PHOTOGRAPH THIS SHEET

AD-A198 638

DTIC ACCESSION NUMBER

LEVEL   DTIC FILE COPY

INVENTORY

ESL 4460-5

DOCUMENT IDENTIFICATION

DEC 1978

DISTRIBUTION STATEMENT

ACCESSION FOR	
NTIS GRA&I	☑
DTIC TAB	☐
UNANNOUNCED	☐
JUSTIFICATION per ltr	
BY	
DISTRIBUTION /	
AVAILABILITY CODES	
DIST	AVAIL AND/OR SPECIAL
A-1 23	

DISTRIBUTION STAMP
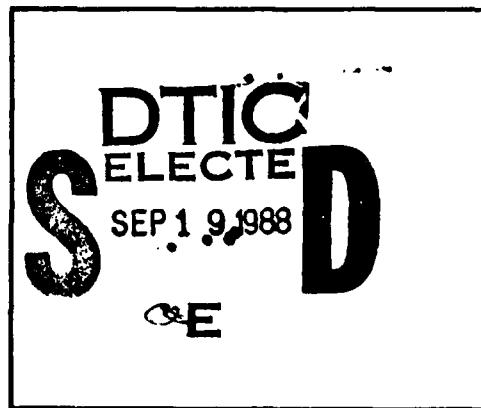
DTIC
COPY
INSPECTED

DTIC
SELECTED
SEP 19 1988
E

DATE ACCESSIONED

DATE RETURNED

88 9 16 240

DATE RECEIVED IN DTIC

REGISTERED OR CERTIFIED NO.

PHOTOGRAPH THIS SHEET AND RETURN TO DTIC-FDAC

METHOD FOR GREY SCALE MAPPING OF UNDERGROUND OBSTACLES
USING VIDEO PULSE RADAR RETURN

D. O. Stapp

The Ohio State University

ElectroScience Laboratory

Department of Electrical Engineering
Columbus, Ohio 43212

TECHNICAL REPORT 4460-5 (784460)

December 1978

Contract DAAG53-76-C-0179

NOTICES

When Government drawings, specifications, or other data are used for any purpose other than in connection with a definitely related Government procurement operation, the United States Government thereby incurs no responsibility nor any obligation whatsoever, and the fact that the Government may have formulated, furnished, or in any way supplied the said drawings, specifications, or other data, is not to be regarded by implication or otherwise as in any manner licensing the holder or any other person or corporation, or conveying any rights or permission to manufacture, use, or sell any patented invention that may in any way be related thereto.

REPORT DOCUMENTATION PAGE		READ INSTRUCTIONS BEFORE COMPLETING FORM
1. REPORT NUMBER	2. GOVT ACCESSION NO.	3. RECIPIENT'S CATALOG NUMBER
4. TITLE (and Subtitle) METHOD FOR GREY SCALE MAPPING OF UNDERGROUND OBSTACLES USING VIDEO PULSE RADAR RETURN		5. TYPE OF REPORT & PERIOD COVERED Technical Report
		6. PERFORMING ORG. REPORT NUMBER ESL 4460-5 (784460)
7. AUTHOR(s) D. O. Stapp		8. CONTRACT OR GRANT NUMBER(s) Contract DAAG53-76-C-0179
9. PERFORMING ORGANIZATION NAME AND ADDRESS The Ohio State University ElectroScience Laboratory, Department of Electrical Engineering Columbus, Ohio 43212		10. PROGRAM ELEMENT, PROJECT, TASK AREA & WORK UNIT NUMBERS
11. CONTROLLING OFFICE NAME AND ADDRESS Department of the Army US Army Mobility Equipment Research		12. REPORT DATE December 1978
& Development Command, Ft. Belvoir, Va 22060		13. NUMBER OF PAGES 156
14. MONITORING AGENCY NAME & ADDRESS(if different from Controlling Office)		15. SECURITY CLASS. (of this report) Unclassified
		15a. DECLASSIFICATION/DOWNGRADING SCHEDULE

16. DISTRIBUTION STATEMENT (of this Report)

17. DISTRIBUTION STATEMENT (of the abstract entered in Block 20, if different from Report)

18. SUPPLEMENTARY NOTES
The material contained in this report is also used as a thesis submitted to the Department of Electrical Engineering, The Ohio State University as partial fulfillment for the degree Master of Science.

19. KEY WORDS (Continue on reverse side if necessary and identify by block number)

Grey level plots   Mapping
Underground radar   Data Processing
Video pulse radar
Tunnels

20 ABSTRACT (Continue on reverse side if necessary and identify by block number)
This work presents a method for detection of underground obstacles through a mapping process. Returns from a Video Pulse Radar system are sampled and interpolated to yield either cross-sectional or plan view plots of the subsurface. The plots are presented in quantized grey scale form. Results of applying the technique to both experimental and analytic data are given, as well as discussion of the interpretation of the plots. Documentation and a user's guide to the computer programs used for plotting are included, as well as suggestions for their improvement.

DD $_{1 \text{ JAN } 73}^{\text{FORM}}$ 1473   EDITION OF 1 NOV 65 IS OBSOLETE

TABLE OF CONTENTS

CHAPTER 1
INTRODUCTION

The ElectroScience Laboratory (ESL) has been involved in the detection of underground targets of one type or another for over a decade. During the past 3 years, part of our efforts have been directed towards the detection of tunnels using the Video Pulse Radar concept developed and used previously for the detection of such targets as utility lines and geological structures. One of the major problems for this kind of radar system is that a wide variety of unwanted targets, classified here as clutter, can be present in the received waveform.

A major effort has been underway at Geo-Centers to provide a target identification capability through mapping techniques using data provided by ESL from Video Pulse Radar Systems. Due to the need for more immediate results to evaluate the progress of our measurement program, a small scale effort has been devoted to an in-house mapping project. Obviously, these results are not to be considered competitive with the major effort but since they contain interesting findings, they are the subject of the present thesis.

An important caveat needs to be included at this point, namely that mapping itself may not be possible at certain sites or times because of restrictions on the placement of the antenna on the surface. This limitation was experienced at several sites, including mountainous terrain and wooded regions. In some cases only a single antenna position is available.

A companion study, modifying techniques developed under contract DAAK70-77-C-0114 appears to have a capability of identifying tunnels on such a single-look basis. This new approach, however, cannot be completed under the present contract because of available time and funding; but some preliminary results are very promising.

Basically the radar used in this study is a simple video, or base-band pulse system. A short pulse, of either 150 picosecond or 6 nanosecond duration, is connected to one element of a crossed, folded, loaded dipole antenna system. This pulse, of course, has a very broad spectrum, extending from the repetition rate of the pulser to the lower microwave region.

1

The crossed antenna pair acts as the principal filter in the system. Its response has been broadened by loading techniques [1-3] and may be modeled in the complex frequency domain by a single pole pair with a significant real component. For the size of tunnel considered in this study, the crossed dipole antenna will pass frequencies up to and just beyond the first tunnel resonance. The crossed antenna configuration also eliminates all returns from planar parallel surfaces. Thus, a great deal of processing of the signal is done in analog fashion by the radar itself.

Four specific antenna systems discussed in detail by Wald [3] are used in this mapping study. They are: a) a Terrascan antenna, b) a modified Terrascan antenna, c) a short box antenna, and d) a long box antenna.

The modification to the Terrascan antenna consisted of moving the balun transformer closer to the antenna terminals, thereby shifting multiple reflections from it out of the desired range window. The box antenna was lengthened just prior to a field test of the antenna because of computations we made of the field scattered by a square tunnel. These computations indicated that the tunnel resonance was lower in frequency than we had expected.

Data was obtained for mapping studies from three sources. The first of those sources was an analytic computation made by Davis [4] using a circular cylinder of $\epsilon_r = 1$ immersed in a homogeneous medium of $\epsilon_r = 9$ and $\sigma = 0.01$ as a model of a tunnel. The other two sources were field trips made to a site in Gold Hill, Colorado known as the Hazel A mine and also to the Curtis Schoolyard in Trumbull County, Ohio where a subsidence problem had been called to our attention by Professor Anne Harris of Youngstown University. Professor Harris, a geologist, and Mr. Richard Myers, of the Bureau of Mines, have both been very helpful to us in our studies.

Before developing the mapping concept, a rather naive discussion of the scattered time domain signal from a tunnel is presented. We model the tunnel as a slab with $\epsilon_r = 1$ immersed in the earth medium of $\epsilon_r > 1$ (see Fig. 1). A pulse is normally incident on the slab from the earth and results in a reflection from the upper interface. The corresponding reflection coefficient is positive. A pulse is also transmitted into the slab and is reflected from the lower interface. The corresponding reflection coefficient here is negative. The reflected pulse now propagates back to the upper interface where it is both transmitted back to the receiving antenna and reflected once again into the slab. Figure 1 illustrates this (note that the rays are actually collinear but are shown separately for clarity). These multiple reflections thus set up a train of reflected pulses that result in a potential multiple lobe signal structure. In the mapping
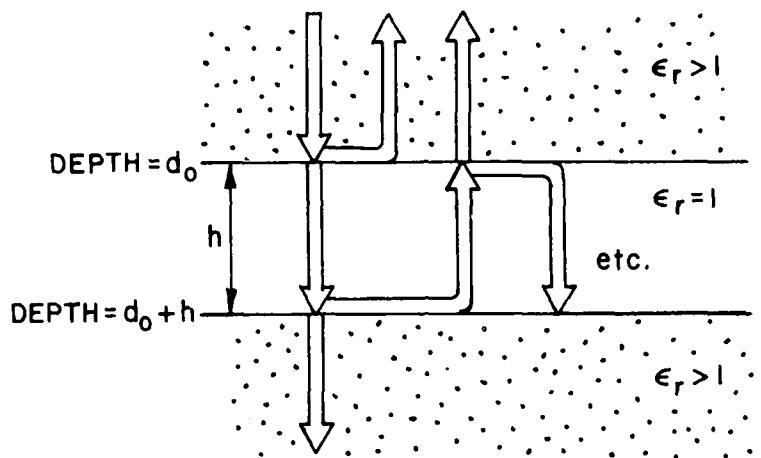
Figure 1. Simplified Tunnel Model.

process, these multiple returns will show up as ʌ train of apparent scatterers at depths (from Fig. 1) related to 2do, 2do+2h, 2do+4h, etc. In fact, the very presence of such a train in a map is an indication that a target whose resonance lies within the bandwidth of the radar system is present.

As has been indicated, the goal of this thesis is to develop a mapping technique and then apply it to experimental data. Since measurements are extremely time consuming, there are a limited number of positions (as stated before) at which an antenna may be placed. This leads to a necessary compromise between the number of data points desired for the construction of a map and the number that can actually be obtained in the time allotted for data gathering. Obviously, even for a very smooth earth one cannot afford to take data with antenna positions separated by one centimeter if an area of say one square kilometer is to be mapped. Even if this were feasible, the ground conditions would very likely change over the time period in which the data was being aquired. As a consequence, the mapping method used must be able to deal with sparsely sampled areas.

Fig. 2 illustrates the mapping technique to be used. In this illustration we have 6 waveforms recorded at 6 successive locations on the surface. These are displayed with the time axis vertical in Fig. 2. Each of these waveforms is stored digitally, consisting of a certain number of samples. The format of our final grey level plot will have the same orientation as the waveforms shown, namely the horizontal axis will be traverse along the ground and the vertical axis will be time or depth. This yields a cross-sectional view of the subsurface. We will be generating one horizontal line of this map at a time.

To start the process, we pick a time delay (or depth if the ground parameters are known) at which to start the map. This is specified as the waveform sample number where we want to start. This starting sample number is shown as the horizontal line labeled "reference depth" in Fig. 2. One sample from each waveform in the traverse (the dot on the reference depth line) is taken at this time delay. The amplitude of these samples is shown plotted again on the lower axis in Fig. 2 (dots on lower curve).

We could at this point make a map from just these waveform samples but it would be extremely small and hard to read. Instead the 6 waveform samples are fed to an interpolator, which fits a smooth curve through them as shown. We may interpolate as many points as we wish between the original waveform samples to yield as large a map as we want.

4
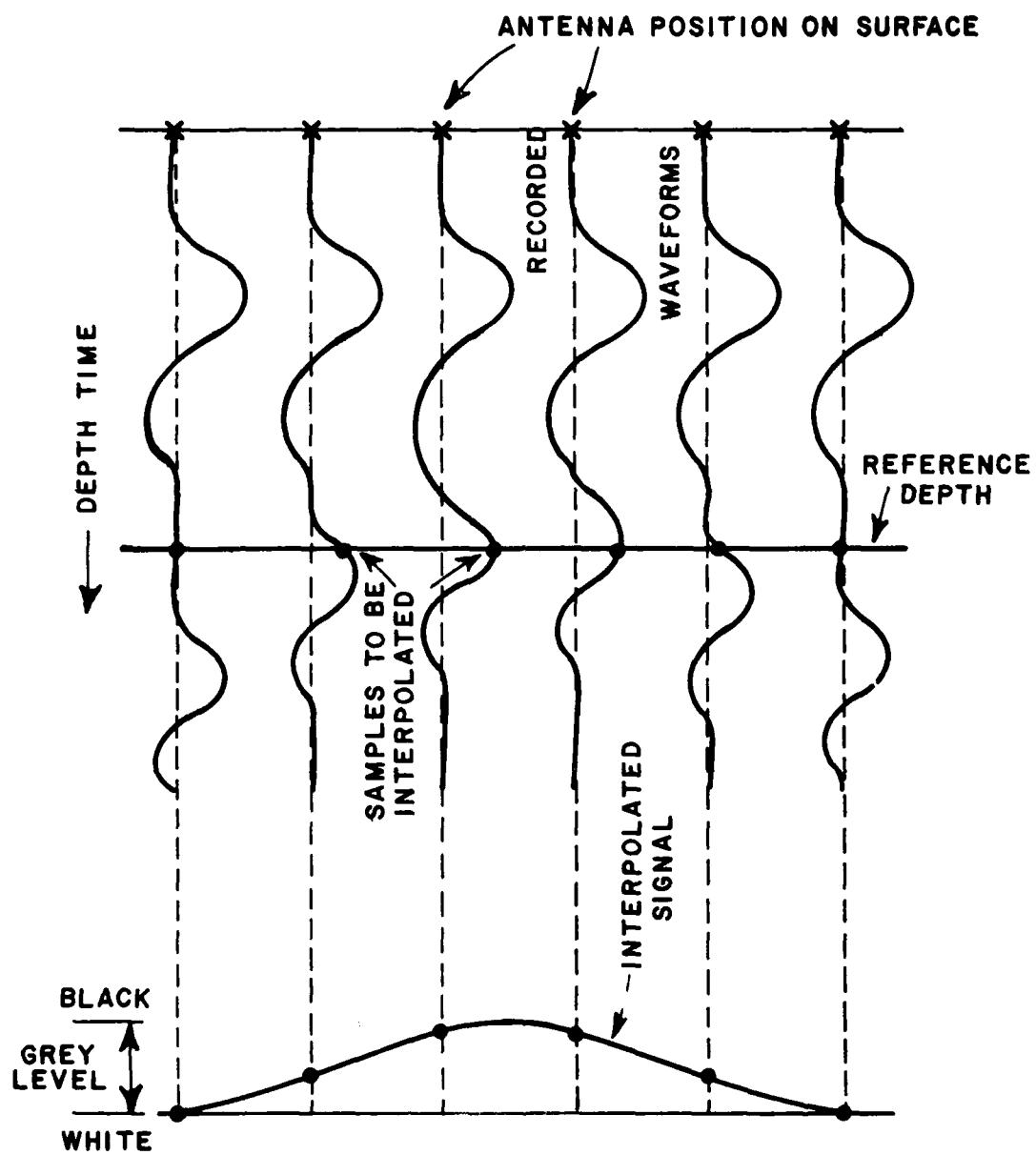
Figure 2. Grey Level Mapping Method.

Since we will be using a line printer as our output medium we do not have a continuum of grey levels available to represent the amplitude of the interpolated signal. For our current installation the limit is 14. Thus, the vertical axis shown as "grey level" in Fig. 2 must be quantized into 14 equal intervals. After this quantization, the interpolated signal is scanned from left to right, and graphic characters representing the grey level of each interpolated point are output to the line printer. Thus, one horizontal line of the map is printed.

To complete the entire map, we return to the original digitized waveforms (top of Fig. 2) and move down one sampling interval on each one. This results in a new reference depth line just one sample below the old one.

The interpolation and quantization processes are repeated and another horizontal line is output to the line printer just below the previous one. We repeat this procedure of moving down one sampling interval on the orginal waveforms until we have mapped as much of the data as we require.

If a two-dimensional grid of antenna positions was used to record data, another type of grey level plot may be produced. By sampling all waveforms in the grid at the reference depth, a "horizontal slice" or plan view may be made. Both the plan view and cross-sectional plot are discussed in detail in Chapter 2.

It can be seen that the mapping technique presented is well suited to produce maps from sparsely sampled grids. The inclusion of interpolation provides a map that is large and smooth enough for the eye to read.

The structure of the remainder of this thesis will be as follows: Chapter 2 presents the interpolation function used in the grey level plotting package, while Chapter 3 discusses the grey level plotting routine itself. Chapter 4 presents results of application of the grey level mapping technique to analytic and experimental data. Finally, Chapter 5 discusses conclusions and recommendations for further improvement to this method of analysis.

CHAPTER II
INTERPOLATION

In this chapter we will derive the interpolation polynomial used as part of the grey level plotting package and discuss the effect this method of interpolation has on the grey level plots themselves.

A formal statement of the interpolation problem is:

Given a continuous $f(x)$ sampled at $x=x_0, x_1, \cdots, x_n$ where $x_i < x_j$ for $i<j$, find a continuous approximation, $F(x)$ to $f(x)$ in the interval $x_0 \leq x \leq x_n$ such that for any $\varepsilon > 0$

$$|f(x) - F(x)| \leq \varepsilon$$

for each $x \varepsilon [x_0, x_n]$. (Note: In this study, x denotes the position of the antenna on the surface of the ground. It is not used to designate time of arrival or the depth of the target.)

By use of the Weierstrauss Theorem[5], it can be shown that $F(x)$ exists for any given $f(x)$ and ε.

After finding $F(x)$, the interpolation process itself consists of finding values of $F(x)$ at points

$$x_i < x < x_{i+1} \qquad i=0,1,\cdots,n-1 \qquad .$$

To derive the approximation polynomial, we define $F_n(x)$ as a polynomial of order n and write

$$F_n(x) = \sum_{k=0}^{n} a_k x^k \qquad (1)$$

where n+1 is the number of sample points.

We then constrain $F_n(x)$ to match $f(x)$ at all of the sampled points $x=x_0, x_1, \cdots, x_n$ so that

$$F_n(x_j) = f(x_j) \qquad j=0,1,\cdots,n \qquad . \qquad (2)$$

We also require that the x_j be distinct.

Using (1) and (2):

$$\sum_{k=0}^{n} a_k \, x_j^k = f(x_j) \qquad j=0,1,\cdots,n$$

in matrix form:

$$\begin{bmatrix} 1 & x_0 & x_0^2 & \cdots & x_0^n \\ 1 & x_1 & x_1^2 & & x_1^n \\ 1 & x_2 & x_2^2 & & x_2^n \\ \cdot & \cdot & \cdot & & \cdot \\ \cdot & \cdot & \cdot & & \cdot \\ \cdot & \cdot & \cdot & & \cdot \\ 1 & x_n & x_n^2 & \cdots & x_n^n \end{bmatrix} \begin{bmatrix} a_0 \\ a_1 \\ a_2 \\ \cdot \\ \cdot \\ \cdot \\ a_n \end{bmatrix} = \begin{bmatrix} f(x_0) \\ f(x_1) \\ f(x_2) \\ \cdot \\ \cdot \\ \cdot \\ f(x_n) \end{bmatrix}$$

$$\underline{X}a = f$$

If the determinant of $\underline{X}$ is non-zero, then a solution exists to $\underline{X}a=f$ and is unique. The determinant DET $\underline{X}$ is well-known and is the Vandermonde Determinant. Its value is given by

$$V_n(x_0,x_1,\cdots,x_n) = \prod_{\substack{i=1 \\ j=0 \\ i>j}}^{\substack{i=n \\ j=n-1}} (x_i - x_j)$$

Since the x_k are distinct, $V_n = $ DET $\underline{X} \neq 0$ and a unique solution to $\underline{X}a=f$ exists.

It can be shown (in a development presented in Appendix A) that the general form of (1) is

$$\begin{vmatrix} F_n(x) & 1 & x & x^2 & \cdots & x^n \\ f(x_0) & 1 & x_0 & x_0^2 & \cdots & x_0^n \\ f(x_1) & 1 & x_1 & x_1^2 & \cdots & x_1^n \\ \cdot & \cdot & \cdot & \cdot & \cdot & \cdot \\ \cdot & \cdot & \cdot & \cdot & \cdot & \cdot \\ \cdot & \cdot & \cdot & \cdot & \cdot & \cdot \\ f(x_n) & 1 & x_n & x_n^2 & \cdots & x_n^n \end{vmatrix} = 0 \qquad (3)$$

8

The coefficients a_k of (1) can be derived by expanding the above determinant by the first row.

A useful form of (3) results when we expand instead by the first column, yielding

$$
F_n(x) \begin{vmatrix} 1 & x_0 & x_0^2 & \cdots & x_0^n \\ 1 & x_1 & x_1^2 & \cdots & x_1^n \\ \cdot & \cdot & \cdot & \cdot & \cdot \\ \cdot & \cdot & \cdot & \cdot & \cdot \\ \cdot & \cdot & \cdot & \cdot & \cdot \\ 1 & x_n & x_n^2 & \cdots & x_n^n \end{vmatrix} - f(x_0) \begin{vmatrix} 1 & x & x^2 & \cdots & x^n \\ 1 & x_1 & x_1^2 & \cdots & x_1^n \\ \cdot & \cdot & \cdot & \cdot & \cdot \\ \cdot & \cdot & \cdot & \cdot & \cdot \\ \cdot & \cdot & \cdot & \cdot & \cdot \\ 1 & x_n & x_n^2 & \cdots & x_n^n \end{vmatrix}
$$

$$
+ \cdots + f(x_n) \begin{vmatrix} 1 & x & x^2 & \cdots & x^n \\ 1 & x_0 & x_0^2 & \cdots & x_0^n \\ \cdot & \cdot & \cdot & \cdot & \cdot \\ \cdot & \cdot & \cdot & \cdot & \cdot \\ \cdot & \cdot & \cdot & \cdot & \cdot \\ 1 & x_{n-1} & x_{n-1}^2 & \cdots & x_{n-1}^n \end{vmatrix} = 0
$$

or

$$
F_n(x) = \sum_{k=0}^{n} f(x_k) L_n^k(x) \tag{4}
$$

where $L_n^k(x)$ is the kth Lagrange Coefficient in x of degree n.

Upon examination, the following properties of the Lagrange Coefficients appear:

(1) they are polynomials of degree n in x

(2) for $j,k=0,1,\cdots,n$ and $j \neq k$

$$L_n^k(x_j)=0$$

(3) for $j,k=0,1,\cdots,n$ and $j=k$

$$L_n^k(x_j)=1$$

9

since we have constrained $F_n(x_j)=f(x_j)$ for $j=0,1,\cdots,n$.

Let us now proceed to derive the explicit form of the $L_n^k(x)$. From properties (1) and (2) we know that $L_n^k(x)$ is an nth degree polynomial with roots $x=x_0,x_1,\cdots,x_{k-1},x_{k+1},\cdots,x_n$ so that

$$L_n^k(x) = \alpha_k(x-x_0)(x-x_1)\cdots(x-x_{k-1})(x-x_{k+1})\cdots(x-x_n)$$

$$\alpha_k \prod_{\substack{j=0 \\ j\neq k}}^{n} (x-x_j) \tag{5}$$

where α_k is an arbitrary (real) constant to be determined.

Using property (3) from above we find

$$\alpha_k = \frac{L_n^k(x_k)}{\displaystyle\prod_{\substack{j=0 \\ j\neq k}}^{n}(x_k-x_j)} = \frac{1}{\displaystyle\prod_{\substack{j=0 \\ j\neq k}}^{n}(x_k-x_j)}$$

substituting back into (5) we have

$$L_n^k(x) = \prod_{\substack{j=0 \\ j\neq k}}^{n} \frac{(x-x_j)}{(x_k-x_j)} \tag{6}$$

which, when used in conjunction with (4) results in our formula for interpolation.

This Lagrange formula for interpolation has several attractive features:

(1)   the $L_n^k(x)$ depend only on x and the constants $\{x_j\}$ (i.e., the sampled points of the original function - Note that the x_j may be arbitrary (but distinct) values. In particular, they need not be equally spaced),

(2)   the $L_n^k(x)$ are dimensionless,

(3)   the form of the equation for the $L_n^k(x)$ is invariant under a change of variable x=a+hs (i.e., invariant under translation by "a" and scale change by "h"). Stated differently,

10

the $L_n^k(x)$ depend only on the relative positions of the points involved in the interpolation,

(4)   the original sampled points are preserved and are not altered as in other forms of curve-fitting (e.g., mean-square approximations).

Figure 3 shows an example of a Lagrange interpolation where the interpolated function was evaluated at 19 points between each known point. The actual waveform is shown at the top with the sampling points (in this case non-uniformly spaced) shown by "x's". We show also a straight-line approximation to the actual waveform since the exact behavior of the actual waveform is known only if the samples satisfy the Shannon sampling theorem for the highest significant frequency component present. The smoothness of the interpolated curve in the botton of Figure 3 is apparent.

However, Figure 4 exhibits the one observed weakness of the Lagrange (or any polynomial) method. Large discontinuities in slope between adjacent points (especially near the ends of the interval) cause an "overshoot" or "peaking" phenomenon which can cause annoying false targets to appear in a grey level plot. The peaking can be seen in the interpolated curve at the bottom of Figure 4 near sampling points 9 and 10. More dense sampling would be the best way to remove this characteristic.

The generalization of the Lagrange interpolation formula to the *two-dimensional case is quite simple*. As shown by Steffensen[6], it is just the product of two one-dimensional interpolations, so that,

$$F_{mn}(x,y) = \sum_{k=0}^{n} \sum_{\ell=0}^{n} f(x_k,y_\ell)L_{mn}^{k\ell}(x,y)$$

$$= \sum_{k=0}^{n} \sum_{\ell=0}^{n} f(x_k,y_\ell)L_m^k(x)L_n^\ell(y) \qquad .$$

After plots were made of the results of several interpolations of experimental data using the entire data set in the interpolation formula, it became apparent that a better mathematical model for including the physical properties in the mapping process was needed. It is intuitively unsatisfactory to let points physically far removed from a section of the map influence the interpolation of that section (e.g., points in the lower right of a map should have little significance in the interpolation of the upper left portion of the map). For this reason, some sort of "localized" interpolation was sought. Several methods were investigated.

11
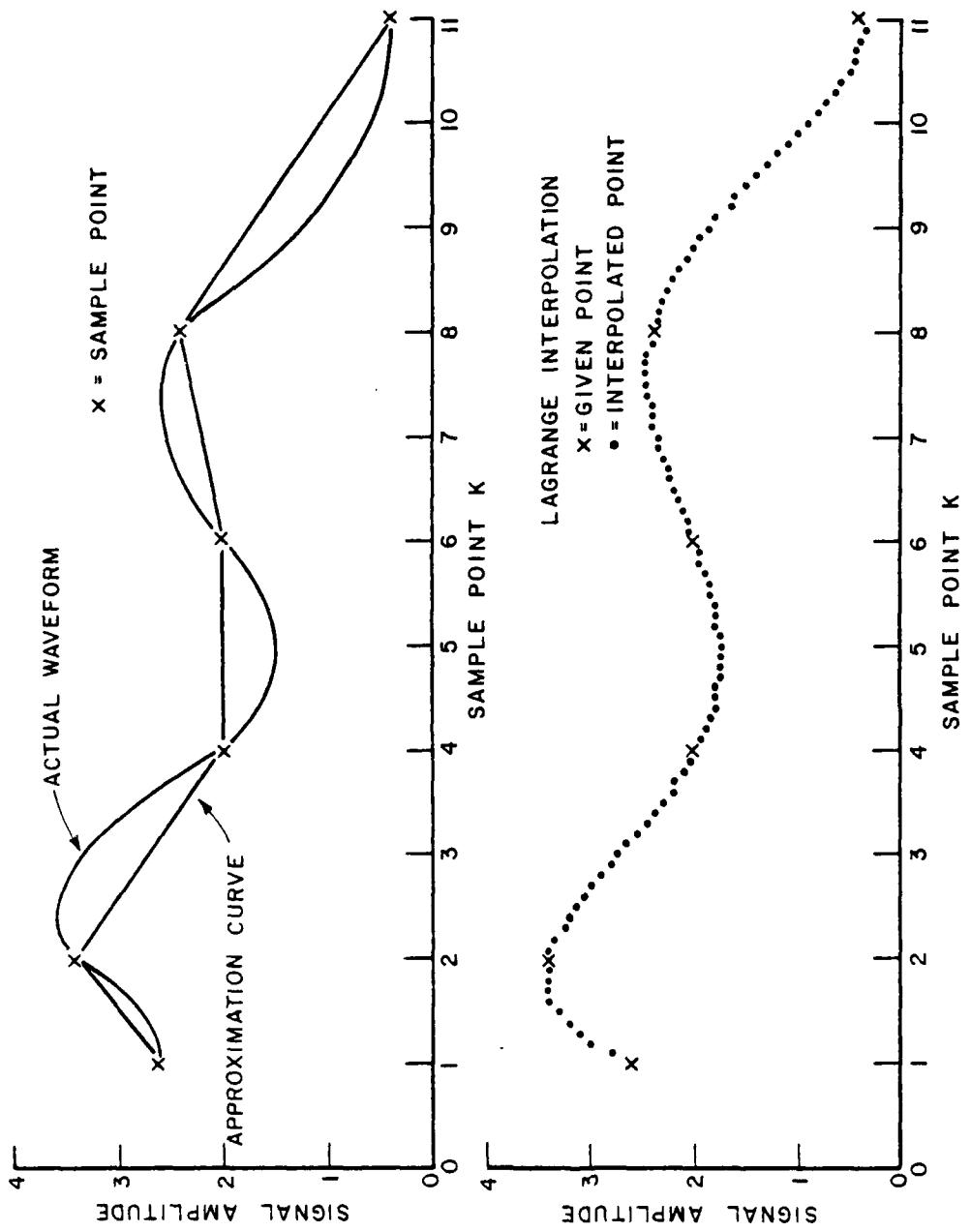
Figure 3. Example of Lagrange Interpolation.

12
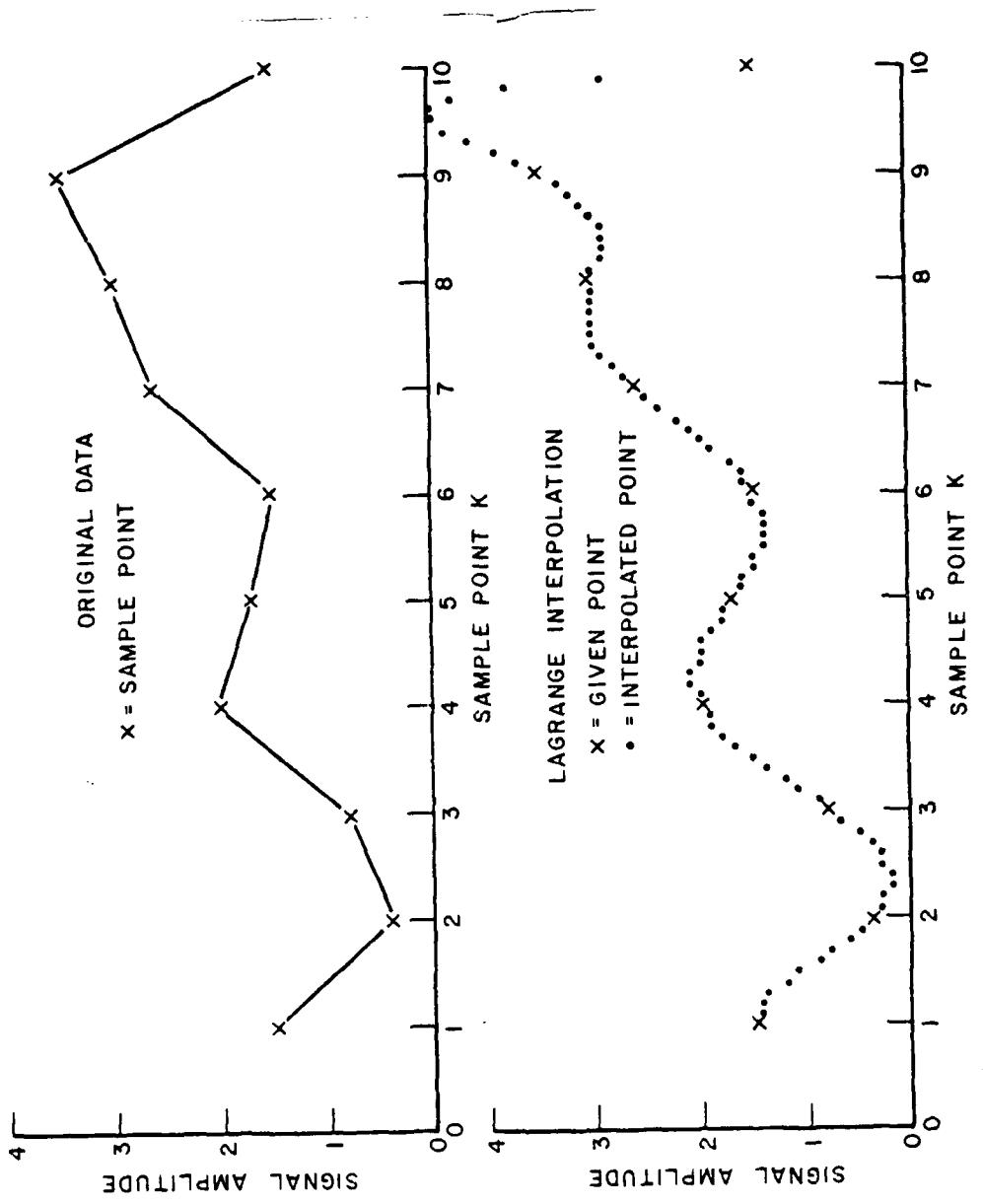
Figure 4. Example of Lagrange Interpolation.

13

(1) Weighting the Lagrange Coefficient

Since the Lagrange coefficients depend only on the relative positions of the points involved in the interpolation, it was felt that by weighting them in proportion to their distance from the desired interpolation point the required localized characteristics could be obtained. The success of this method depends on the unaltered Lagrange coefficients themselves being weighted in proportion to their distance from the interpolation point. Figure 5 is a plot of the Lagrange coefficients for a ten-point grid (i.e., $x_0=1$, $x_1=2,\cdots,$ $x_9=10$) as a function of the interpolation point x.

The coefficients were calculated using (6). If the expected behavior were exhibited in these graphs, the coefficients nearest to the arrows (the position of the interpolation point, x) should be the largest, with magnitudes dropping off as we move away from the arrow. Figure 5 shows that this is not the case. The Lagrange coefficients are not a clear function of the position from the interpolation point (see, e.g., plot for x=1.75). Thus, a localized interpolation method weighting the Lagrange coefficients is not easily accomplished.

(2) Small Interpolation Grids

With this method, the sampled data is partitioned into small, adjacent subsets. Then, each subset is used to interpolate within its boundaries. As can be seen from Figure 6, the smoothness of the resulting curve is very dependent on the method used to partition the data. The points included in each small interpolation are shown enclosed by the brackets at the top of each graph. Each interpolation (encompassing 3 sample points) is butted against the next in the figure. The partitions used in the top curve produce a relatively smooth waveform, but the partitions used in the bottom curve produce large slope discontinuities in the waveform. These discontinuities would have a detrimental effect in any resulting grey level plot.

(3) Overlapping Small Interpolation Grids

The final method tested, and the one that yielded the best results was similar to method (2) but, where different partitions overlapped they were averaged together to yield the final interpolated value. The result of averaging the overlapping portions of Figure 6 is shown in Figure 7. This data was the same as that shown in the top of Figure 4 and the bottom of Figure 4 (using a full data set interpolation) may be compared to Figure 7 ("localized" interpolation). Such a comparison shows that the localized interpolation gives a curve with much less "overshoot" - particularly noticable around points 2, 4, and 9, and yet is still smooth. This result is to be expected since lower-order polynomials are used in the localized method and very fast slope changes cannot occur.

14
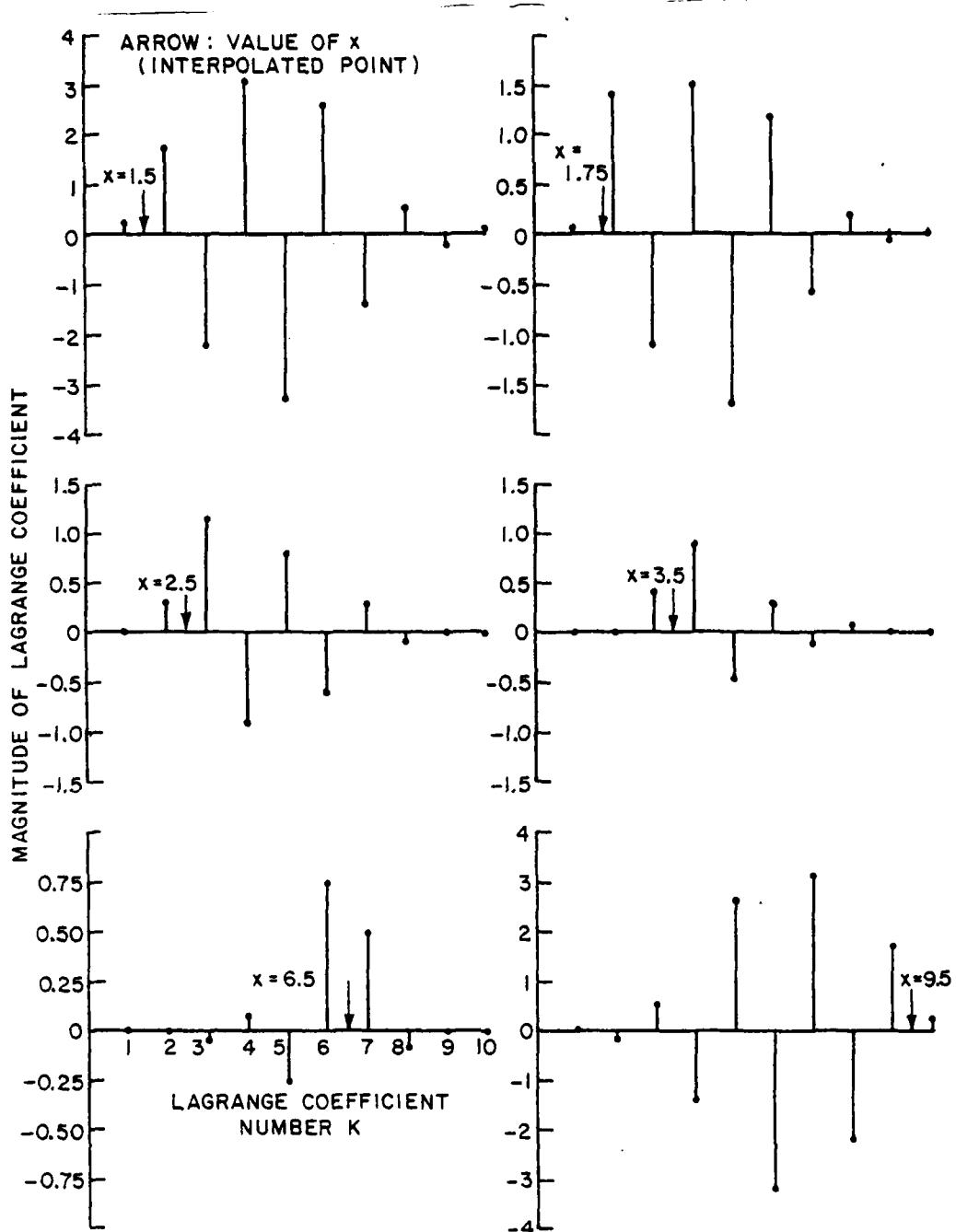
Figure 5. Characteristics of Lagrange Coefficients.
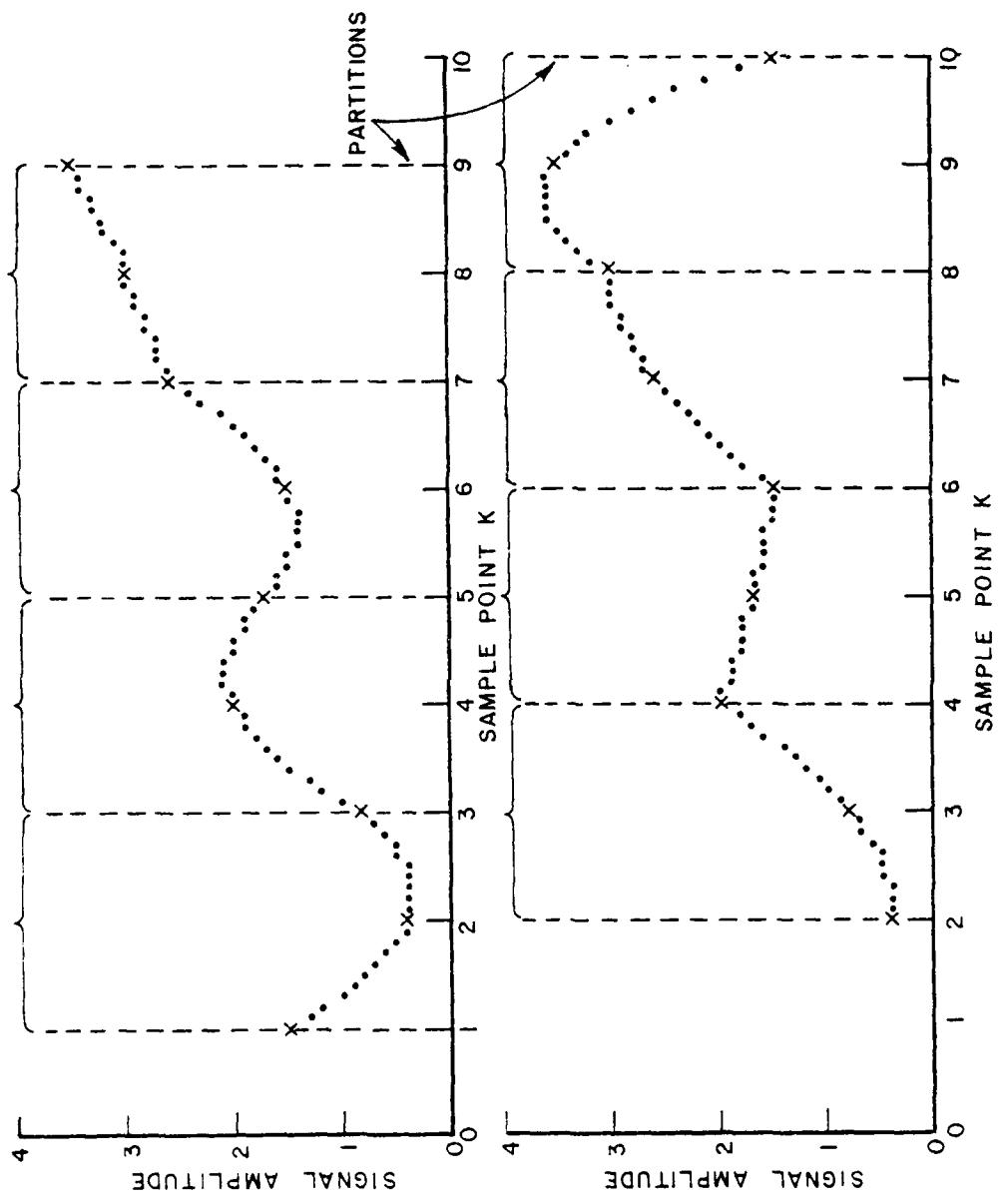
Figure 6. Example Using Small Interpolation Subgrids

16
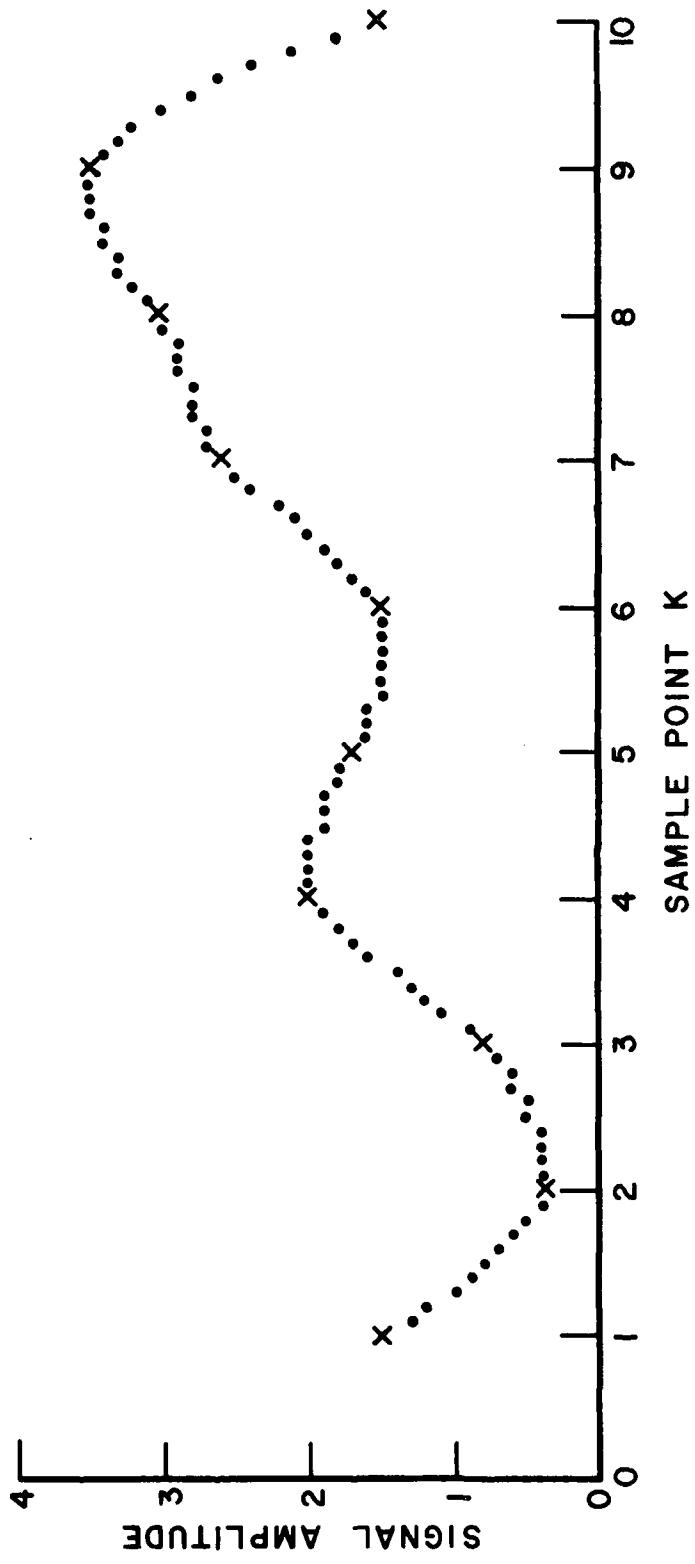
Figure 7. Example of Averaging Overlapping Interpolation
Subgrids.

17

CHAPTER III
GREY LEVEL PLOTTING ROUTINE

The primary function of the grey level plotting routine (here-after GLPR) is to take an array of data, interpolate it to expand it to a given size, quantize the resulting array into a specified number of levels, and then plot that information in the form of grey levels.

Our use of GLPR has been primarily to plot groups of experimental underground radar returns. The resulting grey level plot is then used as an indication of the radar's ability to detect a target of certain prescribed characteristics.

We will now discuss the various inputs to GLPR. The array of known data (the "input array") may be constructed in several ways, depending on the method used to gather the data. If a two-dimensional grid of data is available, this may be used directly as the input array. Subsequent interpolation and plotting will yield "plan views" of the area mapped. Since using only one point from each waveform at the depth of interest for the entry in the input array would be mis-leading (because the equipment used in data taking may not have that high a frequency response) another method for calculating the entries in the input array is used. A depth window (i.e., time window on the waveform) is set up on each waveform and the RMS value of the curve calculated therein. (Choice of the window size is critical. For a discussion of this point see Chapter 4.) The input array then con-sists of these RMS values for a given depth of interest.

If only a one-dimensional, or linear scan is available, the input array may be set up using all sample points from each waveform as a column in the array. This format is similar to that used in seismograms [7]. In order to keep the plots to manageable size, only a portion of the waveforms in the time window of interest is usually plotted.

A summary of all array conventions used in this section is shown in Figure 8.

It is not necessary for the map data to be equally spaced. GLPR will allow non-uniform spacing between known points and will inter-polate to correct for it. Although the spacing may be non-uniform, it must be consistent throughout the map. To understand the differ-ence between consistent and inconsistent non-uniform maps, see Figure 9.

18
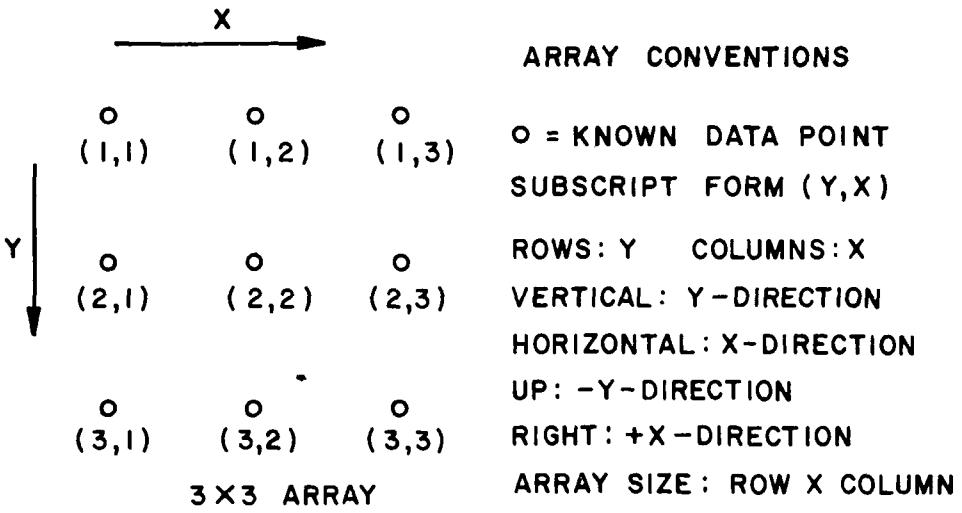
Figure 8. Statement of Array Conventions.

The figure shows a 3×3 array with an X arrow pointing right at the top and a Y arrow pointing down at the left.

```
        X  ───────►

   O          O          O
 (1,1)      (1,2)      (1,3)

 Y │
   │   O          O          O
   │ (2,1)      (2,2)      (2,3)
   ▼

   O          O          O
 (3,1)      (3,2)      (3,3)

        3 × 3  ARRAY
```

ARRAY CONVENTIONS

O = KNOWN DATA POINT

SUBSCRIPT FORM (Y, X)

ROWS: Y   COLUMNS: X

VERTICAL: Y - DIRECTION

HORIZONTAL: X - DIRECTION

UP: - Y - DIRECTION

RIGHT: + X - DIRECTION

ARRAY SIZE: ROW X COLUMN

CONSISTENT NON-UNIFORM MAP

INCONSISTENT NON-UNIFORM MAP
(POINTS NOT LINED UP)

Figure 9.   Consistent and Inconsistent Non-Uniform Maps.

20

Figure 10 shows two examples of physical spacing versus array representations. On the left is a representation of the physical layout of a two-dimensional map. In the uniform case, spacing between all samples is equal and the input array subscripts reflect the physical position of the sample points. In the non-uniform case, however, spacing between samples in the horizontal dimension varies as a function of x and the array subscript no longer reflects the true physical spacing of the sample points. Another array with this spacing information must be supplied to GLPR.

At the right of Figure 10 are the array representations of the input data after interpolation (throughout this chapter a white circle will be used to represent sample (known) points and a black circle will designate an interpolated point). The size of the interpolated array is specified by the user of GLPR in the number of interpolated points desired between each known point (i.e., between each entry of the input array). At the top right of Figure 10, the user has specified two points to be interpolated between known values in the x-direction and one point between values in the y-direction.

In the non-uniform case the interpolation is handled differently. The interpolation attempts to fill in "missing" data points to make the final plot look true (i.e., without the distortion that might result if point (1,2) in Figure 10 was considered to be equidistant from points (1,1) and (1,3). The result is that interpolation beyond that specified by the user is performed. In the lower right of Figure 10, the user has specified one point to be interpolated between known values in the y-direction and no points between values in the x-direction (as seen from the lack of an interpolated point between columns 1 and 2). Note that interpolation was still performed in the x-direction, however, to make the final plot reflect the physical lay-out of the data. Note also that the input array may be non-uniform in one direction only or in both.

In order to fully explain the algorithm used by GLPR, several terms must now be defined.

Block: A block is the area bounded by four adjacent points of known data. Figure 11 shows two examples of blocks: uniform on the left and non-uniform on the right.

Grid: The pattern of measurements (experimental data) that constitute a map.

Subgrid: A subgrid is the rectangular set of known points used to interpolate inside its boundaries. It has dimensions YxX. A sub-grid is identified by its upper left point. Figure 12 shows a 4x5 input array with a 3x3 subgrid consisting of the blocks numbered 1 through 4.

21

PHYSICAL CONFIGURATION   INTERPOLATED
(WITH INPUT ARRAY SUBSCRIPT)   ARRAY CONFIGURATION

```
   O     O     O     O            O••O••O••O
 (1,1) (1,2) (1,3) (1,4)          •••••••••••
                                  O••O••O••O
   O     O     O     O            •••••••••••
 (2,1) (2,2) (2,3) (2,4)          O••O••O••O
                                  •••••••••••
   O     O     O     O            O••O••O••O
 (3,1) (3,2) (3,3) (3,4)
```

UNIFORM CASE

```
  O   O           O       O       O   O   •   •   O   •   O
(1,1)(1,2)      (1,3)    (1,4)     •   •   •   •   •   •   •

  O   O           O       O       O   O   •   •   O   •   O
(2,1)(2,2)      (2,3)    (2,4)     •   •   •   •   •   •   •

  O   O           O       O       O   O   •   •   O   •   O
(3,1)(3,2)      (3,3)    (3,4)
```

NON-UNIFORM CASE

O = KNOWN POINT
• = INTERPOLATED POINT

Figure 10.   Expansion of Input Array by Interpolation.

EXAMPLES OF BLOCKS
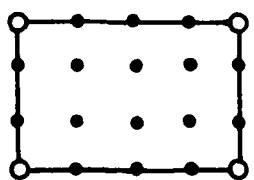
Figure 11.
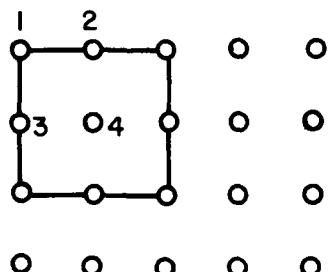
DEFINITION OF SUBGRID
FOR INTERPOLATION

Figure 12.
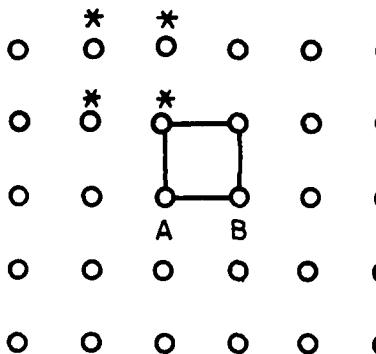
ILLUSTRATION OF
OVERLAP

Figure 13.
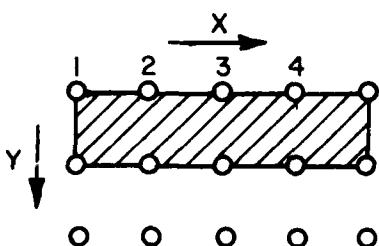
DEFINITION OF
HORIZONTAL SCAN

Figure 14.

23

Overlap: An overlap occurs if a fixed point (Y,X) is contained in more than one subgrid. In Figure 13, if we are using a 3x3 subgrid, then each point in the block shown will be overlapped by the subgrids marked with "*". Overlaps other than those indicated will also occur. Note that the line AB is also overlapped by the subgrid at A and that the point B is overlapped yet again by the subgrid identified by point B. These types of overlap are very cumbersome to deal with computationally and are ignored by GLPR. The consequences of this are discussed below.

"Interpolating a Block with Subgrid (Y,X)" means to interpolate values at all points in a block using the subgrid (Y,X).

"Filling a Block" means to calculate a value for each point inside a block by averaging the overlapping interpolated values at that point.

A "Horizontal Scan" is the filling of all blocks from left to right for some fixed Y. In Figure 14, for the 3x5 input array shown, filling blocks 1-4 constitutes a horizontal scan.

The algorithm used in GLPR is then to perform horizontal scans from top to bottom until all blocks in the input array have been filled. This methodology means that at points where "higher-order" overlaps occur (see "overlap" above), the interpolations using points to the right and downward are preferred and in fact overwrite the results from other interpolations on the left and upward. The detrimental effects, if any, of this method have not yet been observed in practice.

We now state a procedure for parameter choice for the user of GLPR. After statement of the procedure, two examples of its use are given.

I) Choose the dimensions of the input array. One of the dimensions must be less than or equal to 126, as this is the width of a line printer page. If a two-dimensional map of data was taken, the dimensions of the input array are just the dimensions of the area of interest in the map. If a linear scan was taken, the usual choice for the y-dimension is the number of sample points in the waveforms and for the x-dimension is the number of waveforms in the scan.

II) Choose the number of points to be interpolated between the given points. This number is specified independently for the x- and y-dimensions. When choosing these parameters, it must be remembered that in the non-uniform case, even if no points are desired between given points, the GLPR will still interpolate enough points between the given ones to eliminate any distortion that might otherwise result.

As an example, suppose waveforms were recorded at positions 1, 5, 6 and 8 in some reference grid. GLPR would interpolate values for

24

positions 2, 3, 4 and 7 on the grid even if the user specified no interpolated points were to be generated between known values. Conversely, if the user had specified 1 point to be generated between known values, the program would then calculate values for positions 1.5, 2, 2.5, 3, 3.5, 4, 4.5, 5.5, 6.5, 7 and 7.5 on the reference grid.

III) By completing step II, the dimensions of the interpolated array have now been fixed. They may be calculated from the following formulas:

For the uniform case:

interpolated array x-dimension =
total number of points generated in x-direction =
(x-dimension of input array -1)
x (number of interpolated points desired in
x-direction +1) +1

interpolated array y-dimension =
number of points generated in y-direction
in one horizontal scan =
number of interpolated points desired in y-direction +2

For the non-uniform case:

Calculate x-size = highest coordinate in reference grid
- lowest coordinate in reference grid

then interpolated array x-dimension =
total number of points calculated in x-direction =
x-size x (number of interpolated points desired in
x-direction +1) +1

Calculate y-size = maximum spacing of any two
adjacent points on the reference grid.

then interpolated array y-dimension =
maximum number of points generated in y-direction
in any one horizontal scan =
y-size x (number of interpolated points desired
in y-direction +1) +1

It will be noted that the entire interpolated map is never kept in memory at one time. Only the data from one horizontal scan resides in core at any time. This facilitates processing of large maps.

IV) Choose the number of grey levels. A maximum of fourteen levels may be specified. The representation of these levels on a line printer page is shown in Figure 15. Maximum resolution is achieved

GREY LEVEL

| 1 | 2 | 3 | 4 | 5 | 6 | 7 | 8 | 9 | 10 | 11 | 12 | 13 | 14 |

WHITE

BLACK
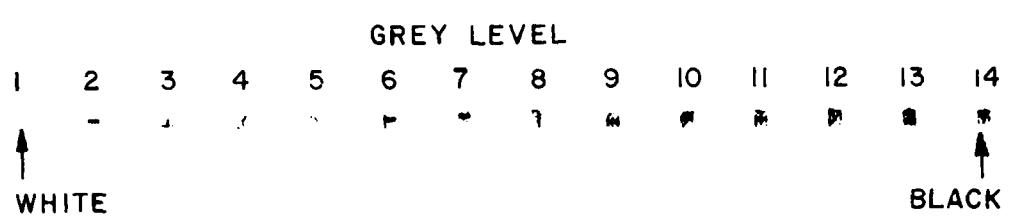
Figure 15. Line Printer Representation of Grey Levels.

with a large number of grey levels and maximum contrast is obtained with a small number, so a compromise is usually necessary. (Also see VI below "clipping").

V.   Choose the subgrid size to be used for interpolation. The subgrid size in the x- and y-dimensions are specified separately. If no interpolation is desired in a given direction, that subgrid size is specified as 1 (and the number of desired interpolated points in that direction (step II) should be declared zero).

The size of the subgrid may be chosen up to the size of the input array itself. Usually, to model the physical processes involved, the entire data set is not used.

In the non-uniform case, data physically far removed from certain points may unduly influence the interpolation around that point, so care must be taken when choosing the subgrid size.

VI.   Specify the clipping level. One method of increasing resolution in a given area of a grey level plot while sacrificing detail in others is by "clipping" the data. That is, data in the interpolated array are tested; if a data value is greater than or equal to a specified threshold value (the clip value) it is set equal to the threshold value. This will sacrifice detail in the clipped areas and will allot more grey levels to the remainder of the map. In practice, one plot is usually made with an arbitrarily high clip value, in order to determine what the most effective clip value will be.

In order to clarify the use of the above procedure, the following two examples are presented:

EXAMPLE 1

We have 17 waveforms of 256 samples each which were taken along a straight line at intervals of 1 foot. The time window seen by each waveform is 200 ns and the ground in which the measurements were taken had a relative permittivity of approximately 9.

Since this is a linear scan, we decide to do a cross-sectional view grey-level plot, using all 17 waveforms and the entire 200 ns time window. We will plot depth down the page and horizontal position across the page. The dimensions of the input array will then be Y=256, X=17. Since the data was taken on a uniform grid, we need not specify the spacing.

Suppose that we wish to plot the data letting the width and height of one grey level character represent the same physical

27

reference dimension. That is, we wish to make the horizontal and vertical scales the same. This will result in a small amount of visual distortion (since the actual width and height of a line printer character are not equal) but is a useful first approximation.

The physical dimensions of the area represented by our grey level plot are:

horizontal: (17 waveforms -1) *1 foot/waveform *0.305 meter/foot = 4.88 meters

vertical: $\dfrac{(200 \text{ ns})*(0.3 \text{ meter/ns})}{\sqrt{9}}$ = 20 meters

but this is the round-trip distance, so the actual range is 20/2 = 10 meters

Let us let one character on the grey level plot represent one sample from the waveform in the y-direction (i.e., no interpolated points in the y-direction). Then the unit of length represented by one character's height or width will be

unit length = $\dfrac{10 \text{ meters}}{256 \text{ points}}$ = 0.0391 meters/point.

Then we should have

$\dfrac{4.88 \text{ meters}}{0.0391 \text{ meters/point}}$ = 125 points

on the horizontal. We can come close to this number by specifying that we want 6 points interpolated between each known value in the horizontal direction. We would then have a plot (see formula in Step III)

(17-1)*(6+1)+1 = 113 characters wide   .

This is a distortion of our original plan for the plot by compression of about 9.6%. We will consider that to be acceptable.

We have now specified the desired number of interpolated points, namely, Y=0, X=6 and the interpolated array dimensions are (see formula in Step III): Y=0+2=2 and X=113.

28

We will initially get as much resolution as possible by specifying fourteen grey levels and an arbitrarily high clip value.

In choosing a subgrid size, we will choose to interpolate in the x-direction only, since we have a fairly high number of samples in the y-direction. We do this by specifying the y-dimension subgrid size as one. We choose the X subgrid size to be 3, as this is the smallest value that still allows overlapping to occur.

EXAMPLE 2

We have a grid of waveforms available in the configuration shown in Figure 16. In one direction the measurements are spaced at half-foot intervals and in the other direction, measurements were taken at 1, 3, and 2 foot intervals.

We choose to display this information in a series of plan views at selected depth windows. Let us assume that some window of interest has been chosen and RMS values of the waveforms in this window are available.

After interpolation, we expect that the non-uniform dimension will be the largest, and therefore choose to plot this down the page (y-direction). The dimensions of the input array are then X=5, Y=4.

Since the data are non-uniformly sampled, we must specify the spacing. In the x-direction, the samples are uniformly spaced, so that we may say the measurements were taken at positions x=1,2,3,4,5. In the y-dimension, we choose 1 foot as our basic unit and specify that the measurements were taken at positions y=1,2,5,7.

Let us once again attempt to present the data in "true" form by making the x- and y-scales on the plot equal. In the x-direction, specify 14 points to be generated between known values. (This was chosen solely as an attempt to fill the width of the page.) The formula (Step III) for the interpolated array x-dimension then gives

$(5-1)*(14+1)+1 = 61$ points .

Let us also try to correct for the fact that the height/width ratio of a line printer character is 5/3. Expanding the x-scale by 5/3 would give 101.67 points. We can come close to this by changing our desired number of interpolated points to 24 instead of 14. Then the interpolated array x-dimension is $(5-1)*(24+1)+1 = 101$ points.

To make the interpolated data "true," we will need twice as many interpolated points in the y-direction (twice the number of points needed before 5/3 correction). This is because our unit of measurement on the y-axis was twice that used in the x-axis (i.e., 1 ft. vs. 0.5 ft). Using the formula from Step III for the non-uniform case, we have:

29
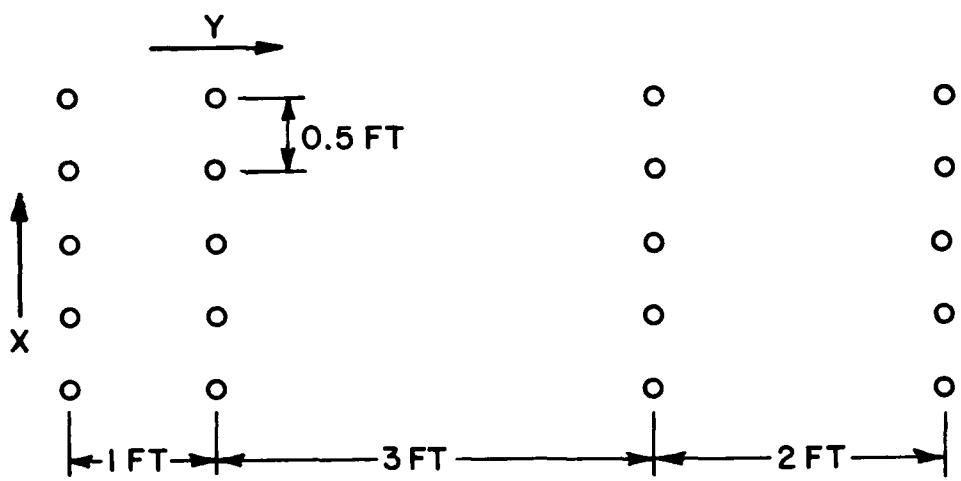
Figure 16.   Layout of Measurement Positions Used in Example 2.

$$Y\text{-size} = \text{MAX}\{2-1, 5-2, 7-5\}$$

$$= \text{MAX}\{1, 3, 2\}$$

$$= 3$$

interpolated array y-dimension =

$$3*(14*2+1)+1 = 88 \text{ points} \qquad .$$

We then choose to obtain 14 grey levels; we set clipping at an arbitrarily high value and choose a subgrid with Y=3, X=3 for interpolation to obtain overlap in both dimensions.

31

CHAPTER IV
GREY LEVEL PLOTS

In this section we will present results of applying the previously discussed grey level plotting program to experimental underground radar returns. We will discuss separately data taken at several locations with different antenna types and different pulsers.

The first location from which data was processed was the Curtis School in Trumbull County, Ohio. The site was a schoolyard with an abandoned coal mine structure underneath. Subsidence had already occurred in areas of the school's playground. The depth of the mine structures in this yard was approximately 2.4 m. The yard has subsequently been drilled using a square grid with 7.62 m spacing between holes. The rock composition was found to be rather complex and included sandstone, shale, and much broken rock.

Several visits have been made to the site. The data presented here is from the first trip, made in January, 1978. The temperature had been below freezing over an extended period and a deep snow had fallen. However, the schoolyard was plowed by local officials prior to our measurements.

Initially, the area was scanned using the Terrascan system. Based on signal returns observed, a portion of the yard was selected for detailed study. Data was taken according to the plan shown in Figures 17 and 18. Figure 17 shows the general layout of the yard with an indication of the area mapped. Figure 18 gives the coordinates used to identify each waveform recorded.

The measurements were made using an unmodified Terrascan crossed-dipole antenna with a 150 ps pulser. The receiver was a Tektronics sampling oscilloscope. Data was recorded using a microprocessor system [8] and floppy disk recorder. Waveforms obtained using this system are shown in Figure 19. Each waveform essentially shows the received signal level as a function of time.

The first type of plot attempted was a plan view of the area. The waveforms were examined and a time window from approximately 30 to 40 ns was chosen as the depth at which the largest returns were occurring.

32
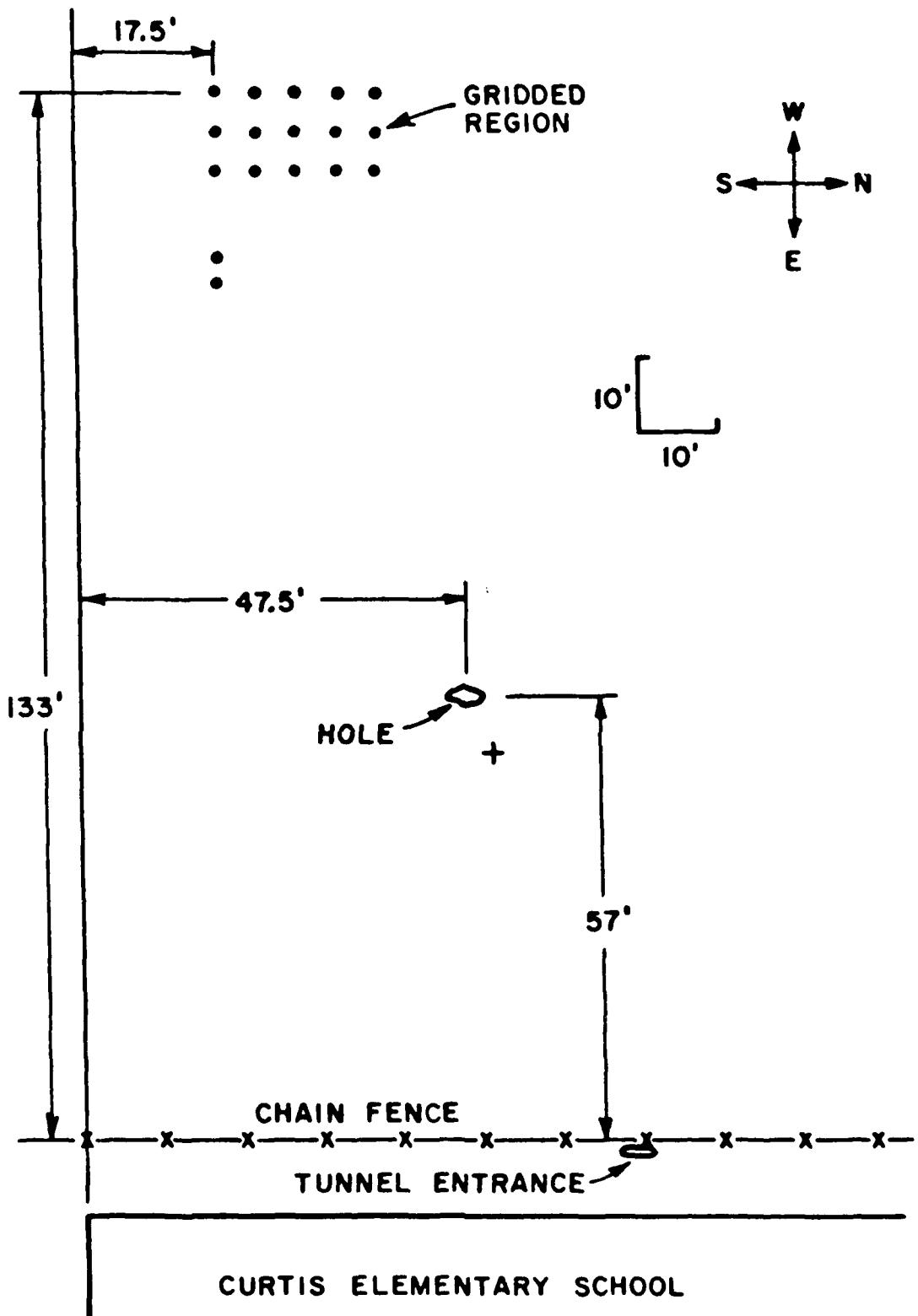
Figure 17. Aerial View of Curtis School Site.
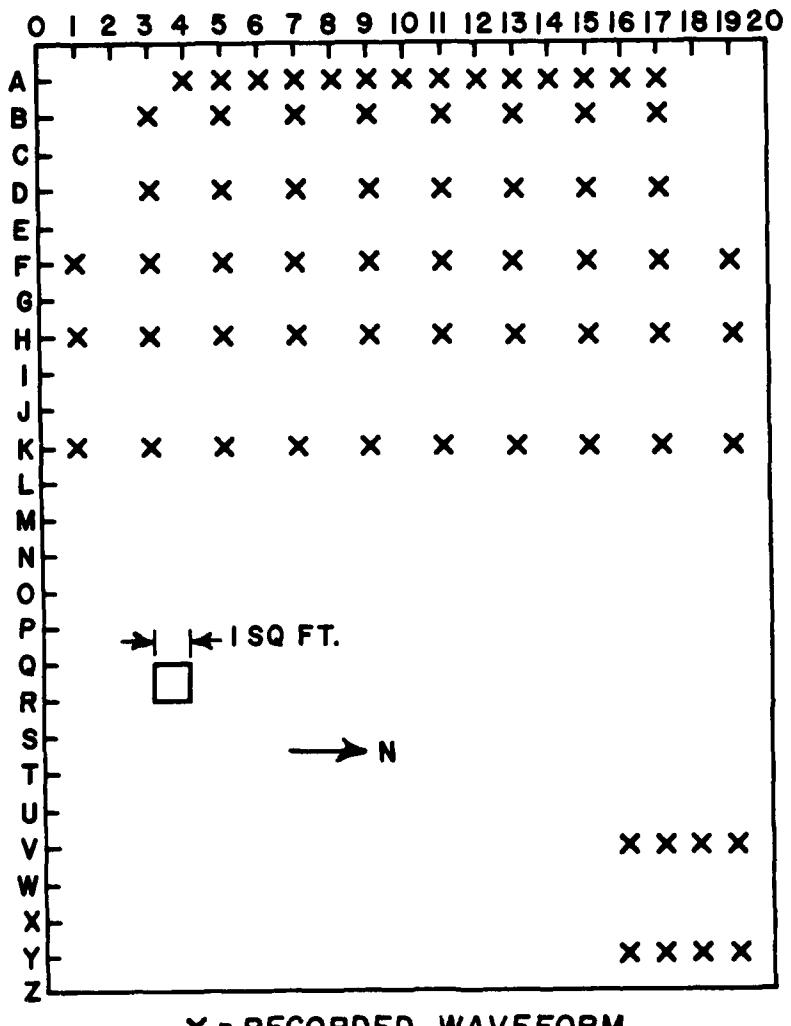
Figure 18. Antenna Positions Used for Recording Data at Curtis Schoolyard.
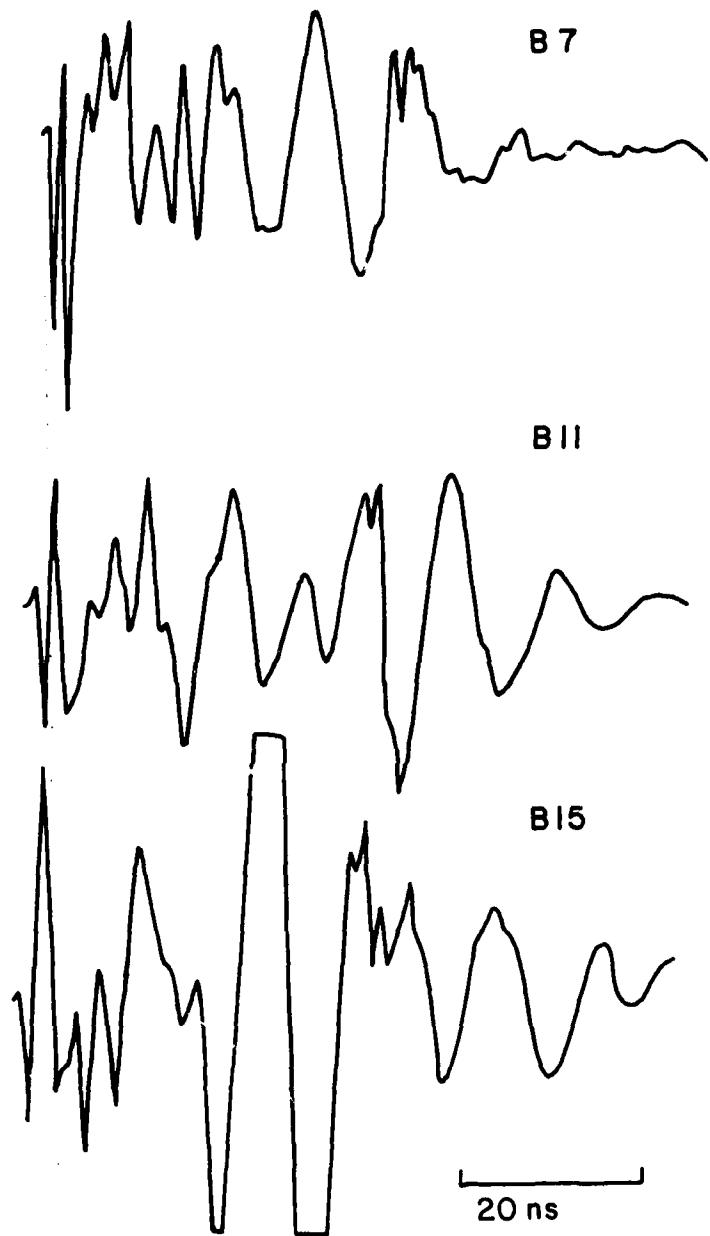
Figure 19. Example Waveforms Recorded at Positions Shown at
Curtis Schoolyard.
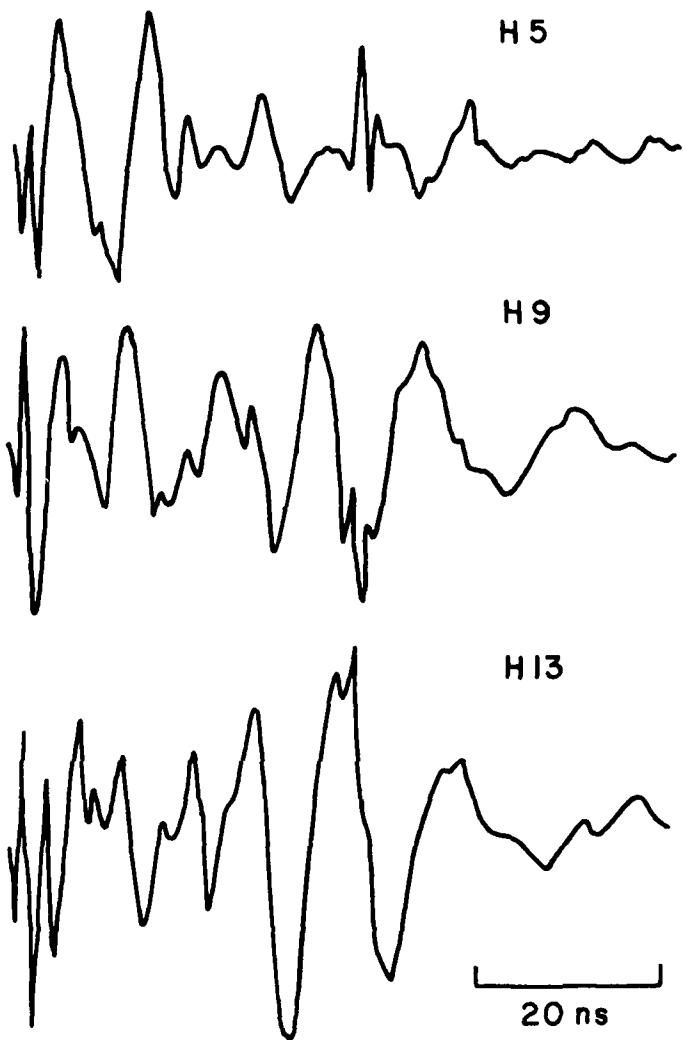
Figure 19 (cont.).   Example Waveforms Recorded at Positions
Shown at Curtis Schoolyard.

Numbers derived from the peak-to-peak signal amplitude were
calculated in this window for each position shown in Figure 18
and the values are shown in Figure 20. Only the waveforms from
columns 5-17, odd and rows A,B,D,F,H,K were used in the grey level
plot. This is the largest set of positions that constitutes a
consistent map (see Chapter III).

It should be noted that at the time this plot was made, the
GLPR could not handle non-uniform grids of data. Thus, the decision
to include rows A and K in the plot results in inherent distortion.
GLPR treats rows A and B and also rows H and K as equidistant from
each other. These rows are also plotted in the same manner so
that the resulting plot is compressed at the top and expanded at
the bottom. Also, this early version of GLPR could only perform
interpolation on entire data sets, hence the interpolation is not
localized.

The grey level plot itself is shown in Figure 21. Contour
lines were added to help distinguish between the different graphic
characters and to observe the charactieristics of the interpolation.

Next, computer calculation of RMS values in a time window
of specified position and width was added to the GLPR. This relieved
the burden of hand calculation of signal amplitudes. GLPR was
also upgraded to handle localized interpolations (as discussed
in Chapter II).

Using the same waveforms as above (i.e., A,B,D,F,H,K, 5-17 odd)
plan views were plotted using a 50-point time window for calculation
of the RMS value. Each waveform consisted of 256 "points" or samples
and spanned 100 ns in time. This gives a scale of (100 ns)/(250
pts.) = 0.391 ns/pt. So a 50-point window would be approximately
20 ns wide. This window was scanned across the waveform set at
25 point ($\sim$10 ns) increments. The results are shown in Figures
22-30.

It should be remembered in viewing these plots that only
42 numbers were input to the interpolator, namely the RMS values
calculated for the waveforms recorded at the intersection of
coordinate lines A,B,D,F,H,K and 5-17 odd. Only these 42 points
on the grey level plot are experimental. All other points were
generated by the interpolation in trying to fit a smooth 2-dimensional
surface of the specified size to the given data points.

An interpolation grid size (see Chapter III) of 3x3 was chosen
for these plots and this resulted in averaging of at most 4 overlaps
at each point in the plot. It sould be mentioned that the compres-
sion/expansion distortion mentioned above is still present in
these plots as the GLPR had not yet been modified to deal with
non-uniform data sets.

37

	1	2	3	4	5	6	7	8	9	10	11	12	13	14	15	16	17	18	19	20
A				0.4	0.9	0.4	1.1	0.2	1.8	3.0	2.3	2.6	2.6	3.4	4.4	2.0	2.05			
B			0.8		1.1		1.9		2.2		2.5		1.5		7.2		0.8			
D			0.4		0.6		1.1		1.5		1.1		3.1		1.1		1.7			
F	1.7		0.9		1.0		1.2		1.5		2.1		3.0		2.0		1.5		1.0	
H	1.5		0.4		0.8		2.0		1.7		1.5		2.6		3.0		3.5		1.5	
K	1.0		1.9		1.3		2.0		0.7		0.4		1.0		3.5		1.6		1.5	
V																3.6	3.0	1.8	1.0	
Y																1.4	0.7	0.7	0.6	
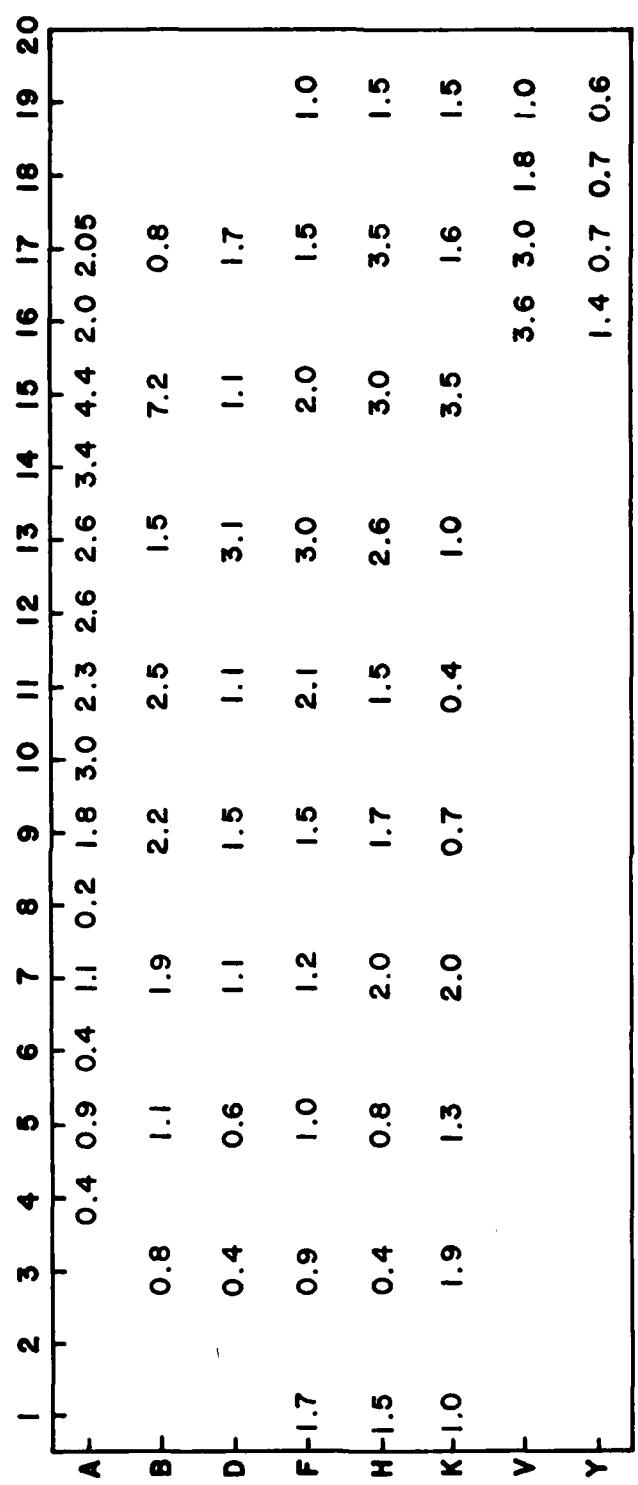
Figure 20. Approximate Maximum Signal Amplitude (Peak-to-Peak) In 30-40 ns. Window for Curtis Schoolyard Data.

38
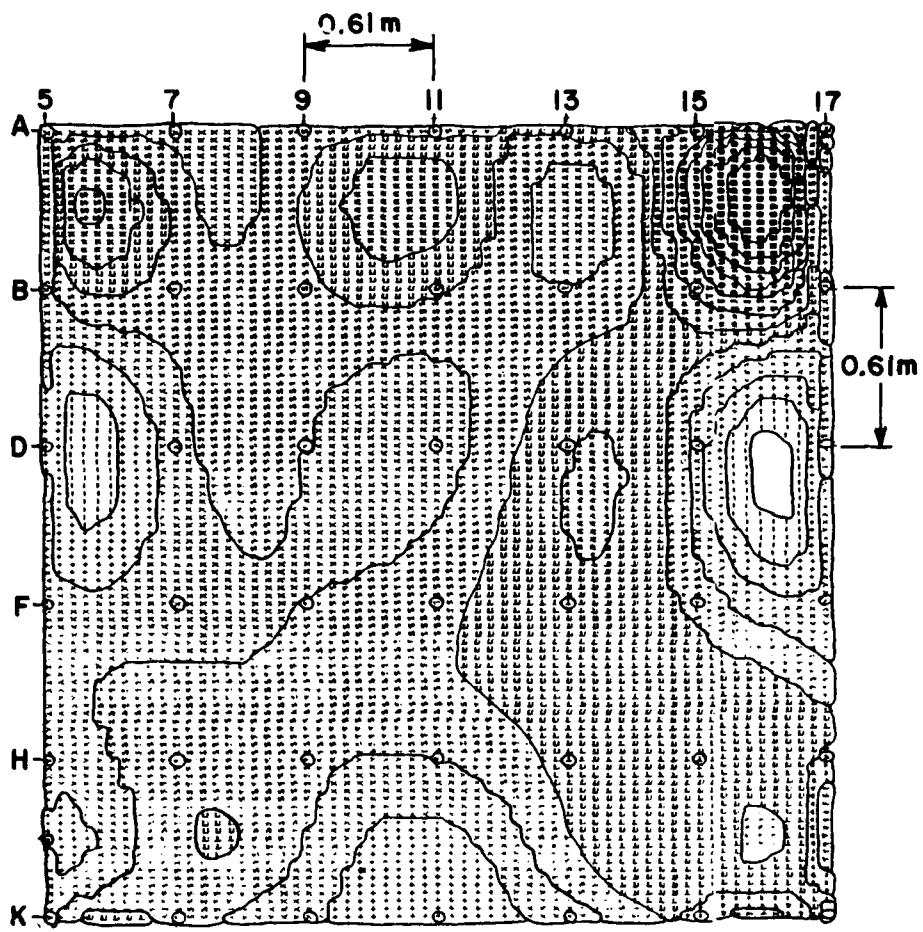
Terrascan Antenna   No Clipping
NXDIV=19 NYDIV=9   Fold First
LIX=6   LIY=7   RMS Window: 30-40 ns.

Figure 21. Curtis School Site   Plan View.

Terrascan Antenna   No Clipping
NXDIV=19   NYDIV=9   Fold First
LIX=3   LIY=3   RMS Window: 0-19.5 ns.
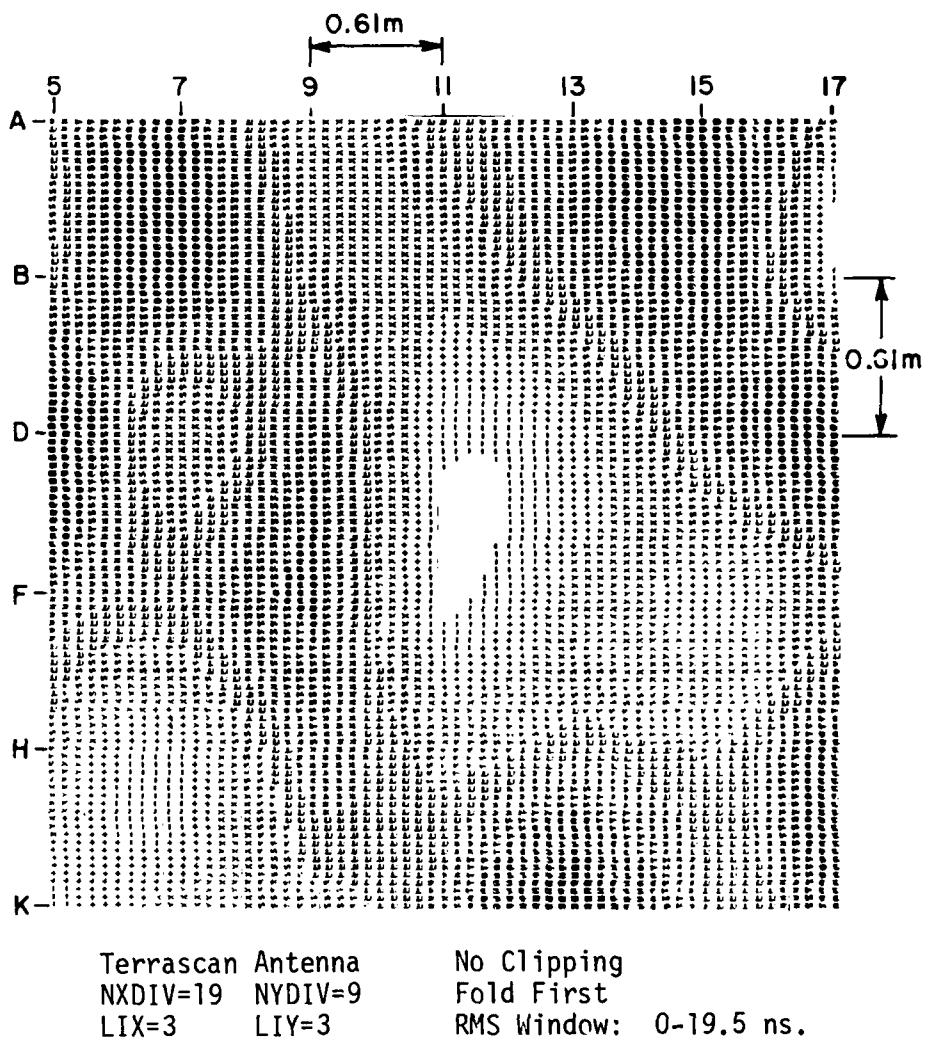
Figure 22.   Curtis School Site   Plan View.

Terrascan Antenna   No Clipping
NXDIV=19 NYDIV=9   Fold First
LIX=3   LIY=3   RMS Window: 10.2-29.3 ns.
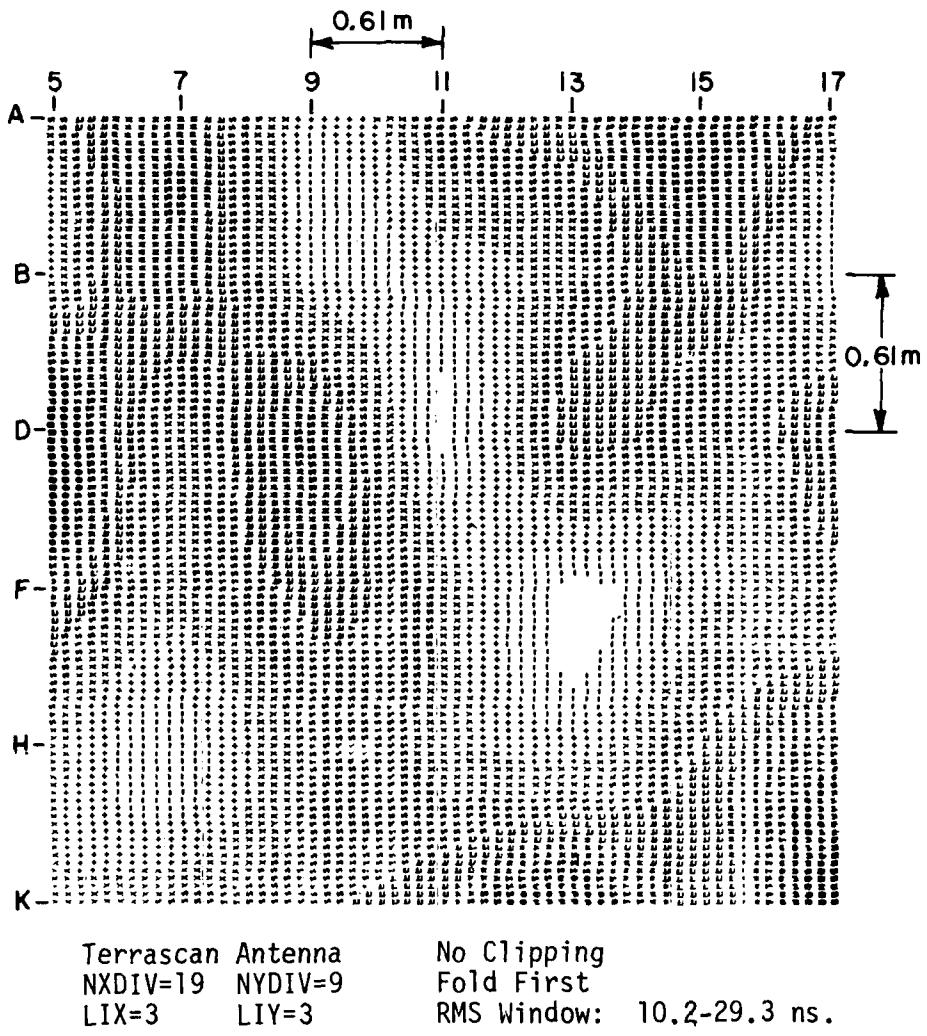
Figure 23. Curtis School Site   Plan View.
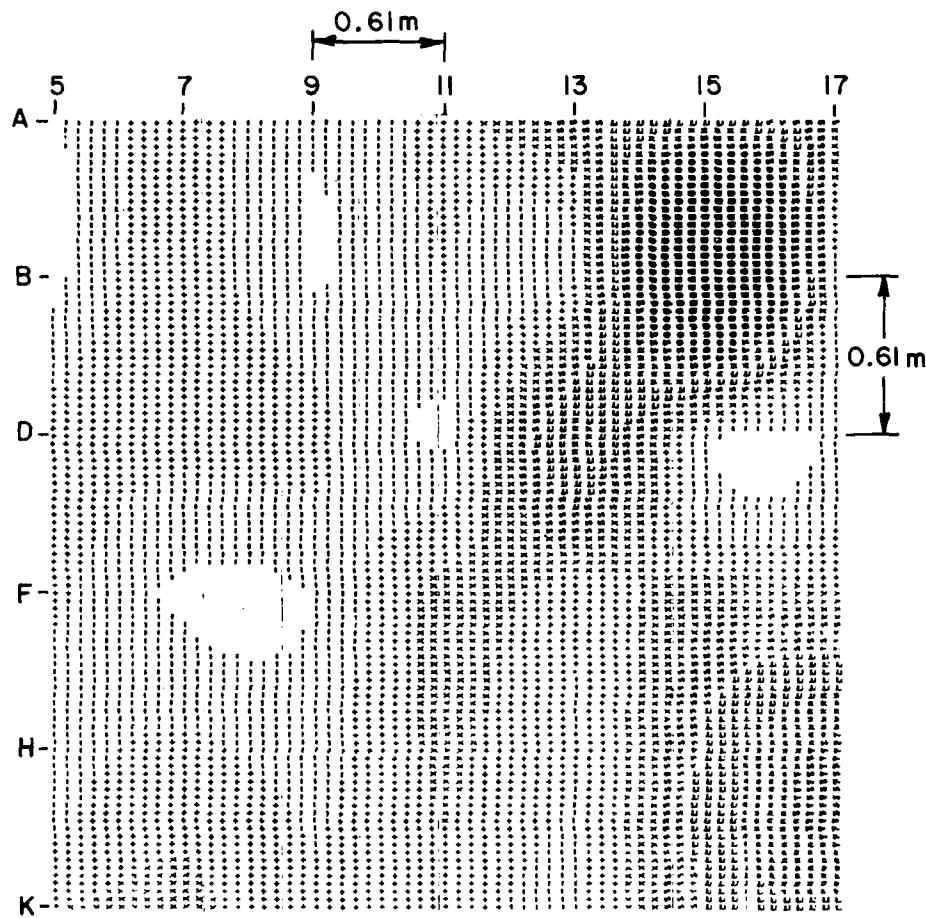
Terrascan Antenna   No Clipping
NXDIV=19 NYDIV=9   Fold First
LIX=3   LIY=3   RMS Window: 19.9-39.1 ns.

Figure 24.   Curtis School Site   Plan View.
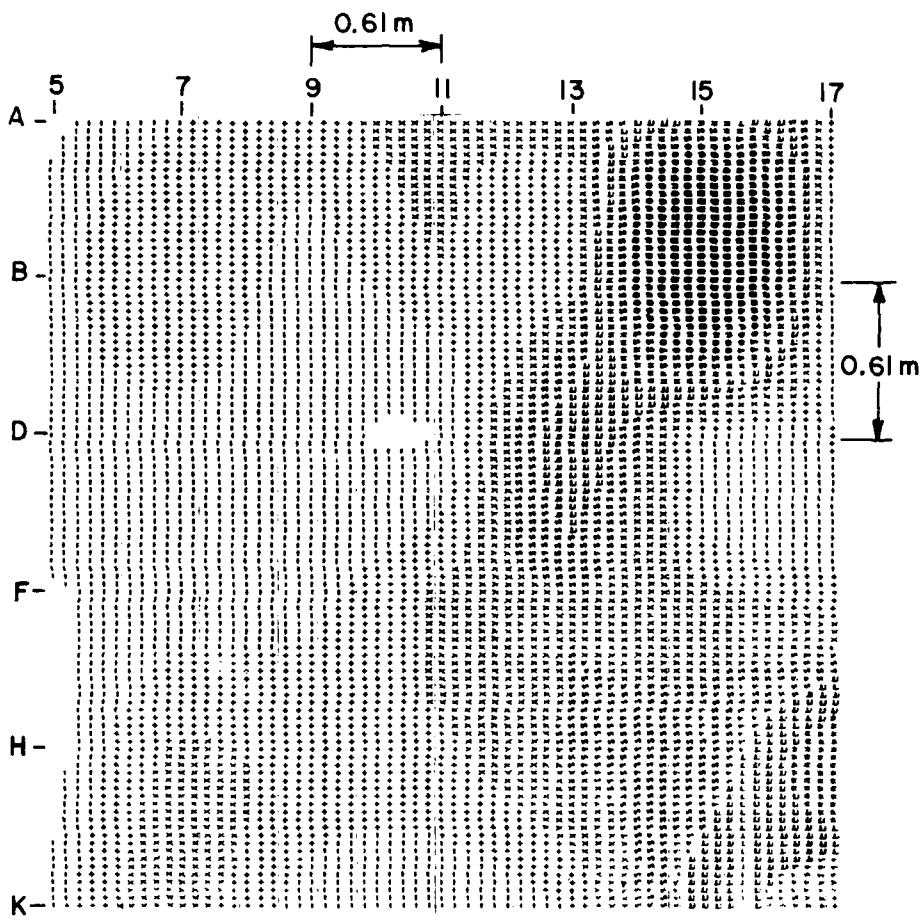
```
Terrascan Antenna        No Clipping
NXDIV=19  NYDIV=9        Fold First
LIX=3     LIY=3          RMS Window:  29.7-48.8 ns.
```

Figure 25. Curtis School Site   Plan View.
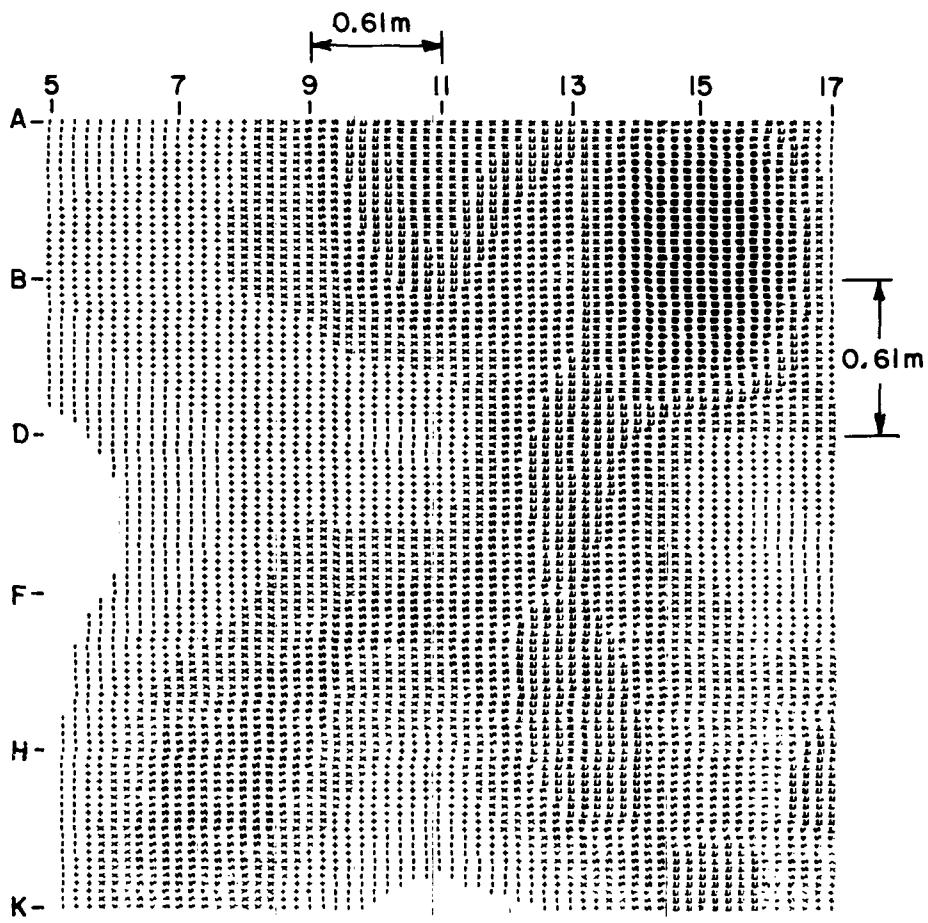
43

Terrascan Antenna   No Clipping
NXDIV=19 NYDIV=9   Fold First
LIX=3   LIY=3   RMS Window: 39.5-58.6 ns.

Figure 26. Curtis School Site   Plan View.
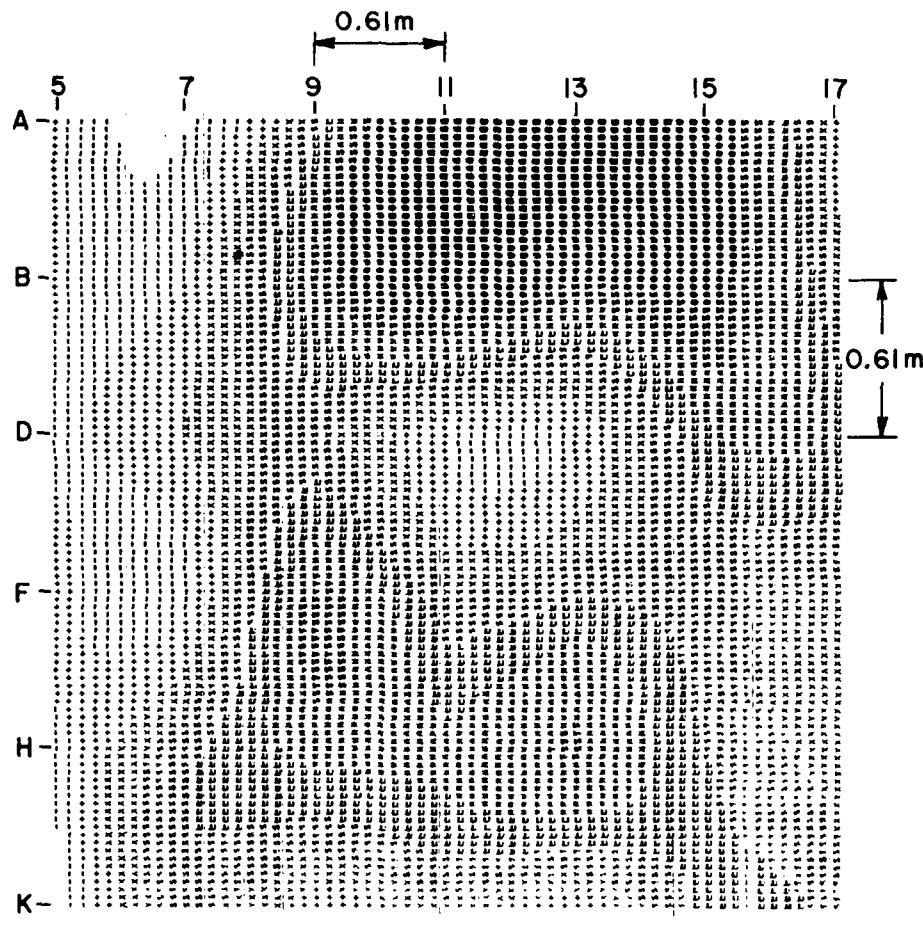
Terrascan Antenna   No Clipping
NXDIV=19 NYDIV=9   Fold First
LIX=3   LIY=3   RMS Window: 49.2-68.4 ns.

Figure 27. Curtis School Site   Plan View.
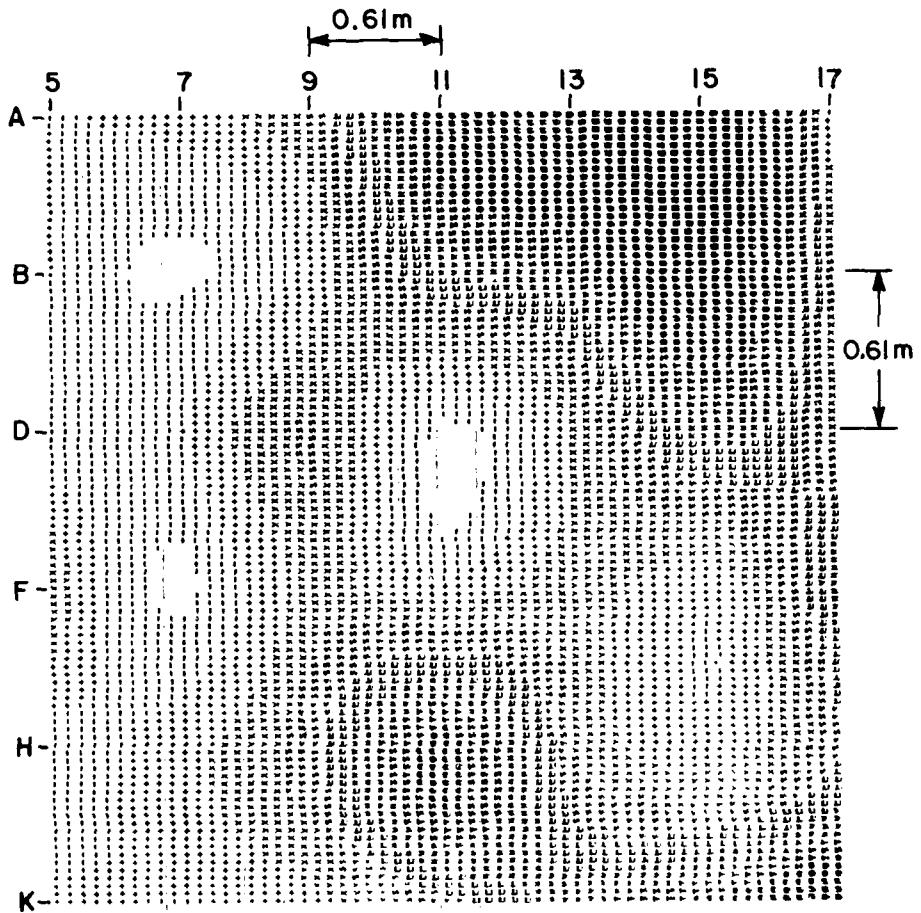
Terrascan Antenna   No Clipping
NXDIV=19   NYDIV=9   Fold First
LIX=3   LIY=3   RMS Window: 59-78.1 ns.

Figure 28. Curtis School Site   Plan View.
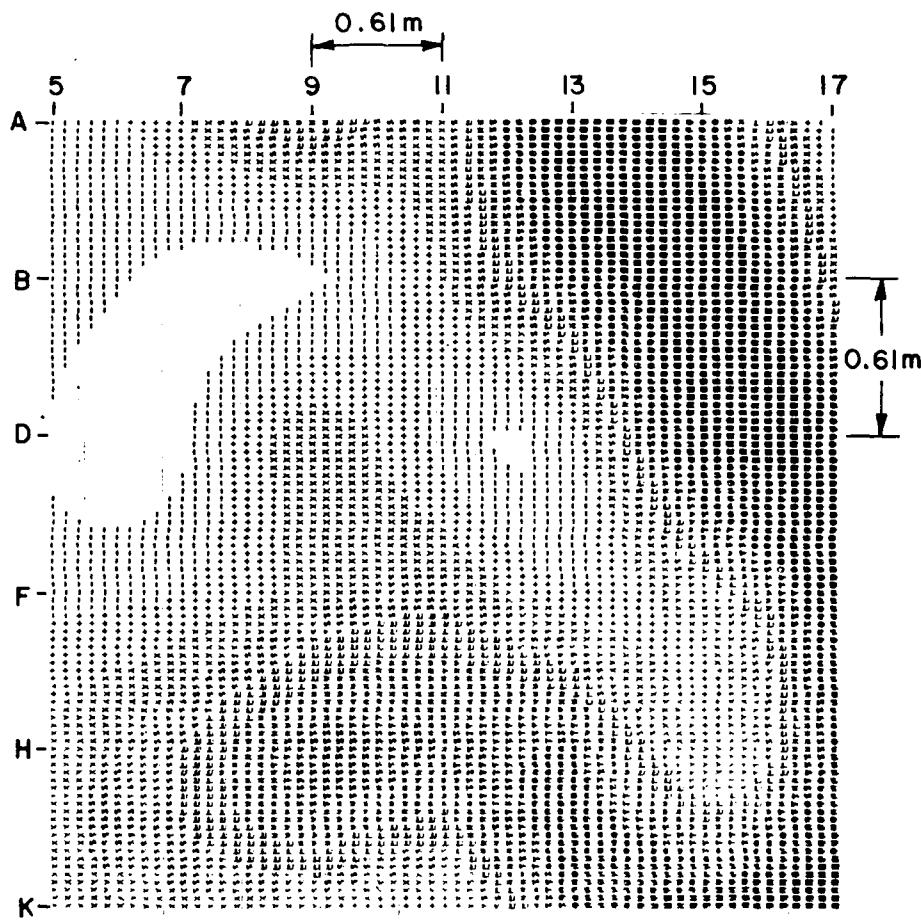
```
Terrascan  Antenna        No Clipping
NXDIV=19   NYDIV=9         Fold First
LIX=3      LIY=3           RMS Window:  68.8-87.9 ns.
```

Figure 29. Curtis School Site   Plan View.
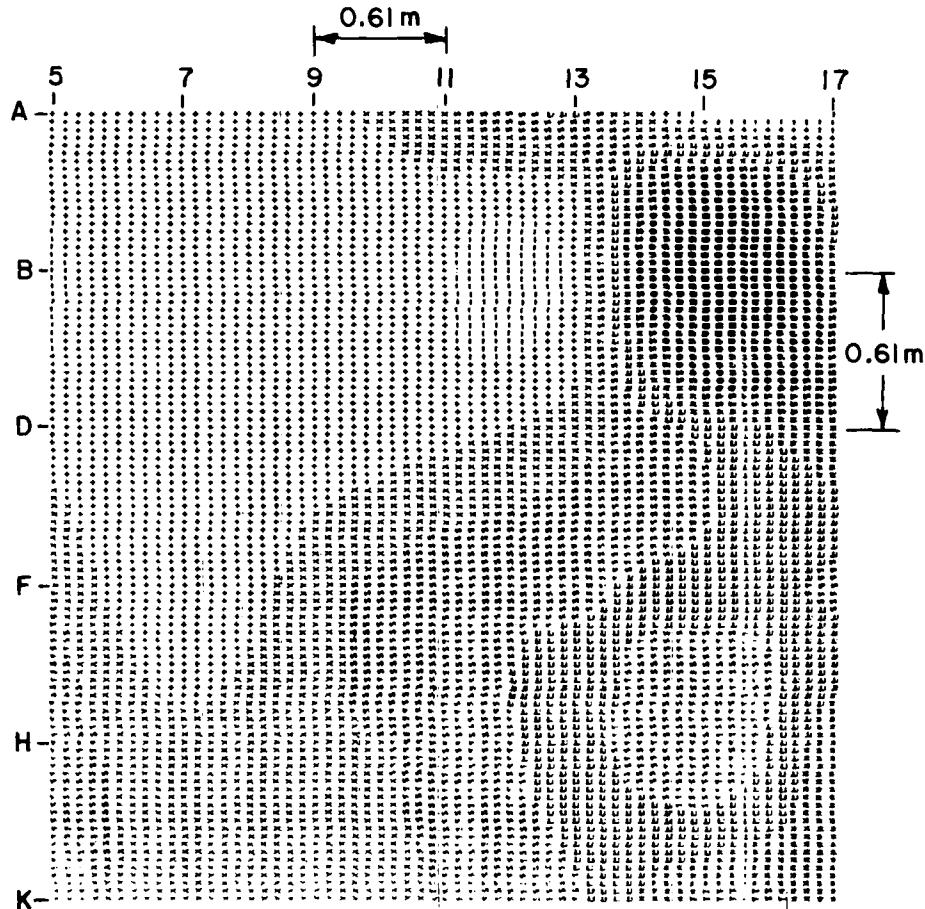
Figure 30. Curtis School Site   Plan View.

Looking at the plots, it is apparent that the area of interest
in all (except plots for 0-19.5 ns and 10.2-29.3 ns) is the upper
right corner. This corresponds to the area around position A15
in Figure 18. Of particular note is the plot for 68.8-87.9 ns
where quite linear edges are present, indicating the possible
presence of a tunnel at this depth.

A rough estimate of the ground permittivity in the area is
$6 \leq \epsilon_r \leq 9$. Using $\epsilon_r = 7.5$ we find that a delay of 69 ns corre-
sponds to a depth of 3.7 m and a delay of 88 ns to a depth of
4.9 m. This agrees with the distance to the floor of the tunnel
of 3.7 m as determined by drilling. The top of the tunnel was
at 2.4 m, corresponding to 44 ns. Examining the grey plots containing
this depth (29.7-48.8 ns and 38.5-58.6 ns) we note strong signal
returns in the A15 position, but these are visible in other plots
also. It appears that the tunnel response is contained in this
data. However, many other features are also present. We believe
that this clutter is caused by inhomogenities in the tunnel over-
burden due to changes in water flow during the nearly 100 years
the tunnel has been in existence. Figure 19 shows the large signal
returns that occur at these shallow depths. It was these large
returns that initially motivated mapping of this area.

Figure 31 shows the grey level distributions of the plots
of Figures 22-30. In each plot, the abscissa is the number of
the grey level from 1 (white) to 14 (black) and the ordinate is
the percentage of the total map occupied by that grey level. It
is interesting to note that the grey level plot that showed the
possible presence of a tunnel most clearly (68.8-87.9 ns) is also
that which has a more nearly uniform grey level distribution.

Perhaps the most critical parameter in processing the plan
view type of grey level plot is the choice of window size for RMS
value calculation. If a window is chosen too large, a target
(which usually appears as a ringing in the waveform) could acci-
dentally be removed. On the other hand, a window size too small
may represent a time resolution in excess of the frequency bandwidth
of the radar system used to take the data.

Another form of grey level plot is the cross-sectional view.
The cross-section differs from the plan view in that it is not
usually necessary (or even desirable) to use the RMS windowing
process discussed above. In this type of plot, the vertical axis
consists of a section of the input waveform plotted point-by-point.
An absolute value of the waveform is taken so that both positive
and negative peaks in the signal will appear on the grey level
plot as darkened areas.

Grey Level Distribution of Figure 22.

Grey Level Distribution of Figure 23.

Grey Level Distribution of Figure 24.

Figure 31.

Grey Level Distribution of Figure 25.

Grey Level Distribution of Figure 26.

Grey Level Distribution of Figure 27.

Figure 31 (cont.).

51

Grey Level Distribution of Figure 28.

Grey Level Distribution of Figure 29.

Grey Level Distribution of Figure 30.

Figure 31 (cont.).

52
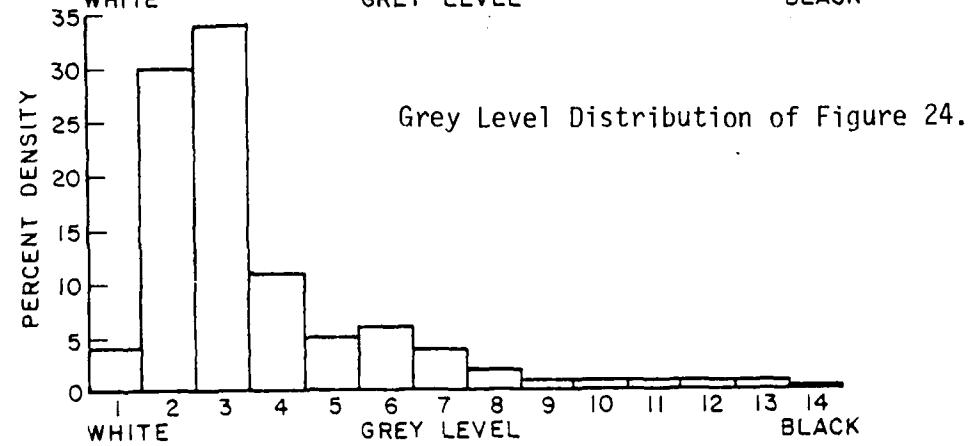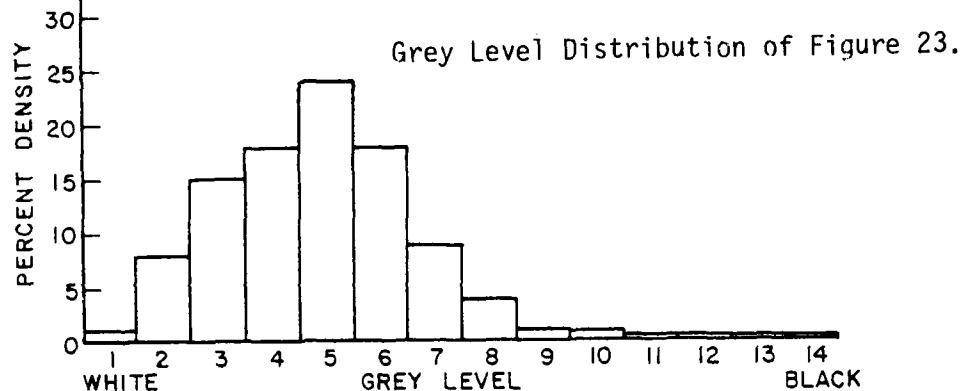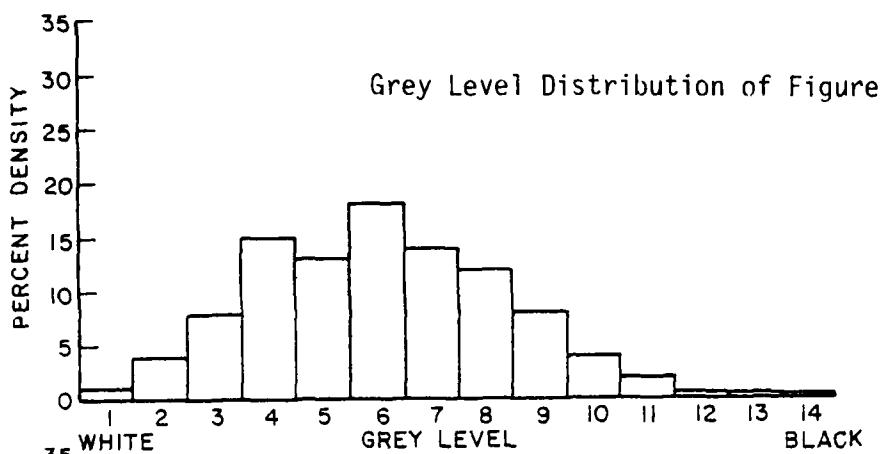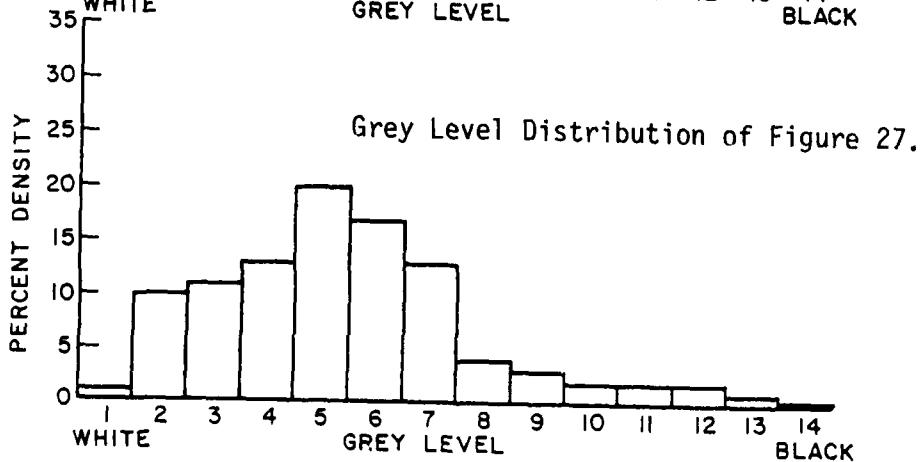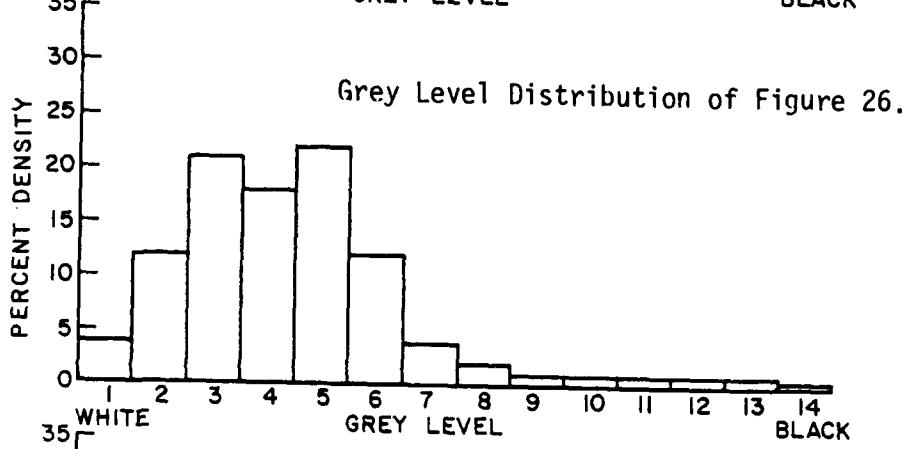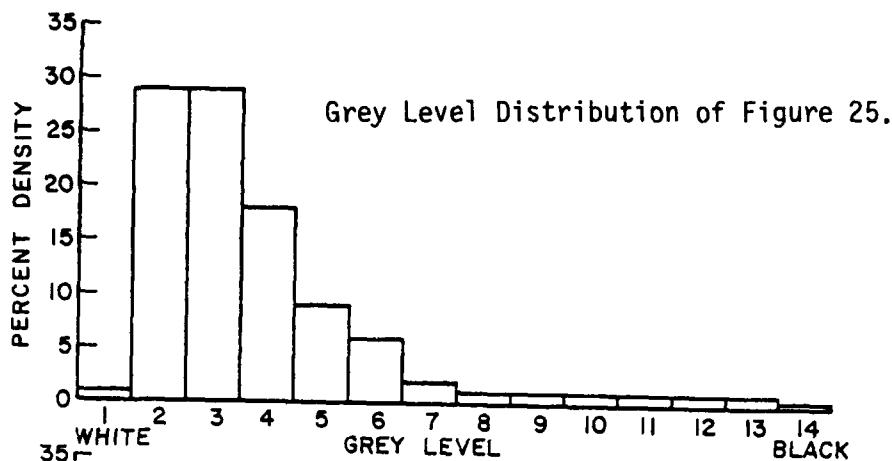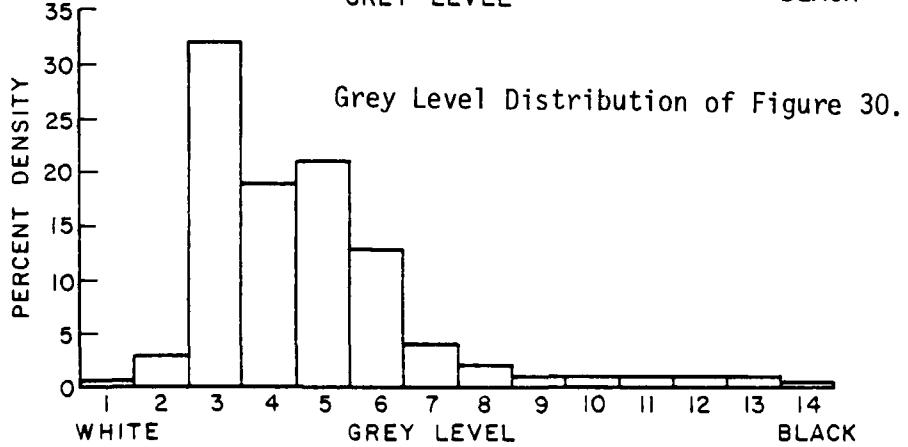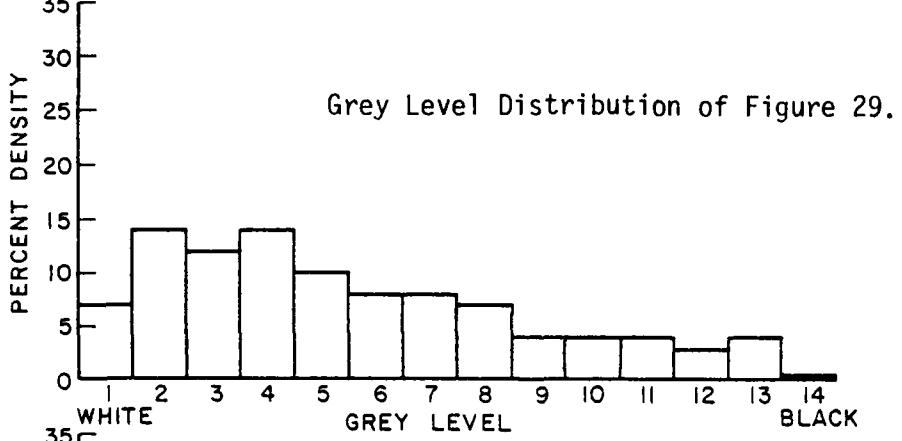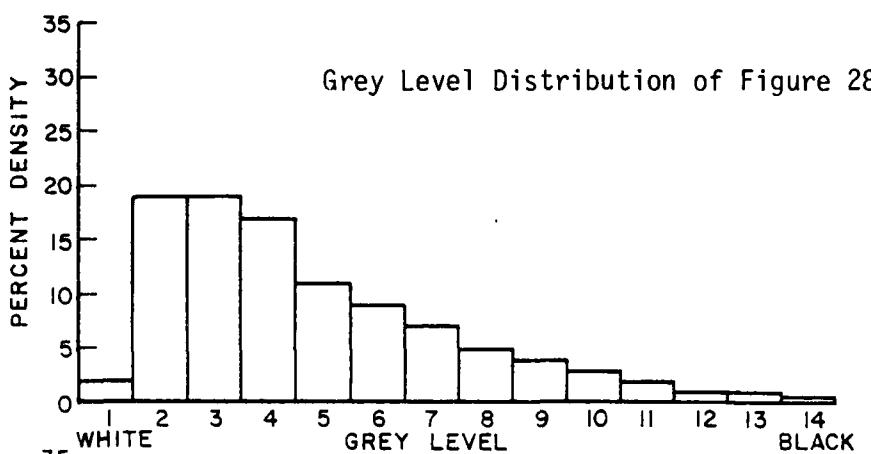
In the cross-section plot the "signature", or shape that a target assumes in the plot is not an actual cross-sectional view of the target itself. As shown in Figure 32, at each point in a linear traverse the distance to the target (in this case a point scatterer) varies as $\ell = \sqrt{x^2 + d^2}$ where ℓ is the distance to the target, d is the depth of the target and x is the horizontal displacement from the position immediately over the target. At each measurement point off-axis from the target, its apparent depth is ℓ. It is at a position corresponding to ℓ in each radar return that the target echo will appear. If these distances, ℓ, are "straightened out" as shown in the lower portion of Figure 32 it can be seen that the position of the target echo traces out a hyperbola. In general then, the type of signature that we are looking for in a cross-sectional view is a hyperbolic curve.

To verify this concept, waveforms calculated by Davis [4] were grey level plotted. Each waveform was derived from a moment-method calculation of the backscatter from a circular cylinder of $\epsilon_r = 1$ immersed in a homogeneous medium of $\epsilon_r = 9$ and $\sigma = 0.01$. The depth to the center of the cylinder was 2.745 m. Nine waveforms were calculated using horizontal offsets from the tunnel ranging from 0 to 2.44 m (i.e., 0.305 m spacing between waveforms). Figure 33 shows a typical waveform from this group.

The resulting grey level plot is shown in Figure 34. To generate this plot, waveforms offset to one side were duplicated on the other side of the cylinder to simulate a traverse over a tunnel. As expected, a hyperbolic shape appears, accompanied by a train of echoes.

To check the possible distortion of the hyperbolic signature by sparse sampling (i.e., too few antenna positions) the above data was re-processed using fewer waveforms. Figure 35 shows the result of using only 5 of the original 9 waveforms and Figure 36 uses only 3. Note in particular the increase in background level in these plots and the widening of the hyperbola.

Returning to experimental data, Figure 37 shows a cross-sectional view derived from one linear traverse of the Curtis School data. This data set consisted of a group of 31 waveforms taken along the H coordinate of Figure 18. Measurements were taken at column positions -5 to 25. The time span of each waveform was 200 ns.

Note that traces of hyperbolic arcs are apparent in this plot, mostly centered about the 17 position on the horizontal axis. The vertical repetition of the arcs is a possible indication of multiple signal reflections inside the tunnel, as discussed earlier.

53
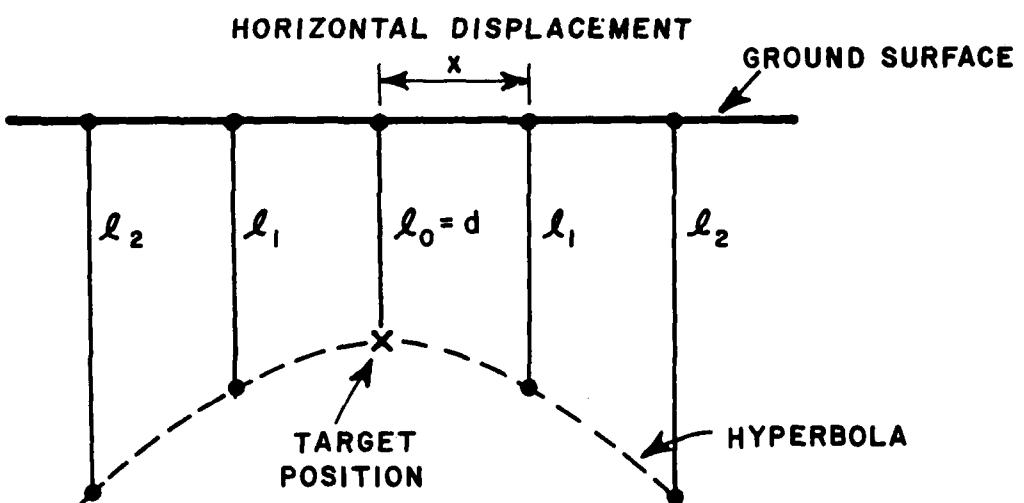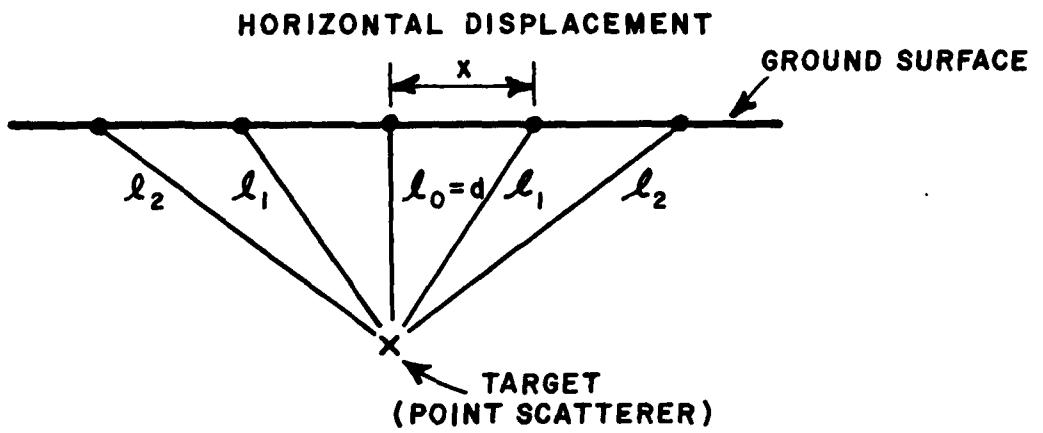
Figure 32. Derivation of Target Signature in Cross Section.

10 ns

5 mV FOR 100 V
GAUSSIAN
PULSE INPUT
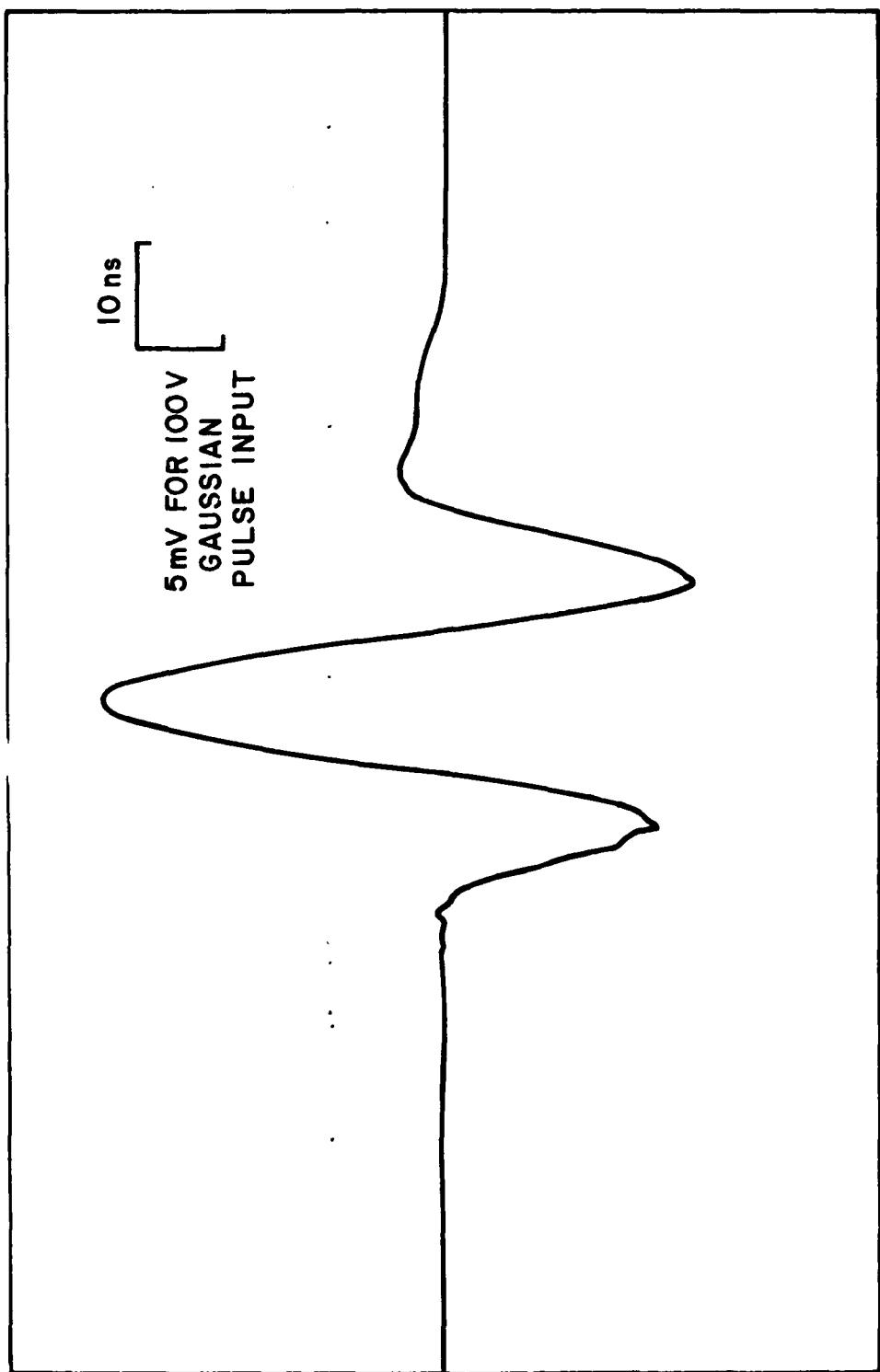
Figure 33.   Calculated Received Waveform.
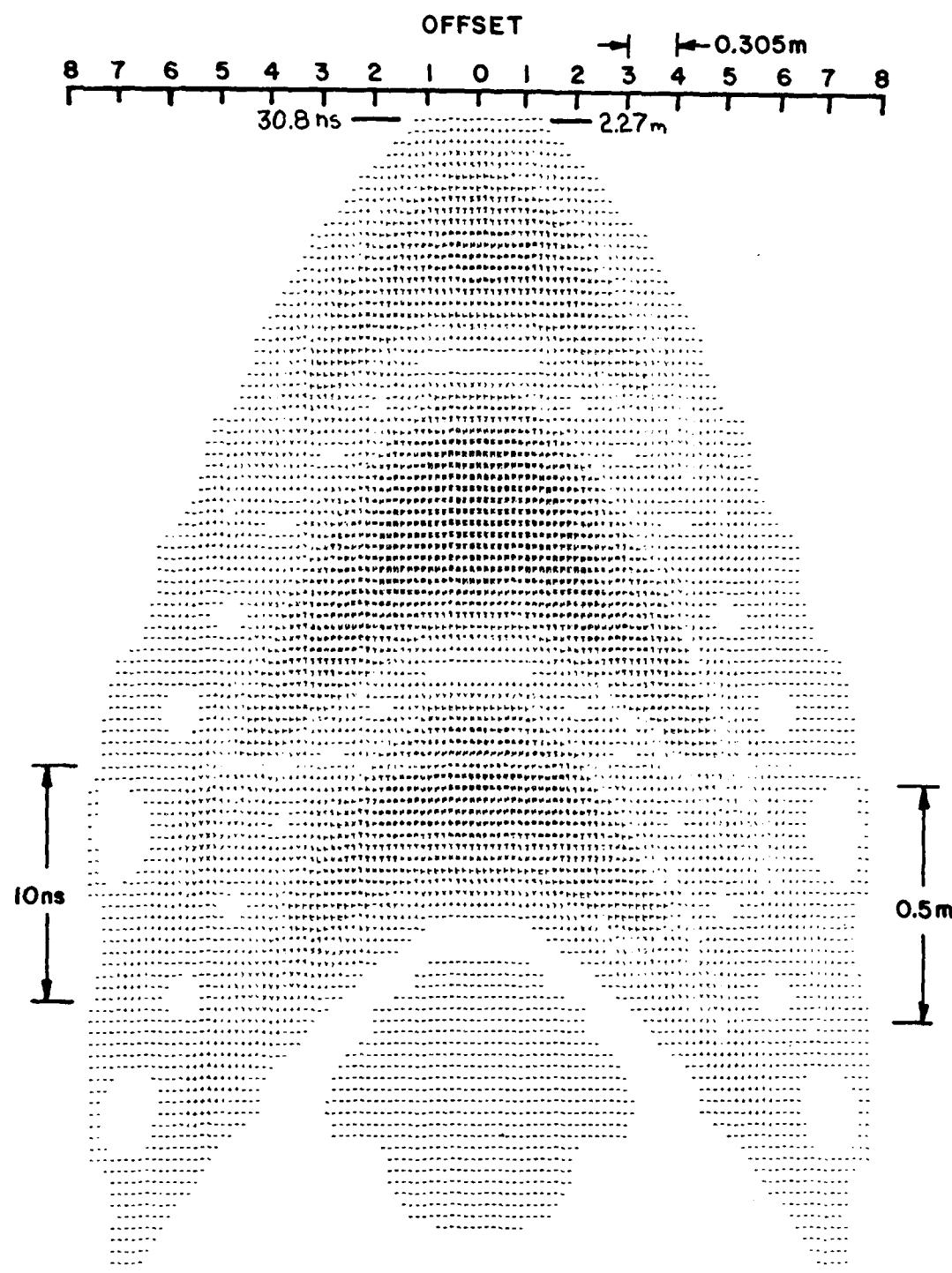
Figure 34. Moment Method Datas Cross Section.

56
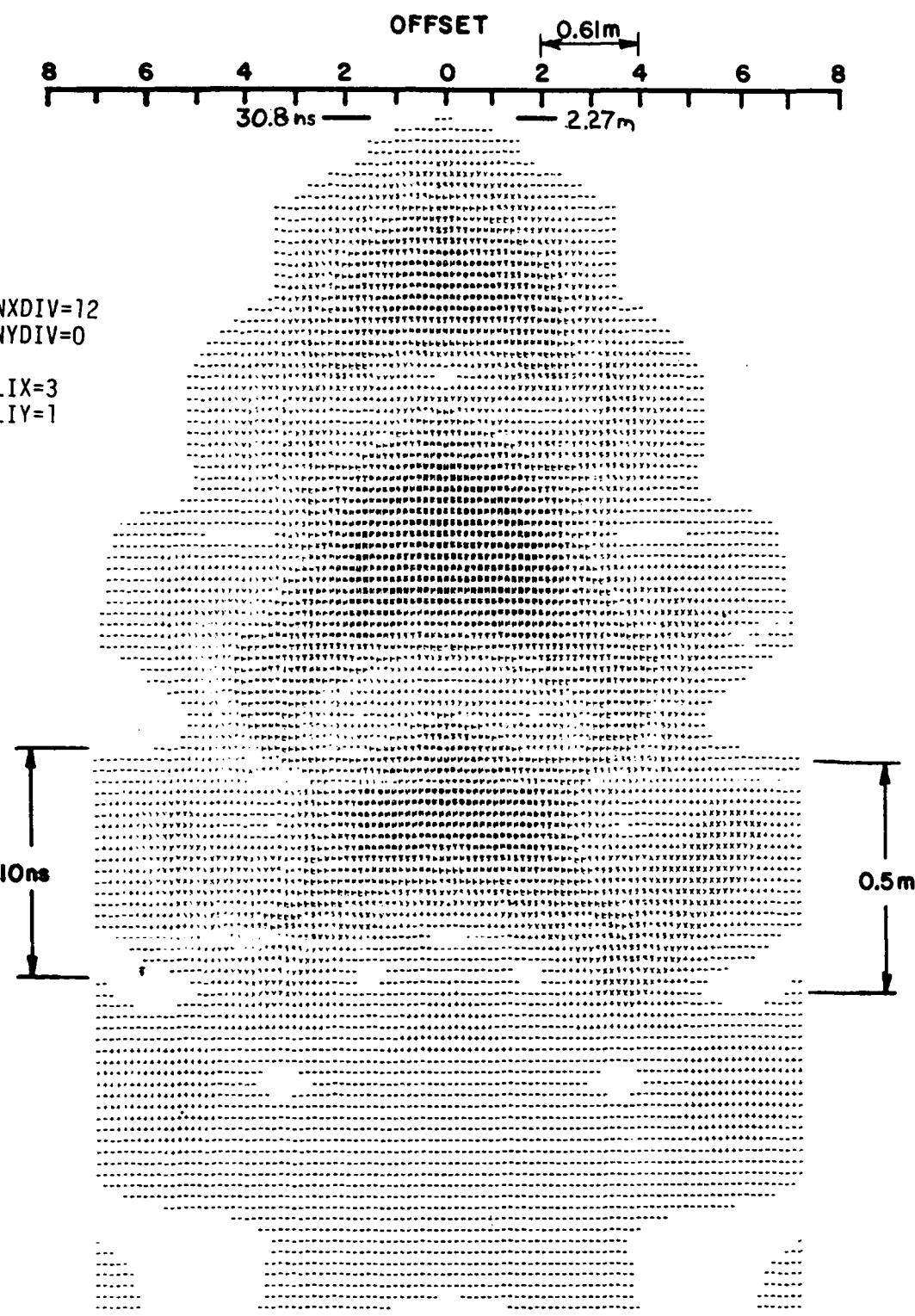
Folded Dipole   No Clipping   Fold First   Using 9 Waveforms
Figure 35.   Moment Method Data   Cross Section.

57

OFFSET

1.22m

8   4   0   4   8

28.9 ns —   — 2.12m

10ns   0.5m
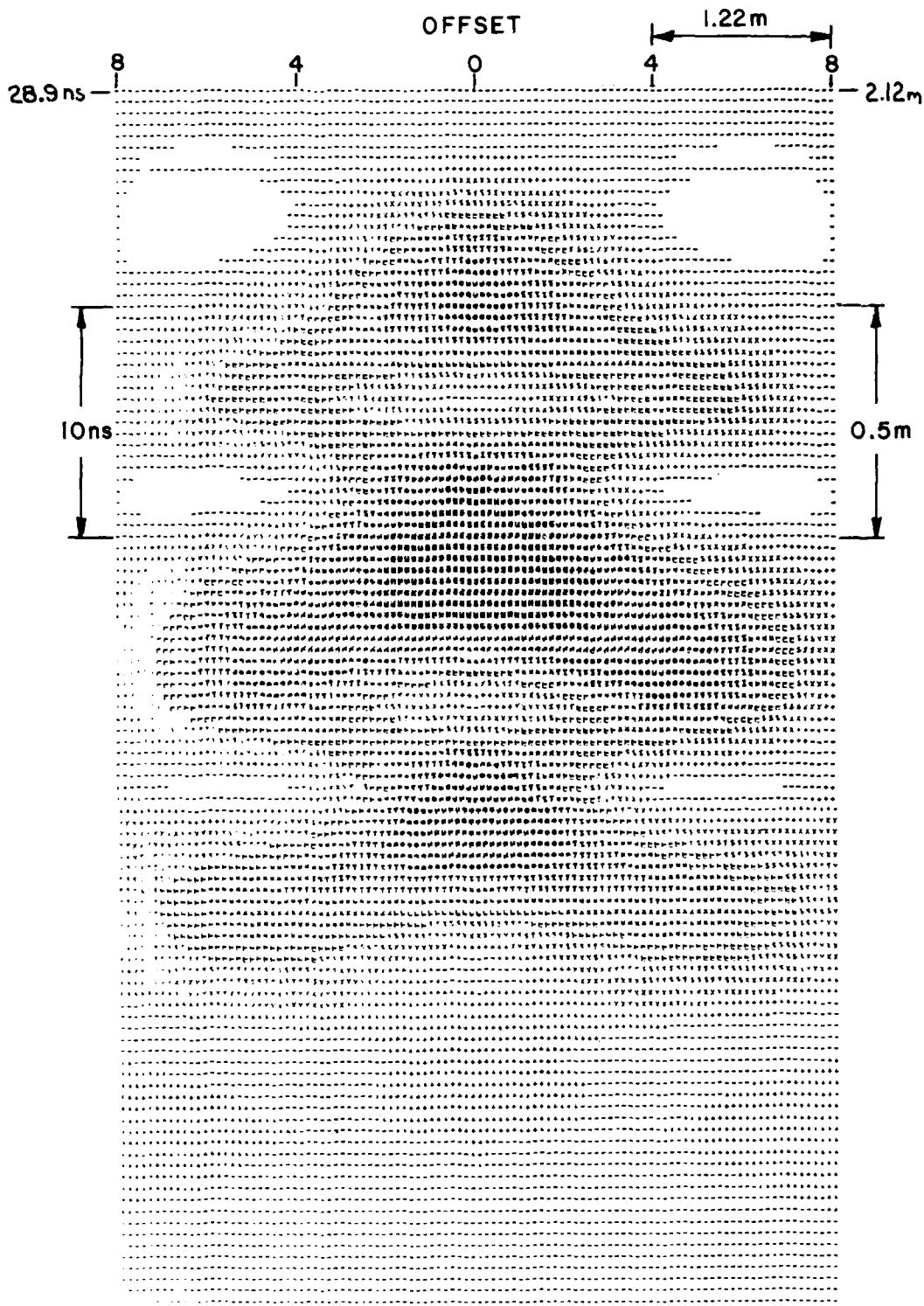
NXDIV=25   NYDIV=0
LIX=3   LIY=1

Folded Dipole   No Clipping   Fold First   Using 5 Waveforms
Figure 36.   Moment Method Data   Cross Section.

58
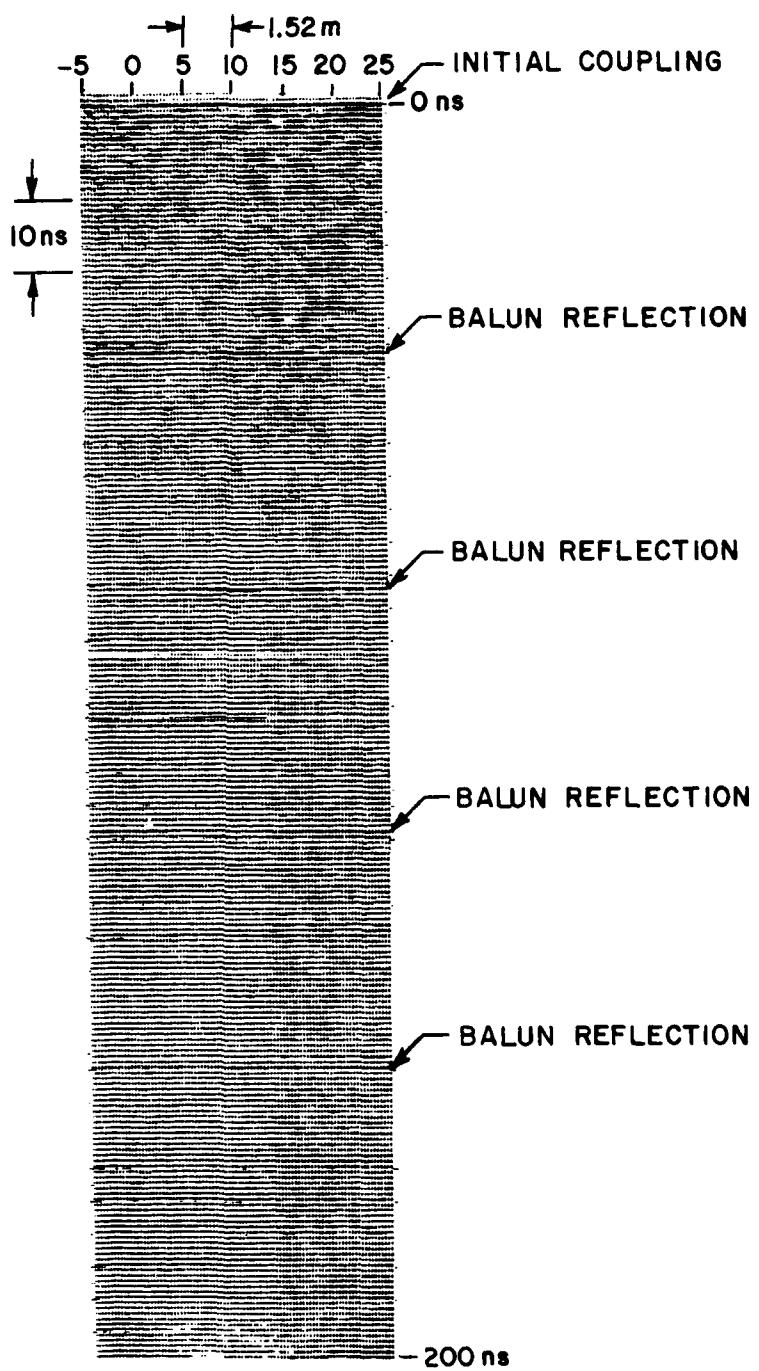
Figure 37. Curtis School Site   Cross Section.

59

The dark line running horizontally across the plot at the
top (labeled "initial coupling") is the coupling signal between
the transmit and receive arms of the antenna and may be used as
a time reference to locate the surface of the ground. The other
horizontal dark lines are caused by reflections from the balun
transformer in the antenna. That is, part of the transmitted pulse
is reflected at the antenna terminals and travels back to be reflected
again at the balun. This is in essence a second transmitted pulse.
These multiple balun reflections then result in the multiple dark
lines seen in the plot. The presence of hyperbolic arcs at a
shallow depth could again be caused by the disturbance of drainage
by the tunnel.

Another site from which data was processed is the Hazel A
mine in Gold Hill, Colorado. This is a former gold mine dug straight
into the side of a mountain. Measurements were taken in a large
grid on this slope according to the scheme shown in Figure 38.

Measurements were taken first using a 6 ns pulser and a
Terrascan antenna redesigned for deep probing. As stated in Chapter
I, the modification consisted chiefly of moving the balun transformer
closer to the antenna terminals to obtain a selected range window
free from balun reflections. Later measurements were taken using
an antenna designed specifically for the type of target found at
Gold Hill. Transmission experiments between the tunnel and the
surface indicated a relative permittivity of approximately 6 for
this site.

First, a plan view of the area was plotted. The depth of
the tunnel throughout this map was between 2.75 and 3.32 m (see
Figure 38). For a midrange value of 3.02 m we calculate the position
of the tunnel echo in the waveforms to be about (3.02 m)/(0.0612
m/ns) $\approx$ 49 ns (not taking into account the lateral distance from
the tunnel). The tunnel depth span of 3.32-2.75 = 0.57 m translates
to a time span of 9.3 ns.

Thus, we choose a time window for RMS value calculation of
approximately 20 ns centered at the 49 ns point on the 100 ns wave-
forms. This corresponds to a depth range of 2.41 to 3.59 m. Figure
39 shows the plan view.

Since contrast is very low in this plot, clipping (see
Chapter III) is used to raise the contour out of the background
(Figures 40 and 41). We expect to see a dark form running from
left to right centered about the 10 coordinate but this is only
partially visible. It is puzzling that a similar shape occurs
centered at the 5 coordinate also. Compounding this problem, we
note that in Figure 42 which shows a plan view at a greater depth
(59-78.2 ns or approximately 3.61-4.78 m) that a similar large
dark area appears. This is perhaps a multiple reflection from
the tunnel.

60
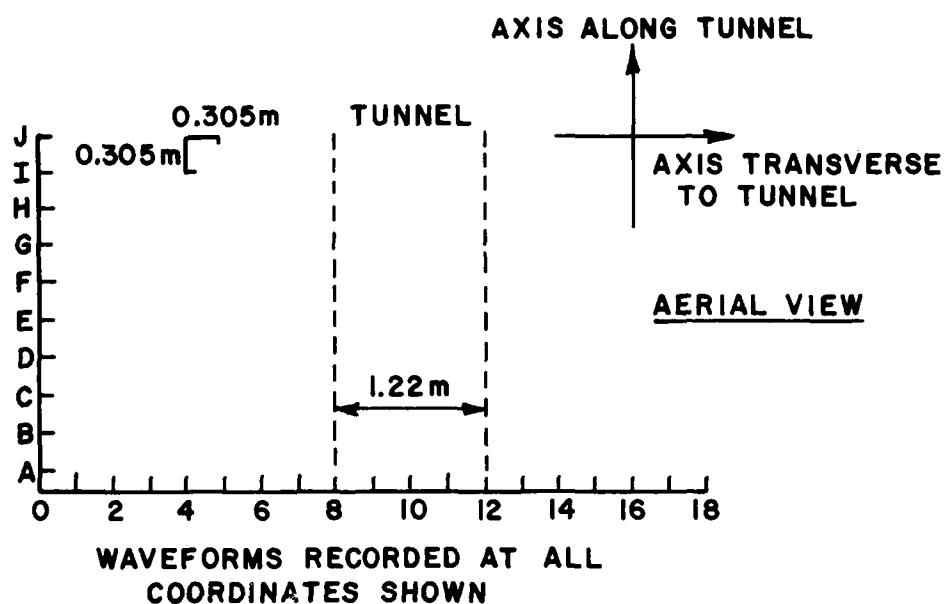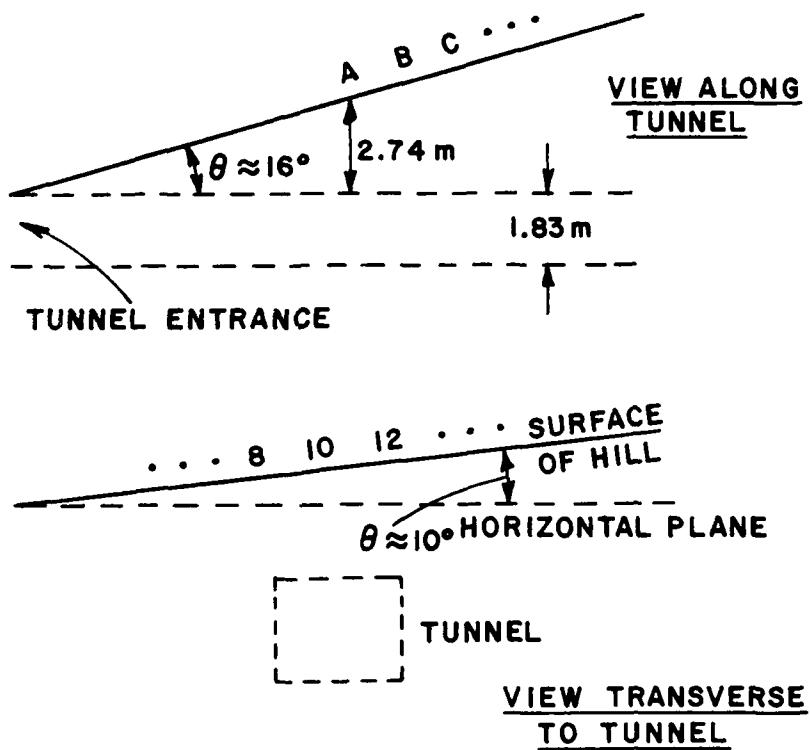
Figure 38. Geometry of Gold Hill Map 1 Site.

Figure 39. Gold Hill Map 1 Plan View

0.305 m

0.305 m

NXDIV=9
NYDIV=5

LIX=3
LIY=3

TUNNEL
WIDTH

Clipped at
1.3 Fold
First
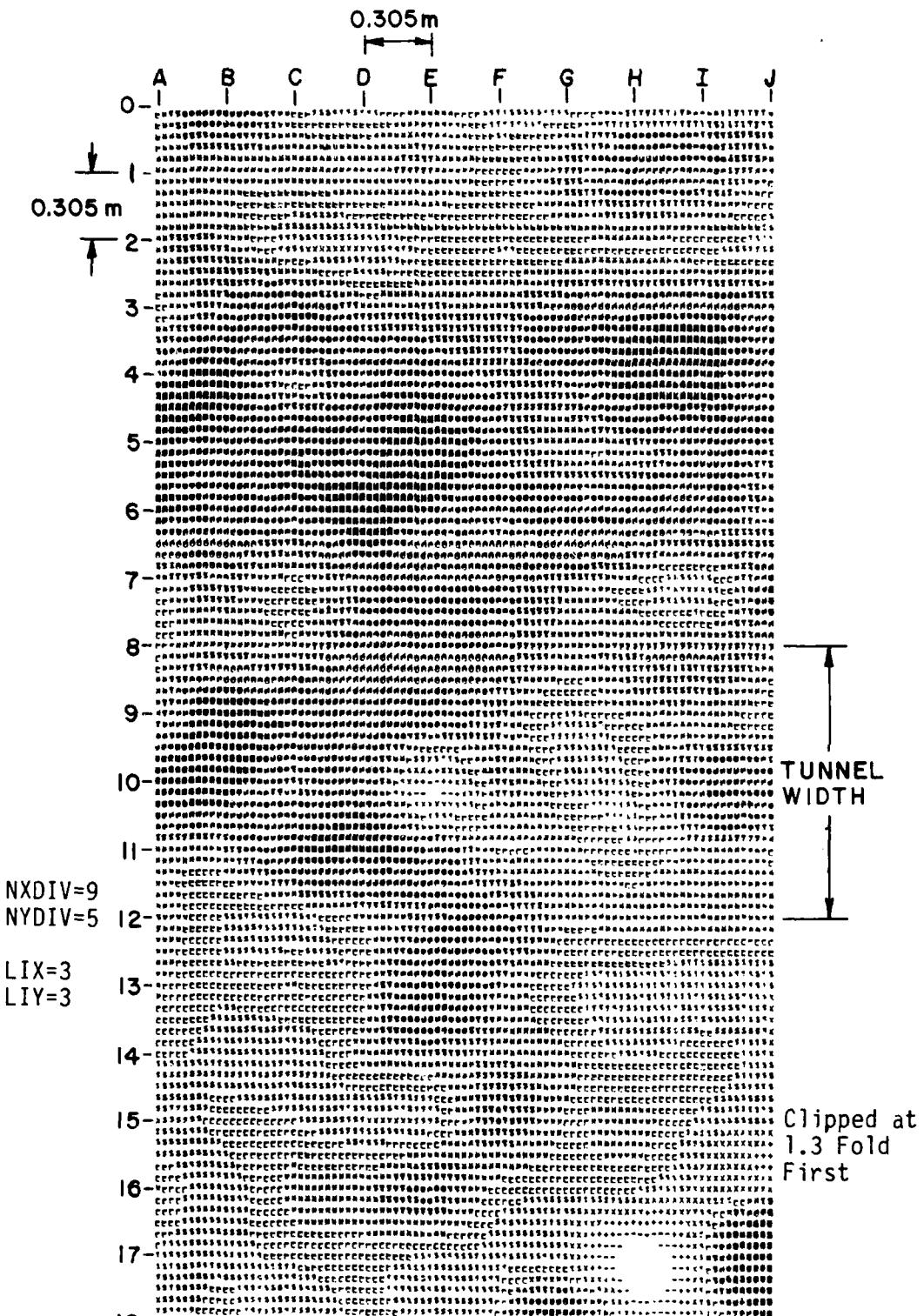
Modified Terrascan Antenna   RMS Window: 39.5-58.6 ns.
Figure 40.   Gold Hill Map 1   Plan View

63
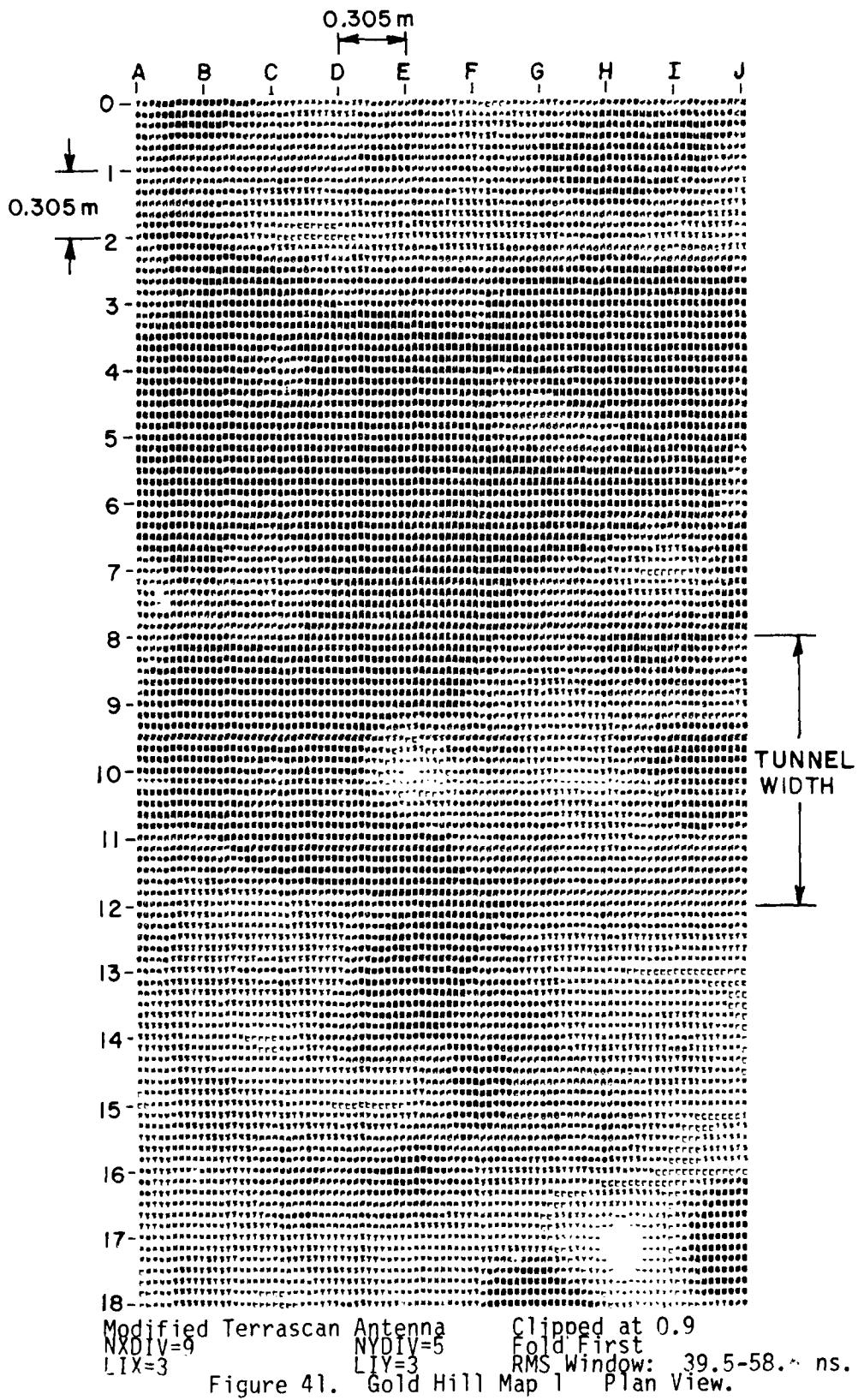
Figure 41. Gold Hill Map 1 Plan View.

Modified Terrascan Antenna   Clipped at 0.9
NXDIV=9   NYDIV=5   Fold First
LIX=3   LIY=3   RMS Window: 39.5-58. ns.

0.305 m

0.305 m

A B C D E F G H I J

NXDIV=9
NYDIV=5

LIX=3
LIY=5

TUNNEL
WIDTH

Clipped at
0.55 Fold
First

Modified Terrascan Antenna   RMS Window: 59-78.1 ns.
Figure 42.   Gold Hill Map 1   Plan View
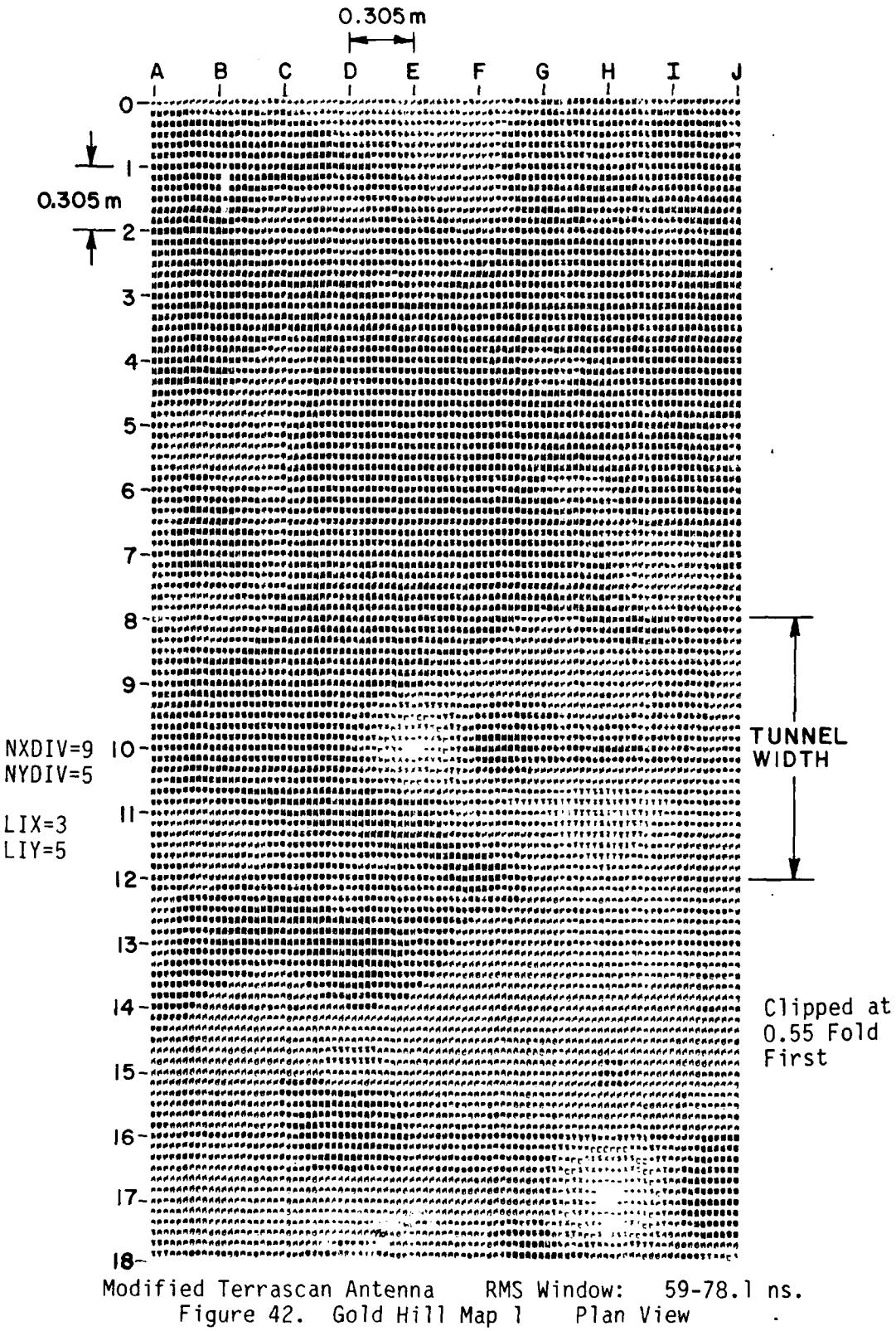
We observe at this time that the data taken with the Terrascan antenna has extremely high clutter levels. It is anticipated that further processing of this data will reduce the clutter level. Later results using the long box antenna will show substantial improvement in this area.

Following a different approach, we next plot a cross-sectional view using only the waveforms in a straight-line traverse directly over the tunnel (i.e., waveforms with coordinate 10 in Figure 38). This is shown in Figure 43. The expected form of this plot would be a dark area spanning the plot from left to right (i.e., along the tunnel) and perhaps dropping towards the right because of the greater depth of the tunnel as we travel uphill. This type of signature is apparent in two places in the figure. The first position is almost exactly where the tunnel location was calculated and the second somewhat higher than the roof of the tunnel. This implies that discontinuities caused by water flow and fracturing during tunnel construction are the source of such signals.

The next step was to again plot cross-sections of the data but using lateral traverses across the tunnel instead of along it. This form of plot would possibly exhibit the hyperbolic form discussed earlier. Figures 44-50 show this type of plot for traverses along the C,D,E,F,G,H, and I coordinates (from 0 to 18) shown in Figure 38.

On these plots, the arrow with a "T" beside it indicates the center of the tunnel and the given tunnel depth shows the height of the tunnel at its center. A consistent dark area occurs in these plots in the general region of the tunnel (spanning 8-12 on the horizontal scale). This dark area is not contained in other regions of the plots as the depth approaches that of the tunnel. In general, this shape appears before the expected time of arrival of the tunnel echo. Note the continuing presence of shallow clutter in these plots.

These plots include an enhancement to the GLPR. In previous plots, folding (absolute value) was done about the zero volt line as shown in Figure 51. While in most circumstances this would not adversely affect the grey level plot, it can be seen in Figure 51 that if the waveform is offset from the zero-volt level, distortion of the peaks can occur, as well as the addition of an annoying "background" grey level. To remedy this, the folding process was changed to fold instead about the mean of the waveform. As shown at the bottom of Figure 51 this results in true representation of peaks and elimination of the background grey level.

66
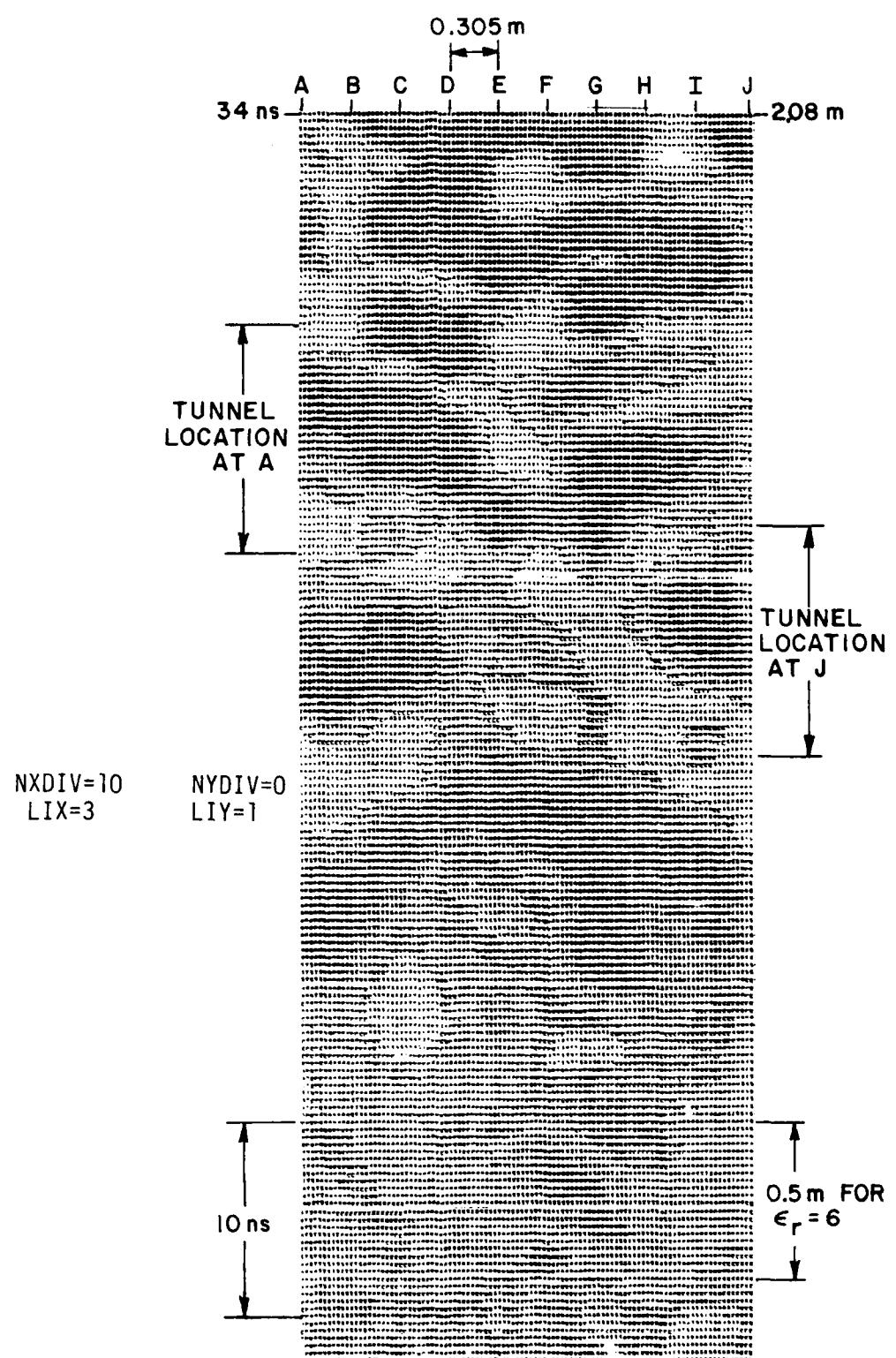
Figure 43.   Gold Hill Map 1 Traverse 10   Cross Section.
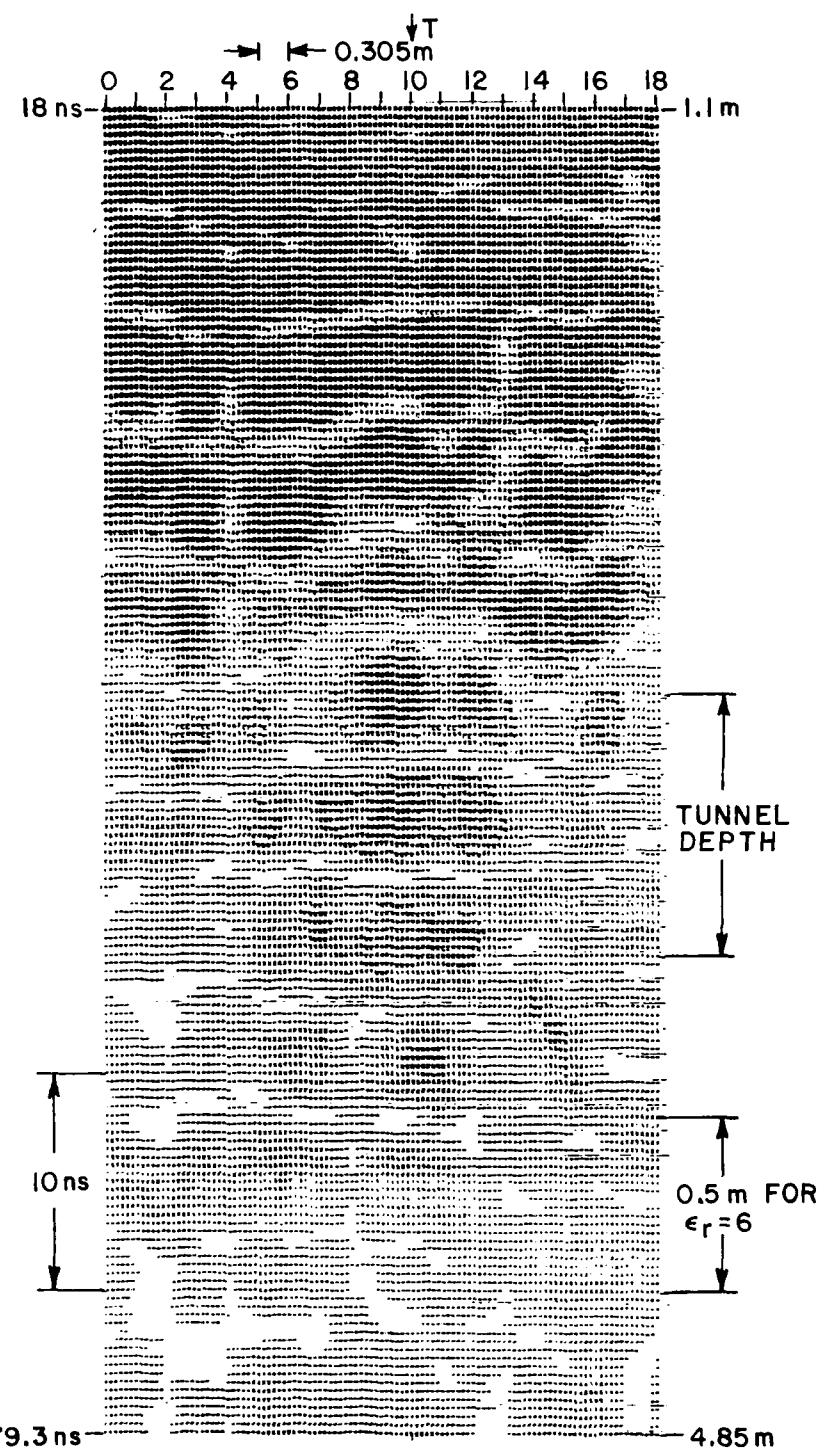
Figure 44. Gold Hill Map 1 Traverse C   Cross Section.
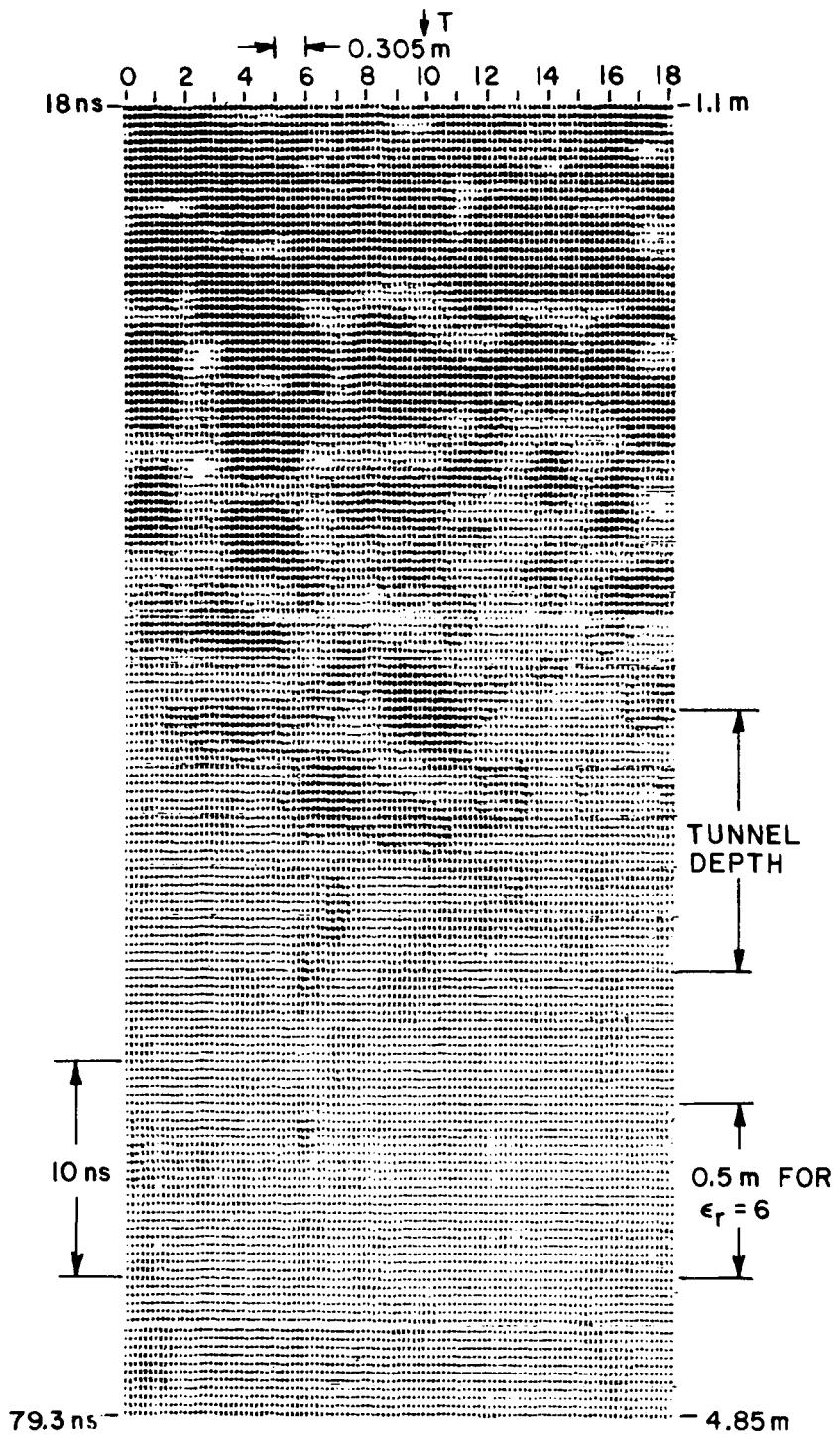
Figure 45. Gold Hill Map 1 Traverse D Cross Section.
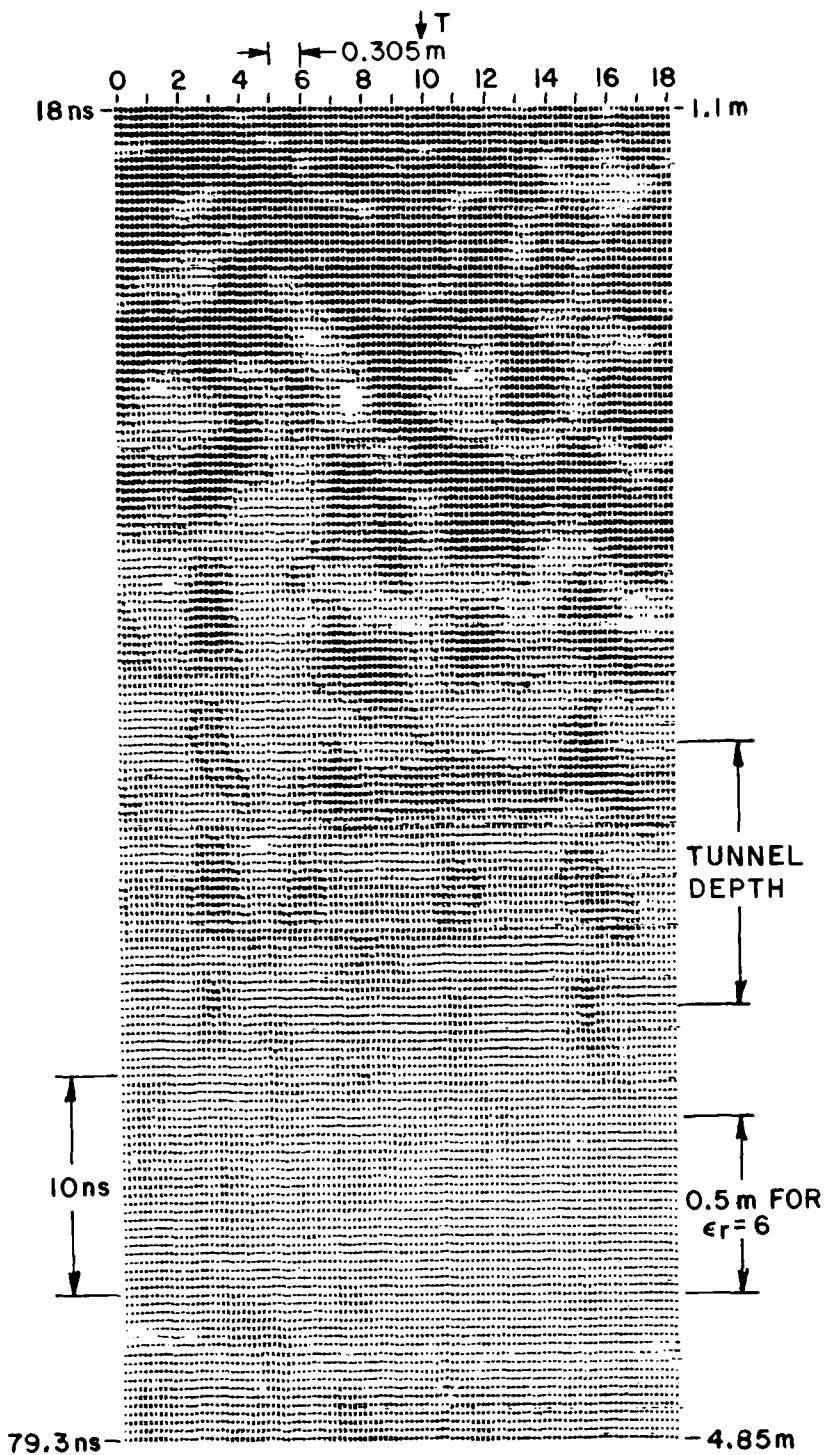
Figure 46. Gold Hill Map 1 Traverse E   Cross Section.

70
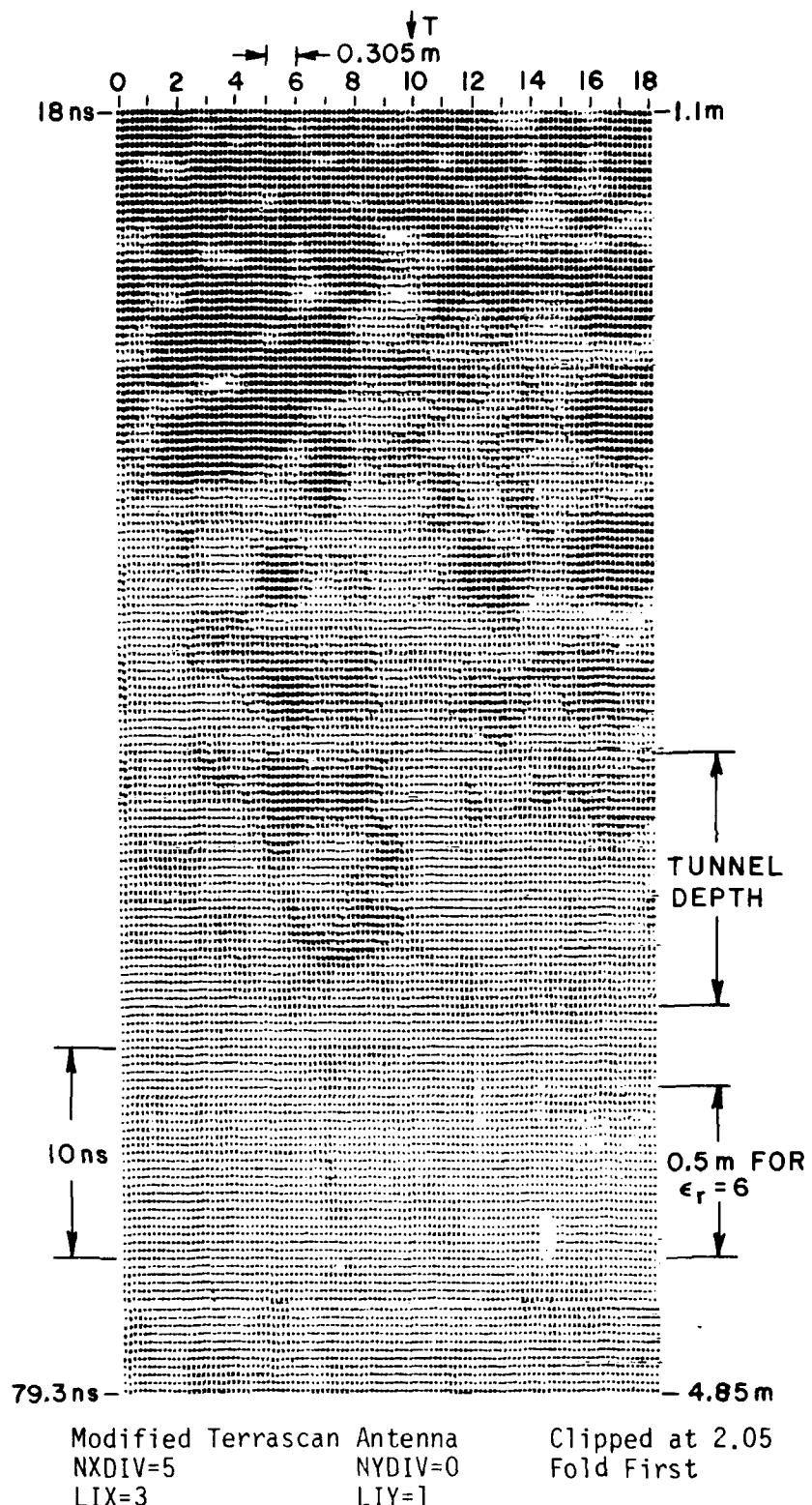
Figure 47. Gold Hill Map 1 Traverse F   Cross Section.

71
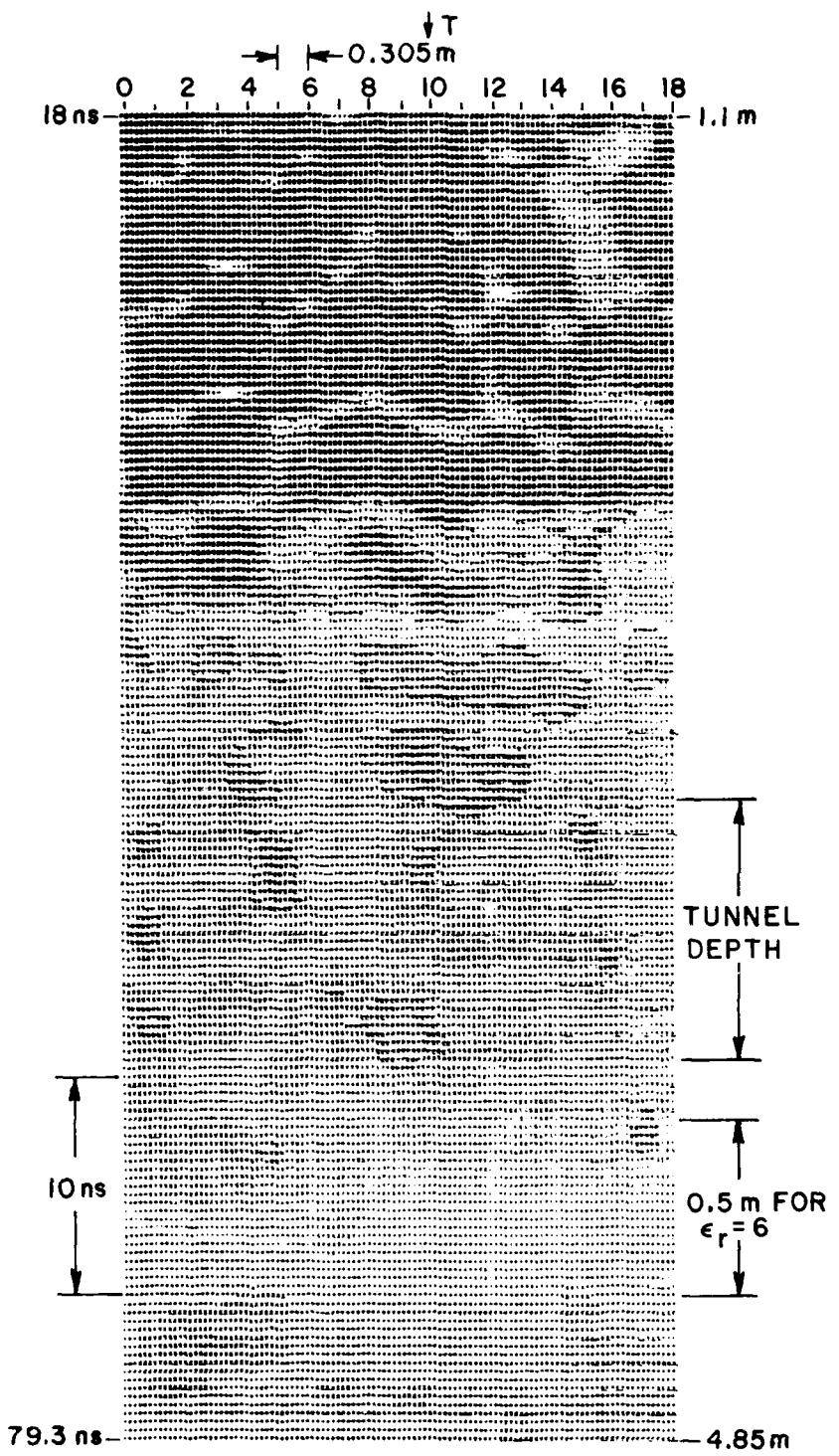
Figure 48.   Gold Hill Map 1 Traverse G   Cross Section
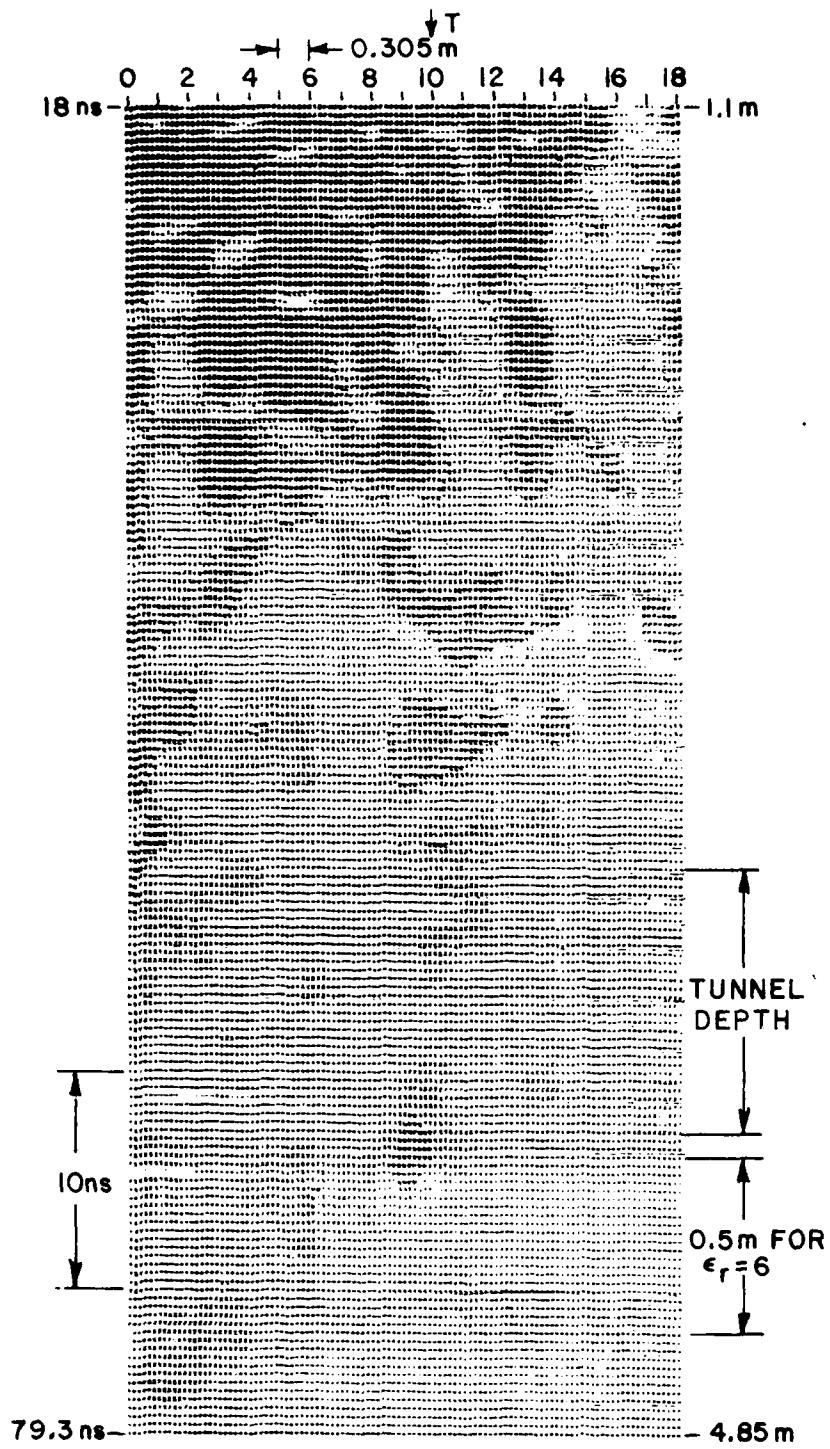
72

Figure 49.   Gold Hill Map 1 Traverse H   Cross Section

73
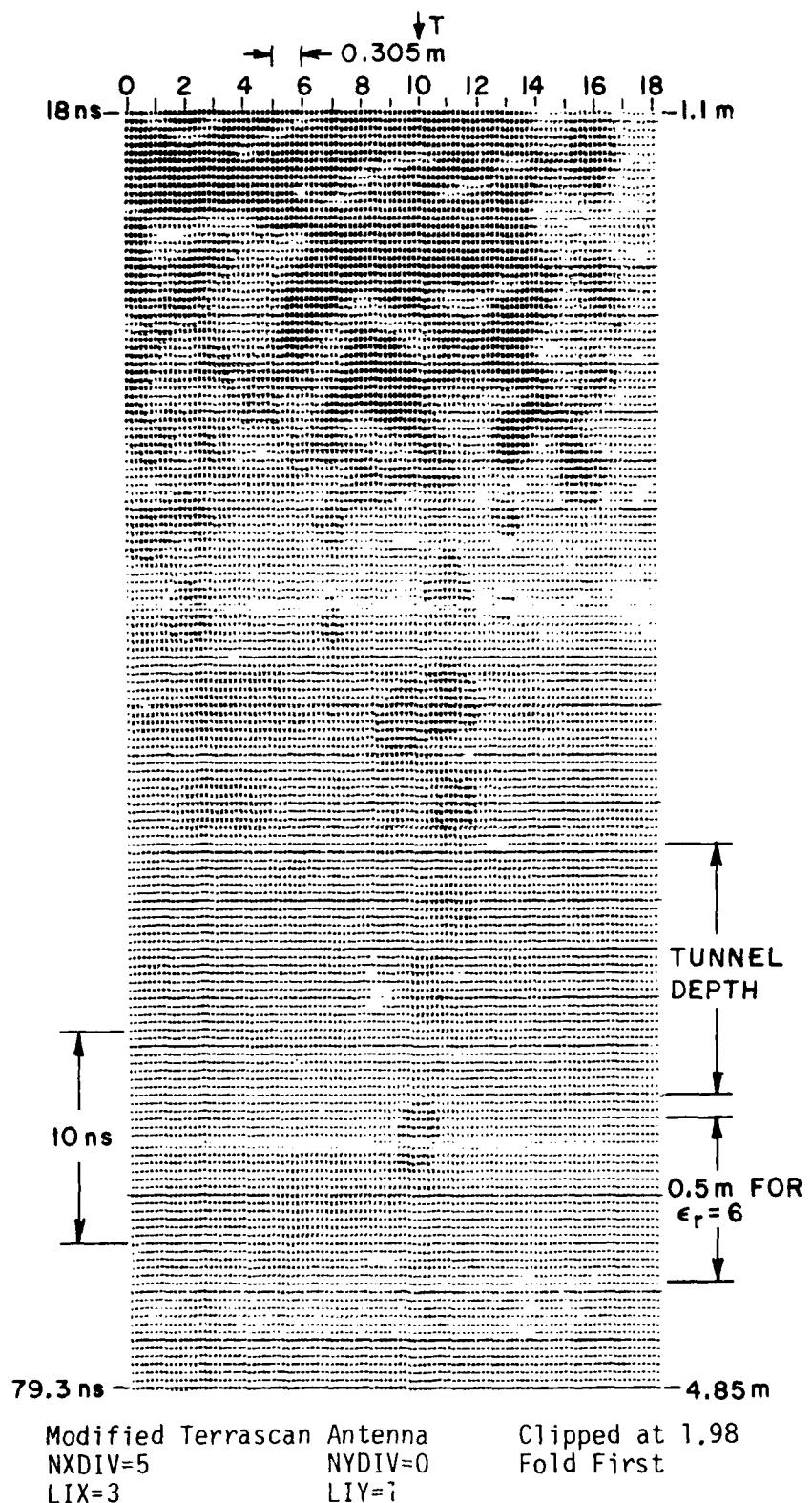
Figure 50. Gold Hill Map 1 Traverse I Cross Section

74
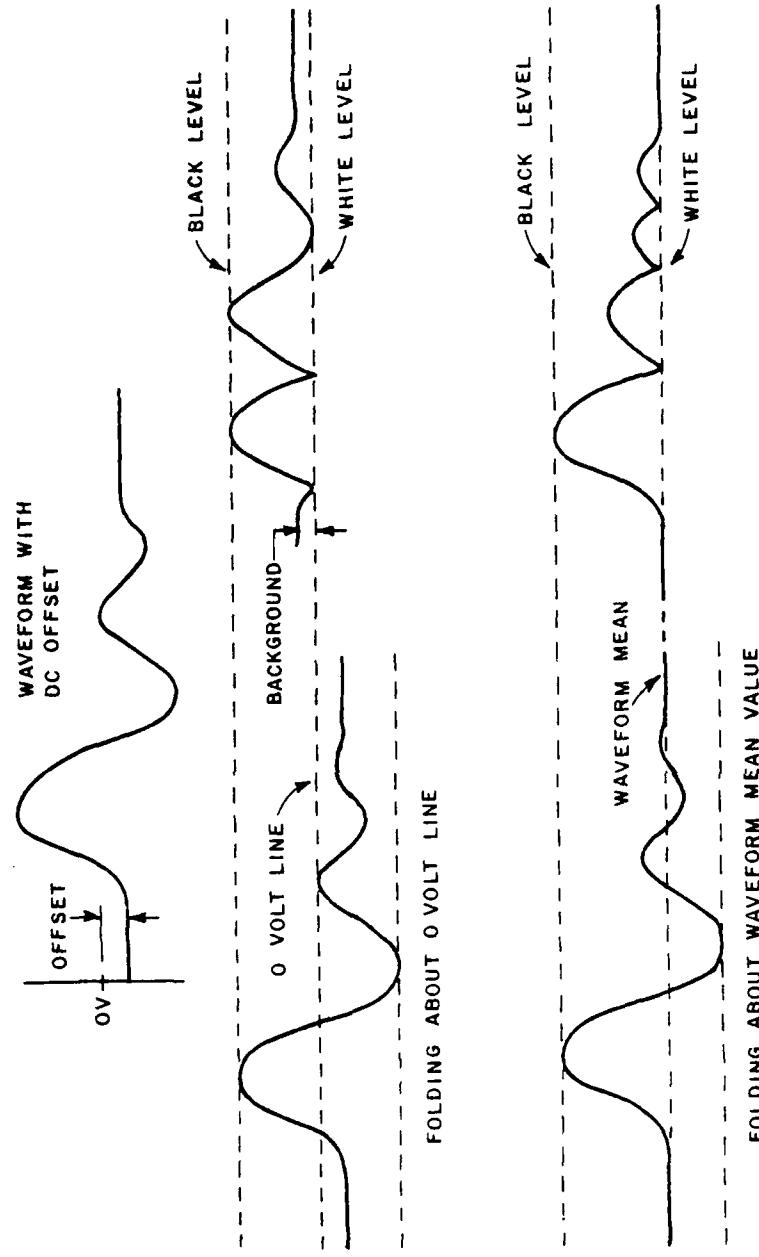
Figure 51. Two Methods for Folding Waveforms.

75

Returning to Figures 44-50, to aid in detection of a possible
target a hyperbolic curve for a point scatterer at the appropriate
depth is shown in Figure 52. The curve has been drawn to the same
scale as the plots. This calculated curve should be used with
care however, since the actual target in this case is not a point
scatterer but a square tunnel. It can be seen, though, that curves
that approximate the appropriate hyperbolic contour are present
in Figures 44-50. This is indicative of the presence of a tunnel-
like target.

One feature of grey level plots (or any display of underground
radar returns) which makes them more difficult to interpret is the
presence of "clutter"; that is, targets in addition to the desired
one. In underground radar some clutter may be caused by surface
roughness or ground inhomogeneities or other factors. Since this
type of signal should be uncorrelated from one measurement position
to the next, averaging of consecutive waveforms in the mapping
traverse may improve the appearance of the data by removing the
clutter. Note that this use of the word clutter does not include
actual subsurface targets other than the desired one (i.e., so
called "false targets"). This clutter reduction method will only
remove those signal components that are uncorrelated with traverse
position.

This technique was implemented by averaging groups of 3 adjacent
waveforms from traverses across the hill and using the resulting
averaged waveforms as input to the GLPR. Figures 53-58 show the
results from applying the technique to traverses C,F, and I. Figures
53, 55 and 57 present the unaveraged data and Figures 54, 56 and
58 present the data averaged for clutter reduction. Note the smoother
appearance of the averaged plots and the absence of some of the
dark areas present in the unaveraged plots. Presumably, the areas
"missing" are clutter signals. Note also the hyperbolic form which
appears rather strikingly in Figure 54. This shape is almost exactly
that of the calculated hyperbola for that depth (see Figure 52).

Some of the figures in this group also used another added
feature to GLPR, namely the ability to clip white as well as black
levels to improve readability.

Comparison of waveforms used as input to the GLPR (Figure
59) and the resulting grey level plots (Figures 44, 53, 54) will
show that the zero crossings of the original data are not readily
apparent on the grey level plots. The reason for this can be seen
by considering the sequence of operations used in generating the
plots. The top of Figure 60 shows the sequence used in the plots
that have been presented thus far. The waveform is first folded
and then interpolated. The interpolation will tend to fit a smooth
curve to the samples and as a result the zero-crossings of the
original signal are "smoothed out". If the sequence of operations

76

FOR 2.74 m DEPTH

FOR 3.60 m DEPTH
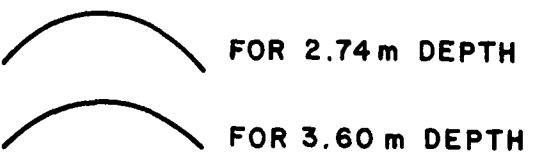
Figure 52. Expected Hyperbolic Shapes To Be Used With Figures 44-50.
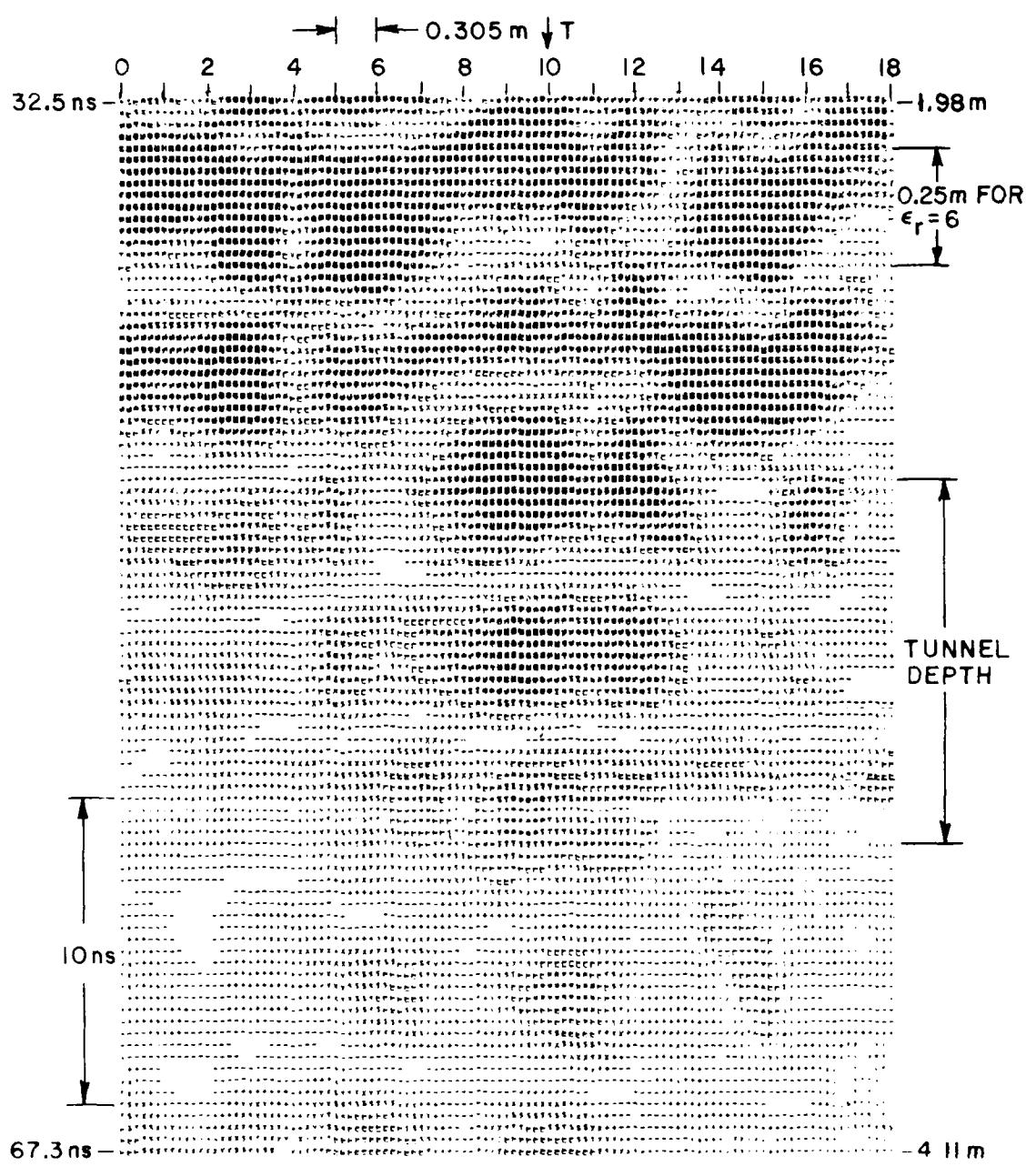
Figure 53. Gold Hill Map 1 Traverse C Cross Section.
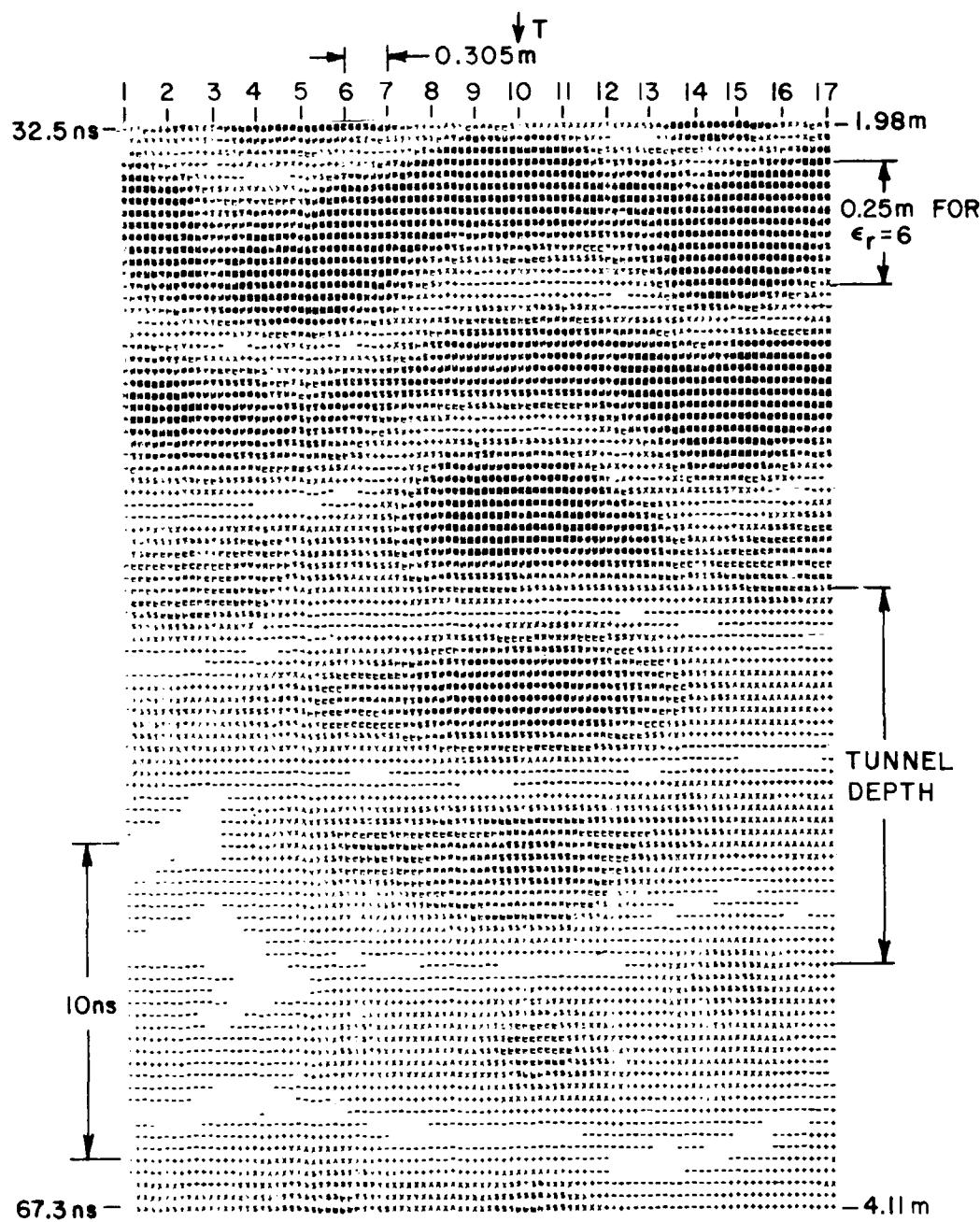
AVERAGED IN GROUPS OF 3

Modified Terrascan Antenna   Clipped at 1.77
NXDIV=5   NYDIV=0   Fold First
LIX=3   LIY=1

Figure 54.   Gold Hill Map 1 Traverse C   Cross Section.
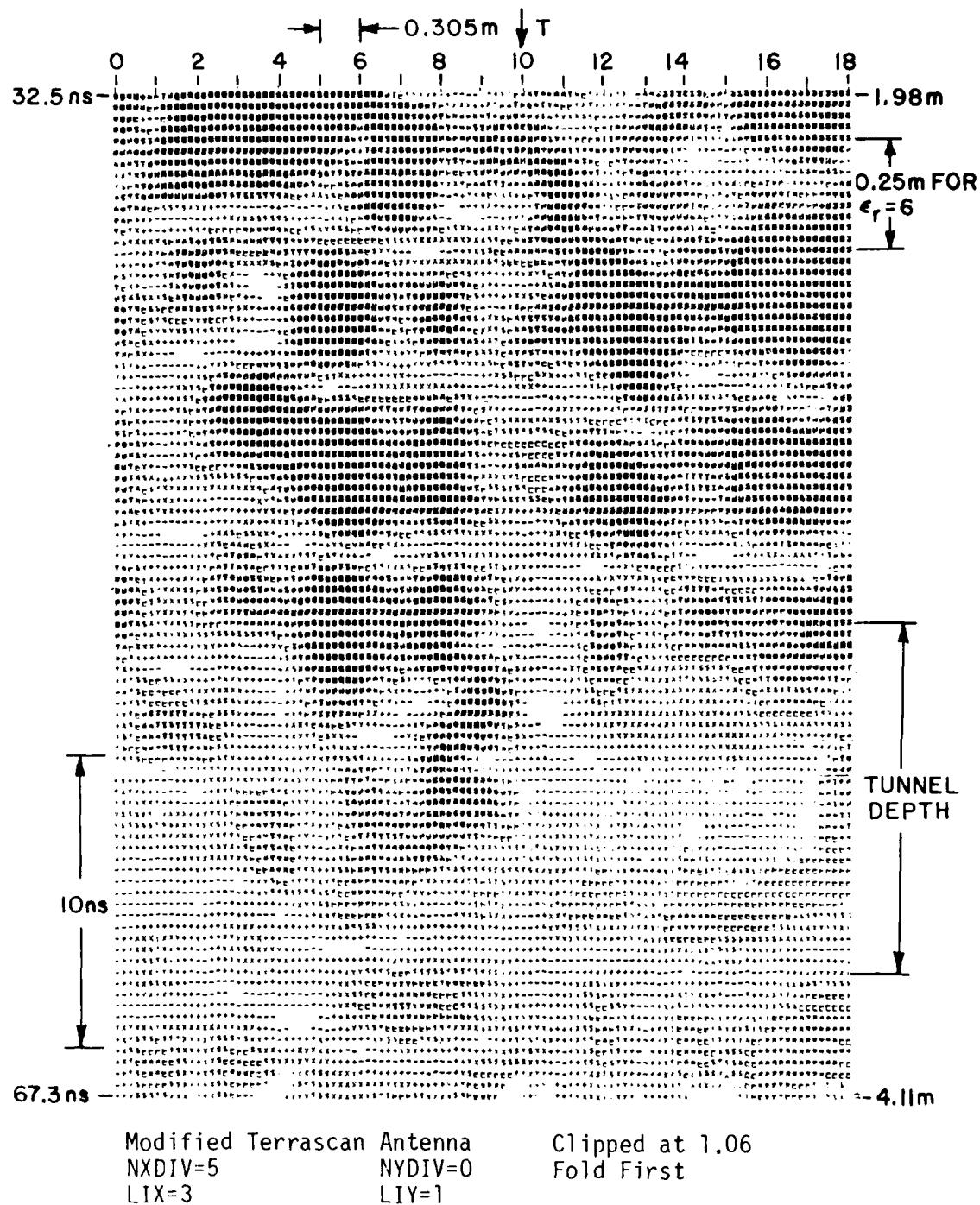
Figure 55. Gold Hill Map 1 Traverse F   Cross Section.
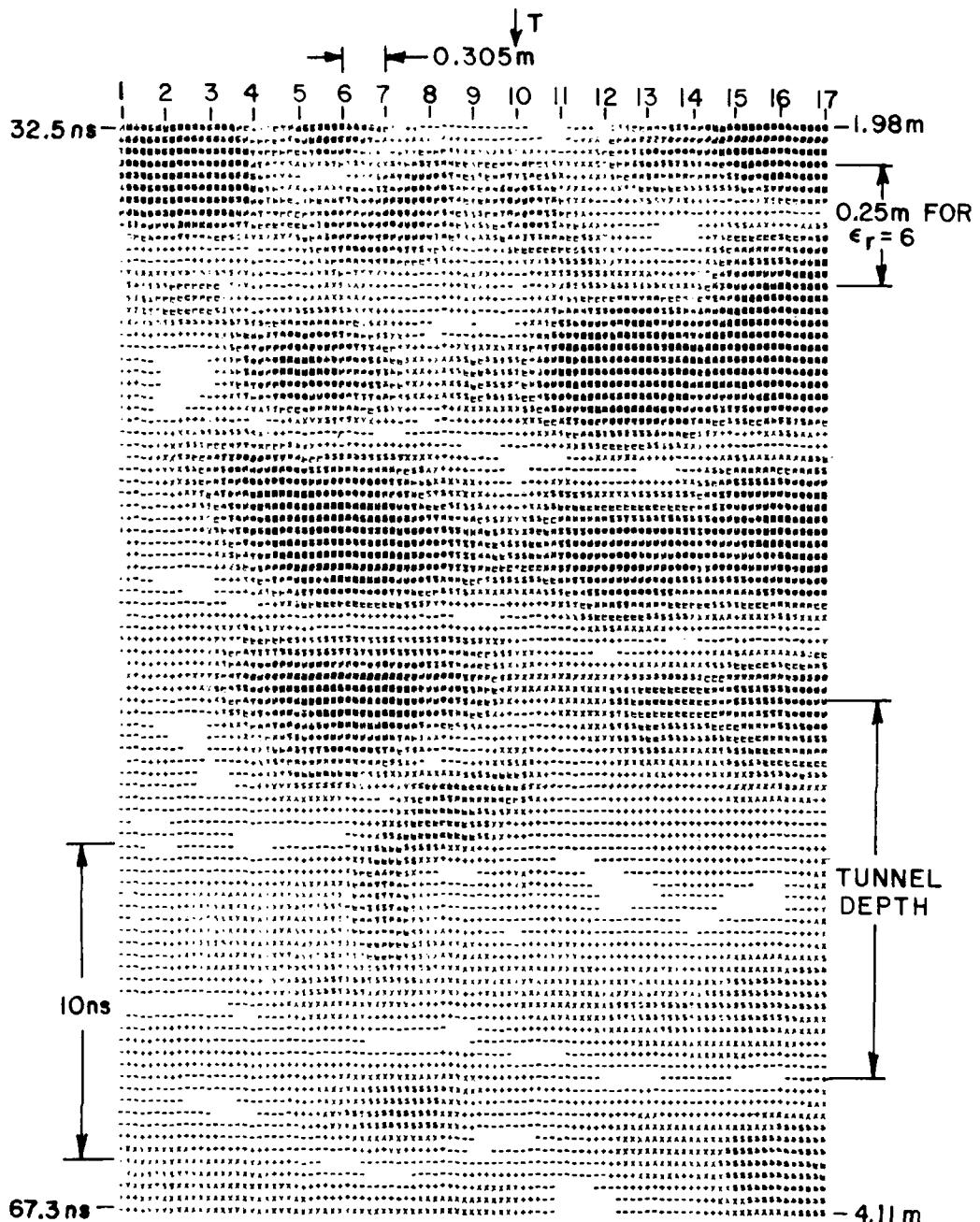
AVERAGED IN GROUPS OF 3

Modified Terrascan Antenna   Clipped at 1.32
NXDIV=5   NYDIV=0   Fold First
LIX=3   LIY=1

Figure 56. Gold Hill Map 1 Traverse F   Cross Section.

81
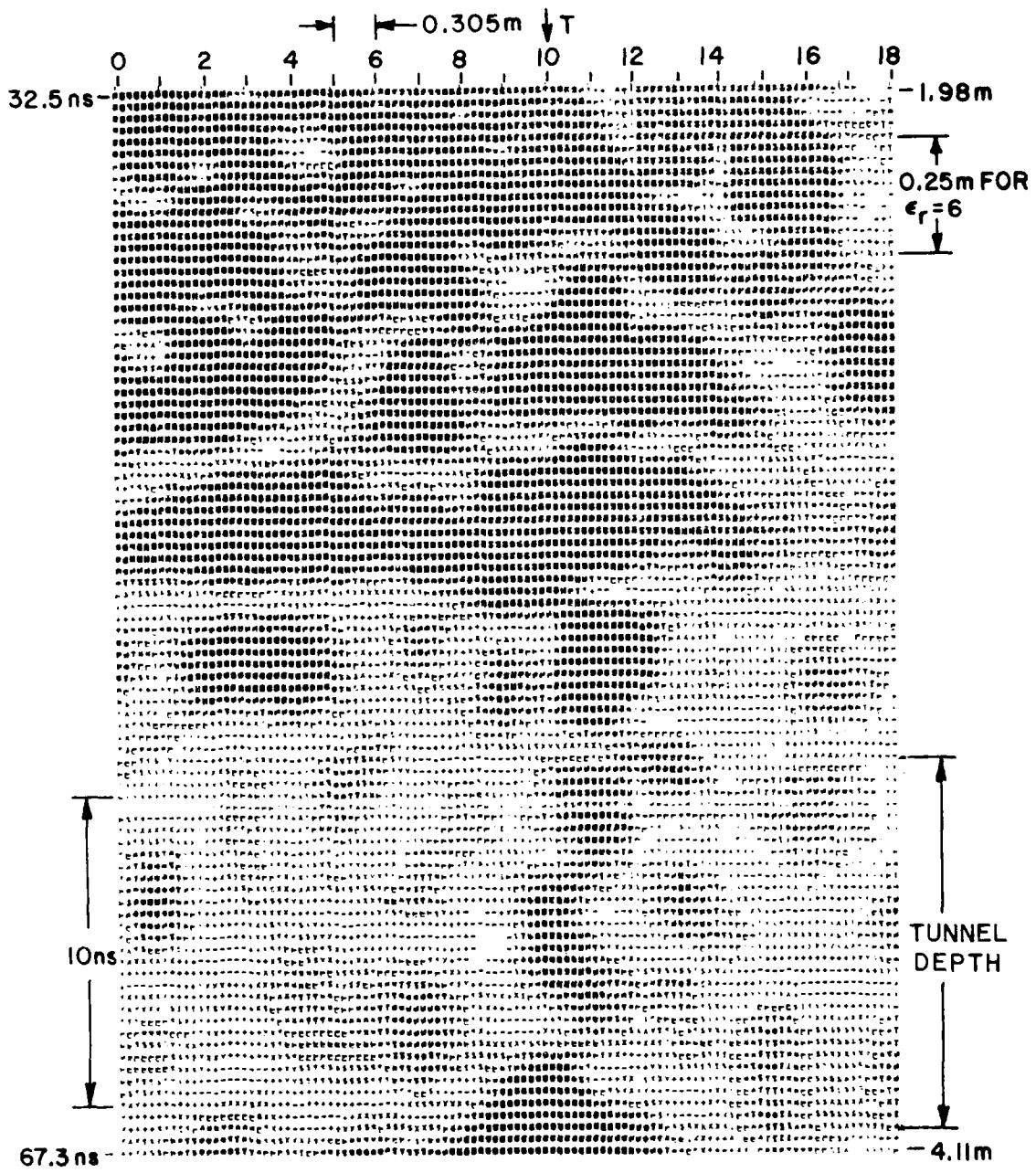
Figure 57.   Gold Hill Map 1 Traverse I   Cross Section.

AVERAGED IN GROUPS OF 3

Modified Terrascan Antenna   Clipped at 0.4
NXDIV=5   NYDIV=0   Fold First
LIX=3   LIY=1
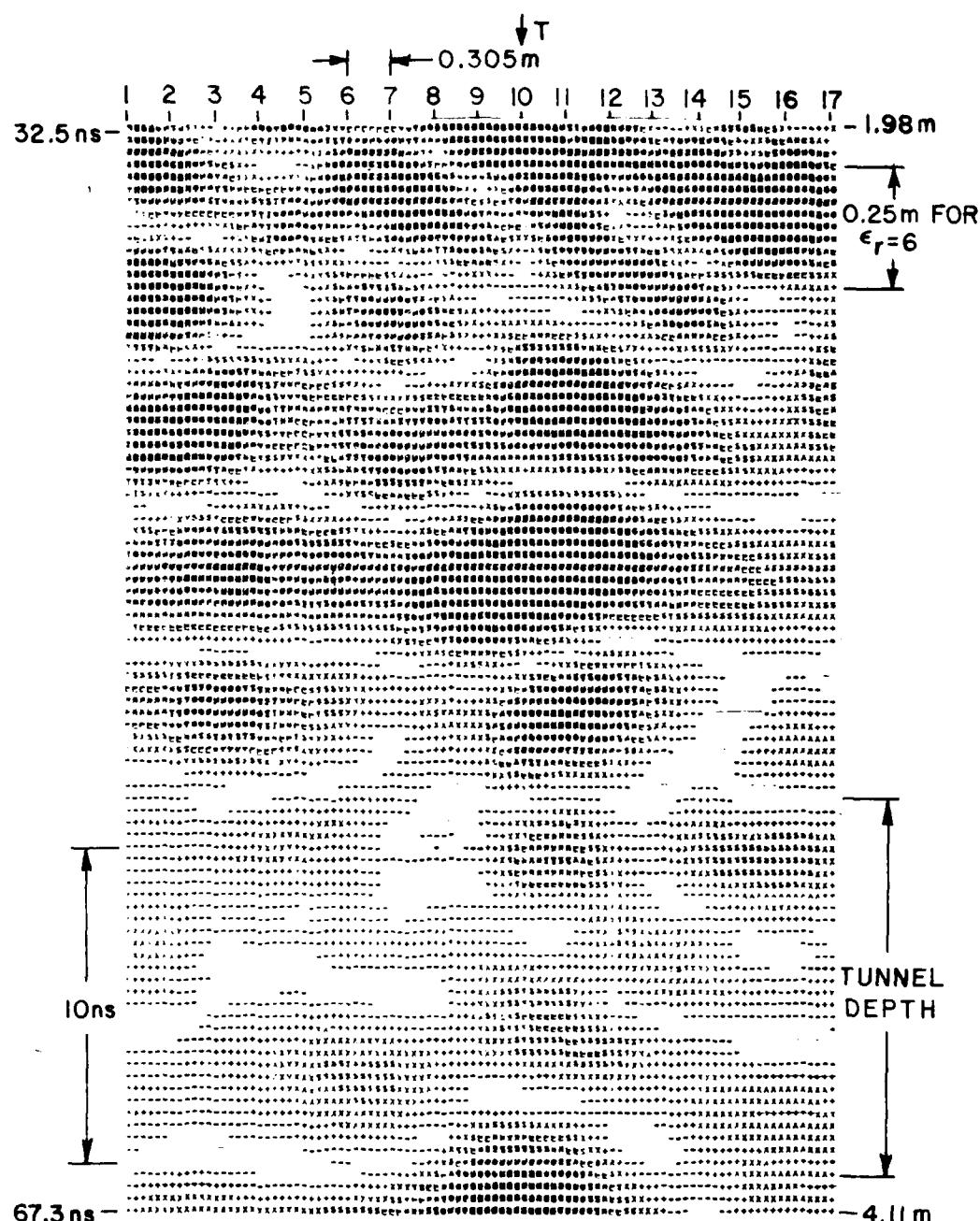
Figure 58. Gold Hill Map 1 Traverse I   Cross Section.

83
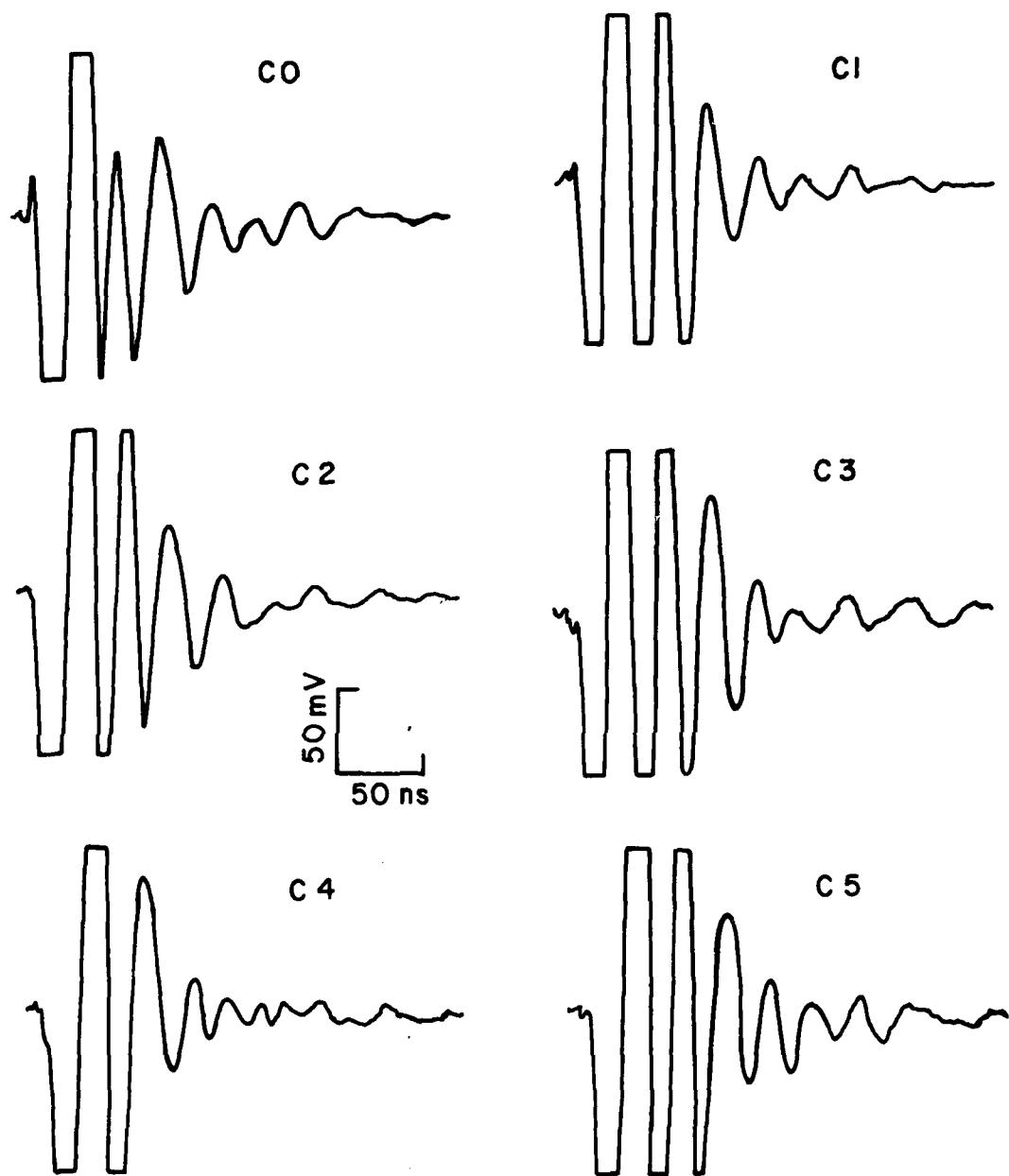
Figure 59. Waveforms From Gold Hill Map 1 Traverse C.

Figure 59 (cont.).   Waveforms From Gold Hill Map 1   Traverse C.

C12

C13

C14

C15

C16

C17

C18

50 mV

50 ns

Figure 59 (cont.). Waveforms From Gold Hill Map 1   Traverse C.

86
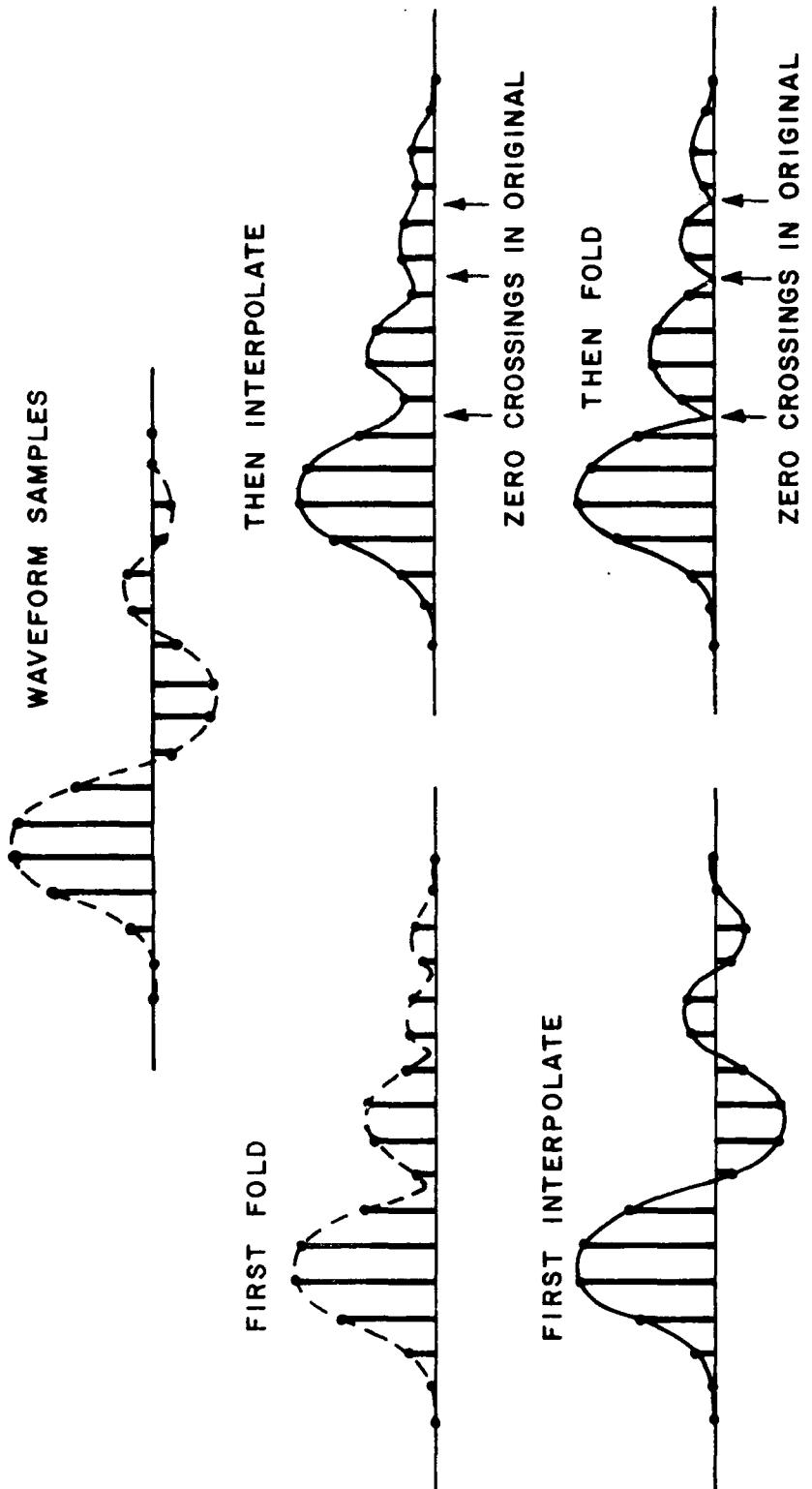
Figure 60. Two Sequences of Operations for Grey Level Plotting.

is changed to that shown in the bottom of Figure 60 the result
is different. This method does not affect the shape of the waveform
near the zero crossings so they should be more apparent in a grey
level plot.

This fact is readily verified by Figure 61 which shows the
result of using this FOLD LAST method of processing in the analytic
data for the circular cylinder. The hyperbolic shapes are now
clearly separated by a white area (compare to Figure 34). Figures
62 and 63 show also the effect of more sparse sampling, as shown
earlier in Figures 35 and 36. Note the reduction in background
level in these FOLD LAST plots.

Experimental data processed using this technique is shown
in Figures 64-73 which present the same data as shown earlier.
Figures 64-70 correspond respectively to Figures 44-50 and Figures
71-73 present the clutter reduced data shown before in Figures
54, 56 and 58.

In observing these plots, it should be noted that the zero-
crossings (white areas) serve only to delineate polarity changes
in the waveforms and should not be focused upon as possible targets.
Only the darkened areas represent strong signal returns.

One feature noted in the grey level plots presented thus
far is the presence of a large number of echoes coming from scatterers
closer to the surface than the roof of the tunnel. This is perhaps
explained as the result of reflections from locations in the tunnel
overburden where fissures filled with water or air are present.
In certain cases, this clutter could conceivably prevent detection
of the tunnel.

One traverse was also taken across this section of Gold Hill
using a different antenna. This was the long box antenna, designed
specifically for this type of target. Data was taken at 0.61 m
intervals instead of 0.305 m as before. The measurement positions
as identified using the coordinates in Figure 38 were C2, C4, C6,....,
C14, C16, C18. As a preliminary step in evaluation of this data,
all 256 samples were plotted in a cross-sectional view using the
FOLD FIRST technique. The result is shown in Figures 74 and 75.
These are two distinct grey level plots. If an attempt were made
to plot all 256 samples in one graph, either the data near the
bottom would be too light or, after clipping to raise the grey
level at the bottom, the top would be too dark. These figures
then consist of two halves of the waveform set, each clipped at
an appropriate level. The difficulty with this plotting method
is that two different interpolations are being presented and they
may distort the data near the border between the two plots. A
possible remedy to this situation would be to multiply the data
by a linear gain, increasing with depth.

88

Figure 61. Moment Method Data   Cross Section.
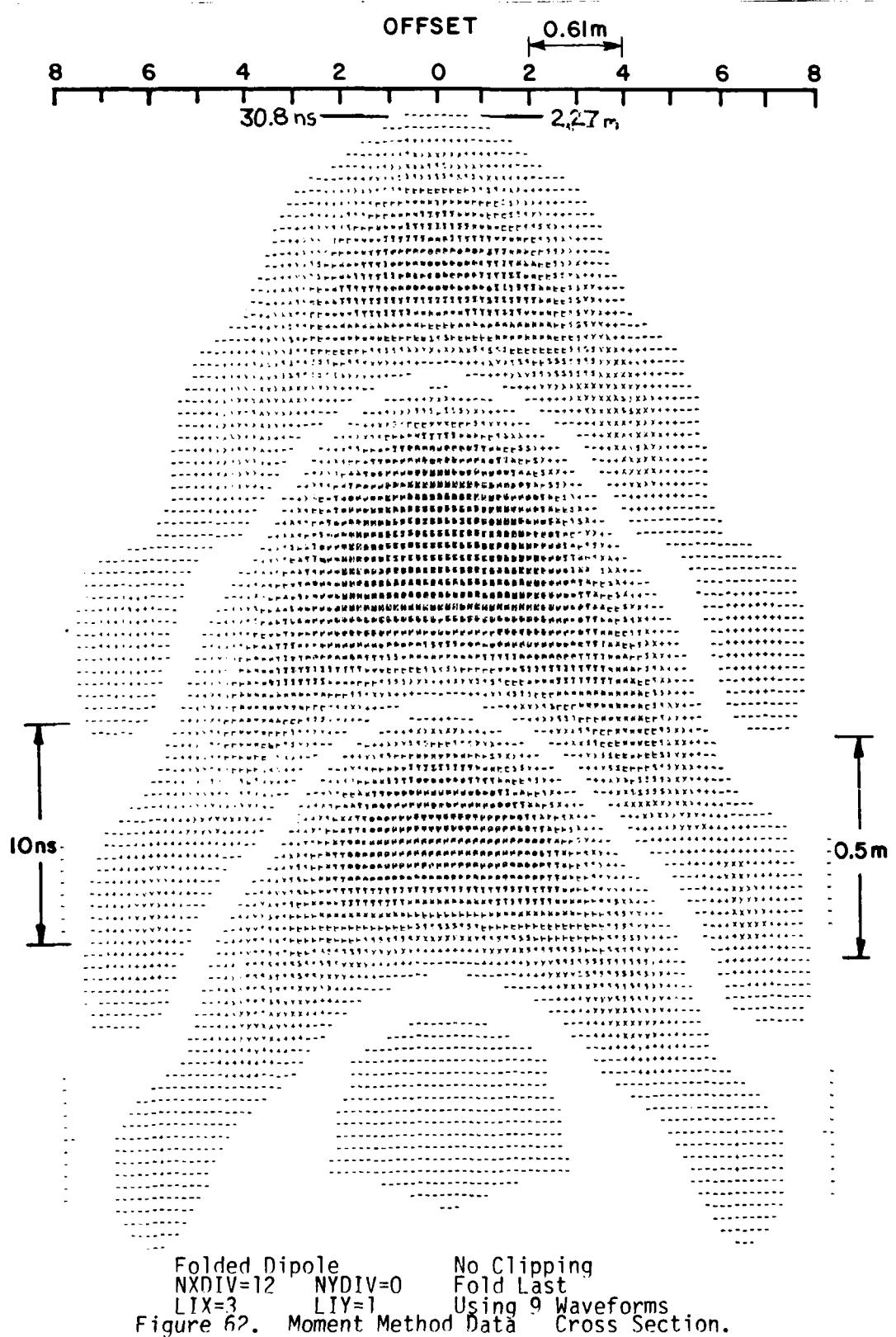
Figure 62. Moment Method Data Cross Section.
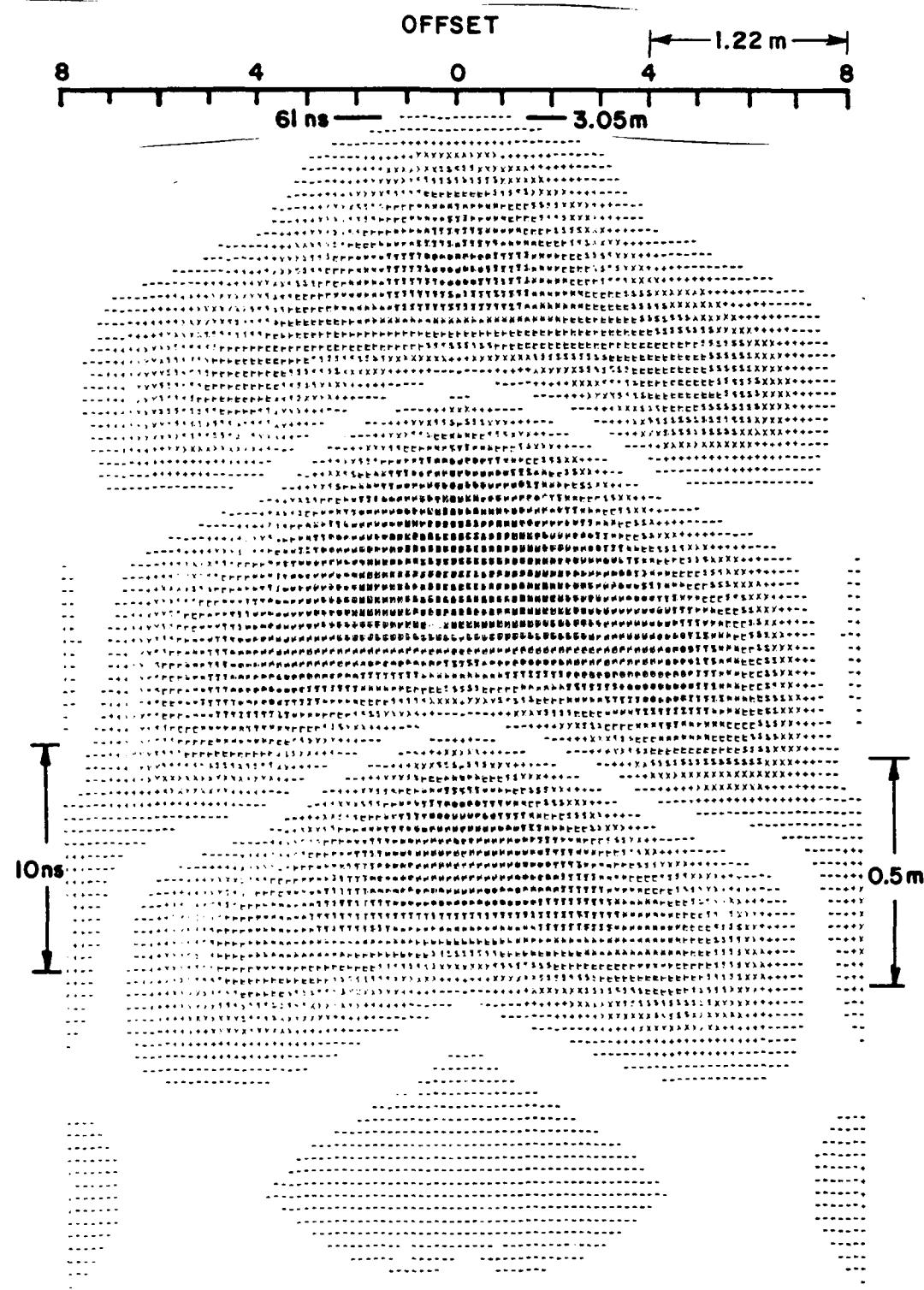
Folded Dipole   No Clipping
NXDIV=25 NYDIV=0   Fold Last
LIX=3   LIY=1   Using 5 Waveforms
Figure 63.   Moment Method Data   Cross Section.

91
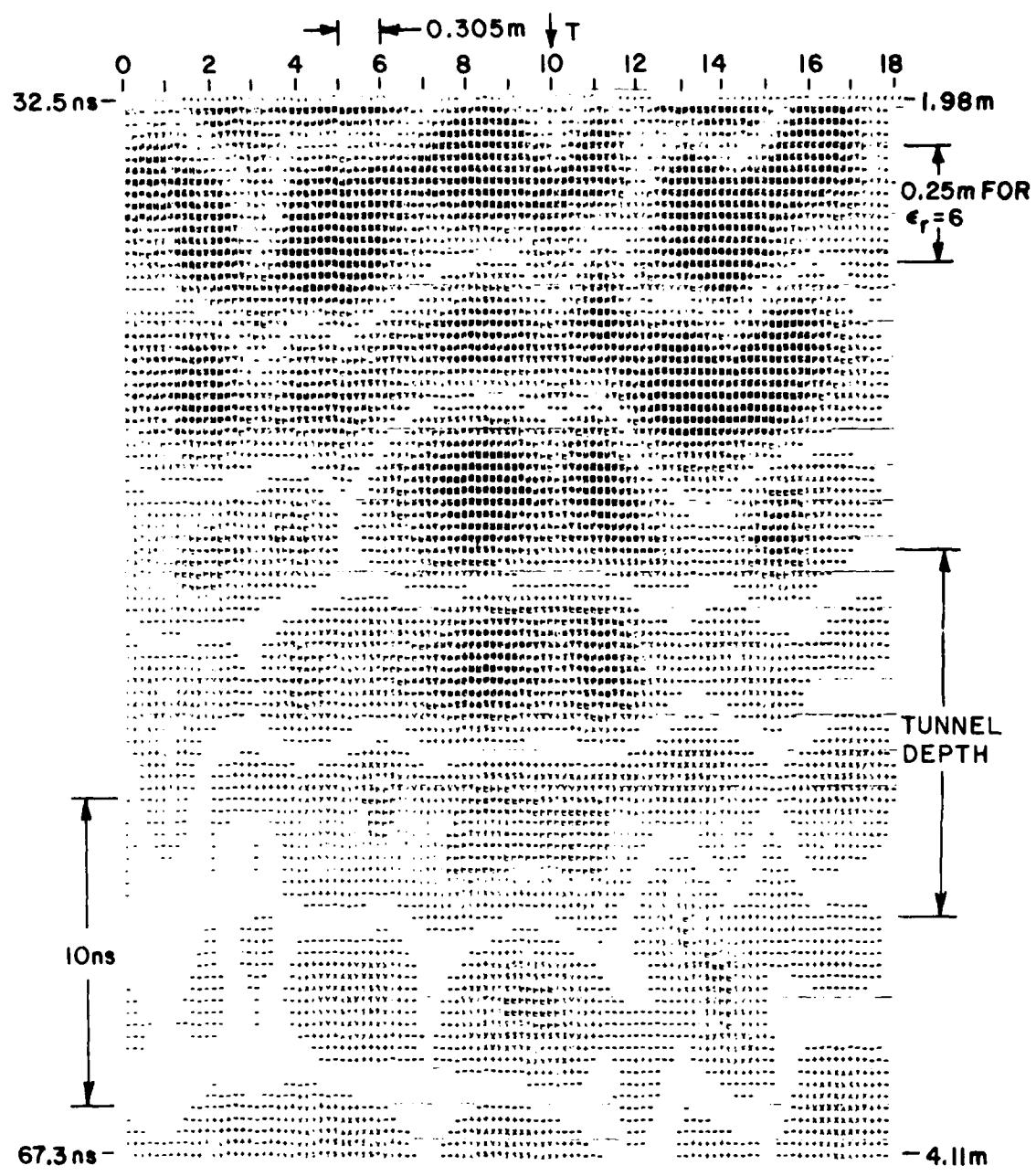
Figure 64. Gold Hill Map 1 Traverse C   Cross Section.
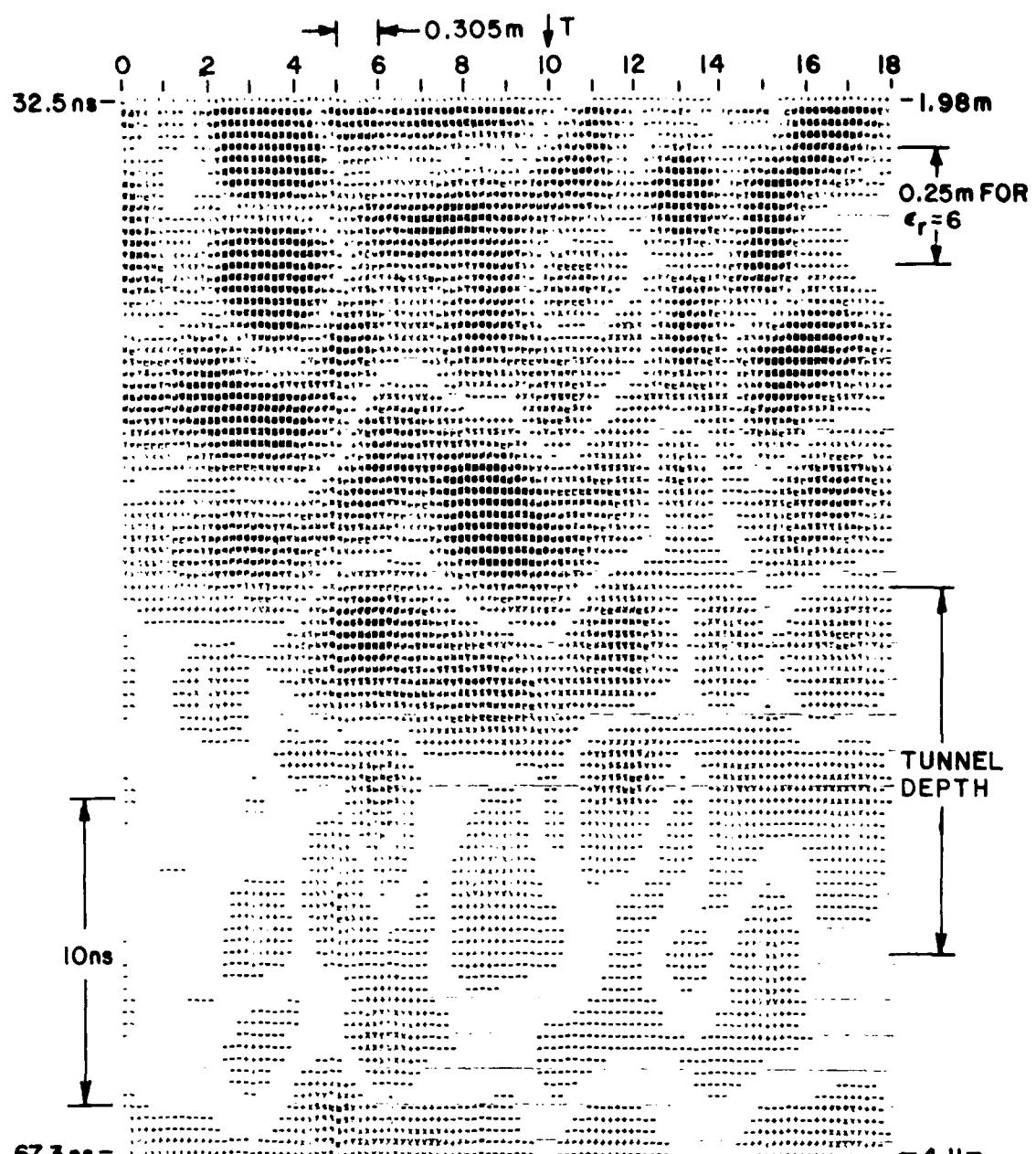
92

Figure 65. Gold Hill Map 1 Traverse D   Cross Section.
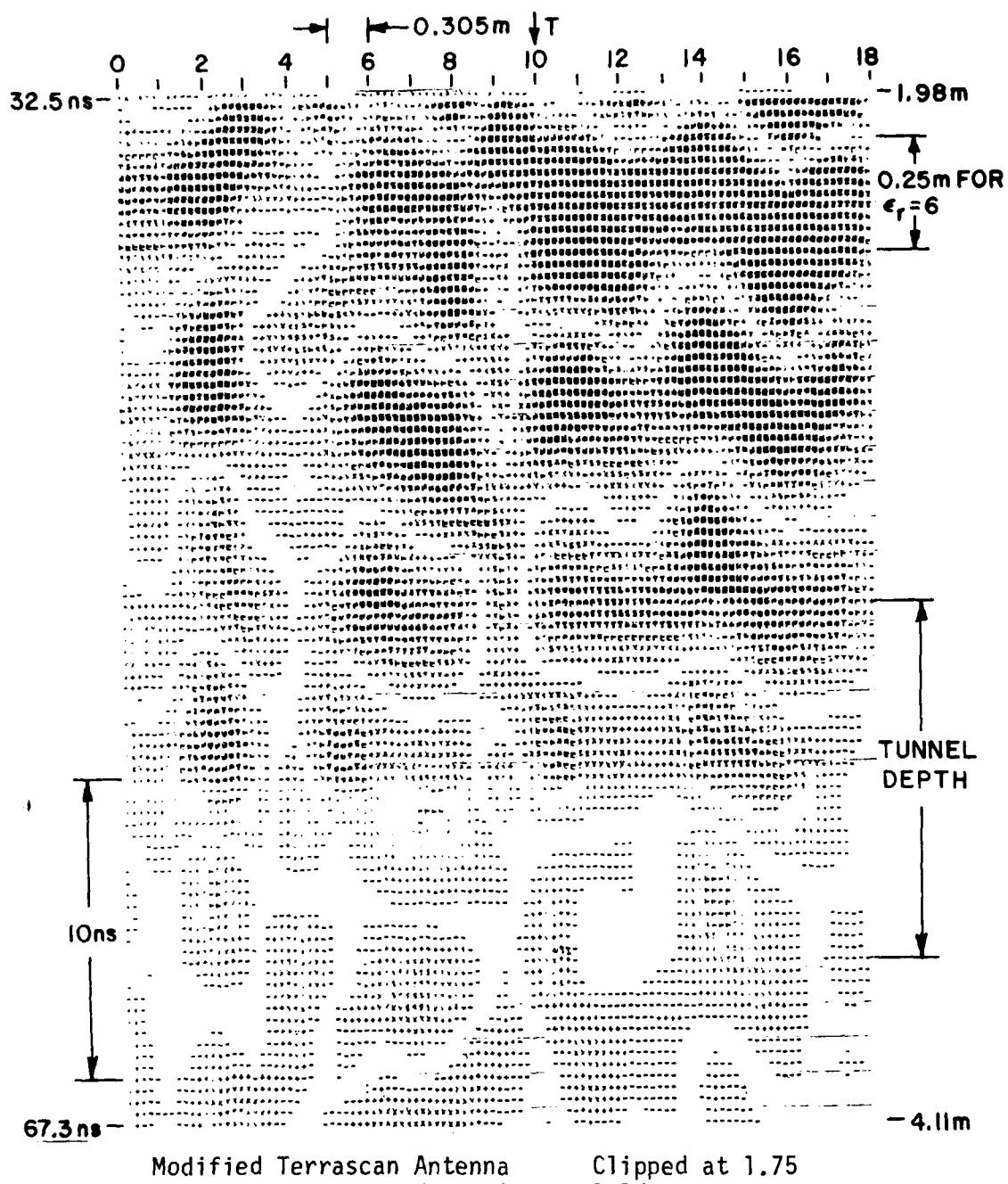
Figure 66. Gold Hill Map 1 Traverse E Cross Section.

94

Figure 67. Gold Hill Map 1 Traverse F   Cross Section.
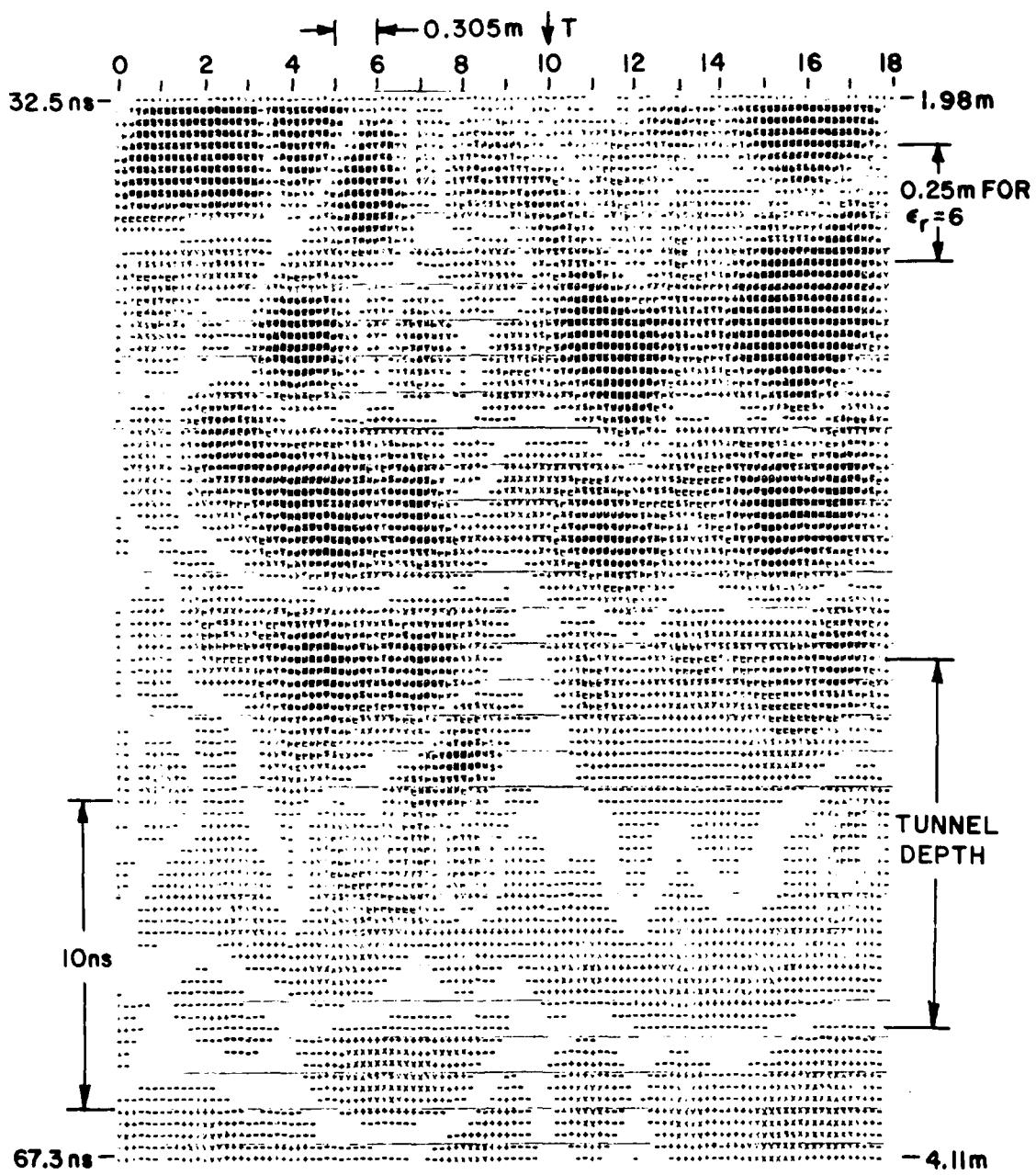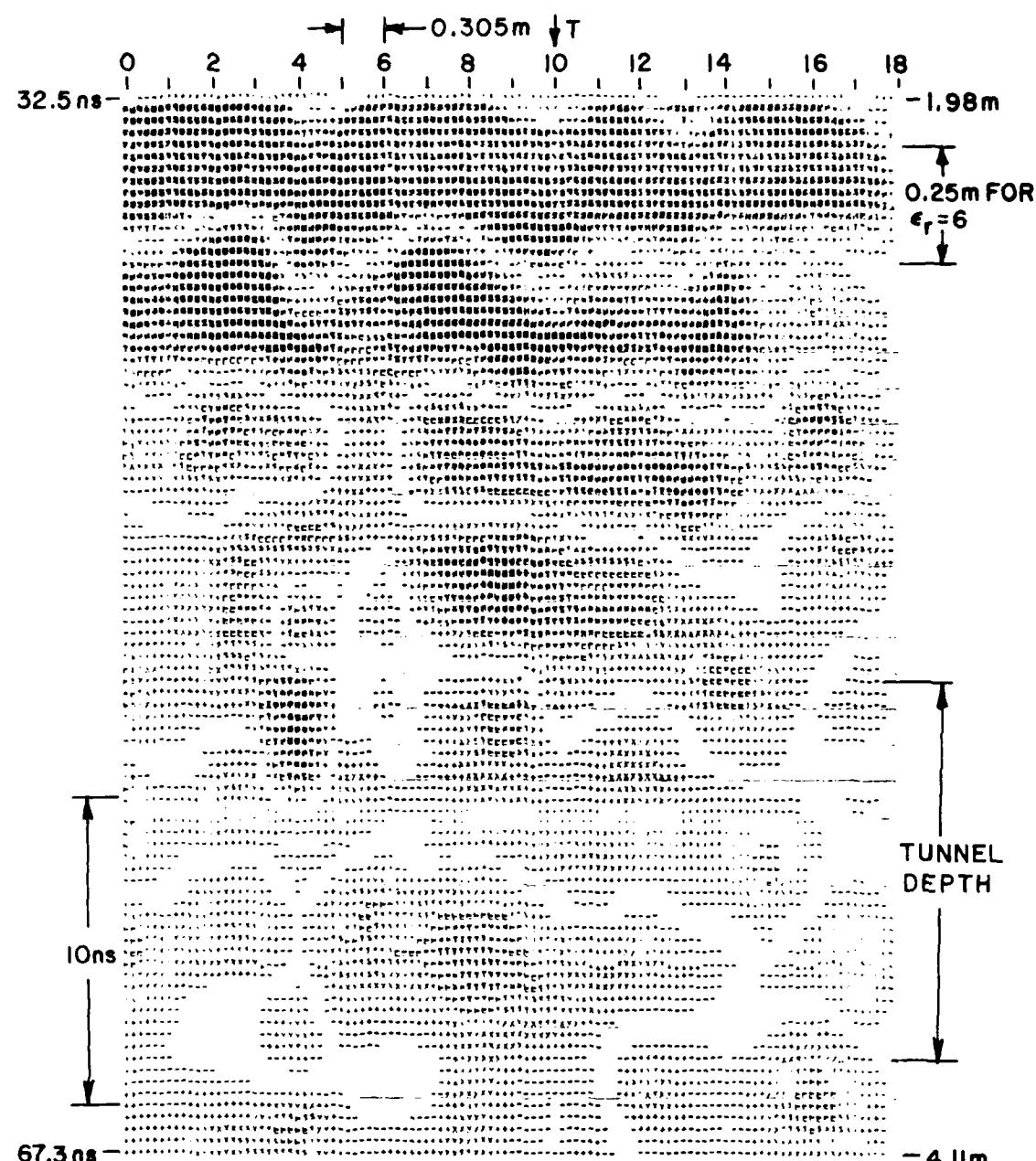
Modified Terrascan Antenna   Clipped at 1.67
NXDIV=5   NYDIV=0   Fold Last
LIX=3   LIY=1

95

Figure 68. Gold Hill Map 1 Traverse G   Cross Section.
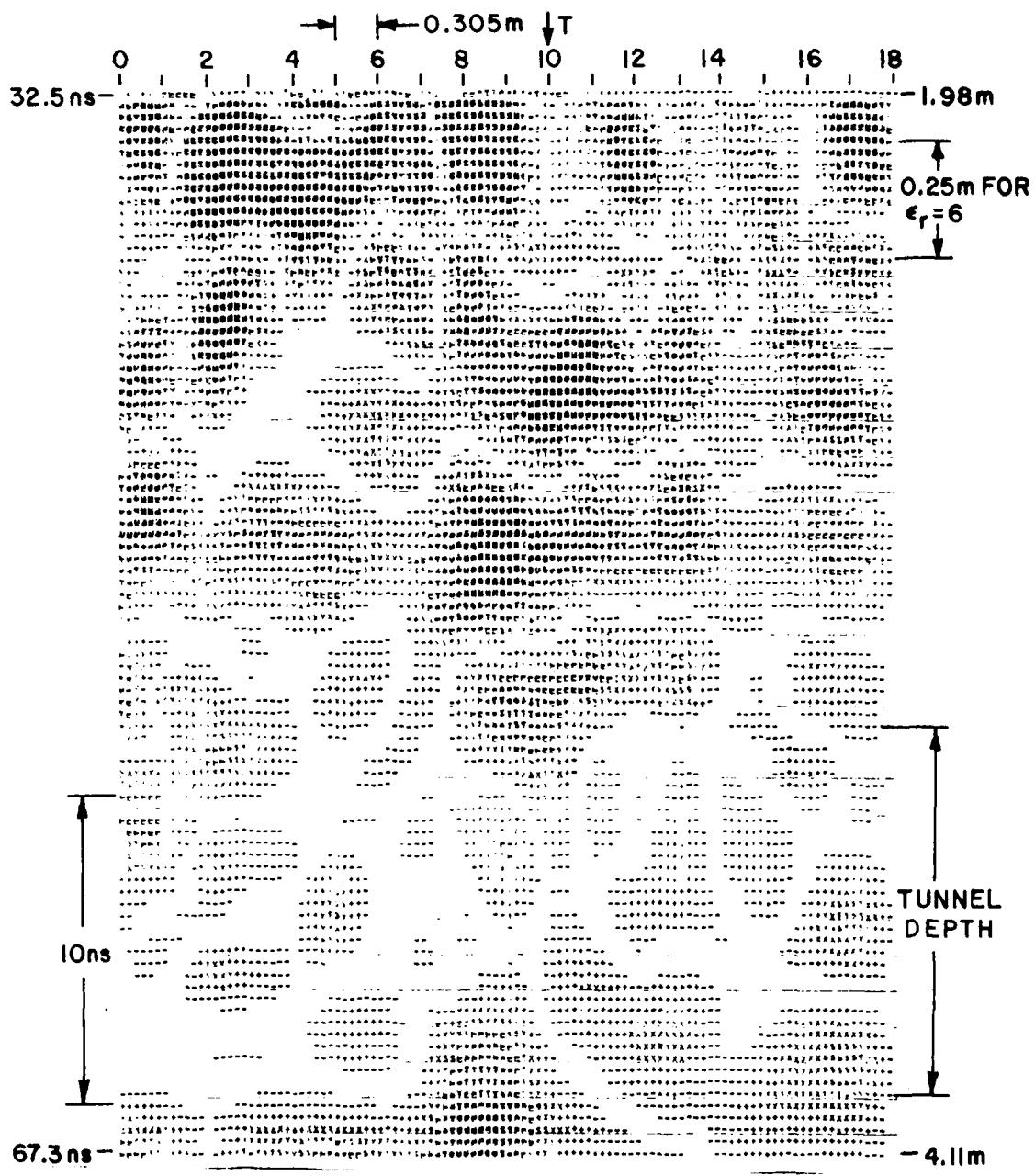
Figure 69. Gold Hill Map 1 Traverse H   Cross Section.
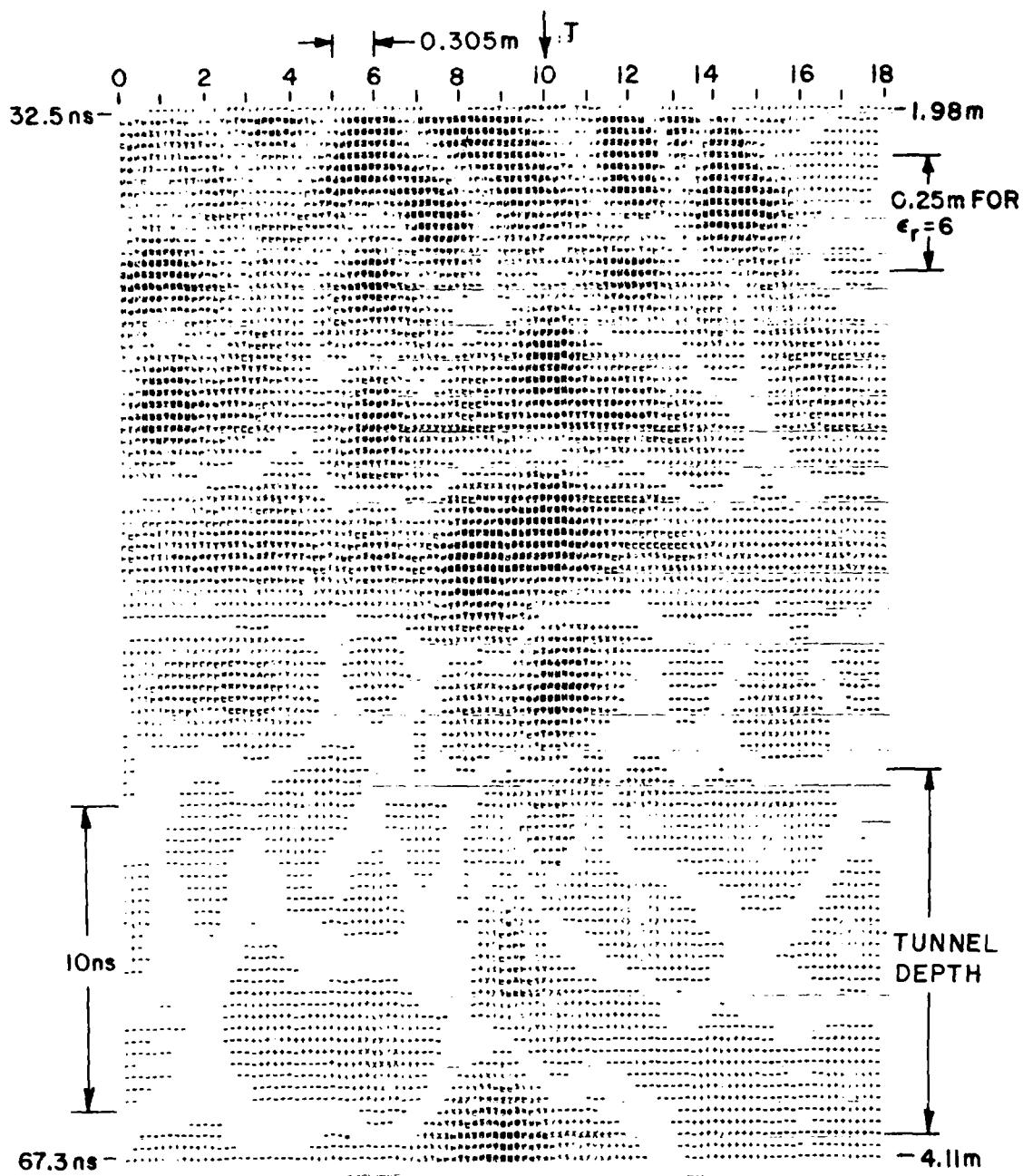
Figure 70.   Gold Hill Map 1 Traverse I   Cross Section.
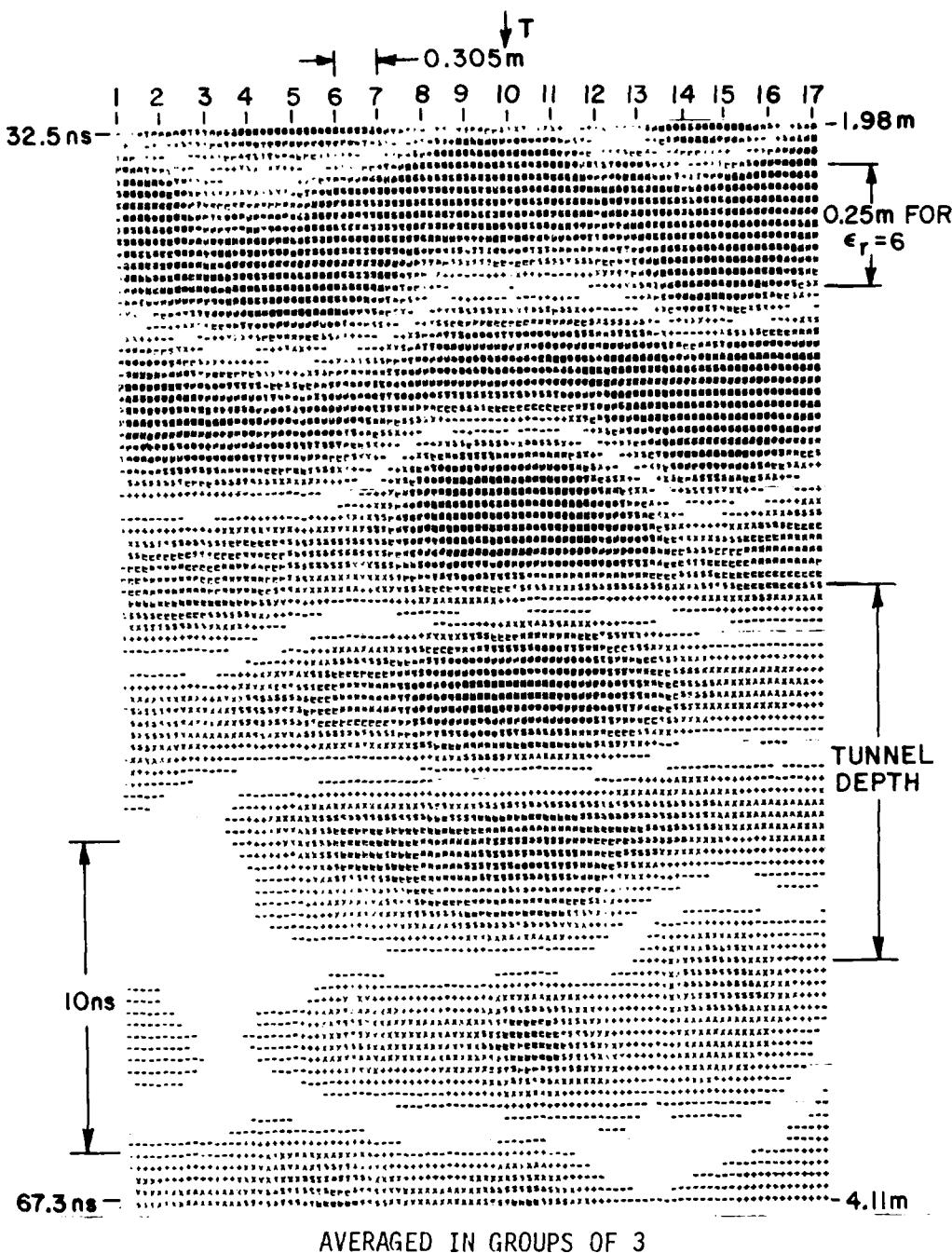
Figure 71. Gold Hill Map 1 Traverse C Cross Section.
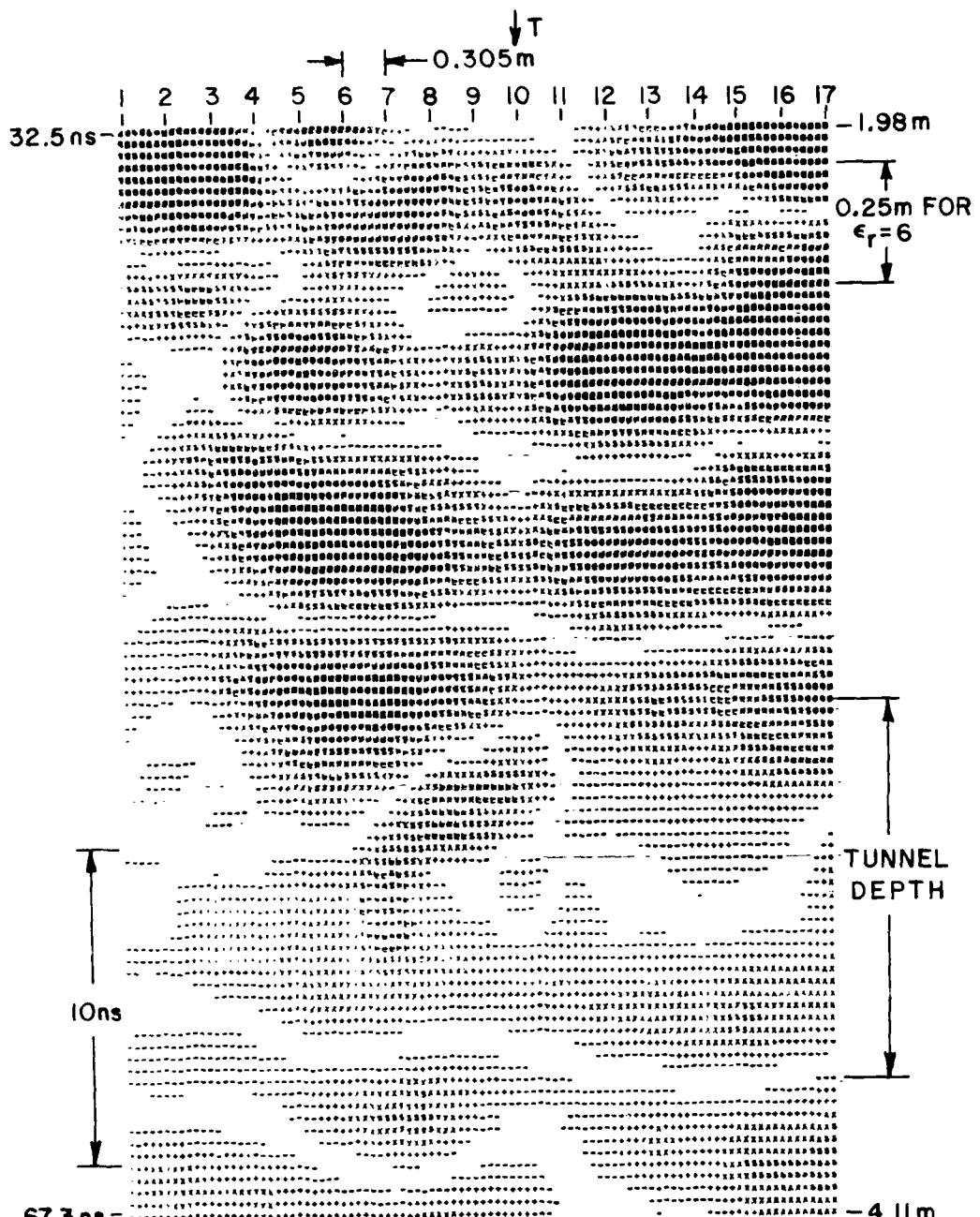
Figure 72. Gold Hill Map 1 Traverse F   Cross Section.
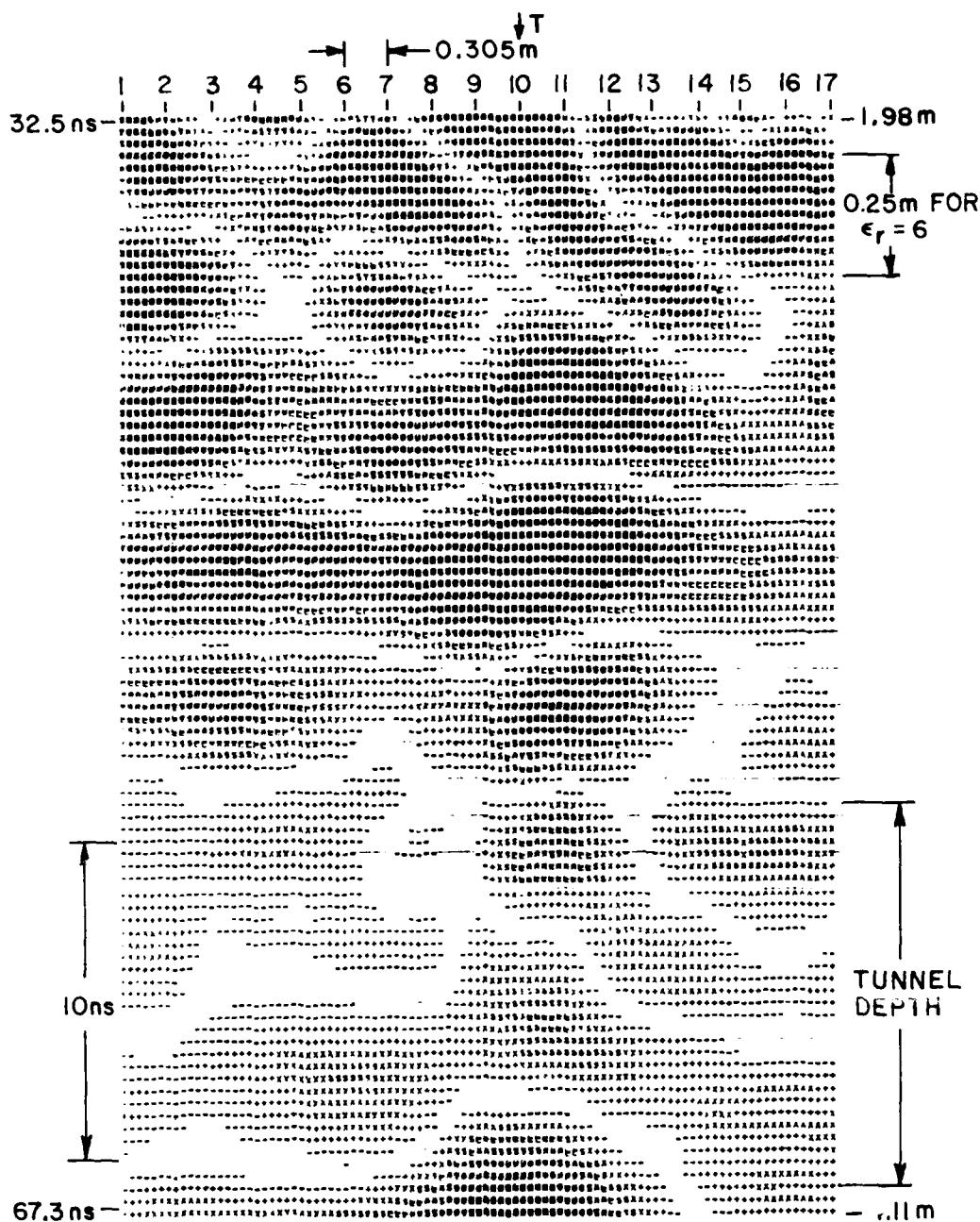
100

Figure 73. Gold Hill Map 1 Traverse I Cross Section.

101
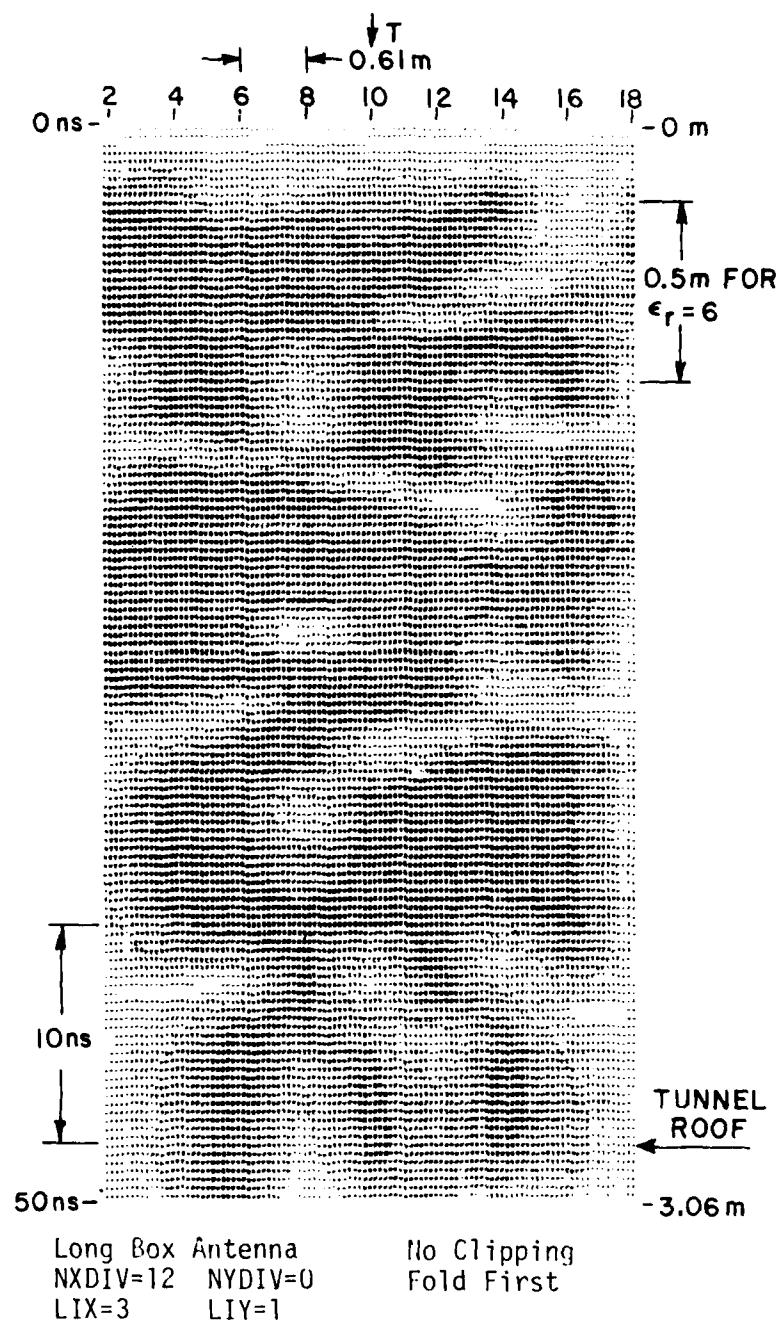
Figure 74. Gold Hill Map 1 Traverse C   Cross Section.
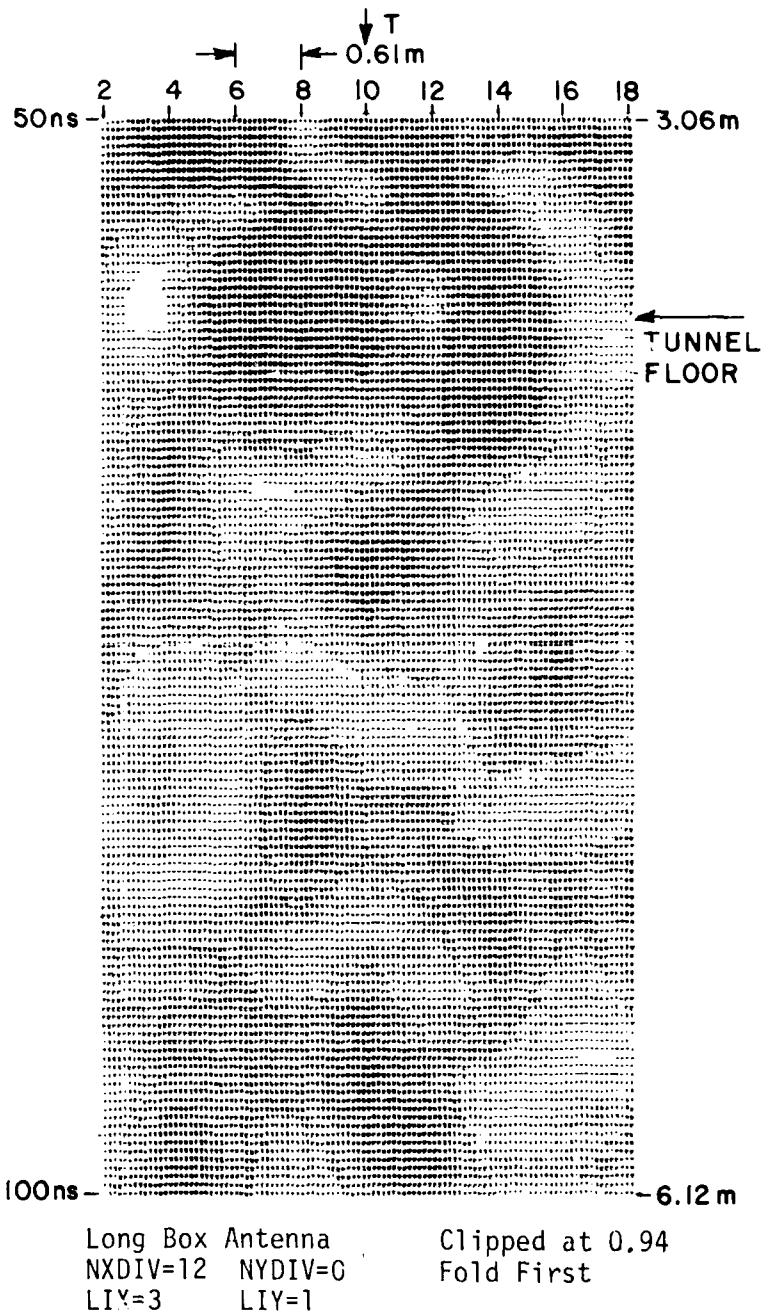
Figure 75. Gold Hill Map 1 Traverse C   Cross Section.

Figures 76 and 77 show the data plotted in a range window of approximately 2-4 m (32.5-67.3 ns). Figure 76 is a normal grey level plot and Figure 77 is a plot using the 3 waveform averaging technique for clutter reduction discussed above. Figure 78 shows the shape of hyperbola to be expected.

Figure 76 exhibits this expected shape at a position less than 10 ns above the roof of the tunnel. We may also compare Figure 76 with Figure 53 which presents data from the same traverse across the hill but obtained with the Terrascan antenna. Because of the different antenna structures, the clutter should appear differently in each plot; and the figures show this, but note the darkened area that appears in both plots near the tunnel position.

The spreading out of the hyperbolic shape in the plot using the long box antenna can be explained in two ways. First, the spreading could be due to the lower frequency response of the antenna. Secondly, the traverse taken with the box antenna had antenna positions separated by 0.61 m, or twice the spacing of the Terrascan version. As was shown earlier in Figures 35 and 36, more sparse mapping results in broader hyperbolic forms in the grey level plot.

Plots were also made using the FOLD LAST method. Figure 79 shows the unaveraged data and Figure 80 shows the averaged data. Note once again the smoothness of the clutter reduced plot and its tendency to single out one or two hyperbolic forms as candidates for consideration as targets. Observe that the averaging process tends to remove the rapid variations in null positions which are also clutter-related.

Other data from the Gold Hill site was also subjected to grey level processing. Two diagonal traverses were made using the long box antenna at a location further uphill than that of Figure 38. Figure 81 shows the layout of the measurements taken at this site. These antenna positions were the only ones available in this region because of the rough ground and presence of many obstacles.

We will first discuss the traverse from L-2 to S12. The complete 256 point waveforms are shown plotted in grey scale in Figures 82 and 83. They are two separate plots, as discussed under Figures 74 and 75 above.

After selection of an approximate depth window of 4.6-8.84 m (or 75-145 ns) for the tunnel depth of 6.1 m in this area, a variety of processing techniques were used on the data. Figure 84 shows the basic plot, clipped to highlight the areas of interest. The calculated hyperbolic shape for this map is shown in Figure 85. Figure 86 shows the same data after clutter reduction by averaging. Note in particular the noise evident in the lower portion of these plots and also in the typical waveform from this traverse shown at the top left of Figure 87.

104
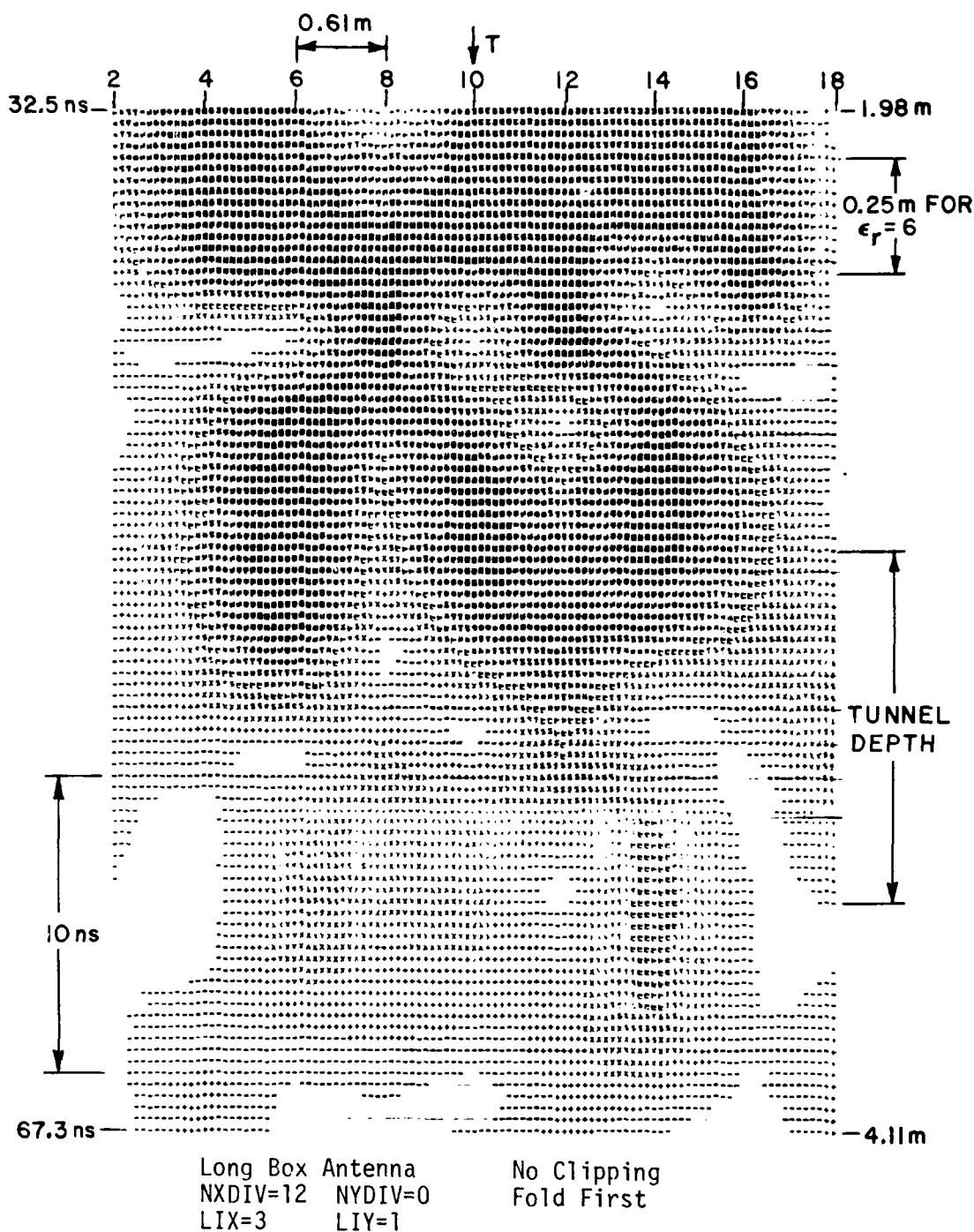
Figure 76. Gold Hill Map 1 Traverse C   Cross Section.

105
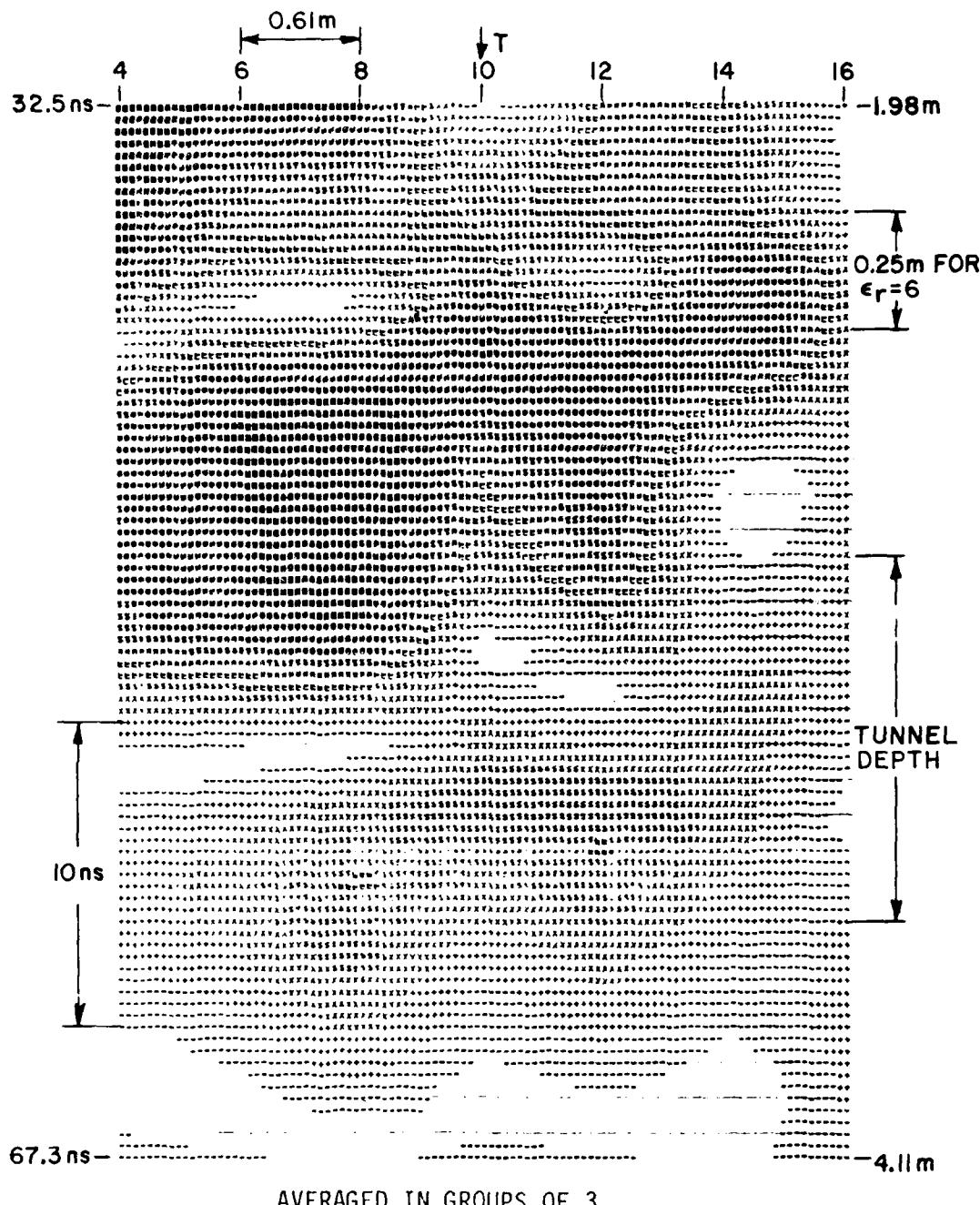
Figure 77.   Gold Hill Map 1 Traverse C   Cross Section.

106

FOR 2.74 m DEPTH

FOR 3.66 m DEPTH
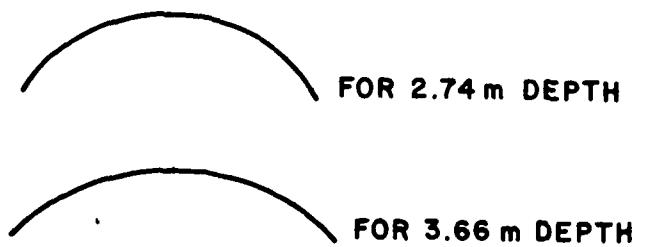
Figure 78.   Expected Hyperbolic Shape To Be Used With Figures
76, 77, 79, 80.
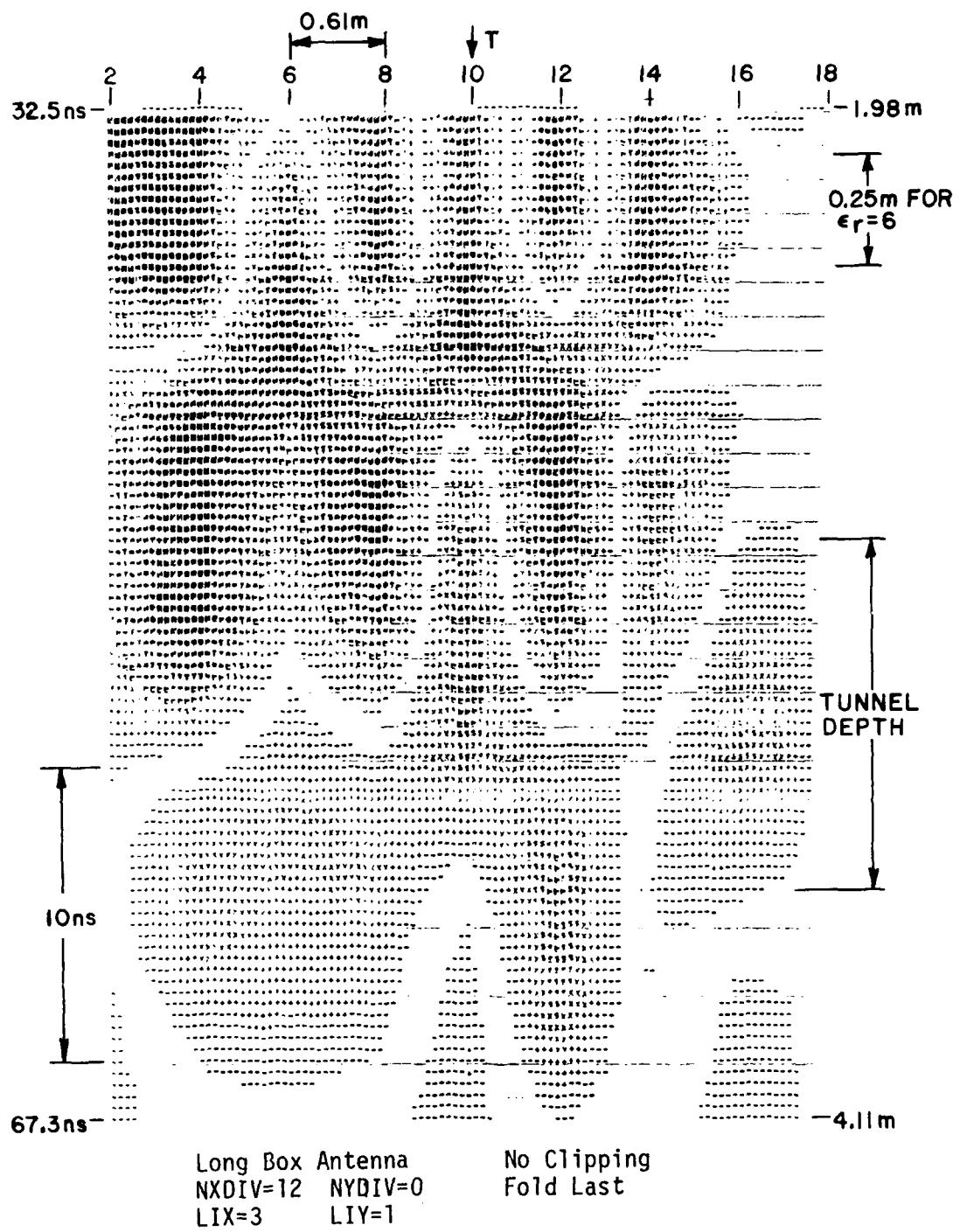
Figure 79. Gold Hill Map 1 Traverse C   Cross Section.

AVERAGED IN GROUPS OF 3
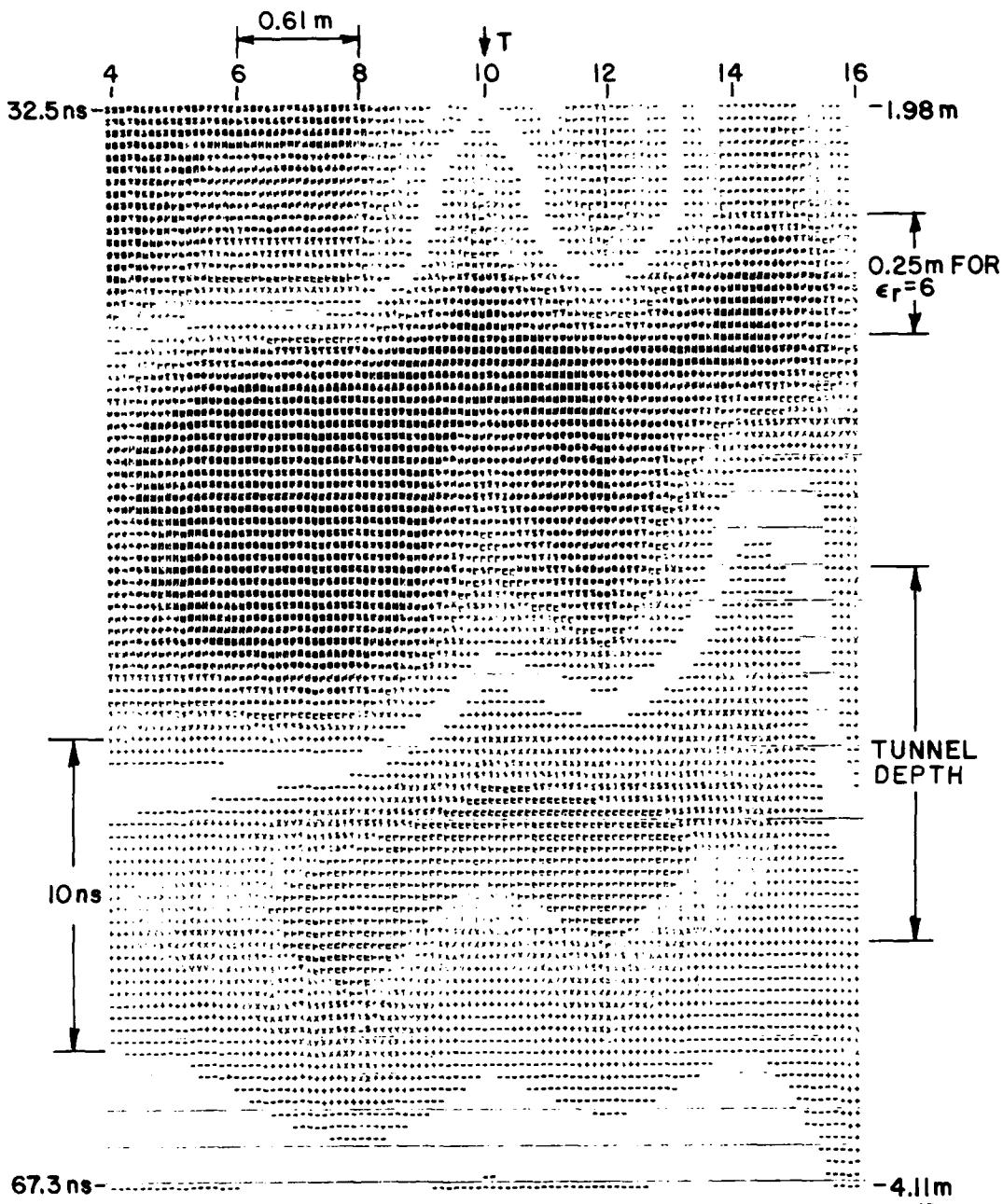
Long Box Antenna   Clipped at 2.4
NXDIV=16 NYDIV=0   Fold Last
LIX=3   LIY=1

Figure 80.   Gold Hill Map 1 Traverse C   Cross Section.

109
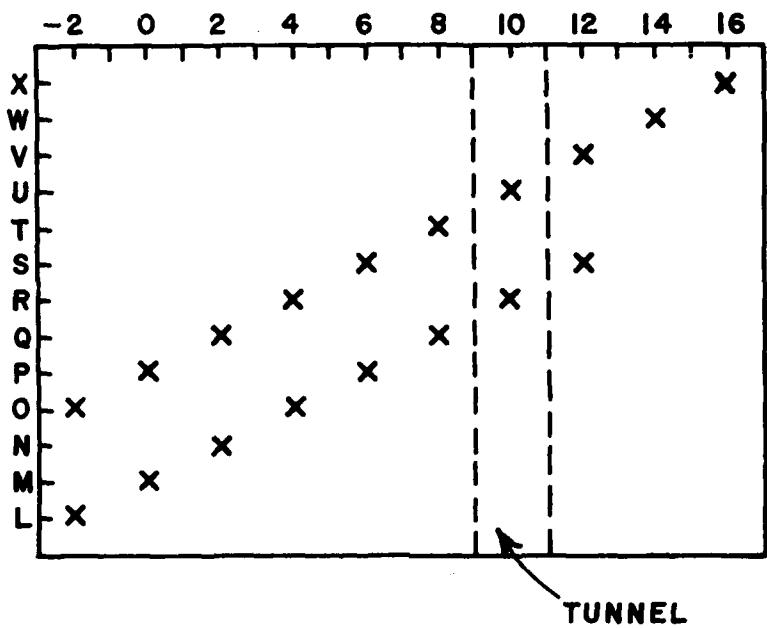
X = RECORDED WAVEFORM

GOLD HILL MAP 2

MEASUREMENT COORDINATES

Figure 81.
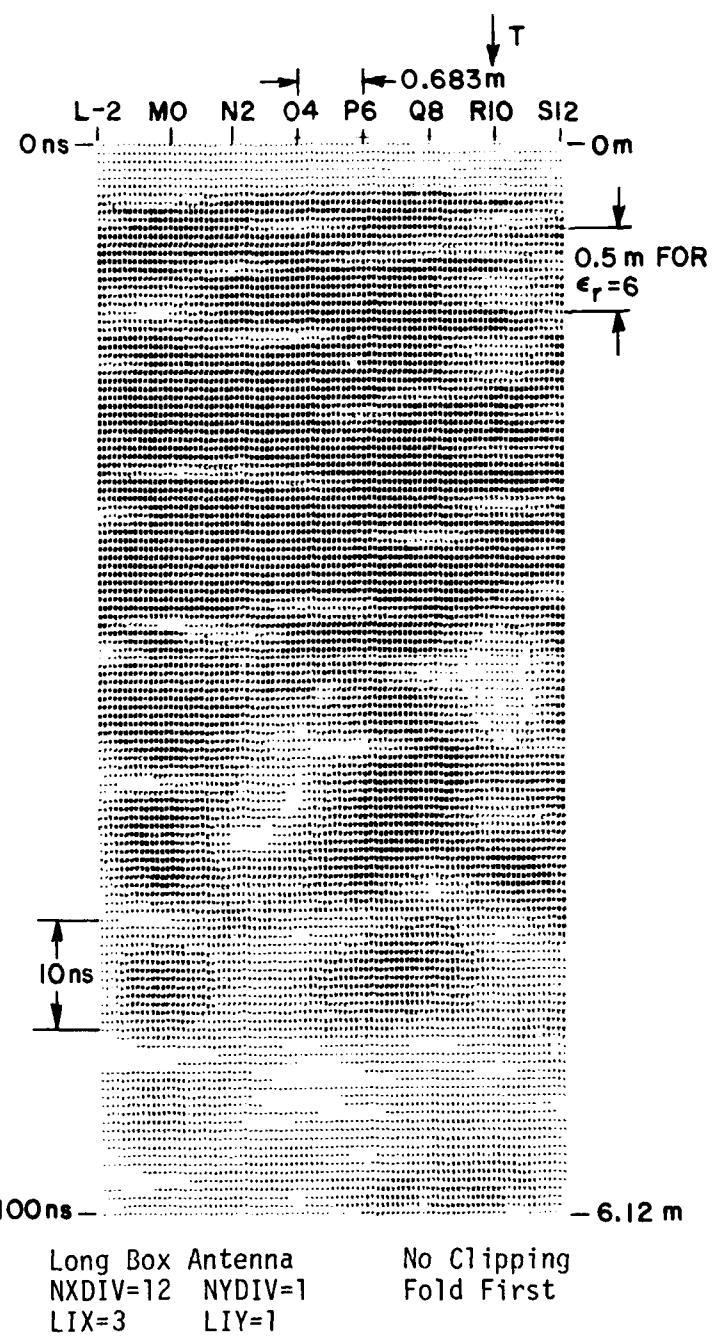
Figure 82. Gold Hill Map 2 Traverse L-2 to
S12   Cross Section.
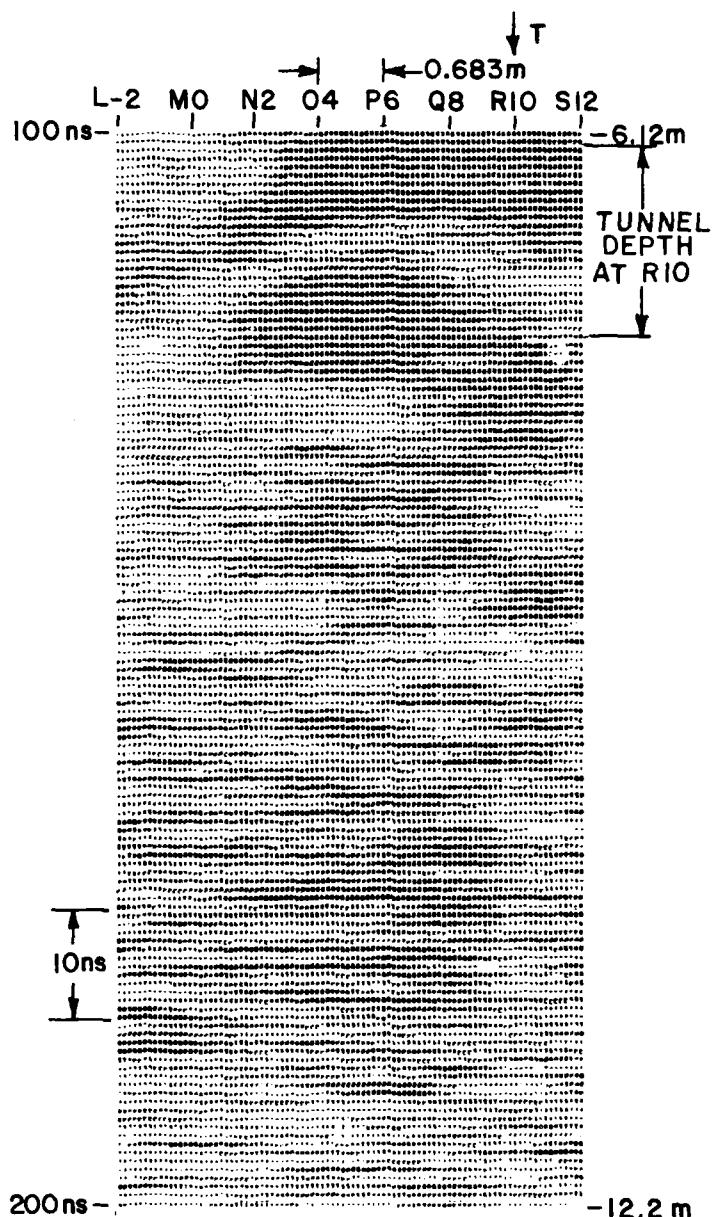
111

Figure 83.   Gold Hill Map 2 Traverse L-2 to
             S12   Cross Section.
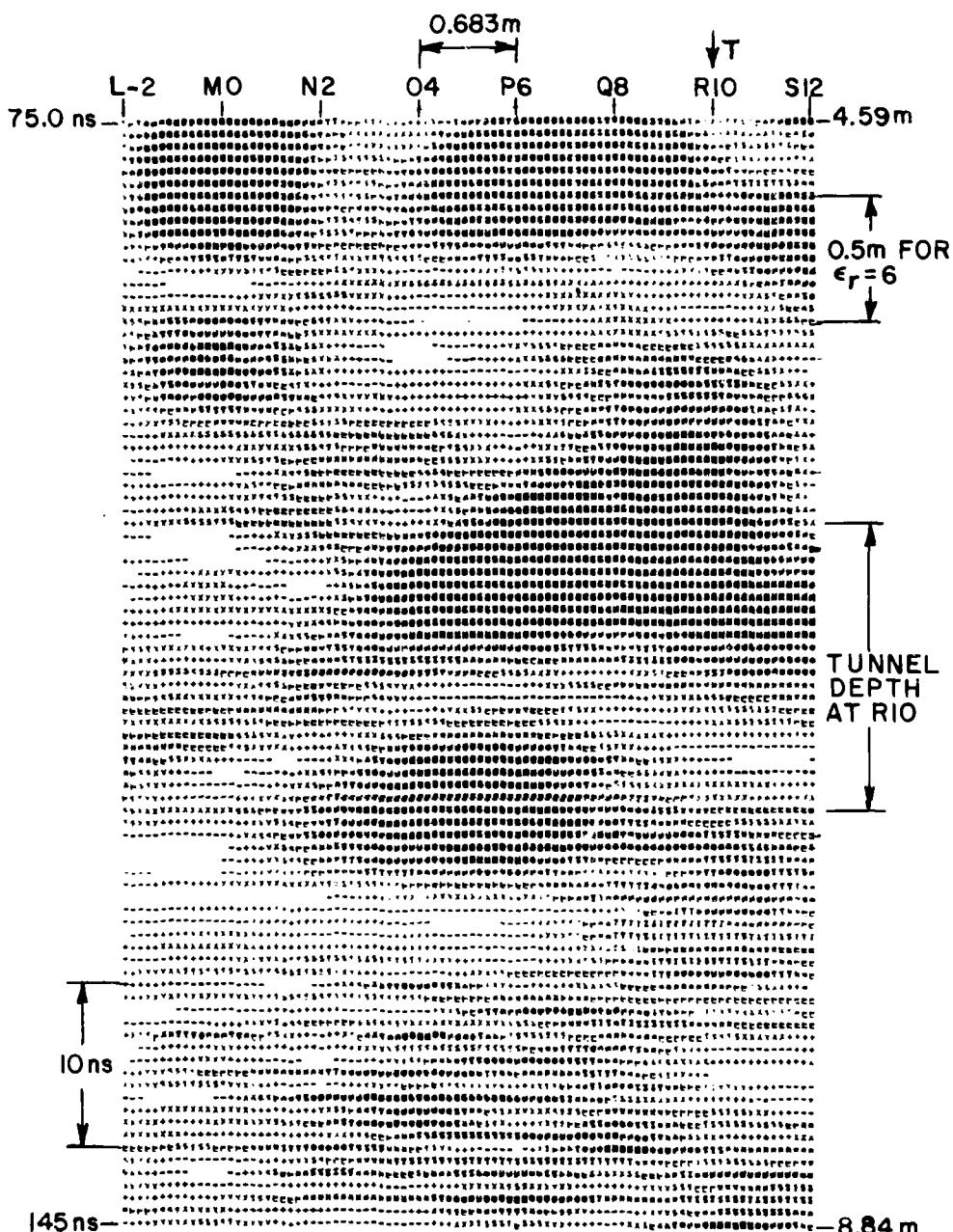
Figure 84. Gold Hill Map 2 Traverse L-2 to
S12   Cross Section.

113

FOR 6.1 m DEPTH

Figure 85.   Expected Hyperbolic Shape To Be Used With Figures
84, 86, 88-93, 96-103, 105, 106.
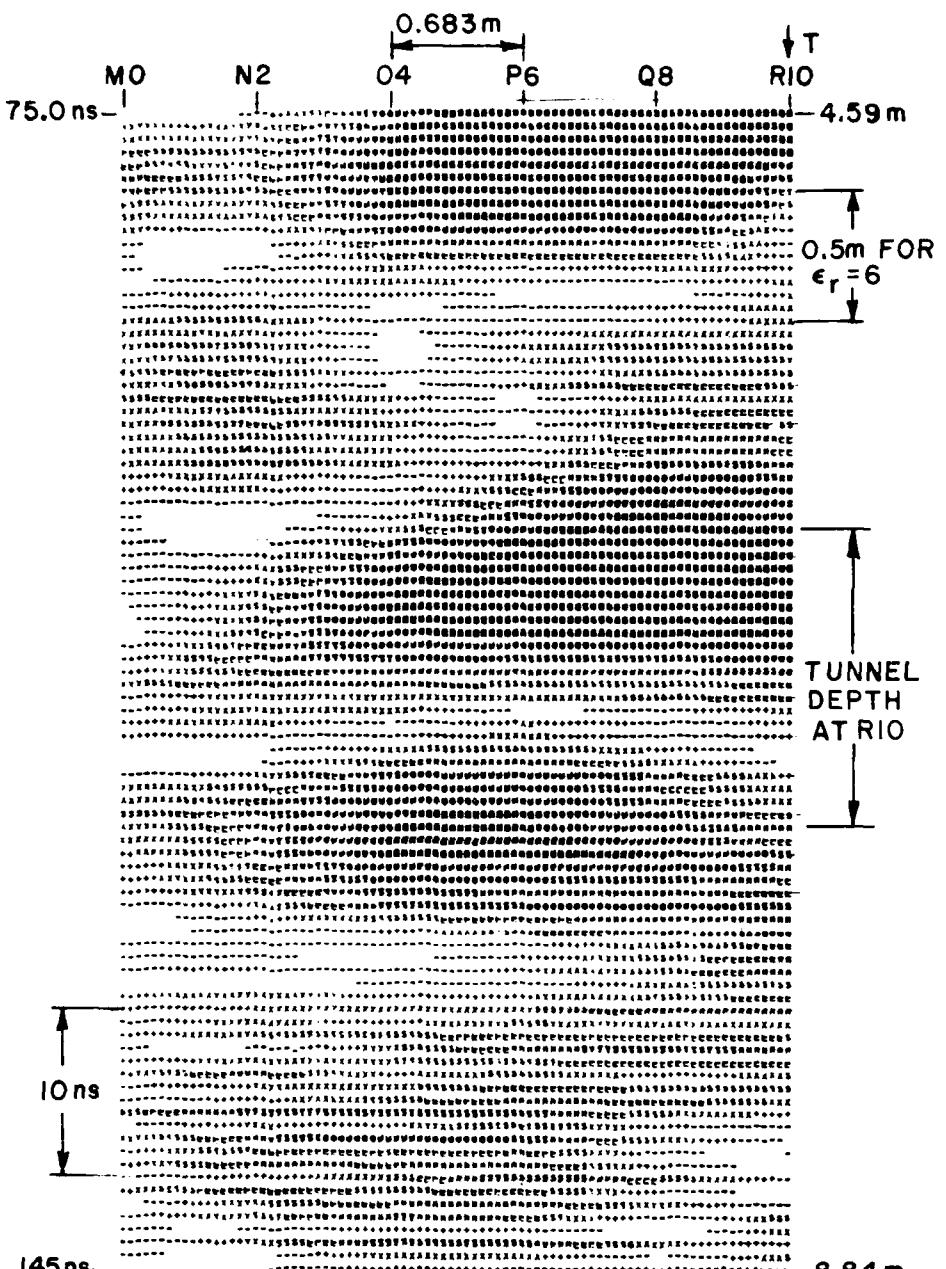
AVERAGED IN GROUPS OF 3

Long Box Antenna   Clipped at 1.61
NXDIV=16   NYDIV=0   Fold First
LIX=3   LIY=1

Figure 86.   Gold Hill Map 2 Traverse L-2 to
             S12   Cross Section.

115

TYPICAL
SIGNAL (MO)

FFT OF TYPICAL
SIGNAL

40ns

0 MHz   1270 MHz

FILTER CORNERS
320, 360 MHz

FILTER CORNERS
160, 200MHz

FILTER CORNERS
100, 140 MHz

FILTER CORNERS
60, 100MHz

FILTER CORNERS
40, 80 MHz
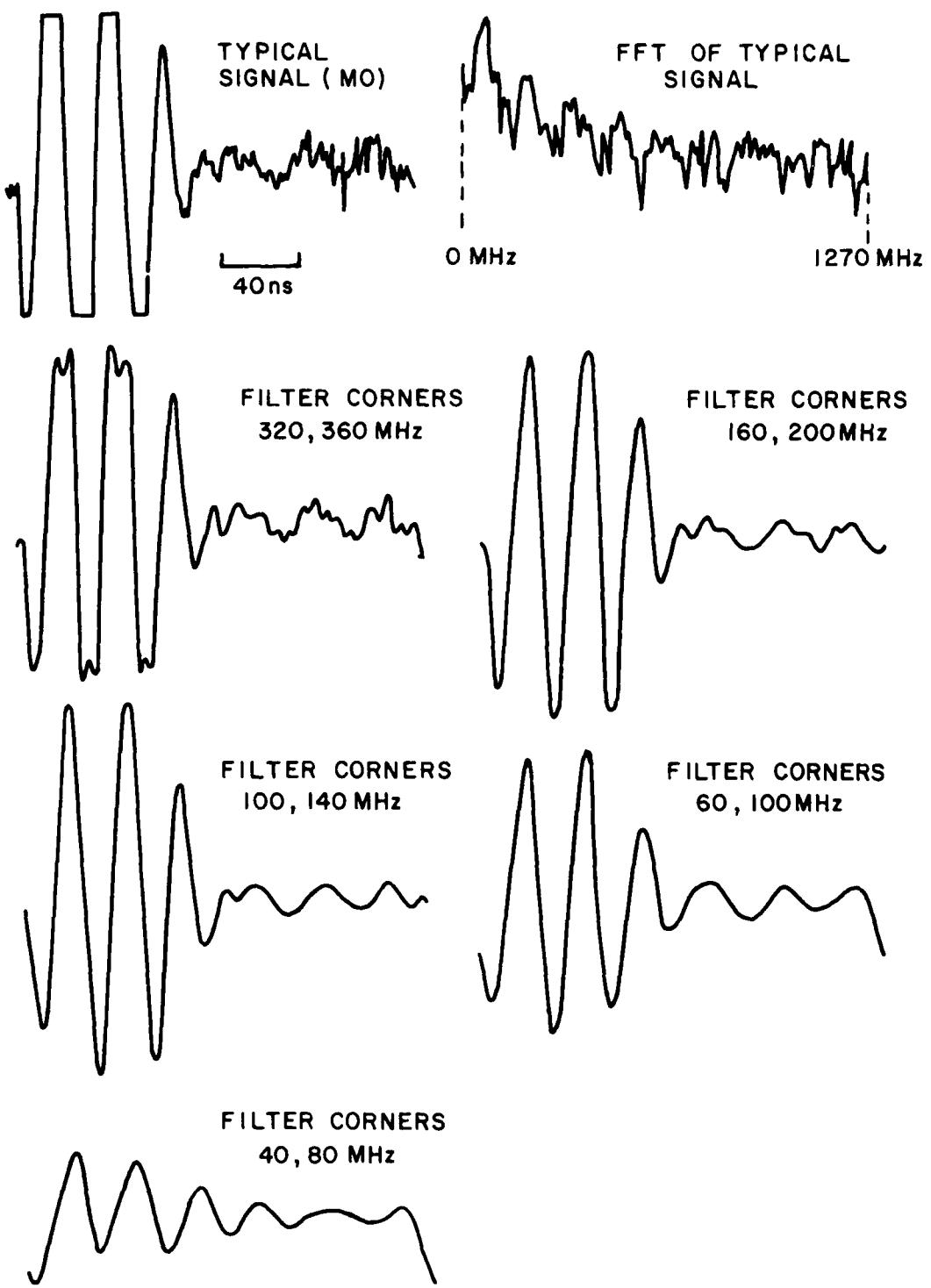
Figure 87.   Determination of Best Trapezoidal Low-Pass Filter
for Gold Hill Map 2 Data.

116

Low-pass filtering was chosen as the method to remove this noise. That is, the waveforms used as input to GLPR would be filtered. Figure 87 shows the effect of several successively narrower low pass filters on one waveform from this traverse. A trapezoidal filter was finally chosen with lower corner frequency at 100 MHz and upper corner frequency at 140 MHz. This filter removed most of the noise without adversely affecting the waveshape. Figure 88 then shows the grey scale plot of the filtered data. Figure 89 results from first filtering the data and then averaging it for clutter reduction. This clearly shows the appropriate darkened area in the region where the tunnel response is expected. It also contains the response from both the roof and floor of the tunnel.

The data from this traverse was also processed using the FOLD LAST method. The same set of processing techniques was used as before. Figures 90-93 show the results of: 1) just clipping, 2) 3-waveform averaging, 3) filtering and 4) filtering and then averaging, respectively. Note that in this group of plots there are two hyperbolic forms at approximately the right depth and that they have the same general shape as the calculated curve (Figure 85). This could perhaps be explained as reflections from both the roof and floor of the tunnel.

The next group of figures presents the data from the other diagonal traverse shown in Figure 81, namely that from 0-2 to X16. Figures 94 and 95 are two halves of the complete waveform set with Figure 94 spanning 0-100 ns and Figure 95 100-200 ns. It can readily be seen that noise was a problem on these measurements also by observing Figure 95.

The depth window chosen for the last traverse (75-145 ns) was also used here. Figure 96 shows the basic grey level plot while Figure 85 is the expected hyperbolic shape. Figure 97 is the clutter-reduced version.

The same low pass filtering method (with the same filter corners) was used also. Figure 98 is the unaveraged but filtered data and Figure 99 is the data after first filtering then averaging.

Versions of these plots using the FOLD LAST method were also made. Figures 100-103 are the 0-2 traverse after 1) normal grey level plotting, 2) 3-waveform averaging, 3) low-pass filtering and 4) filtering then averaging, respectively.

Another useful processing technique was also tried out on this data. As shown in Figure 104, the normal use of the folding function (i.e., absolute value) in grey level plotting, using either the FOLD FIRST or FOLD LAST methods, causes positive and negative peaks to be mixed.
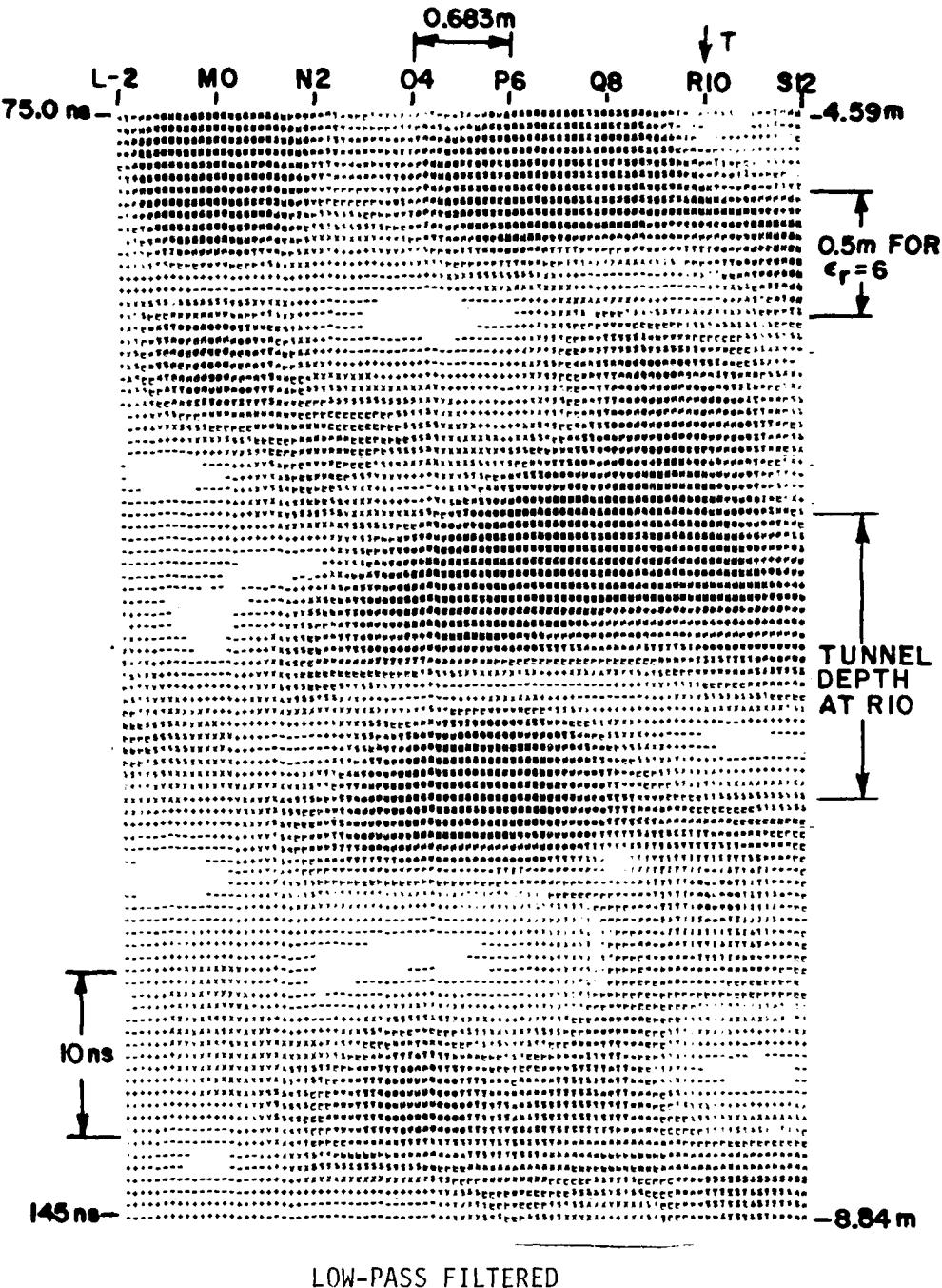
LOW-PASS FILTERED

Long Box Antenna   Clipped at 1.62
NXDIV=12   NYDIV=0   Fold First
LIX=3   LIY=1

Figure 88.   Gold Hill Map 2 Traverse L-2 to S12   Cross Section.
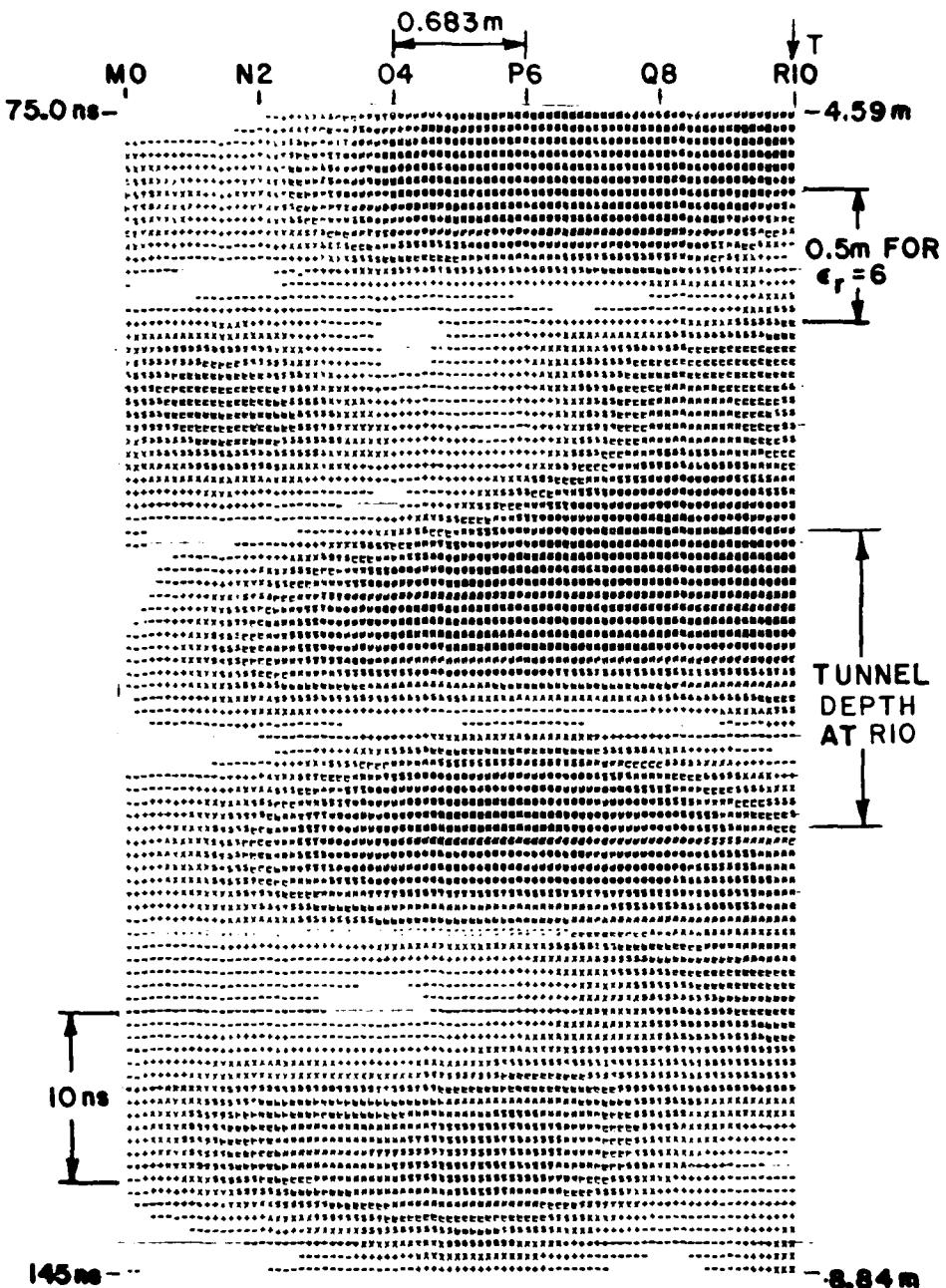
LOW-PASS FILTERED AND AVERAGED IN GROUPS OF 3

Long Box Antenna   Clipped at 1.6
NXDIV=16   NYDIV=0   Fold First
LIX=3   LIY=1

Figure 89.   Gold Hill Map 2 Traverse L-2 to S12
Cross Section.
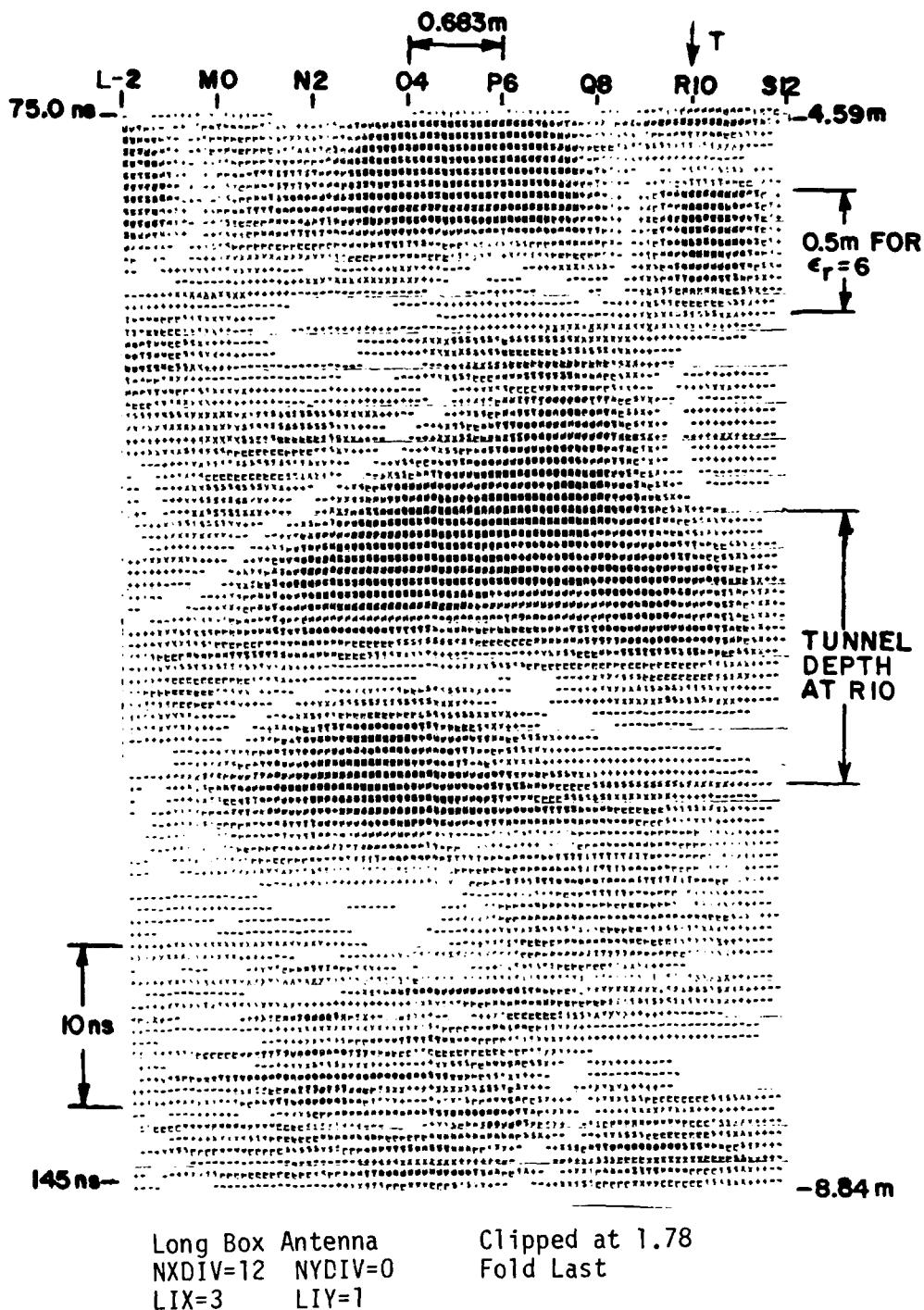
Figure 90. Gold Hill Map 2 Traverse L-2 to S12
Cross Section.

AVERAGED IN GROUPS OF 3
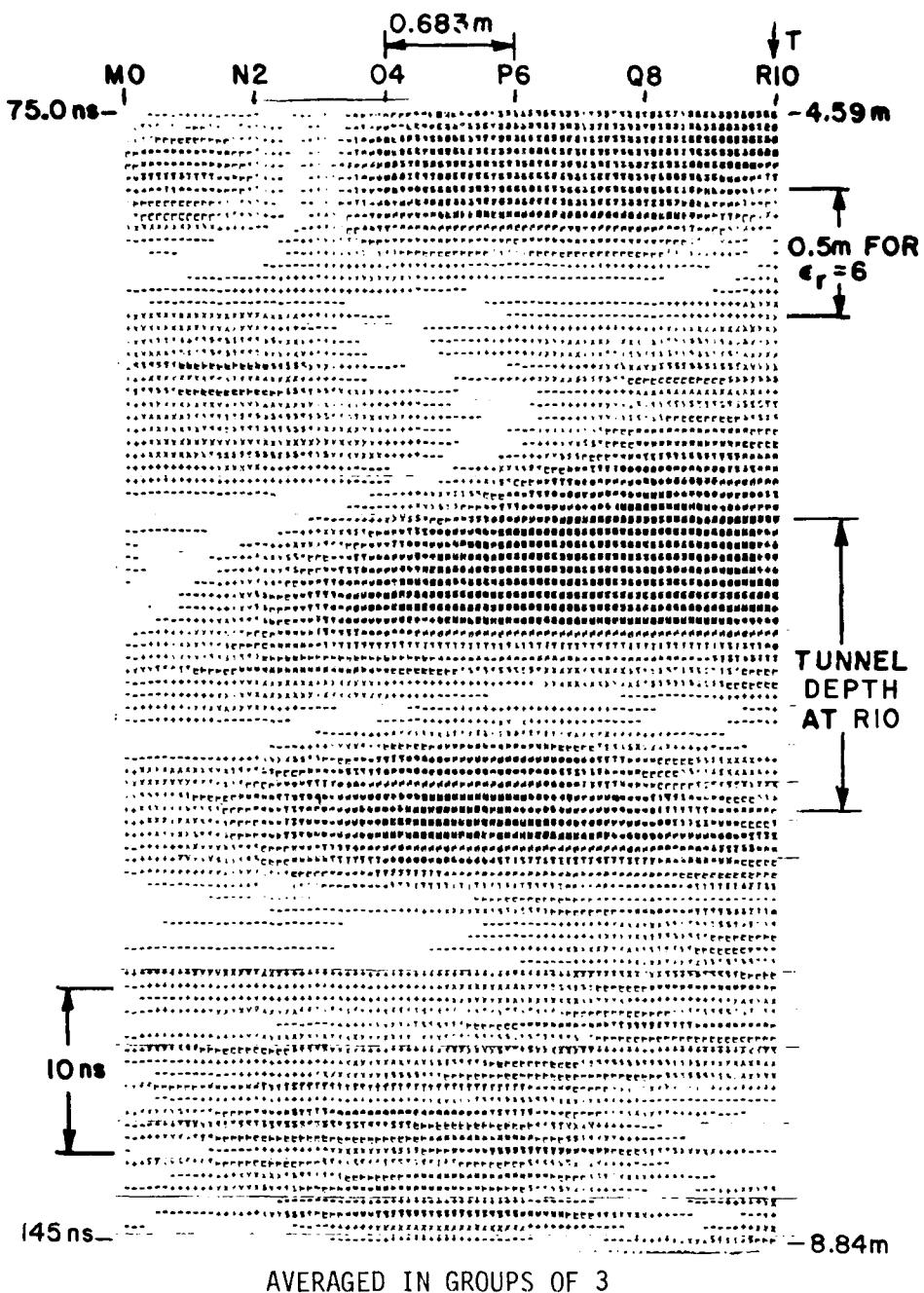
Long Box Antenna   Clipped at 1.63
NXDIV=16   NYDIV=0   Fold Last
LIX=3   LIY=1

Figure 91. Gold Hill Map 2 Traverse L-2 to S12
            Cross Section.
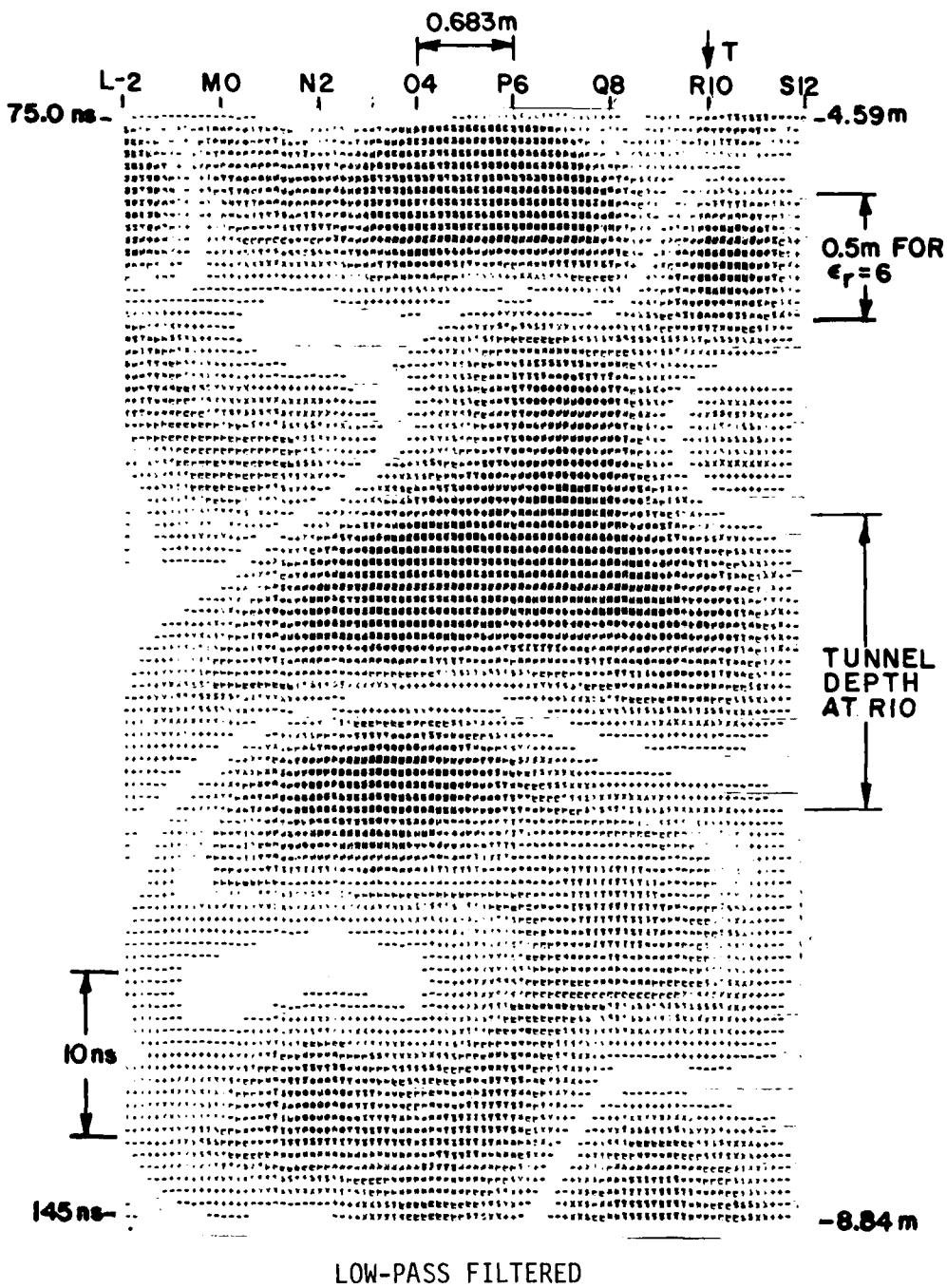
LOW-PASS FILTERED

Long Box Antenna   Clipped at 1.65
NXDIV=12   NYDIV=0   Fold Last
LIX=3   LIY=1

Figure 92.   Gold Hill Map 2 Traverse L-2 to S12
             Cross Section.
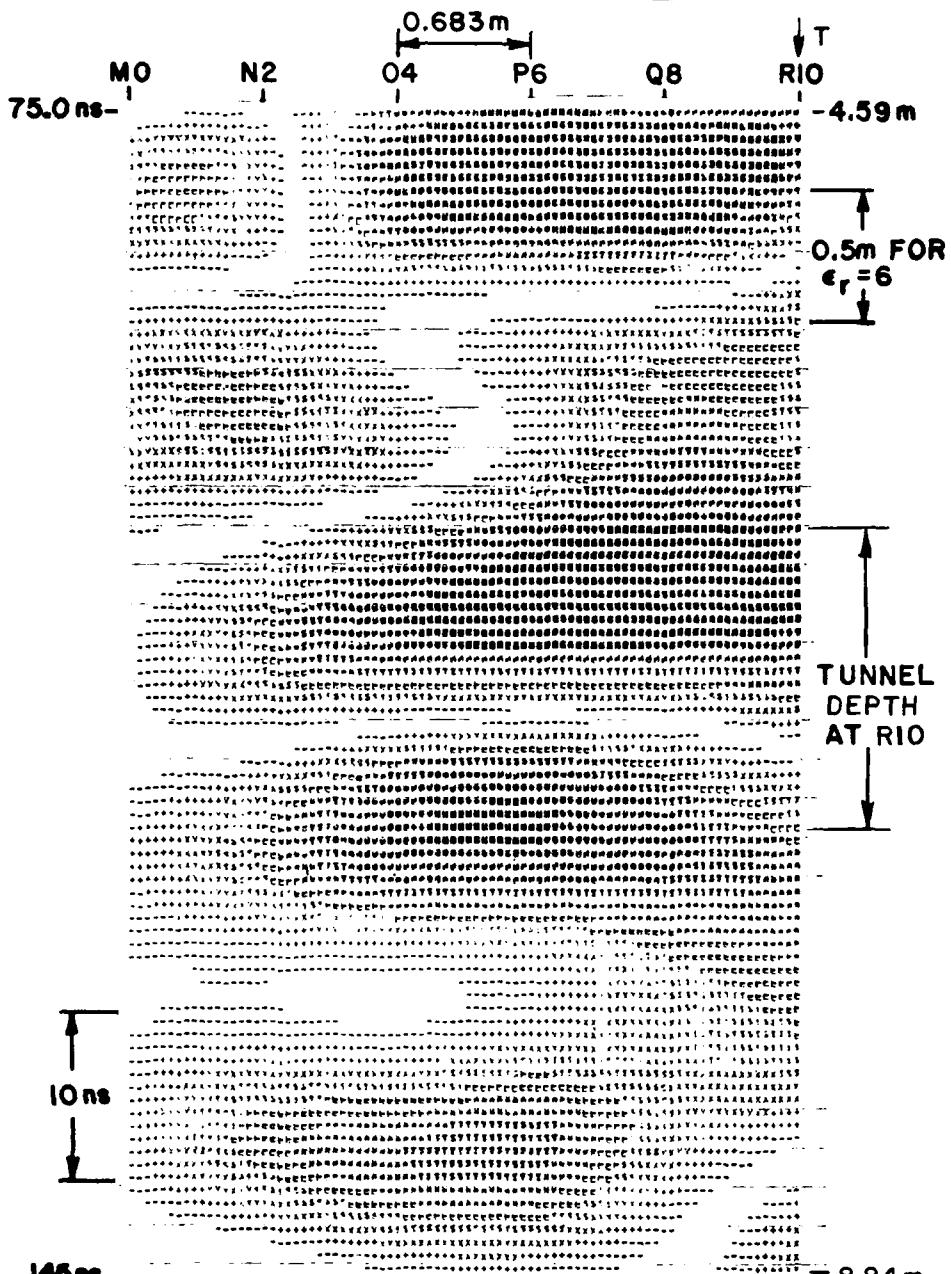
122

LOW-PASS FILTERED AND AVERAGED IN GROUPS OF 3

Long Box Antenna	Clipped at 1.61
NXDIV=16 NYDIV=0	Fold Last
LIX=3 LIY=1	

Figure 93. Gold Hill Map 2 Traverse L-2 to S12
Cross Section.
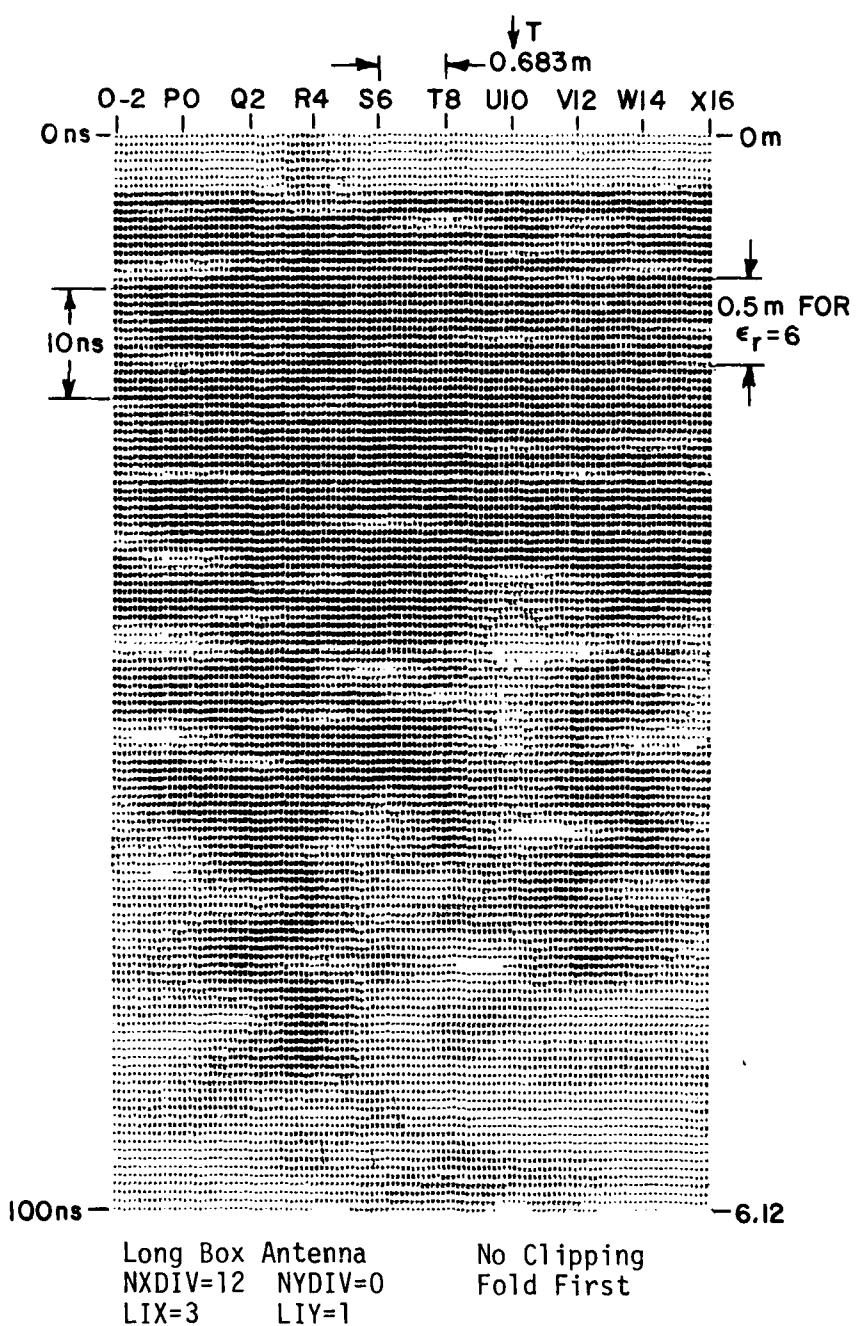
Figure 94. Gold Hill Map 2 Traverse O-2 to X16
Cross Section.
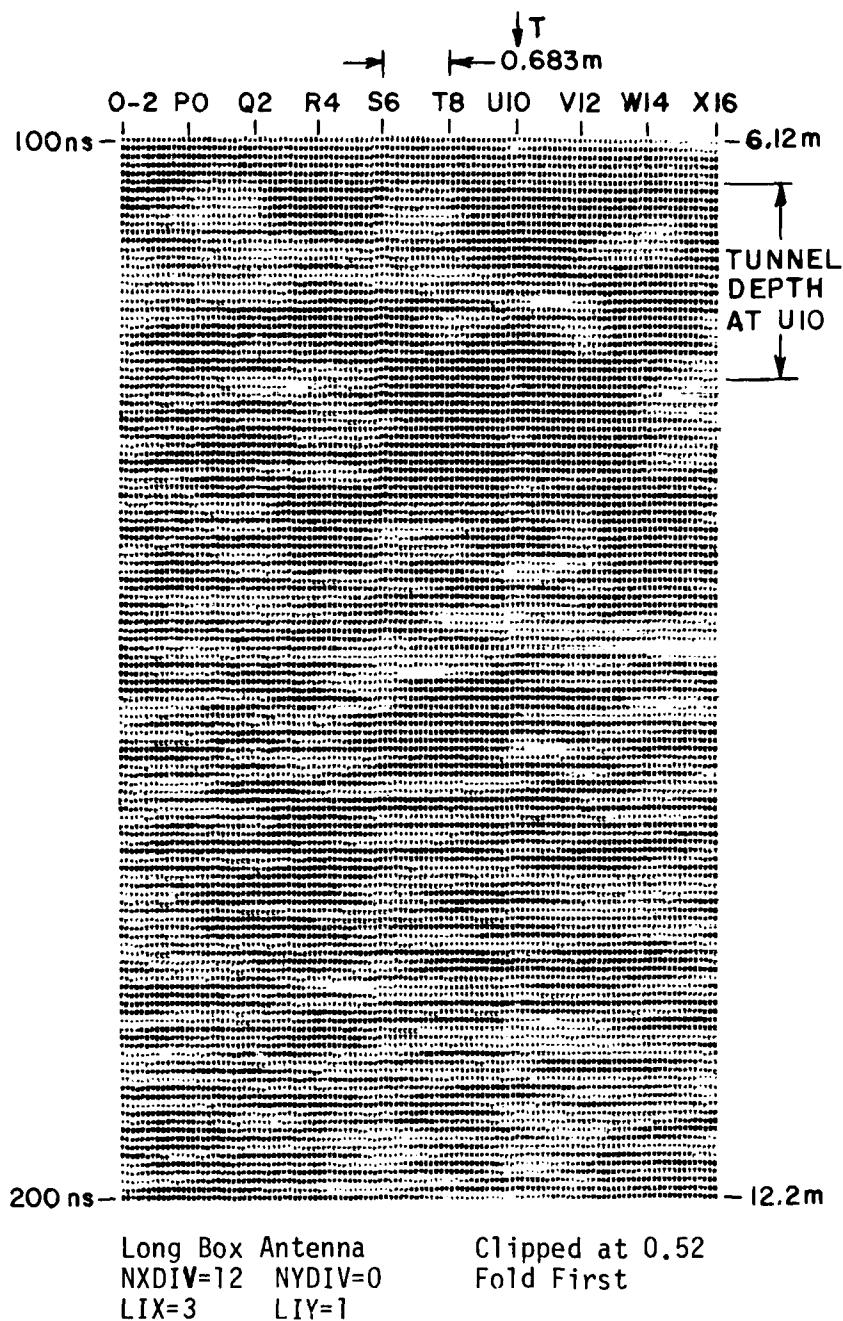
Figure 95.   Gold Hill Map 2 Traverse O-2 to X16
             Cross Section.

125

Long Box Antenna   Clipped at 1.95
NXDIV=12 NYDIV=0   Fold First
LIX=3   LIY=1
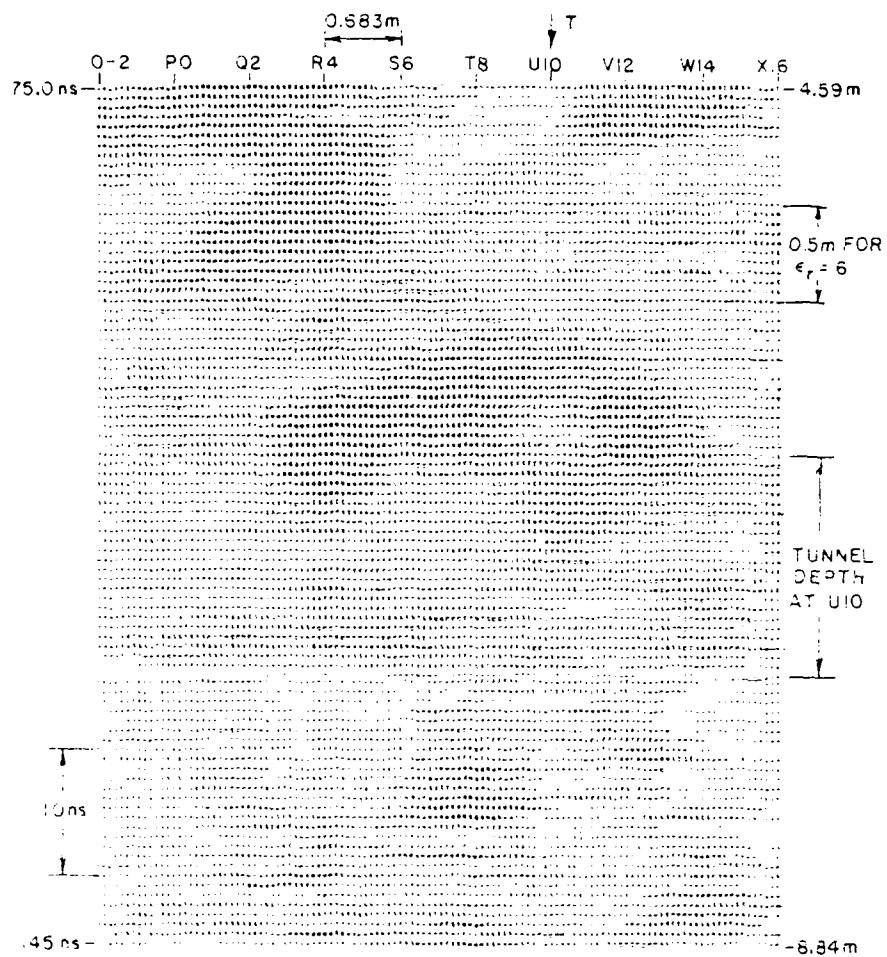
Figure 96.   Gold Hill Map 2 Traverse 0-2 to X16
Cross Section.
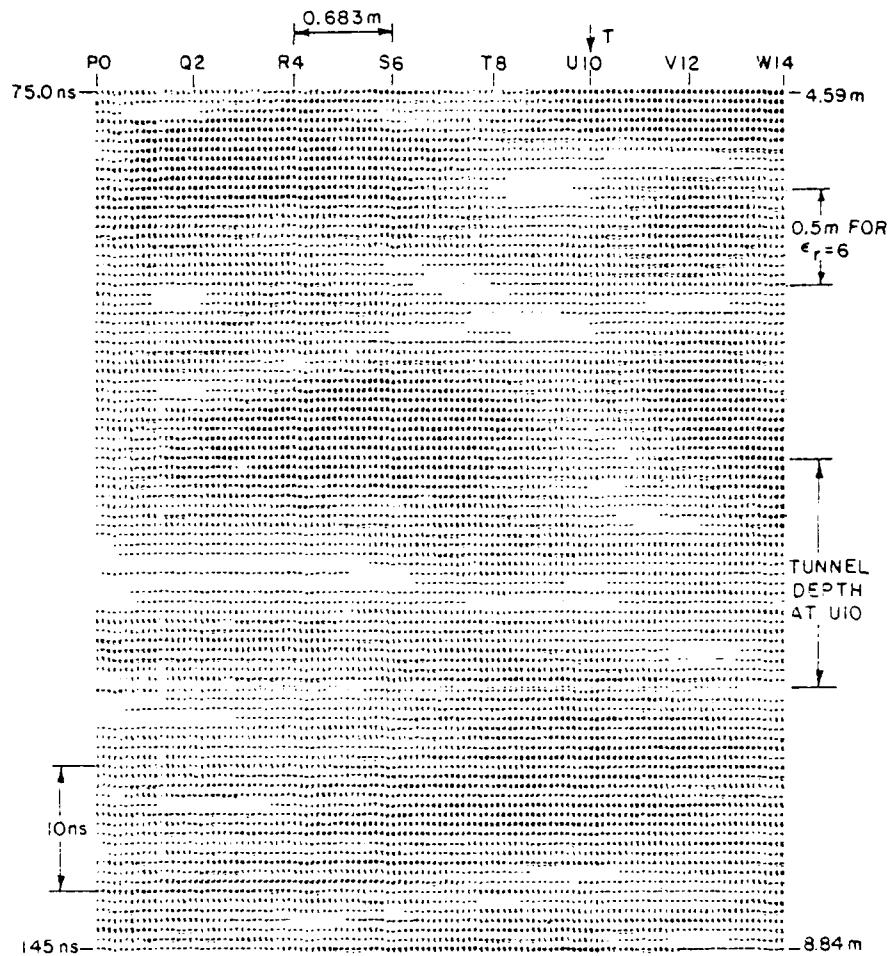
AVERAGED IN GROUPS OF 3

Long Box Antenna		Clipped at 1.15
NXDIV=16	NXDIV=0	Fold First
LIX=3	LIY=1	

Figure 97. Gold Hill Map 2 Traverse 0-2 to X16 Cross Section.

127
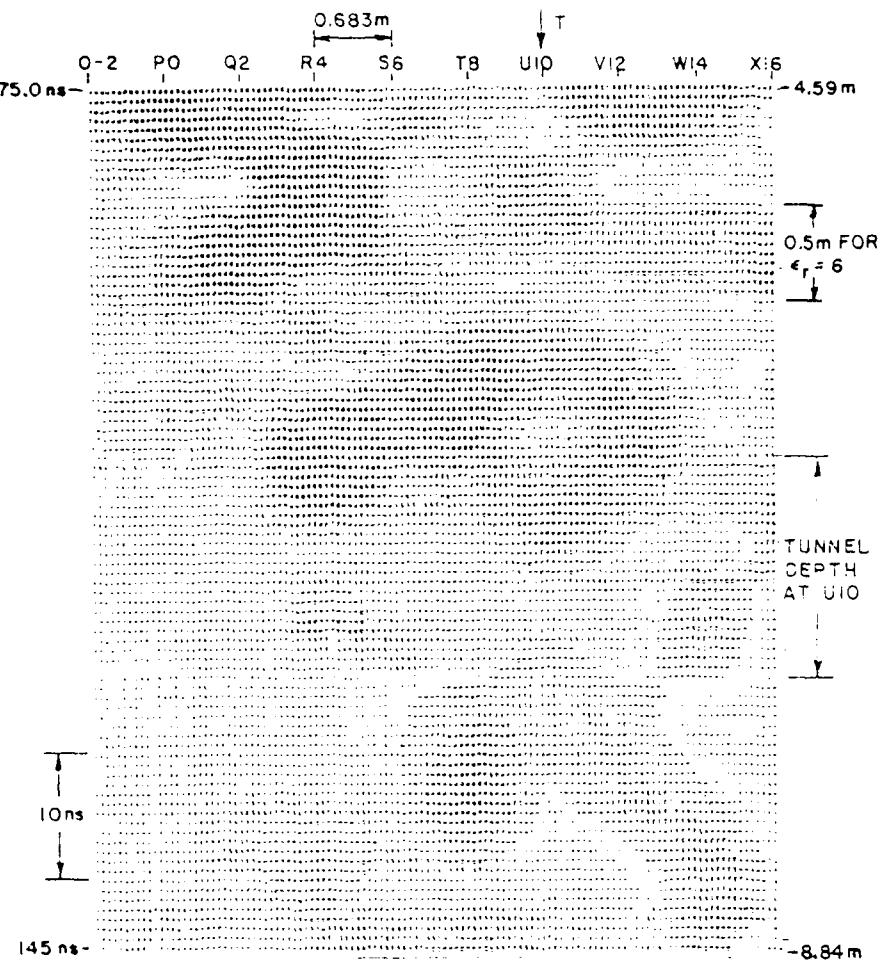
LOW-PASS FILTERED

Long Box Antenna   Clipped at 1.8
NXDIV=12   NYDIV=0   Fold First
LIX=3   LIY=1

Figure 98.   Gold Hill Map 2 Traverse 0-2 to X16
            Section.
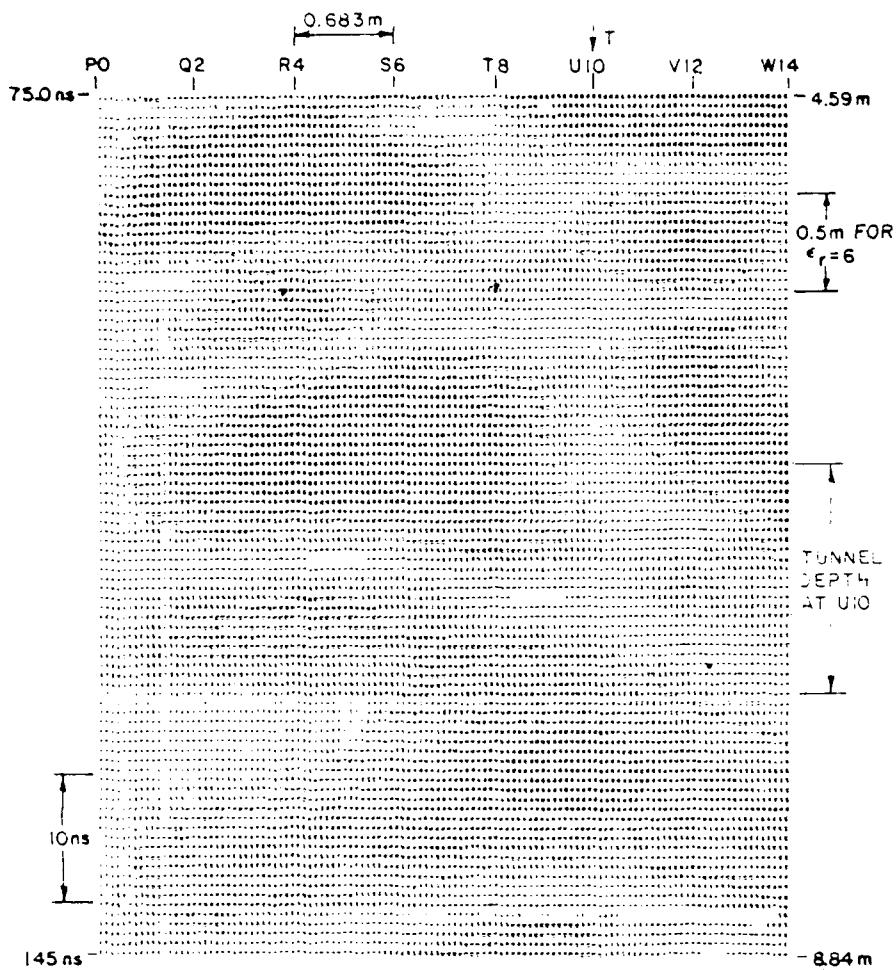
LOW-PASS FILTERED AND AVERAGED IN GROUPS OF 3

Long Box Antenna   Clipped at 1.14
NXDIV=16   NYDIV=0   Fold First
LIX=3   LIY=1

Figure 99.   Gold Hill Map 2 Traverse 0-2 to X16
             Cross Section.
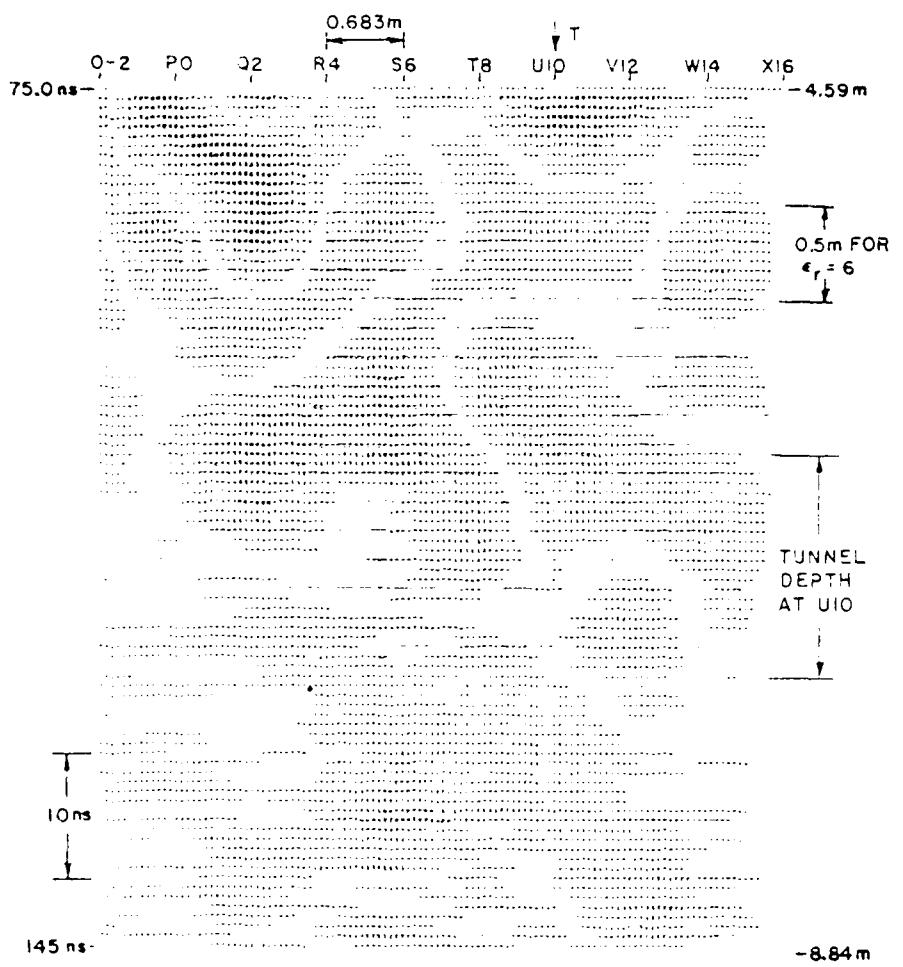
Figure 100. Gold Hill Map 2 Traverse 0-2 to X16 Cross Section.
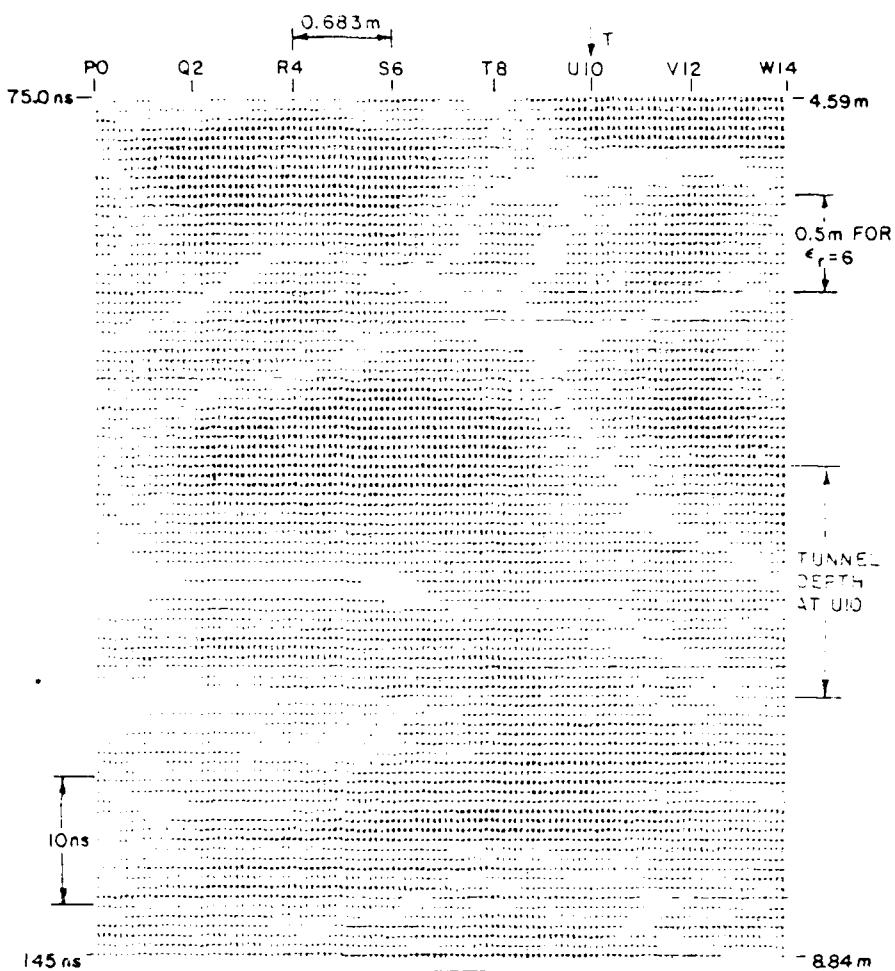
AVERAGED IN GROUPS OF 3

Long Box Antenna   Clipped at 1.17
NXDIV=16   NYDIV=0   Fold Last
LIX=3   LIY=1

Figure 101.   Gold Hill Map 2 Traverse 0-2 to X16
              Cross Section.
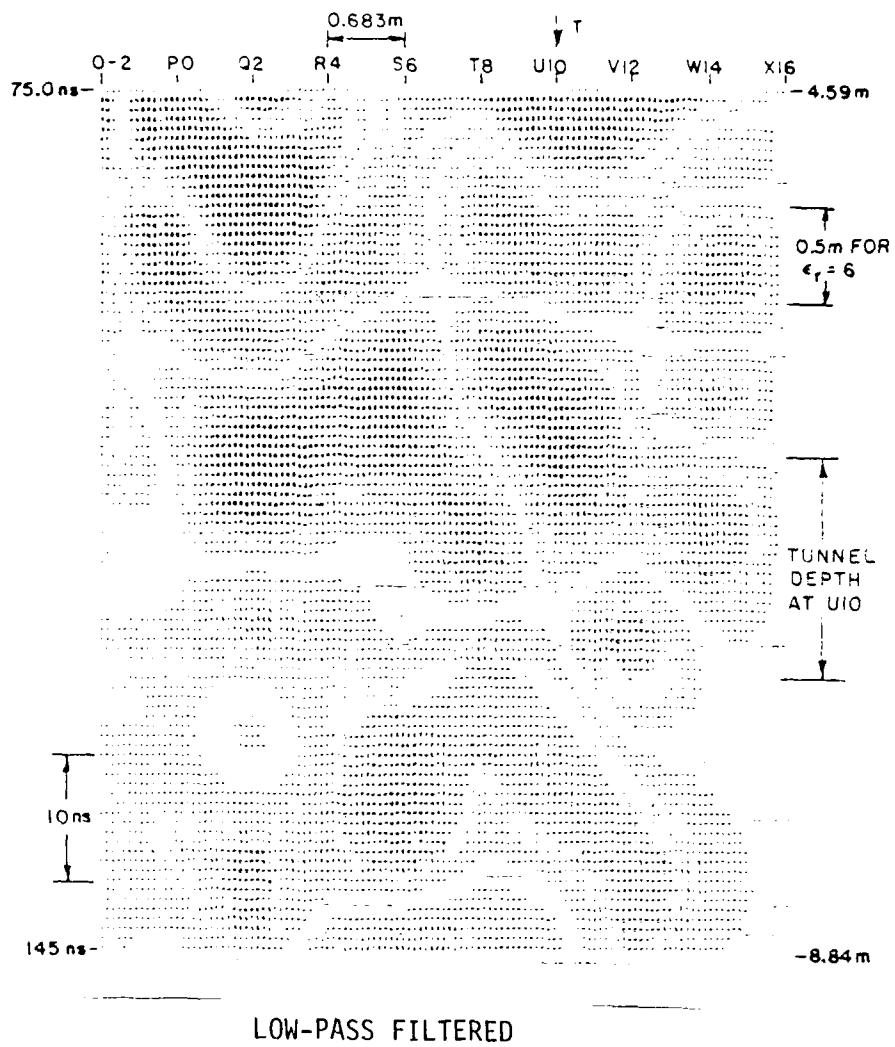
LOW-PASS FILTERED

Long Box Antenna   Clipped at 1.91
NXDIV=12   NYDIV=0   Fold Last
LIX=3   LIY=1

Figure 102. Gold Hill Map 2 Traverse 0-2 to X16
             Cross Section.
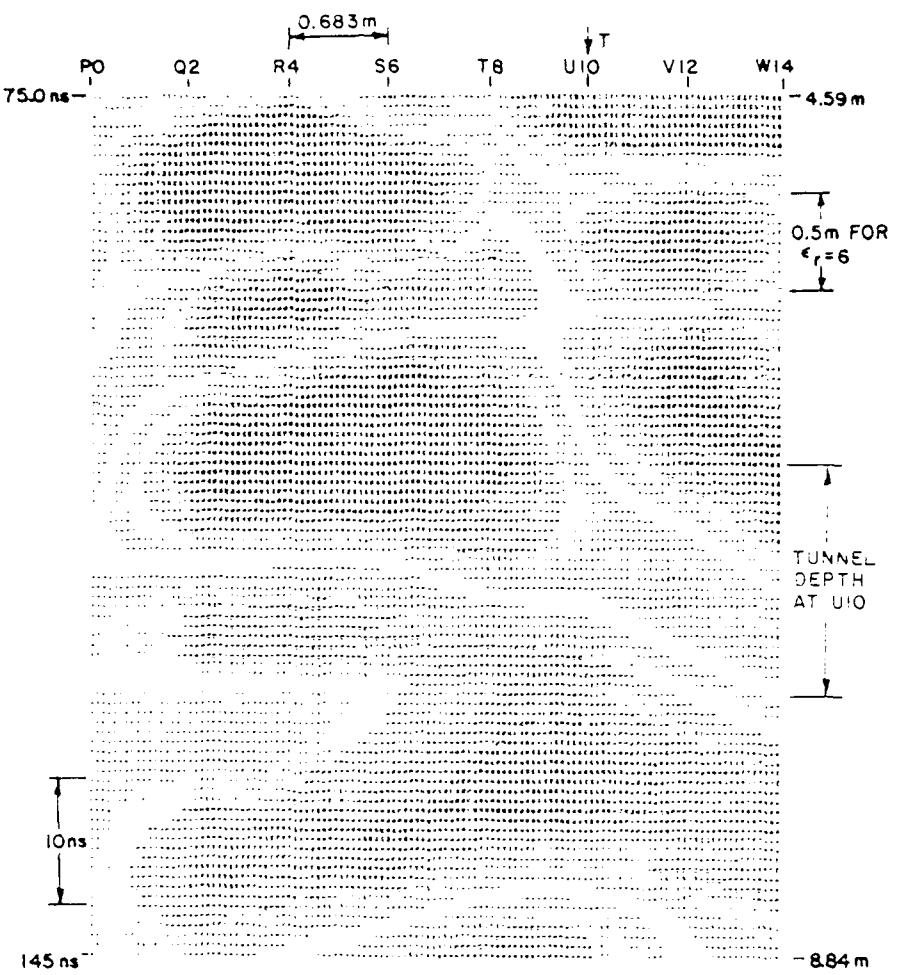
LOW-PASS FILTERED AND AVERAGED IN GROUPS OF 3

Long Box Antenna   Clipped at 1.01
NXDIV=16   NYDIV=0   Fold Last
LIX=3   LIY=1

Figure 103:   Gold Hill Map 2 Traverse 0-2 to X16
              Cross Section.
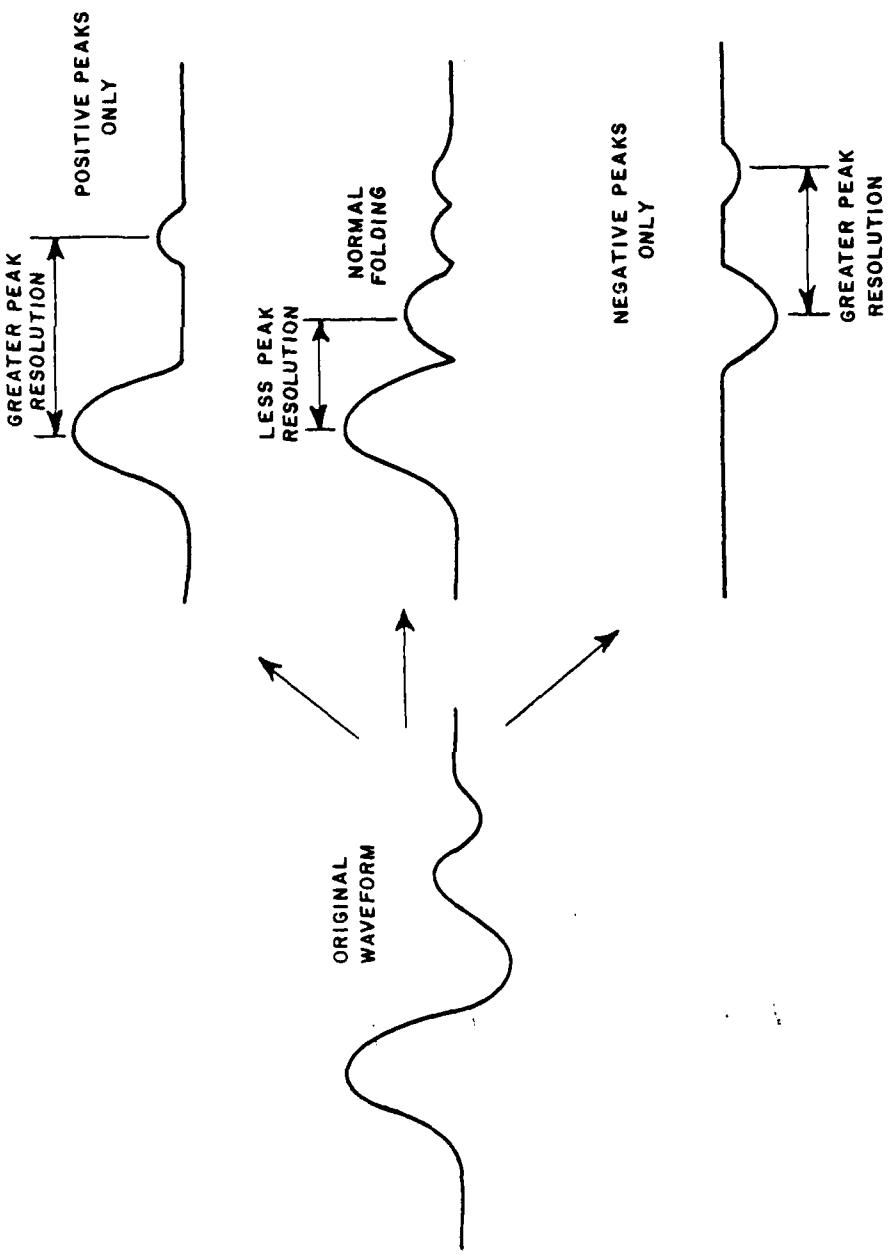
Figure 104. Method to Improve Peak Resolution.

134

If only one polarity needs to be tracked to detect the tunnel then plotting both polarities on one graph increases the visual "confusion" level. Plotting only one polarity of a waveform set should increase the ability to discern a target, as is also shown in Figure 104.

This type of plotting was done using the O-2 traverse data without filtering or averaging. The results are shown in Figures 105 and 106. Figure 105 exhibits the positive portions only and Figure 106 exhibits the negative portions only. These plots may be compared to Figure 100 in which both polarities are plotted. Figure 105 would presumably show the reflection from the top of the tunnel and it does appear to be present in the midst of much clutter. Figure 106 should show the reflection from the floor of the tunnel since the reflection coefficient at the lower interface is opposite in sign.

Just prior to completion of the present thesis, a new processing technique which appears to offer much promise for future mapping efforts was developed. Using data from the Gold Hill Map 2 traverses (specifically waveforms T8-X16), a set of poles describing each waveform in the Z-transform domain was calculated. Using the physical dimensions of the tunnel to determine its natural resonances, only poles near these resonances are kept for further processing, effectively deconvolving out the unwanted signal components from the antenna structure.

A new waveform is then generated using only the selected poles. This waveform should include the tunnel response almost exclusively. Some clutter may be present. Figure 107 shows the grey level plot obtained from this deconvolved data. Note that the tunnel height and vertical position correspond exactly to the calculated values and that the shape that appears is very similar to the analytic one shown in Figure 63. The only apparent error is the lateral displacement of the hyperbolic shape to the left. This is possibly explained by the fact that position calculations for the tunnel did not include the side slope of the hill on which measurements were taken. As shown in Figure 108, if the traverse over the tunnel is not horizontal, the minimum depth to the tunnel (corresponding to the vertex of the hyperbola) would occur at a position offset to the left.

135
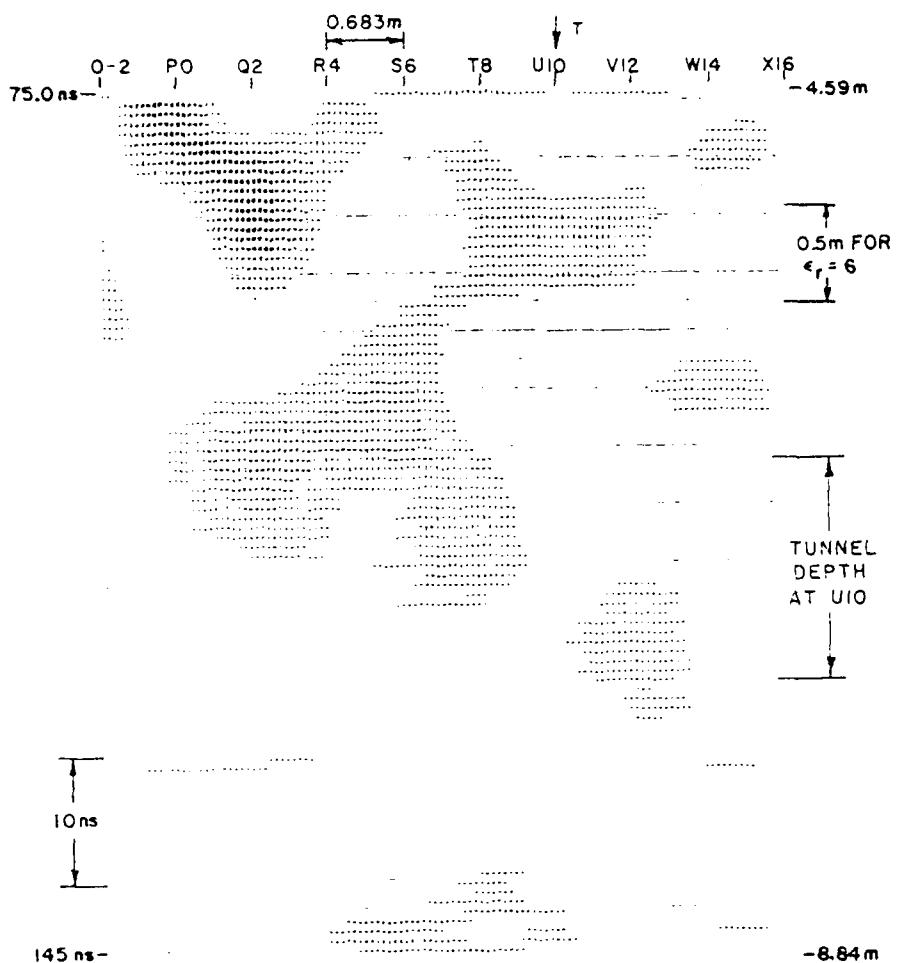
POSITIVE PORTIONS ONLY

Long Box Antenna   No Clipping
NXDIV=12 NYDIV=0   Fold Last
LIX=3   LIY=1

Figure 105. Gold Hill Map 2 Traverse 0-2 to X16
             Cross Section.

136
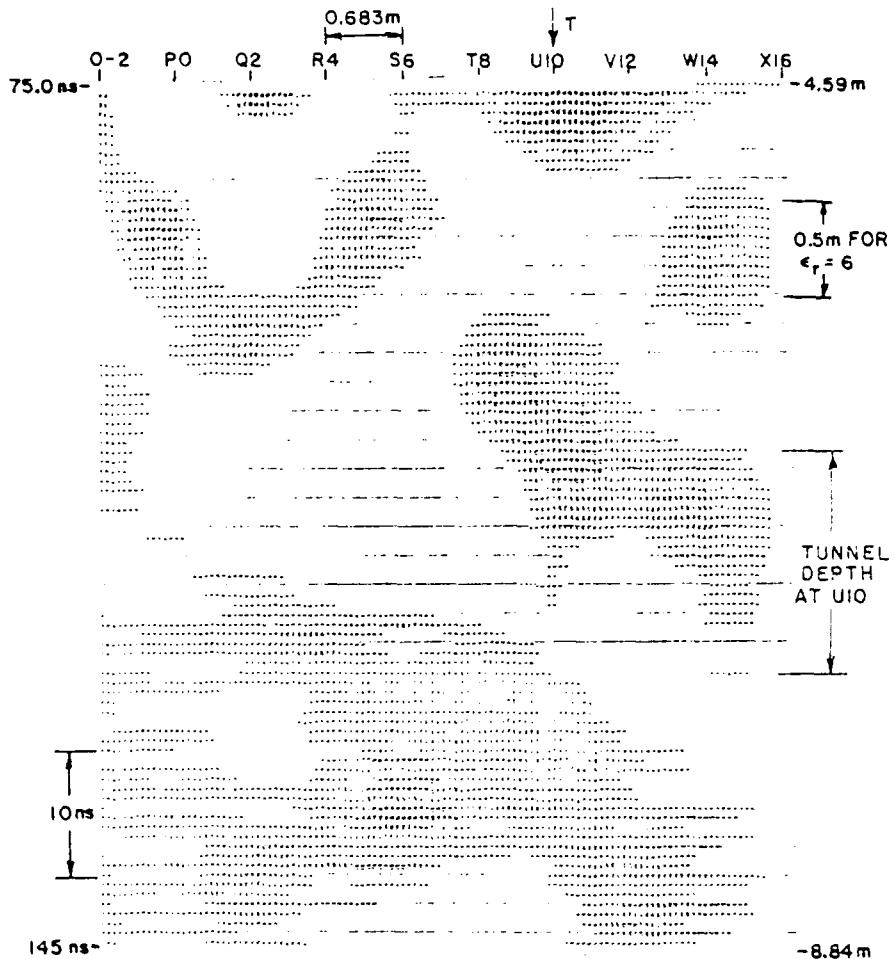
NEGATIVE PORTIONS ONLY

Long Box Antenna   No Clipping
NXDIV=12   NYDIV=0   Fold Last
LIX=3   LIY=1

Figure 106. Gold Hill Map 2 Traverse O-2 to X16
             Cross Section.

137
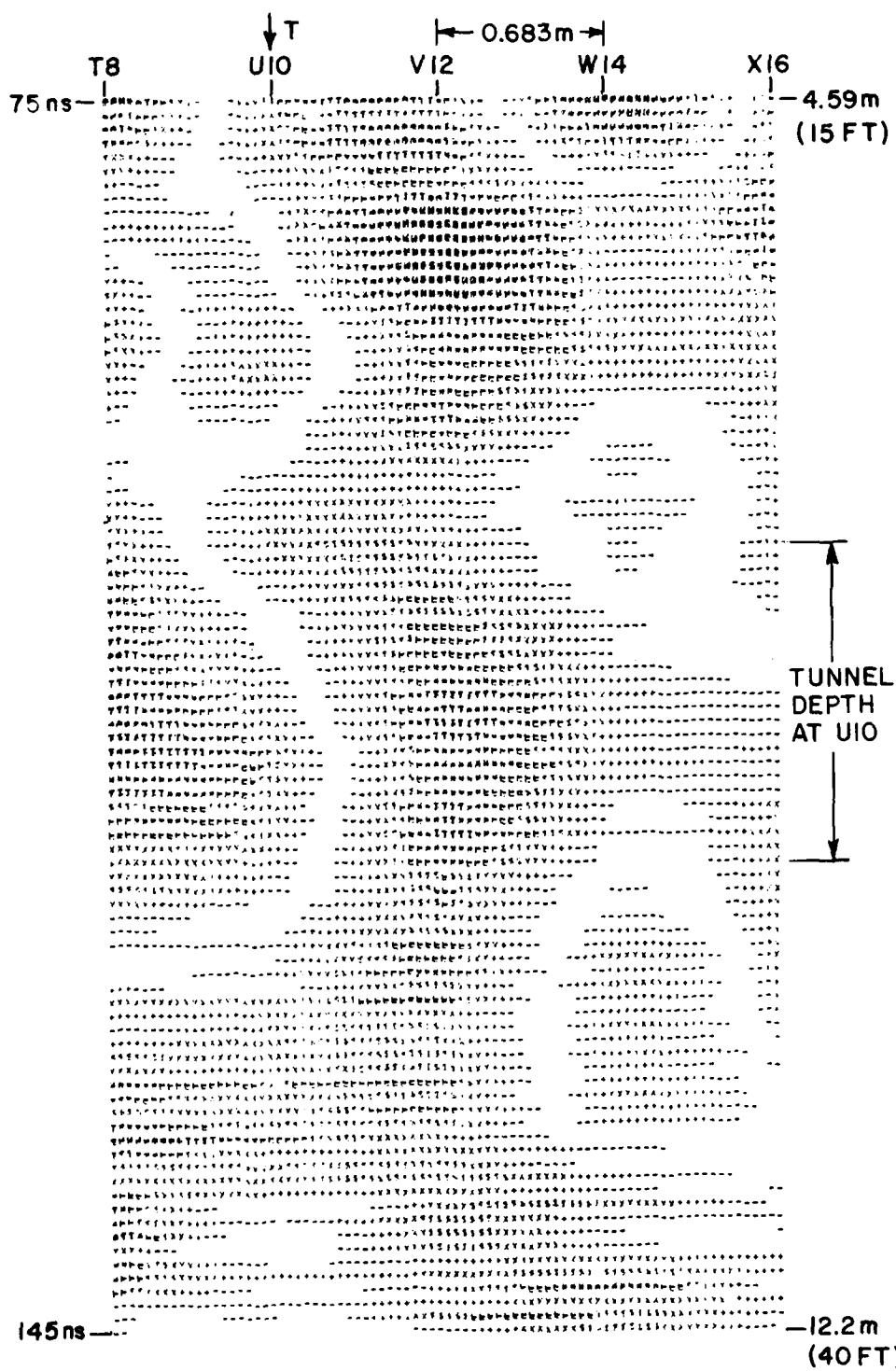
DECONVOLVED DATA
Long Box Antenna   No Clipping
NXDIV=10   NYDIV=0   Fold Last
LIX=3   LIY=1
Figure 107. Gold Hill Map 2 Traverse T8 to X16   Cross Section.
(An improved version of Figure 107 is given in
Figure 49 of Report 4460-11.)
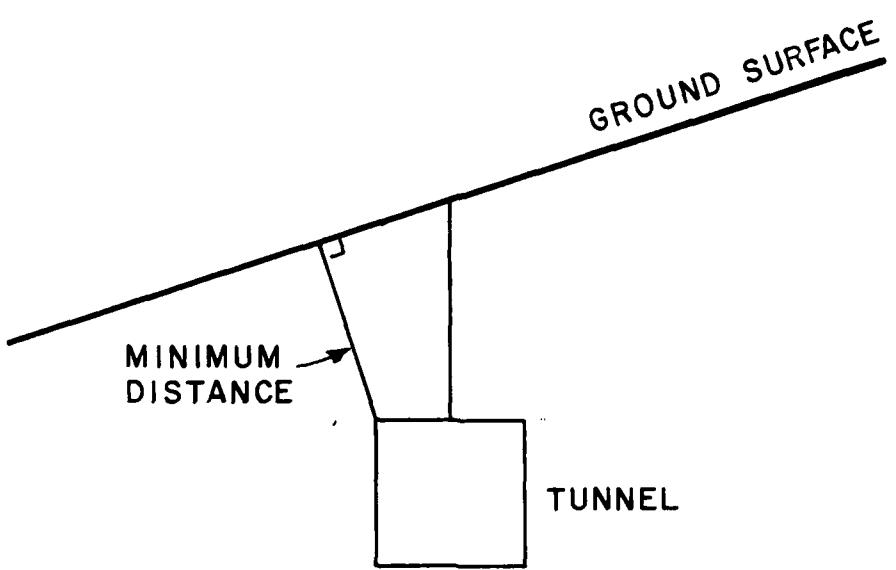
Figure 108. Minimum Distance to Tunnel in a Non-Horizontal Traverse.

CHAPTER V
CONCLUSIONS

From the results presented earlier, it is clear that tunnel detection through the use of grey scale plotting can be accomplished. Some of the best examples of this are Figures 29, 43, 54 and 107 in Chapter 4. Although the detection capability appears to be quite good in these plots, the limitations of the mapping technique must be kept in mind.

There is a "learning period" in which one must become familiar with target characteristics as exhibited in the plots. In certain situations it is necessary to be familiar with the properties of the interpolation method used in order to distinguish between "real" targets and those which are created by the interpolation. Use of a localized interpolation controls this phenomenon quite well. Thus, in the plan view type of plot, where actual 2-dimensional interpolation takes place, it is unsatisfactory to use large subgrids for the interpolation because of the high probability that such false targets will appear. These are due chiefly to the higher-order polynomials involved in this case. As has been discussed before, RMS window size is also a critical parameter in a plan view plot.

Preprocessing of the radar return before input to GLPR is almost always necessary, as evidenced by the above cited figures. Techniques used to generate these plots ranged in difficulty from simple DC removal to deconvolution using the Z-transform.

One limitation of GLPR is its speed. The preprocessing certainly lengthens the time required to generate one plot, but the real time constraint is the interpolation speed and size of map to be generated. For a YDIM x XDIM sample array, processing a grey level plot is of computational complexity

$$\emptyset(XDIM*YDIM*NXDIV*NYDIV*(LIX^3LIY+LIX^2LIY))$$

where

   XDIM,YDIM   are the dimenisions of the waveform sample array.

   NXDIV,NYDIV are the number of interpolated points required
                       between samples in the x- and y-dimensions,
                       respectively, and

LIX,LIY   are the x- and y-dimensions of the subgrid to be   .
          used for interpolation, respectively.

It can be seen that an increase in interpolation subgrid size causes cubic growth in computation time.

Lastly, a fundamental problem with our particular plotting method is the use of a line printer as the output device. Unequal character dimensions, uneven inking, white areas between characters, and character skewing all detract from the final plot.

In our use of GLPR, however, the above limitations have not been crucial. Our interest is not to provide full-scale detection capability with these plots but merely to be able to discern in a simple way our ability to detect certain types of targets with given radar systems. This plotting method is also useful as a measure of the effectiveness of various signal processing techniques.

Improvements to GLPR are possible. Recent developments in interpolation using the Discrete Fourier Transform[9] suggest that computation time could be improved. A basic MxN interpolation using the Lagrange method is of order M^2+N^2 while the Discrete Fourier Transform method using the FFT algorithm is only of order $M\log_2+N\log_2 N$ (for a rectangularly separable interpolation function, as we have used).

Another improvement would be the use of color instead of grey levels in plotting. The eye can distinguish differences between adjacent colors more readily than adjacent grey levels that are close in value. This is useful since the reading of a grey level plot usually involves tracking the interface between two grey levels. Assignment of colors to signal levels would be user-controlled to allow enhancement of areas of interest.

141

REFERENCES

[1] J.D. Young and R. Caldecott, "Underground Pipe Detector,"
U.S. Patent 3,967,282, June 29, 1976.

[2] C.A. Tribuzi, "An Antenna for Use in an Underground (HFW) Radar
System," Report 4460-4, The Ohio State University ElectroScience
Laboratory, Department of Electrical Engineering; prepared under
Contract DAAG53-76-C-0179 for U.S. Army Mobility Equipment
Research and Development Command, November 1977.

[3] L.W. Wald, "Modification of the HFW Underground Antenna
Based on Experimental Studies," M.Sc. Thesis, The Ohio State
University ElectroScience Laboratory, Department of Electrical
Engineering, December 1978.

[4] C.W. Davis, III, Ph.D. Dissertation, The Ohio State University
ElectroScience Laboratory, Department of Electrical Engineering.

[5] C.B. Tompkins and W.L. Wilsor, Jr., Elementary Numerical
Analysis, Englewood Cliffs, NJ, Prentice-Hall, Inc., 1969,
pp. 207-241.

[6] J.F. Steffensen, Interpolation, New York, Chelsea Publishing
Co., 1950, pp. 21-22, 203-216.

[7] K.H. Waters, Reflection Seismology, New York, John Wiley and
Sons, 1978, pp. 151-184.

[8] D.W. Wise, "A Microcomputer-Controlled System for the
Aquisition and Processing of Radar Returns from Underground
Targets," Report 479X-6, The Ohio State University Electro-
Science Laboratory, Department of Electrical Engineering;
prepared under tcontract for Columbia Gas System Service
Corporation, January 1978.

[9] P.N. Keating, "More Accurate Interpolation Using Discrete
Fourier Transforms," IEEE Transactions on Acoustics, Speech, and
Signal Processing, Volume ASSP-26, No. 4, August 1978,
pp. 368-369.

[10] J.N. Franklin, Matrix Theory, Englewood Cliffs, NJ,
Prentice-Hall Inc., 1968, p. 48.

[11] Ibid, p. 44.

APPENDIX A
DERIVATION OF GENERAL FORM OF INTERPOLATION PROBLEM

As stated in Chapter II, we are looking for a polynomial estimate $F_n(x)$ of degree n to a continuous function $f(x)$ of the form

$$F_n(x) = \sum_{k=0}^{n} a_k x^k \qquad \text{(A1)}$$

We also constrain $F_n(x)$ so that

$$F_n(x_j) = f(x_j) \qquad j=0,1,\cdots,n \qquad \text{(A2)}$$

Combining (A1) and (A2) we have:

$$\sum_{k=0}^{n} a_k x_j^k = f(x_j) \qquad j=0,1,\cdots,n$$

or in matrix form:

$$
\begin{bmatrix}
1 & x_0 & x_0^2 & \cdots & x_0^n \\
1 & x_1 & x_1^2 & \cdots & x_1^n \\
1 & x_2 & x_2^2 & \cdots & x_2^n \\
\cdot & \cdot & \cdot & & \cdot \\
\cdot & \cdot & \cdot & & \cdot \\
\cdot & \cdot & \cdot & & \cdot \\
1 & x_n & x_n^2 & \cdots & x_n^n
\end{bmatrix}
\begin{bmatrix}
a_0 \\
a_1 \\
a_2 \\
\cdot \\
\cdot \\
\cdot \\
a_n
\end{bmatrix}
=
\begin{bmatrix}
f(x_0) \\
f(x_1) \\
f(x_2) \\
\cdot \\
\cdot \\
\cdot \\
f(x_n)
\end{bmatrix}
$$

We want a solution to exist to (A1) for all x in some interval $a \leq x \leq b$, so we append this equation to the matrix also, yielding

143

$$
\begin{bmatrix}
1 & x & x^2 & \cdots & x^n \\
1 & x_0 & x_0^2 & \cdots & x_0^n \\
1 & x_1 & x_1^2 & \cdots & x_1^n \\
\vdots & \vdots & \vdots & & \vdots \\
1 & x_n & x_n^2 & \cdots & x_n^n
\end{bmatrix}
\begin{bmatrix}
a_0 \\
a_1 \\
\vdots \\
\vdots \\
a_n
\end{bmatrix}
=
\begin{bmatrix}
F_n(x) \\
f(x_0) \\
f(x_1) \\
\vdots \\
f(x_n)
\end{bmatrix}
\tag{A3}
$$

$$\underline{X}_1 a = f$$

where

the dimensions of $\underline{X}_1$ are $(n+2) \times (n+1)$

the dimensions of a are $(n+1) \times 1$, and

the dimensions of f are $(n+2) \times 1$

From linear algebra[10], for an MxN system of inhomogeneous equations, $\underline{X}_1 a = f$ such as this, the condition for solvability is that the Mx(N+1) matrix $\underline{X}_2$ formed by adjoining column vector f to $\underline{X}_1$ has

$$\text{RANK } \underline{X}_2 = \text{RANK } \underline{X}_1 \tag{A4}$$

So we must have that

$$
\text{RANK}
\begin{bmatrix}
1 & x & x^2 & \cdots & x^n \\
1 & x_0 & x_0^2 & \cdots & x_0^n \\
1 & x_1 & x_1^2 & \cdots & x_1^n \\
\vdots & \vdots & \vdots & & \vdots \\
1 & x_n & x_n^2 & \cdots & x_n^n
\end{bmatrix}
$$

$$
= \text{RANK}
\begin{bmatrix}
F_n(x) & 1 & x & x^2 & \cdots & x^n \\
f(x_0) & 1 & x_0 & x_0^2 & \cdots & x_0^n \\
f(x_1) & 1 & x_1 & x_1^2 & \cdots & x_1^n \\
\vdots & \vdots & \vdots & \vdots & & \vdots \\
f(x_n) & 1 & x_n & x_n^2 & \cdots & x_n^n
\end{bmatrix}
\tag{A5}
$$

144

We must consider two cases for (A5)

Case 1:

$$x \neq x_j \qquad j=0,1,\cdots,n$$

Since the columns and rows of $\underline{X}_1$ are independent (x_j distinct and $x \neq x_j$) we have

$$\text{RANK } \underline{X}_1 = n+1 \qquad . \tag{A6}$$

To find the rank of $\underline{X}_2$ we use the following theorem from linear algebra[11]:

Let $\underline{A}$ be an MxN matrix. If $\underline{A}$ has an rxr submatrix $\underline{S}$ with DET $\underline{S} \neq 0$ and if every $(r+1)x(r+1)$ submatrix $\underline{T}$ of which $\underline{S}$ is a submatrix has DET $\underline{T}=0$ then RANK $\underline{A}=r$.

In our case the matrix $\underline{A}$ corresponds to $\underline{X}_2$. We wish to have RANK $\underline{X}_2$=RANK $\underline{X}_1$=n+1, so we look for submatrix $\underline{S}$ with DET $\underline{S} \neq 0$ and r=n+1.

We take as submatrix $\underline{S}$ the matrix

$$\underline{S} = \begin{bmatrix} 1 & x_0 & x_0^2 & \cdots & x_0^n \\ 1 & x_1 & x_1^2 & \cdots & x_1^n \\ \vdots & \vdots & \vdots & & \vdots \\ 1 & x_n & x_n^2 & \cdots & x_n^n \end{bmatrix}$$

which is $(n+1)x(n+1)$. Since the x_j are distinct

$$\text{DET } \underline{S} \neq 0$$

satisfying the first part of the theorm.

The only $(n+2)x(n+2)$ submatrix $\underline{T}$ that we can have is the matrix $\underline{X}_2$ itself. So, in order to satisfy $(\overline{A}4)$ we must have:

$$\text{DET } \underline{X}_2 = 0 \tag{A7}$$

or

145

$$\begin{vmatrix} F_n(x) & 1 & x & x^2 & \cdots & x^n \\ f(x_0) & 1 & x_0 & x_0^2 & \cdots & x_0^n \\ f(x_1) & 1 & x_1 & x_1^2 & \cdots & x_1^n \\ \vdots & \vdots & \vdots & \vdots & & \vdots \\ f(x_n) & 1 & x_n & x_n^2 & & x_n^n \end{vmatrix} = 0 \qquad (A8)$$

This is the condition for solvability of (A3) in this case.

Case 2:

$x = x_j \qquad\qquad j \epsilon \{0,1,\cdots,n\}$

Since two rows of the matrix $\underline{X}_1$ are equal, we have that

no. independent rows = no. independent columns =
$n+1$ = RANK $\underline{X}_1$ which is the same as Case 1.

Using (A8) we must have

$$\begin{vmatrix} F_n(x_j) & 1 & x_j & x_j^2 & \cdots & x_j^n \\ f(x_0) & 1 & x_0 & x_0^2 & \cdots & x_0^n \\ \vdots & \vdots & \vdots & \vdots & & \vdots \\ f(x_j) & 1 & x_j & x_j^2 & \cdots & x_j^n \\ \vdots & \vdots & \vdots & \vdots & & \vdots \\ f(x_n) & 1 & x_n & x_n^2 & \cdots & x_n^n \end{vmatrix} = 0 \qquad (A9)$$

This is satisfied since we have made the constraint that $F_n(x_j) = f(x_j)$. Therefore (A8) is the general statement of the interpolation problem presented in (A1) and (A2).

146

```
  1  C      >>>>INTERPOLATE AND PLOT GREY LEVELS SUBROUTINE
  2  C
  3  C
  4  C
  5  C
  6  C      >>PURPOSE:GIVEN AN ARRAY OF KNOWN DATA POINTS, SUBROUTINE
  7  C              TAPED WILL INTERPOLATE THE ARRAY, QUANTIZE IT INTO
  8  C              GREY LEVELS, AND WRITE IT TO A SPECIFIED FILE
  9  C              WHICH MAY THEN BE PRINTED ON THE LINE PRINTER BY
 10  C              RUNNING PROGRAM OVERS.0046.
 11  C      >>ALGORITHM USED:SEE ACCOMPANYING DOCUMENTATION.
 12  C
 13  C      >>SUBROUTINES USED:INTERP
 14  C
 15  C      >>CALLING PARAMETERS:
 16  C        A: INPUT ARRAY OF KNOWN POINTS (SAMPLES).
 17  C        XDIM,YDIM: DIMENSIONS OF A (I.E. A(YDIM,XDIM) )
 18  C        AI: ARRAY HOLDING INTERPOLATED DATA FROM ONE HORIZONTAL
 19  C            SCAN.
 20  C        XSIZ,YSIZ: DIMENSIONS OF AI (I.E. AI(YSIZ,XSIZ) )
 21  C                MUST BE CALCULATED ACCORDING TO THE FOLLOWING
 22  C                FORMULAS...
 23  C
 24  C            FOR UNIFORMLY SPACED DATA:
 25  C
 26  C                XSIZ=(XDIM-1)*(NXDIV+1)+1
 27  C                YSIZ=NYDIV+1
 28  C
 29  C            FOR NON-UNIFORMLY SPACED DATA:
 30  C
 31  C                XSIZ=(FX(XDIM)-FX(1))*(NXDIV+1)+1
 32  C                YSIZ=FY(1)*(NYDIV+1)+1
 33  C
 34  C                WHERE
 35  C                    FY(P)=AVE( FY(N+1)-FY(N) )    N=1,...,YDIM-1
 36  C
 37  C        FX,FY: ARRAYS (OF DIMENSIONS XDIM AND YDIM, RESPECTIVELY)
 38  C               CONTAINING COORDINATES OF KNOWN POINTS IN A
 39  C               NON-UNIFORMLY SPACED SAMPLE ARRAY. (SEE DIAGRAM)
 40  C
 41  C               1 23   45 : SUBSCRIPT OF ARRAY FX
 42  C               X XX   XX : KNOWN POINTS
 43  C               123456789 : REFERENCE COORDINATES
 44  C
 45  C               FX(1)=COORD. OF 1ST KNOWN POINT=1
 46  C               FX(2)=  "    "   2ND  "      "   =3
 47  C               FX(3)=  "    "   3RD  "      "   =4
 48  C               FX(4)=  "    "   4TH  "      "   =8
 49  C               ETC.
 50  C
 51  C        LX,LY: DIMENSIONS OF INTERPOLATION GRID
 52  C        NXDIV,NYDIV: NUMBER OF INTERPOLATED POINTS DESIRED BETWEEN
 53  C                KNOWN VALUES IN THE X- AND Y-DIRECTIONS
 54  C        EQUAL: 1=ARRAY OF KNOWN DATA IS NOT UNIFORMLY SPACED
 55  C               0=ARRAY OF KNOWN DATA IS UNIFORMLY SPACED
```

```
56  C        CLIPU,CLIPL: VALUES AT WHICH INTERPOLATED DATA WILL BE
57  C                    CLIPPED. (I.E. VALUES GREATER THAN CLIPU
58  C                    WILL BE SET EQUAL TO CLIPU AND VALUES LESS
59  C                    THAN CLIPL WILL BE SET EQUAL TO CLIPL.)
60  C        LEV: NUMBER OF GREY LEVELS DESIRED. (UP TO 14)
61  C        LU: LOGICAL UNIT NUMBER FOR PLOT OUTPUT
62  C    >>AUTHORS: D.G.STAFF        ESL 264
63  C
64  C
65  C
66  C
67         SUBROUTINE  IANDP(A,XDIM,YDIM,AI,YSIZ,YSIZ,FX,FY,
68       *                   LIX,LIY,NXDIV,NYDIV,NGRID,CLIPU,
69       *                   CLIPV,LEV,LU)
70         INCLUDE  INTERP,39194
71         INTEGER  XDIM,YDIM,XS,YS,X1,Y1,PASS,POSITN,QNT2
72         INTEGER  XSCALE,YSCALE,XINTLM,YINTLM,XSIZ,YSIZ
73         INTEGER  CH(64,14),OUT(6,132)
74         DIMENSION  A(YDIM,XDIM),AI(YSIZ,XSIZ),FX(1),FY(1),PER(14)
75         DIMENSION  STACK(20)
76         DATA  CH/1680
77       *                                       I  3     0  *        0  /  -
78       *    T  -        N  N  V  7  N  7  -  S  U  T  X  $  /
79         VMIN=1.E30
80         VMAX=-1.E30
81         NXDIV=NXDIV+1
82         NYDIV=NYDIV+1
83         WRITE(LU,900)
84  900    FORMAT(1H1)
85  C    >>PASS=1 DETERMINE EXTREMA OF INTERPOLATED VALUES.
86  C    >>     =2 PLOT GREY LEVELS.
87         DO 50 PASS=1,2
88           IF(PASS.EQ.1)GO TO 15
89              WRITE(7,901)
90  901        FORMAT(" STARTING 2ND PASS.")
91  C          >>FILL OUT WITH SPACES.
92              DO 11 I=1,6
93              DO 11 J=1,132
94  11          OUT(I,J)=CH(1,1)
95  C          >>CLEAR DENSITY ARRAY.
96              DO 12 I=1,14
97  12          PER(I)=0.
98  C          >>DELTA IS THE SPACING BETWEEN GREY LEVELS.
99              DELTA=(VMAX-VMIN)/FLOAT(LEV)
100 C          >>MARGIN IS THE WIDTH OF MARGIN NEEDED TO CENTER THE
101 C          >>GREY LEVEL PLOT ON THE LINE PRINTER.
102              MARGIN=(132-XSIZ)/2
103 C    >>XSCALE,YSCALE ARE THE NUMBER OF BLOCKS IN THE X- AND
104 C    >>Y-DIRECTIONS,RESPECTIVELY.
105 15       YSCALE=YDIM-1
106          IF(LIY.EQ.1)YSCALE=YDIM
107          YSCALE=YDIM-1
108          IF(LIY.EQ.1)YSCALE=YDIM
109 C    >>YC,YS ARE THE COORDINATES OF THE BLOCK TO BE FILLED.
110          DO 50 YS=1,YSCALE
```

148

```
111                DO 100 YS=1,XSCNUM
112  C              >>XINTLR,YINTLR ARE THE COORDINATES OF THE UPPERMOST
113  C              >>AND LEFTMOST GRID THAT WILL OVERLAP THE CURRENT
114  C              >>BLOCK.
115                 XINTLR=YS-LIX+2
116                 IF(XINTLR.GT.XS)XINTLR=XS
117                 IF(XINTLR.LT.1)XINTLR=1
118                 YINTLR=YS-LIY+2
119                 IF(YINTLR.GT.YS)YINTLR=YS
120                 IF(YINTLR.LT.1)YINTLR=1
121  C              >>ILIM AND JLIM ARE THE NUMBER OF POINTS TO
122  C              >>INTERPOLATE IN THE X- AND Y-DIMENSIONS OF
123  C              >>EACH BLOCK, RESPECTIVELY.
124                 ILIM=NXDIV+1
125                 JLIM=NYDIV+1
126                 IF(NORUNT.NE.1)GO TO 199
127                   IF(LIX.EQ.1)GO TO 20
128                   S=(FX(XS+1)-FX(XS))*NXDIV+1
129                   IF(S-IFIX(S).GT.1E-6)STOP NXE
130                   ILIM=IFIX(S)
131                   GO TO 21
132  20               ILIM=1
133  21               IF(LIY.EQ.1)GO TO 22
134                   S=(FY(YS+1)-FY(YS))*NYDIV+1
135                   IF(S-IFIX(S).GT.1E-6)STOP NYD
136                   JLIM=IFIX(S)
137                   GO TO 199
138  22               JLIM=1
139  199            DO 100 I=1,ILIM
140  C              >>RX,RY ARE THE COORDINATES OF THE POINT TO
141  C              >>INTERPOLATE.
142                 RX=XS+FLOAT(I-1)/NXDIV
143                 IF(NORUNT.EQ.1)RX=RX-XS+FX(XS)
144                 DO 100 J=1,JLIM
145                   RY=YS+FLOAT(J-1)/NYDIV
146                   IF(NORUNT.EQ.1)RY=RY-YS+FY(YS)
147  C                >>FILL BLOCK.
148  C                >>LEVL IS A POINTER TO THE STACK OF OVERLAPPING
149  C                >>INTERPOLATED VALUES.
150                   LEVL=1
151  C                >>XI,YI ARE COORDINATES OF THE GRID USED TO
152  C                >>INTERPOLATE THE CURRENT BLOCK.
153                   DO 200 XI=XINTLR,XS
154                     DO 200 YI=YINTLR,YS
155  C                    >>IF GRID WILL NOT FIT IN ARRAY, SKIP IT.
156                       IF(XI.GT.XINTLR-LIX+1)GO TO 200
157                       IF(YI.GT.YINTLR-LIY+1)GO TO 200
158                       CALL INTERP(Z,FY,FX,XDIM,XDIM,LIY,LIX,YI,XI,
159       .                          RY,RX,ATN,NORUNT)
160  C                    >>STACK HOLDS OVERLAPPING VALUES FOR ONE POINT.
161                       STACK(LEVL)=ATN
162                       LEVL=LEVL+1
163  200              CONTINUE
164                   LEVL=LEVL-1
165                   IF(LEVL.EQ.0)GO TO 100
```

149

```
166  C          >>AVERAGE OVERLAPPING VALUES.
167            AIN=0.
168            DO 300 K=1,LEVL
169  300       AIN=AIN+STACK(K)
170            AIN=AIN/LEVL
171  C          >>CLIP INTERPOLATED VALUE.
172            IF(AIN.GT.CLIPH)AIN=CLIPH
173            IF(AIN.LT.CLIPL)AIN=CLIPL
174  C          >>PUT INTERPOLATED DATA INTO HOLDING ARRAY.
175  C          >>IC IS THE HORIZONTAL POSITION OF THE INTER-
176  C          >>POLATED VALUE IN THE HOLDING ARRAY.
177            IC=(XS-1)*DYDIV+I
178            IF(NOPROT.EQ.1)IC=(IY(XS)-IY(1))*DYDIV+I
179            AI(J,IC)=AIN
180  C          >>VMAX AND VMIN ARE THE MAXIMUM AND MINIMUM
181  C          >>INTERPOLATED VALUES. THEY ARE USED TO
182  C          >>QUANTIZE THE ARRAY INTO GREY LEVELS.
183            IF(AIN.LT.VMIN)VMIN=AIN
184            IF(AIN.GT.VMAX)VMAX=AIN
185  100      CONTINUE
186          IF(PASS.EQ.1)GO TO 50
187  C        >>OUTPUT SECTION.
188  C        >>JLIM IS THE DIMENSION OF THE HOLDING ARRAY
189  C        >>IN THE Y DIMENSION.
190          JLIM=JLIM-1
191          IF(YS.EQ.YSCOLD)JLIM=JLIM+1
192          IF(IIY.EQ.1)JLIM=1
193          DO 400 J=1,JLIM
194            DO 410 I=1,XSIZ
195  C            >>POSITN IS THE HORIZONTAL POSITION (COLUMN
196  C            >>NUMBER) OF THE OUTPUT CHARACTER ON THE LINE
197  C            >>OF PRINT.
198              POSITN=I+MARGIN
199  C            >>QNTZ IS THE NUMBER OF THE GREY LEVEL TO
200  C            >>WHICH THE INTERPOLATED VALUE IS QUANTIZED.
201  C            >>1=LIGHTEST  LEV=DARKEST
202              QNTZ=1.0+(AI(J,I)-VMIN)/DELTA
203              IF(QNTZ.EQ.LEV+1)QNTZ=LEV
204  C            >>PER HOLDS GREY LEVEL DENSITIES.
205  C            >>PER(N) IS DENSITY OF LEVEL N.
206              PER(QNTZ)=PER(QNTZ)+1.
207              DO 410 K=1,4
208                OUT(K,POSITN)=CL(K,QNTZ)
209  410       CONTINUE
210  C        >>WRITE ONE LINE OF OUTPUT.
211  600       WRITE(IO,902)((OUT(II,JJ),JJ=1,132),II=1,4)
212  902       FORMAT(1X,132A1,3(/4X,132/))
213  50       CONTINUE
214  C        >>PRINT SUMMARY.
215  C        >>CALCULATE PERCENT DENSITY OF EACH SYMBOL.
216          TOT=0.
217          DO 500 I=1,LEV
218  500     TOT=TOT+PER(I)
219          DO 550 I=1,LEV
220  550     PER(I)=PER(I)*100./TOT
```

```
221          WRITE(LU,903) VMAX,VMIN,LEV
222   903    FORMAT(" MAX.VALUE=",F10.3,/," MIN.VALUE=",F10.3,/,
223        *           " NO.LEVELS=",2X,I2,/," SYMBOL DENSITY",5X,
224        *           "SYMBOL DENSITY")
225          LEV2=LEV/2
226          DO 575 I=1,LEV2
227          II=I+LEV2
228   575    WRITE(LU,904)(CH(J,I),CH(J,II),J=1,4),PER(I),PER(II)
229   904    FORMAT(4X,A1,18X,A1,3(/,"+    ",A1,18X,A1),/,"+",
230        *           7X,F5.2,"%",13X,F5.2,"%")
231          RETURN
232          END
```

151

```
 1  C     >>>>TWO-DIRECTIONAL LAGRANGE INTERPOLATION SUBROUTINE
 2  C
 3  C
 4  C     >>PURPOSE: INTERPOLATES A 2-D FUNCTION F(X,Y) INSIDE A
 5  C       RECTANGULAR ARRAY OF KNOWN VALUES (SAMPLES). SPACING
 6  C       BETWEEN SAMPLES IN EITHER X- OR Y-DIRECTION (OR BOTH)
 7  C       MAY BE ARBITRARY. ANY RECTANGULAR SUBSET OF THE KNOWN
 8  C       DATA MAY BE USED AS THE INTERPOLATION GRID.
 9  C       NOTE: THE X-DIMENSION DENOTES THE ROWS OF F(X,Y) AND
10  C             THE Y-DIMENSION DENOTES THE COLUMNS OF F(X,Y).
11  C
12  C     >>FORMULA USED:
13  C          F(X,Y)=L(0,0,X)L(0,0,Y)F(X(0),Y(0))
14  C                +L(1,0,X)L(0,0,Y)F(X(1),Y(0))
15  C            +...+L(N,0,X)L(0,0,Y)F(X(N),Y(0))
16  C
17  C                +L(0,0,X)L(1,0,Y)F(X(0),Y(1))
18  C                +L(1,0,X)L(1,0,Y)F(X(1),Y(1))
19  C            +...+L(N,0,X)L(1,0,Y)F(X(N),Y(1))
20  C
21  C                +...
22  C
23  C                +L(0,0,X)L(M,0,Y)F(X(0),Y(M))
24  C                +L(1,0,X)L(M,0,Y)F(X(1),Y(M))
25  C            +...+L(N,0,X)L(M,0,Y)F(X(N),Y(M))
26  C
27  C     WHERE L(J,K,Z) ARE THE LAGRANGE COEFFICIENTS GIVEN
28  C       BY:
29  C       L(J,K,Z)=(Z-X(0))...(Z-X(J-1))(Z-X(J+1))...(Z-X(K))/
30  C       (X(J)-X(0))...(X(J)-X(J-1))(X(J)-X(J+1))...(X(J)-X(K))
31  C
32  C       X( ),Y( ) :COORDINATES OF KNOWN POINTS
33  C
34  C     >>CALLING PARAMETERS:
35  C       X,Y : COORDINATES OF POINT TO INTERPOLATE
36  C       FINT: INTERPOLATED VALUE
37  C       F   : ARRAY OF KNOWN DATA
38  C       N,M : DIMENSIONS OF F
39  C       LN,LM : DIMENSIONS OF INTERPOLATION GRID
40  C       NI,MI : STARTING COORDINATES OF INTERPOLATION GRID
41  C             (I.E. GRID IS X=X(NI),X(NI+1),...X(NI+LN-1)
42  C                           Y=Y(MI),Y(MI+1),...,Y(MI+LM-1)
43  C       NONUNI: 1=ARRAY OF KNOWN DATA IS NOT UNIFORMLY SPACED
44  C               0=ARRAY OF KNOWN DATA IS UNIFORMLY SPACED
45  C       FX,FY : ARRAYS(OF DIMENSIONS N AND M,RESPECTIVELY)
46  C             CONTAINING COORDINATES OF KNOWN POINTS IN A
47  C             NON-UNIFORMLY SPACED SAMPLE ARRAY. (SEE DIAGRAM)
48  C
49  C             1 23   45 : ARRAY ELEMENTS EX
50  C             X YX   XY : KNOWN POINTS
51  C             123456789 : REFERENCE COORDINATES
52  C
53  C             FX(1)=COORD. OF 1ST KNOWN POINT=1 (ALWAYS)
54  C             FX(2)=  "    "  2ND  "      "   =3
55  C             FY(2)=  "    "  2ND  "      "   =4
```

```
56  C          (X(M)=   "     "  NTH  "       "  =0
57  C          ETC.
58  C
59  C    >>AUTHOR : D.C. STAPP FSI 264
60  C
61  C
62  C
63          SUBROUTINE INTERP(F,FX,FY,N,M,LN,LM,N1,M1,X,Y,FIN,
64         .          NONUNI)
65          DIMENSION F(N,M),FX(N),FY(M)
66          FIN=0.
67  C    CALCULATE ENDPOINTS OF GRID
68          N2=N1+LN-1
69          M2=M1+LM-1
70  51      DO 100 I=N1,N2
71          A=1.
72          B=1.
73  C    CALCULATE LAGRANGE COEFFICIENT A/B FOR X
74          DO 200 K=N1,N2
75          IF(K.EQ.I)GO TO 200
76          IF(NONUNI.EQ.1)GO TO 250
77  C       UNIFORM CASE
78          A=A*(X-K)
79          B=B*(I-K)
80          GO TO 200
81  C       NON-UNIFORM CASE
82  250     A=A*(X-FX(K))
83          B=B*(FX(I)-FX(K))
84  200     CONTINUE
85          DO 100 J=M1,M2
86          C=1.
87          D=1.
88  C    CALCULATE LAGRANGE COEFFICIENT C/D FOR Y
89          DO 300 K=M1,M2
90          IF(K.EQ.J)GO TO 300
91          IF(NONUNI.EQ.1) GO TO 350
92  C       UNIFORM CASE
93          C=C*(Y-K)
94          D=D*(J-K)
95          GO TO 300
96  C       NON-UNIFORM CASE
97  350     C=C*(Y-FY(K))
98          D=D*(FY(J)-FY(K))
99  300     CONTINUE
100 C       ACCUMULATE VALUE
101         FIN=FIN+F(I,J)*(A*C)/(B*D)
102 100     CONTINUE
103         RETURN
104         END
```

153

MAIN PROGRAM

```
 1          INCLUDE  NAMPKD,4460X:TANDUB,XP:DATETI:SAD,4460X
 2          DIMENSION A(96,13),AT(1,103),D(256),FX(13),FY(96)
 3          DIMENSION IETLES(8,50),LAB(60)
 4          INTEGER  YDIT,YDIM,YSIZ,YSIZ
 5          DATA FX/1.,'...9..,13..,16..,20..,24..,32..,36..,40..,44..,48..,52./
 6          OPEN 9 GLAPH
 7          DO 2 I=1,96
 8   2      FY(I)=FLOAT(I)
 9          TOP=56.
10          TL=0.
11          TUT=161
12          TNF=256.
13          YDIM=13
14          YDIP=0.
15          YSIZ=103
16          YSIZ=1
17          LIY=3
18          LIY=1
19          NXDIV=1
20          NYDIV=0
21          CLIPU=1.E6
22          CLIPW=-106.
23          LEV=14
24          LU=4
25          NUMDUL=1
26          CALL  WAVES(IETLES,NWAV,IDEADC)
27  10      CALL  WAVEP(IETLES,NWAV,IDEADC,D,256,LAB,TL,IER)
28          IF(IER.EQ.-1)STOP
29          IF(IER.EQ.-2)STOP
30          IF(IER.EQ.1)GO TO 20
31          AVG=0.
32          DO 12 I=1,256
33  12      AVG=AVG+D(I)
34          AVG=AVG/256.
35          DO 16 I=IV1,IVF
36          TI=I-IV1+1
37  16      A(TI,IDEADC-1)=4.*(D(I)-AVG)
38          GO TO 30
39  20      WRITE(9,201)
40  201     FORMAT("LABEL:")
41          READ(9,202) (LAB(I),I=1,27)
42  202     FORMAT(26A4,A2)
43          WRITE(9,204)
44  204     FORMAT("REASSIGN?")
45          READ(9,205) T
46  205     FORMAT(A1)
47          IF(T.EQ.1GYABY6)CALL  GLAPH
48          CALL  ICUDE(A,YDIT,YDIP,AT,YSIZ,YSIZ,FX,FY,LIY,LIY,NXDIV,NYDIV,
49       *              NUMDUL,CLIPU,CLIPW,LEV,LU)
50          WRITE(9,203)
51  203     FORMAT(3(/))
52          WRITE(9,202) (LAB(I),I=1,27)
53          END
```

```
 1          INCLUDE  WAVCKD,99GOXITANDUD,X2IoAIFTLFAD,44FoX
 2          DIMENSION A(96,10),A1(1,97),STACK(256,3),TETLES(4,50)
 3          DIMENSION D(256),LAB(92),FX(10),FY(96)
 4          INTEGER XDIM,YDIM,XSIZ,YSIZ
 5          DATA FY/1.,5.,18.,29.,43.,55.,63.,71.,79.,87./
 6          OPEN 4 GRAPE
 7          DO 2 I=1,96
 8  2       FY(I)=FLOAT(I)
 9          TI =42
10          TWT=161
11          TWF=256
12          NAV=5
13          XDIM=10
14          YDIM=96
15          XSIZ=67
16          YSIZ=1
17          FIX=5
18          FIY=1
19          NXDIV=3
20          FYDIV=0
21          NUPUNT=1
22          CLIPR=1.16
23          CLIPW=-160.
24          FFV=19
25          FD=4
26          TD=256
27          CALL WAVES(TETLES,NWAV,IREADC)
28  C          READ IN NAV WAVEFORMS.
29          DO 10 I=1,NAV
30          CALL WAVEF(TETLES,NWAV,IREADC,D,ID,FLAB,TI,IF)
31          IF(IF.FO.-1)STOP FERE
32          IF(IF.FO.-2)STOP
33          AVG=0.
34          DO 12 J=1,TD
35  12      AVG=AVG+D(J)
36          AVG=AVG/FLOAT(TD)
37          DO 15 J=1,TD
38  15      STACK(J,I)=D(J)-AVG
39  10      CONTINUE
40          M=1
41          NGEN=1
42  C          AVERAGE THE STACK.
43  20      DO 24 I=1,TD
44          AVG=0.
45          DO 22 J=1,NAV
46          AVG=AVG+STACK(I,J)
47  22      CONTINUE
48          D(I)=AVG/FLOAT(NAV)
49  24      CONTINUE
50  C          PROCESS THE GENERATED WAVEFORM.
51          DO 26 I=II,IWF
52          TI=I-II+1
53          A(TI,NGEN)=D(I)
54  26      CONTINUE
55          NGEN=NGEN+1
```

```
56  C          PUT NEXT RAW WAVEFORM INTO THE STACK.
57         CALL WAVEL(TITLES,NNAV,TPEADC,0,IP,LAB,IL,IF)
58         IF(IF.EQ.-1)STOP ERR2
59         IF(IF.EQ.-2)STOP THIS2
60         IF(IF.EQ.1)GO TO 100
61         AVG=0.
62         DO 31 I=J,IL
63         AVG=AVG+P(I)
64  30     CONTINUE
65         AVG=AVG/(FLOAT(IP)
66         DO 32 I=1,IP
67         STACK(I,NT)=P(I)-AVG
68  32     CONTINUE
69         NT=NT+1
70         IF(NT.GT.NAV)NT=1
71         GO TO 20
72  100    WRITE(5,901)
73  901    FORMAT("LABEL:")
74         READ(8,902) (LAB(I),I=1,27)
75  902    FORMAT(26A3,F2)
76         WRITE(5,904)
77  904    FORMAT("REASSIGN?")
78         READ(8,905) I
79  905    FORMAT(A1)
80         IF(I.EQ.2H5376)CALL REASSN
81         CALL LANDP(P,XDIM,YDIM,AT,XSIZ,YSIZ,FX,FY,LIX,LIY,NXDIV,
82        .          NYDIV,NCOUNT,CLIPP,CLIPW,LEV,LU)
83  .      WRITE(LU,903) (LAB(I),I=1,27)
84  903    FORMAT(A(7),26A3,F2)
85         END
```

156

END

DATE

FILMED

DTIC

10-88